Mathematisch-Naturwissenschaftliche Fakultät

Institut für Biochemie und Biologie

DISSERTATION

zum erwerb des akademischen grades

doctor rerum naturalium

Implications of Microcystin Production in *Microcystis aeruginosa* PCC 7806

vorgelegt von

Sven Meißner

geboren am

10.11.1981 in Berlin

Potsdam-Golm, 30.09.2014

Published online at the
Institutional Repository of the University of Potsdam:
URN urn:nbn:de:kobv:517-opus4-75199
http://nbn-resolving.de/urn:nbn:de:kobv:517-opus4-75199

Erklärung

Hiermit erkläre ich, die vorliegende Arbeit eigenständig verfasst und keine anderen als die angegebenen Hilfsmittel und Quellen benutzt zu haben.

Potsdam-Golm, den 30. September 2014

_____

Contents

Summary

Cyanobacteria produce about 40 percent of the world's primary biomass, but also a variety of often toxic peptides such as microcystin. Mass developments, so called blooms, can pose a real threat to the drinking water supply in many parts of the world. This study aimed at characterizing the biological function of microcystin production in one of the most common bloom-forming cyanobacterium *Microcystis aeruginosa*.

In a first attempt, the effect of elevated light intensity on microcystin production and its binding to cellular proteins was studied. Therefore, conventional microcystin quantification techniques were combined with protein-biochemical methods. RubisCO, the key enzyme for primary carbon fixation was a major microcystin interaction partner. High light exposition strongly stimulated microcystin-protein interactions. Up to 60 percent of the total cellular microcystin was detected bound to proteins, i.e. inaccessible for standard quantification procedures. Underestimation of total microcystin contents when neglecting the protein fraction was also demonstrated in field samples. Finally, an immuno-fluorescence based method was developed to identify microcystin producing cyanobacteria in mixed populations.

The high light induced microcystin interaction with proteins suggested an impact of the secondary metabolite on the primary metabolism of *Microcystis* by e.g. modulating the activity of enzymes. For addressing that question, a comprehensive GC/MS-based study was conducted to compare the accumulation of metabolites in the wild-type of *Microcystis aeruginosa* PCC 7806 and the microcystin deficient $\Delta mcyB$ mutant. From

all 501 detected non-redundant metabolites 85 (17 percent) accumulated significantly different in either of both genotypes upon high light exposition. Accumulation of compatible solutes in the $\Delta mcyB$ mutant suggested a role of microcystin in fine-tuning the metabolic flow to prevent stress related to excess light, high oxygen concentration and carbon limitation.

Co-analysis of the widely used model cyanobacterium *Synechocystis* PCC 6803 revealed profound metabolic differences between species of cyanobacteria. Whereas *Microcystis* channeled more resources towards carbohydrate synthesis, *Synechocystis* invested more in amino acids. These findings were supported by electron microscopy of high light treated cells and the quantification of storage compounds. While *Microcystis* accumulated mainly glycogen to about 8.5 percent of its fresh weight within three hours, *Synechocystis* produced higher amounts of cyanophycin. The results showed that the characterization of species-specific metabolic features should gain more attention with regard to the biotechnological use of cyanobacteria.

1

General Introduction

1.1 Cyanobacteria

Cyanobacteria are Gram-negative eubacteria that owe their name to the presence of bluish pigments. Those accessory pigments are linked to the photosystems required for oxygen-evolving photosynthesis. First cyanobacteria-type organisms could have occurred as early as 3 billion years ago, leading to substantial oxygenation of the earth's atmosphere about 2.4- 2.1 billion years ago (Lyons et al., 2014).

Today's cyanobacteria populate diverse habitats ranging from glaciers to hot thermal springs (Whitton et al., 2012) and as symbionts associated with other organisms such as fungi, heterotrophic bacteria, corals and many more (Usher et al., 2007).

The ultra-structure of cyanobacteria is marked by thick cell walls, more typical for Gram-positive bacteria that ensure a high structural rigidity (Hoiczyk and Hansel, 2000). Many cyanobacteria show characteristic intracellular inclusions such as polyphosphate- and cyanophycin granules; gas vesicles and carboxysomes (Komarek and Anagnostidis, 1998).

Most relevant for global photosynthetic carbon fixation by cyanobacteria are phytoplankton species. In many fresh- and brackish water environments, some cyanobacteria species are regularly involved in undesired mass developments, so called blooms.

1.2 Formation of freshwater blooms by cyanobacteria

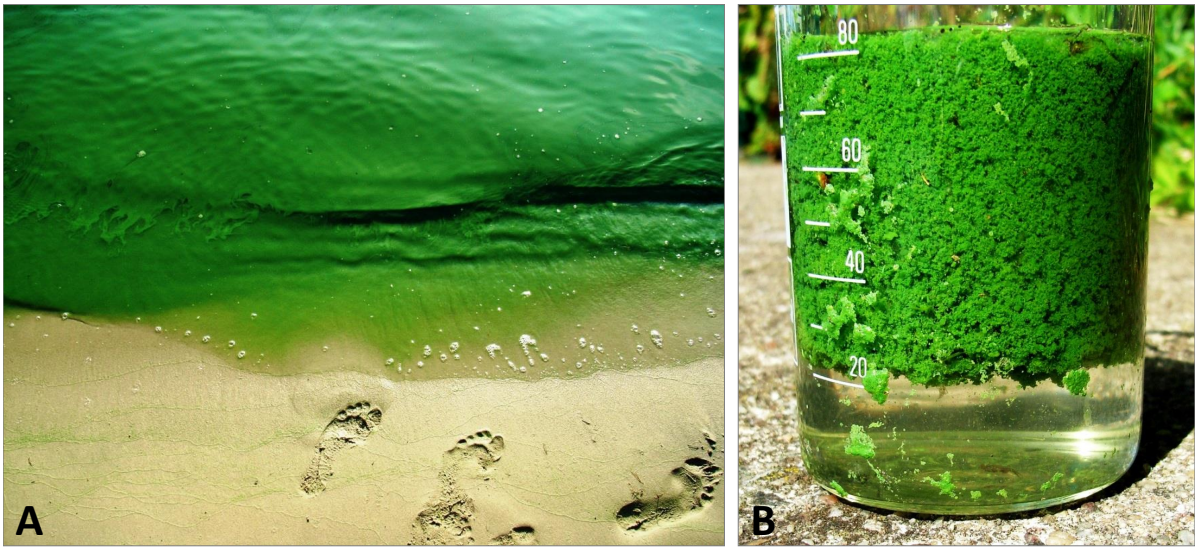

Figure 1.1: Blooms of *Microcystis*, A: Picture of a beach at Lake Templiner See near Potsdam, Germany in August 2009; **B:** Buoyant *Microcystis* colonies in a scoop sample from the surface of river Spree near Friedrichshagen, Germany in August 2009

Nutrient rich fresh water bodies in temperate to tropical climate zones are prone to mass developments of *Microcystis* and some other cyanobacteria species, see Table 1.2. Blooms find their most extreme expression in the formation of floating scums and dense mats.

In eutrophic waters of temperate regions, the composition of the phytoplankton community, usually, follows a distinct seasonal succession, with the establishment of cyanobacterial dominance during summer (Sommer et al., 2012). Abiotic factors related to the formation of blooms include the absence of rain, high temperature and low wind velocity, which support pronounced stratification of the water column into distinct layers (Huisman et al., 2004; Jöhnk et al., 2008; Paerl and Huisman, 2008).

Bloom forming cyanobacteria express gas-filled vesicles, which enables them to float (Thomas and Walsby, 1986; Reynolds et al., 1987). Floating cyanobacteria shade deeper layers and effectively suppress the growth of eukaryotic phytoplankton and macrophytes concurring for light and nutrients (Reynolds et al., 1987; Huisman et al., 2004). Additionally, CO_2 from the atmosphere can directly be assimilated at the surface (Paerl and Ustach, 1982). Increased light absorption by buoyant cyanobacteria further elevates water temperature at the surface and manifests stratification (Paerl and Huisman, 2008). Net oxygen consumption in shaded deeper layers and low mixing within the water column eventually lead to anoxia and mass fish killings (Havens, 2008).

The buoyancy of cyanobacteria is a function of the number and the extent of gas vesicles over the amount of carbohydrate ballast from photosynthesis and turgor pressure (Reynolds et al., 1987). Colony forming *Microcystis* species can vertically migrate within the water column. According to Stoke's law, macroscopic colonies can do this much quicker than smaller ones or single cells. Vertical migration enables *Microcystis* colonies to occupy the most favorable position for e.g. nutrient acquisition in deeper layers, or photosynthesis at the surface.

During cyanobacterial mass developments, the affected habitats are characterized by sharp diurnal changes of oxygen- and inorganic carbon concentrations and the ambient pH (Dunn, 1967; Dokulil and Teubner, 2000). Cells at the water surface are furthermore confronted with high light intensities and damaging UV-radiation. Nonetheless, the formation of floating scum by buoyant colonies is regarded as an elemental part in the life of bloom-forming cyanobacteria (Paerl and Ustach, 1982). To prevent damage and to maintain high photosynthetic activity, effective mechanisms to channel light energy and

to concentrate inorganic carbon are essential.

1.3 Photoprotective and antioxidant mechanisms

Aerobic life is mutually connected with the generation of reactive oxygen species (ROS). Organisms performing oxygenic photosynthesis are in particular exposed to ROS generating conditions, namely high energy flow rates through the photosynthetic electron transport chain and high oxygen concentration. Excess ROS have damaging effects on membranes, proteins and DNA. In that situations, the cells suffer from oxidative stress. Energy-rich UV-radiation also has the potential to damage cellular components directly. However, cyanobacteria evolved a variety of protection mechanisms against oxidative stress and the damaging effects of UV-radiation (Latifi et al., 2009), as summarized in table 1.1.

Table 1.1: Oxidative stress and the defense mechanisms according to (Latifi et al., 2009).

Stressor	**Target/ Effect**	**Defense mechanism**
UV-radiation	DNA, proteins, lipids	Sunscreens: mycosporines, MAAs, scytonemin
Excess energy	$^1O_2$, $O_2^{\bullet -}$ generation	Energy dissipation: NPQ, Flv1/3, Flv2/4
$^1O_2$	DNA, proteins, lipids	Antioxidants: α-tocoperol, carotenoids
$O_2^{\bullet -}$	Lipids, proteins	SOD
H_2O_2	Forms $OH^{\bullet}$ with Fe^{2+}	Catalases, peroxidases
$OH^{\bullet}$	DNA, lipids, proteins	None

The first line of defense comprises small molecules serving as sunscreens to prevent damage by UV-radiation. Mycosporines and mycosporine-like amino acids (MAAs) are small water-soluble molecules, which effectively absorb UV-B radiation (310-365 nm). Scytonemin is a cyanobacteria-specific, lipid soluble pigment deposited at the cell surface. It has an absorption maximum at 370 nm (UV-A) *in vivo* (Latifi et al., 2009).
In the light, ROS evolve at the photosynthetic electron transport chain. The formation of singlet oxygen ($^1O_2$) occurs at the excited reaction center of photosystem II (PS II),

when the plastoquinone (PQ) pool cannot accept additional electrons. Antioxidants like α-tocopherol and carotenoids can detoxify ($^1O_2$). The superoxide anion radical $O_2^{\bullet -}$ is formed by the Mehler reaction at photosystem I (PS I), when electrons are transferred to oxygen instead of ferredoxin. $O_2^{\bullet -}$ is detoxified by metal containing superoxide dismutase, to form molecular oxygen and hydrogen peroxide (H_2O_2). H_2O_2 is further reduced to water by the action of catalase and peroxidase. Detoxification of H_2O_2 is particularly important, since it can be reduced by Fe^{2+} *via* the Fenton reaction to form the highly reactive hydroxyl radical ($OH^{\bullet}$). However, as long as ROS-levels do not exceed a certain threshold, the cells are not suffering oxidative stress.

Energy dissipating mechanisms effectively suppress ROS generation during episodes of over-saturating illumination and carbon limitation. Those include non-photochemical quenching (NPQ) of excitation energy at PS II by the orange carotenoid protein (OCP) sitting at the core of phycobilisomes (Bailey and Grossman, 2008). Excess energy dissipates as heat. Recently, the essential role of flavodiiron proteins in adjustment of the energy flow through the photosystems was described (Helman et al., 2003). The Flv2/Flv4 heterodimer located at the PS II acceptor side serves as photochemical protection mechanism. It allows the control of the PQ-pool redox state and prevents the formation of excess $^1O_2$ (Bersanini et al., 2014). Additionally, Flv1 and Flv3 proteins sitting at the acceptor side of PS I serve as efficient electron sink, when the amount of the available oxidized ferredoxin is limiting. The electrons are directly transferred to oxygen to form water, and the formation of $O_2^{\bullet -}$ by the Mehler reaction is effectively circumvented (Allahverdiyeva et al., 2013).

1.4 Carbon concentrating mechanism (CCM)

Planktonic cyanobacteria require the CCM for optimal growth under atmospheric CO_2 concentrations and bicarbonate utilization from the surrounding medium. It serves the purpose to deliver sufficient CO_2 for primary carbon fixation by the enzyme ribulose-1,5-bisphosphate carboxylase/ oxygenase (RubisCO) and to suppress the loss of carbon

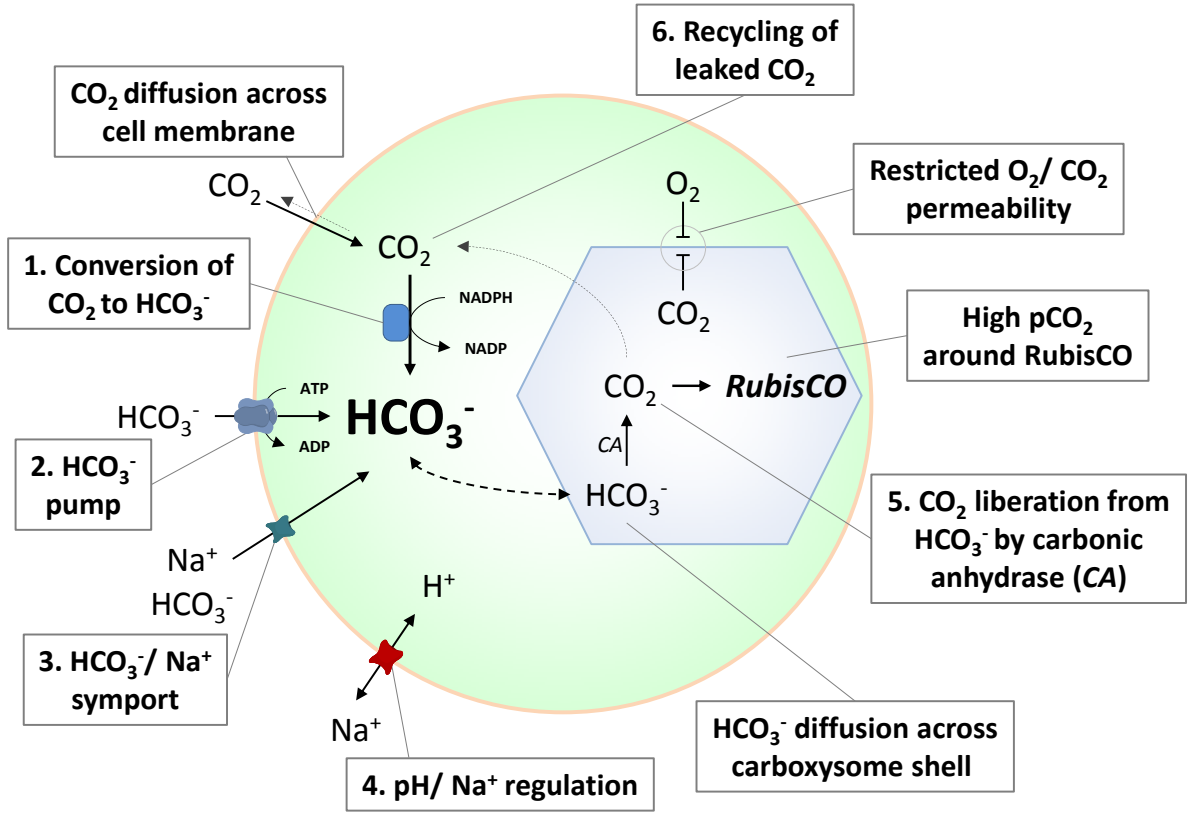

Figure 1.2: Schematic illustration of the β-cyanobacterial carbon concentrating mechanism, broadly adapted from (Price et al., 2008; Price, 2011): The conversion of CO_2 to bicarbonate inside the cell requires energy in the form of NADPH (1). HCO_3^- is actively taken up by ATP-fueled pumps (2), or by Na^+/ HCO_3^- symport (3). PH homeostasis and sodium ion extrusion is realized by Na^+/ H^+ antiport (4). HCO_3^- enters the caboxysome passively, where it is converted to CO_2 by carbonic anhydrase (5). Liberated CO_2 is mostly trapped inside carboxysomes. High CO_2/ O_2 ratios inside carboxysomes favor RubisCO carboxylase activity. CO_2 leaking from carboxysomes is recycled by the CCM (6).

due to photorespiration. Accordingly, the CCM is fully active under carbon limitation, whereas it is broadly suppressed to a basal level at high CO_2 availability (Price et al., 2008). Figure 1.2 summarizes the components of the cyanobacterial carbon concentrating mechanism according to (Price et al., 2008; Sandrini et al., 2014). CO_2 either passively entering the cell or produced by cellular respiration is converted to bicarbonate (HCO_3^-) in the cytoplasm by modified plastoquinone oxidoreductase NADPH dehydro-

genase (NDH-1) complexes. In contrast to CO_2, the charged HCO_3^- molecule hardly diffuses across the cell membrane. Inorganic carbon (C_i) is actively taken up by ATP-fueled, high-affinity bicarbonate transporter BCT1, and by Na^+/ HCO_3^- symporters like BicA and SbtA[1] along a sodium-ion electrochemical gradient. Conversion of imported HCO_3^- to CO_2 requires equal amounts of protons, i.e. pH balancing by Na^+/ H^+ antiport (probably by NhaS3). Bicarbonate accumulates in the cytoplasm up to 1.000 times the ambient concentration (Price, 2011).

Carbon fixation by RubisCO takes place inside carboxysomes. Carboxysomes are compartments of capsid-like shape with a proteinaceous shell. In contrast to lipid bilayers, small charged molecules like bicarbonate can passively diffuse through the shell, whereas CO_2 is effectively retained inside. CO_2 liberates from bicarbonate by the action of carbonic anhydrase inside carboxysomes, where it is utilized by RubisCO. CO_2 leaking from carboxysomes or produced by respiration is broadly recycled by the CCM. Oxygen is probably also excluded from the compartment, further suppressing the oxygenase activity of RubisCO (Marcus et al., 1992; Kinney et al., 2011).

1.5 *Microcystis aeruginosa*

The model organism studied in this work was *Microcystis aeruginosa* strain PCC 7806. *Microcystis aeruginosa* is a typical cyanobacterium frequently involved in fresh water blooms. The single spherical cells have a diameter of 2-7 μm and replicate by binary fission. Colonies form from daughter cells, which remain embedded in a common clear mucilage of homogeneous structure. It mostly consists of acetic polysaccharides (Nakagawa et al., 1987) and serves as a matrix to build up colonies of up to 8 mm in size (Komarek and Anagnostidis, 1998). The colonies are of net-like to lobate shape with irregular outlines. *Microcystis* colonies are morphologically diverse and a relation between particular morphotypes and the occurrence of toxic metabolites was reported (Via-Ordorika et al., 2004; Le Ai Nguyen et al., 2012). However, phylogenetic analy-

[1] SbtA is not present in every *Microcystis* strain, e.g. PCC 7806 (Sandrini et al., 2014)

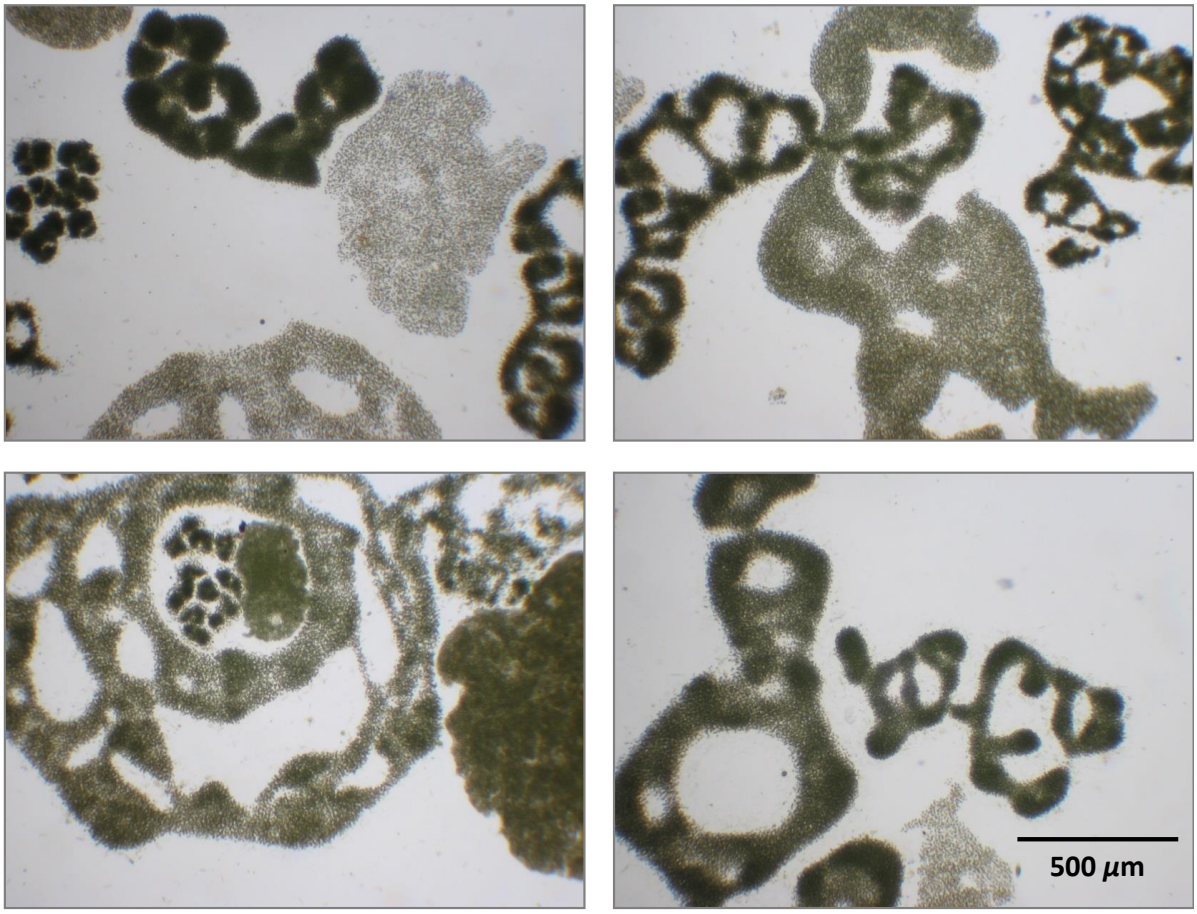

Figure 1.3: Diverse morphology of *Microcystis* colonies in a sample from Lake Wannsee in August, 2013.

sis does not support a clear distinction between different species (Otsuka et al., 2001; Le Ai Nguyen et al., 2012). Moreover, the genomes of *Microcystis aeruginosa* strains are characterized by a common core genome and individual subsets of flexible genes, which indicate a high genetic diversity (Humbert et al., 2013).

1.6 Toxin production by cyanobacteria

Cyanobacterial mass developments have a negative impact on the aesthetic value of most ecosystems. However, many bloom-forming cyanobacteria of fresh- and brackish waters can produce a variety of substances toxic to humans, livestock and wild animals

(Jochimsen et al., 1998; Stewart et al., 2008). The occurrence of toxic cyanobacteria becomes particularly problematic, when reservoirs for drinking water are affected. Table 1.2 lists the most common cyanotoxins found in fresh and brackish water environments and the producers. An early report on fatal intoxication of cattle by cyanotoxins dates back to the 19-th century (Francis, 1878). Especially microcystins are highly problematic cyanotoxins because of their frequent occurrence and high toxicity. Symptoms of oral microcystin consumption include diarrhoea, vomiting and general weakness (DeVries et al., 1993; Briand et al., 2003). Continuous exposition to microcystins could also cause tumor promotion in the liver (Sivonen and Jones, 1999).

Table 1.2: Cyanobacterial toxins and the producing genera involved in harmful fresh- and brackish water algal blooms; Toxicity as lethal dose for 50 % of treated specimens (LD_{50}) in [μg/ kg] when intra-peritoneally admistered to mice; adapted from (Sivonen and Jones, 1999; Paerl and Otten, 2013).

Compound	**Toxicity, LD_{50}**	**Producing genera**
Cyclic peptides		
Microcystin	Liver, 50-300	*Microcystis, Anabaena, Planktothrix, Anabaenopsis, Aphanizomenon, Cylindrospermopsis, Nostoc*
Nodularin	Liver, 50-150	*Nodularia*
Alkaloids		
Anatoxin-a	Nerve synapse, 200	*Anabaena, Aphanizomenon, Cylindrospermopsis, Oscillatoria, Planktothrix, Raphidiopsis, Woronichinia*
Anatoxin-a(S)	Nerve synapse, 20	*Anabaena*
Saxitoxin	Nerve axons, 3-10	*Anabaena, Aphanizomenon, Cylindrospermopsis, Oscillatoria, Planktothrix*
Cylindrospermopsin	Liver, 200	*Anabaena, Aphanizomenon, Cylindrospermopsis, Oscillatoria, Raphidiopsis*

1.7 Microcystin and its synthesis

Microcystins are cyclic heptapeptides. All microcystins share a common basic structure, see figure 1.4. Positions X and Z are variable L-amino acids and modifications might occur on every amino acid residue. A general feature of all microcystins (and nodularin) is the existence of Adda (3-amino-9-methoxy-2,6,8-trimethyl-10-phenyl-4,6-decadienoic acid).

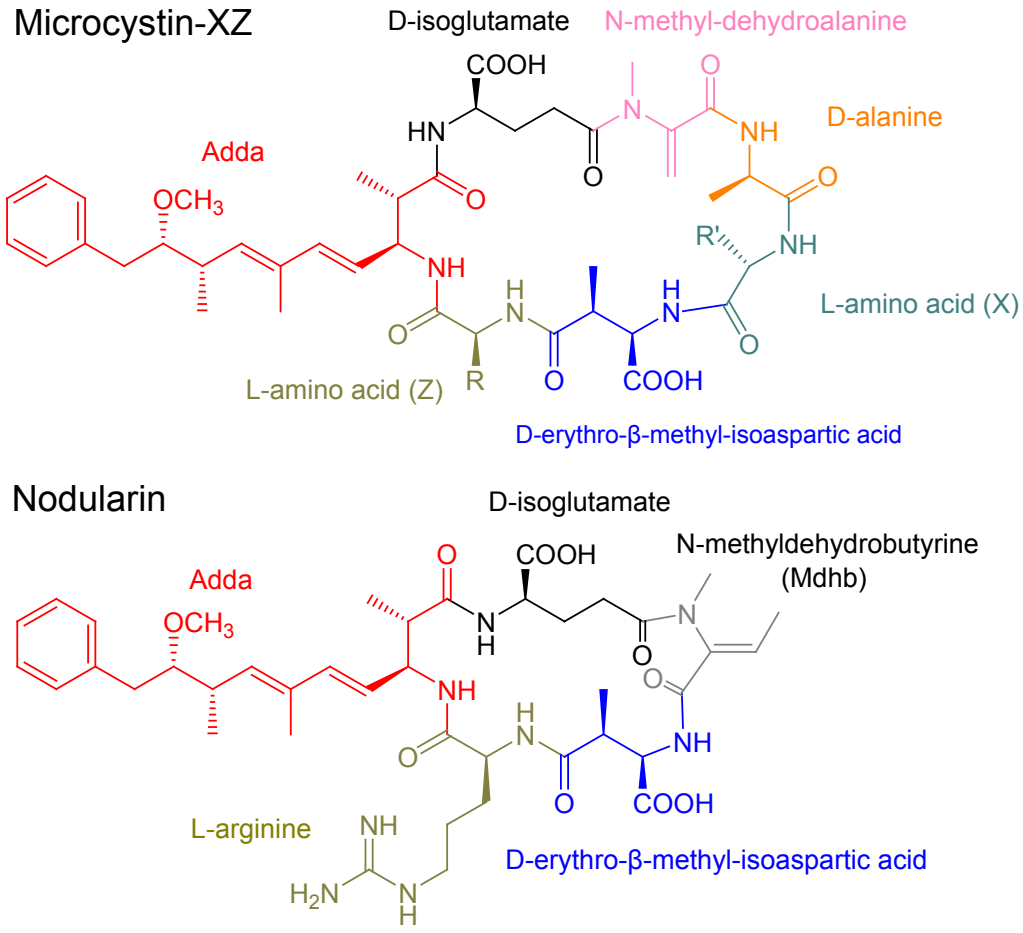

Figure 1.4: Chemical structures of microcystin and nodularin.

A 55 kB gene cluster encodes the machinery required for microcystin biosynthesis (Tillett et al., 2000). It consists of a large multi-enzyme complex including non-ribosomal peptide synthetases (NRPS) for incorporation of non-proteinogenic amino acids, polyketide synthases (PKS), as well as additional modifying enzymes are involved in microcystin synthesis, see figure 1.5. The PKS domains of McyG, D and E synthesize Adda. The PKS modules catalyze the sequential condensation of activated carbonic acids. Modification by the *O*-methyltransferase activity of McyJ and the aminotransferase of McyE completes Adda formation. The other six amino acids are subsequently recognized, activated and incorporated into the peptide chain by the modular NRPS sequence of McyG, A, B, and C. McyI and F are required for D-erythro-ß-methyl-aspartic acid formation prior to its incorporation (Dittmann et al., 2013). The thioesterase domain of McyC finally releases the complete heptapeptide.

Nodularins are cyclic pentapeptides produced solely by *Nodularia* species. Their assembly is functionally similar to that of microcystins, except the deletion of two NRPS modules and the activation and incorporation of L-Tyrosine instead of L-Serine, yielding N-methyl-dehydrobutyrate (Mdhb) instead of N-methyl-dehydroalanine (Mdha) (Dittmann et al., 2013).

Many strains of potentially toxic genera had lost the ability to produce microcystins as consequence of point mutations or gene deletion events by insertions of transposable elements into the mcy-gene cluster (Rantala et al., 2004; Christiansen et al., 2006, 2008; Fewer et al., 2011). The co-occurrence of toxic and non-toxic strains raises the question, whether the ability to produce microcystin has an impact on the competitiveness of a strain under certain environmental conditions.

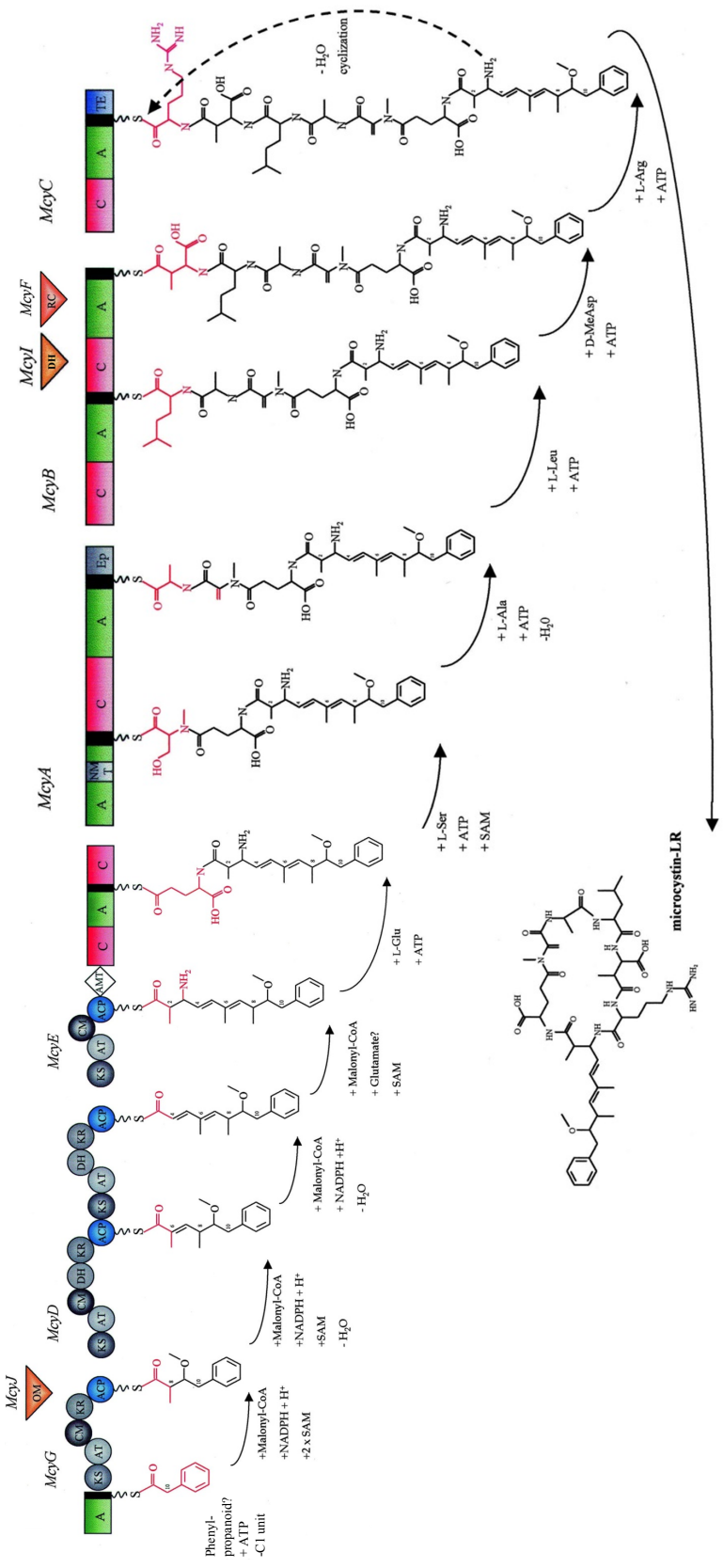

Figure 1.5: Microcystin assembly line: circles, PKS domains; rectangles, NRPS domains; black bars, NRPS thiolation motifs/peptidyl carrier protein; KS, ketoacylsynthase; AT, acyltransferase; CM, C-methyltransferase; KR, ketoacyl reductase; DH, dehydratase; ACP, acyl carrier protein; AMT, aminotransferase; C, condensation domain; A, aminoacyl adenylation domain; NMT, N-methyltransferase; OM, *O*-methyltransferase; Ep, epimerase; DH, dehydrogenase; RC, racemase; TE, thioesterase (Tillett et al., 2000; Dittmann et al., 2013).

1.8 Toxicity mechanism of microcystin-LR

Microcystin-LR is a frequently occurring and highly toxic microcystin variant (Sivonen and Jones, 1999). The hepatotoxicity of microcystin is owed to the fact that it is selectively imported into liver cells by the multi-specific bile acid transport system (Eriksson et al., 1990a). Its toxicity is based on the ability to inhibit eukaryotic protein phosphatases PP1 and PP2A (Runnegar et al., 1995). The Adda (3-amino-9-methoxy-2,6,8-trimethyl-10-phenyl-4,6-decadienoic acid) moiety of microcystin interacts hydrophobically with the active site of the enzymes. In a second step, microcystin binds covalently *via* the electrophilic alpha-beta unsaturated carbonyl of its methyldehydroalanine residue to specific cysteines of the protein phosphatases. Enzyme inhibition leads to hyper-phosphorylation of proteins (Eriksson et al., 1990b), resulting in disorganization of the cytoskeleton microfilaments (Toivola et al., 1994) with necrosis and dissociation of hepatocytes (DeVries et al., 1993; Briand et al., 2003).

1.9 Eco-physiological aspects of microcystin production

Still, the role of microcystin production by cyanobacteria is under debate. Microcystin can account for more than one percent of the dry weight in cyanobacteria samples (Sivonen and Jones, 1999) ; thus, a certain eco-physiological relevance might be anticipated. Since microcystin is a potent inhibitor of eukaryote protein phosphatases, it appears plausible that it primarily serves as a deterrent against grazing zooplankton. However, the microcystin biosynthesis genes are reported to be relatively ancient and that they even pre-date the entire eukaryotic lineage (Rantala et al., 2004). Additionally, grazing on *Microcystis* cells by zooplankton is inhibited regardless of microcystin being present or not (Rohrlack et al., 1999, 2001; Kaebernick et al., 2001). Cyanobacteria in general are of rather poor nutritious value, when compared to e.g. dinoflagellates or diatoms (Muller-Navarra et al., 2004) and are hard to ingest and digest due to mucilaginous envelopments and thick cell walls respectively (Rohrlack et al., 2001). Thus, substantial

decimation of cyanobacteria by filter-feeding zooplankton might not be expected, irrespectively of microcystin production. The assumption that microcystin could primarily function as extracellular allelochemical against eukaryotic algae and macrophytes might also be negated, considering the ancient origin of microcystin synthesis genes.

The currently proposed functions of microcystin production, as well as the environmental factors, which might influence microcystin synthesis, were reviewed recently (Neilan et al., 2013), see figure 1.6. In summary, several studies report effects of culture parameters like phosphorus, nitrogen, trace elements, light, temperature and pH on microcystin production. However, the impact of the changed culture parameters on microcystin synthesis could not be clearly separated from the effects of the parameters on general cell proliferation.

The presence of microcystin outside the cells lead to the assumption that it could serve as info chemical or signal peptide (Schatz et al., 2007). Although McyH shares some homology with ABC-transporters, an active export *via* this route was not demonstrated. However, the addition of external microcystin to *Microcystis* cultures stimulates its production by the cells (Schatz et al., 2007).

The transcription of mcy-genes is initiated at a bidirectional promoter between mcyA and mcyD genes in *Microcystis*. Sequence motifs for the DNA binding proteins Fur (ferric uptake regulator) and NtcA (global nitrogen transcription factor) are located in proximity to the promoter (Ginn et al., 2010). The involvement of NtcA is in particular interesting since it potentially links microcystin synthesis directly with components of energy and carbon metabolism (Alfonso et al., 2001; Vazquez-Bermudez et al., 2002; Tanigawa et al., 2002; Su et al., 2005). Furthermore, the proposed co-induction of microcystin synthesis with iron uptake mechanisms might also point towards a close connection with photosynthesis since flavodiiron proteins are needed for tuning the energy flow through the photosynthetic apparatus (Bersanini et al., 2014; Allahverdiyeva et al., 2013). ROS scavenging enzymes like SOD and catalase also require iron, see 1.1. Analysis of mcy-gene expression was performed to figure out, which specific environmen-

tal stimuli influence the regulation of microcystin synthesis. Accordingly, altered light regimes and iron starvation indeed seem to have an impact on microcystin production (Kaebernick et al., 2000; Sevilla et al., 2008).
Competition experiments with toxic and non-toxic strains furthermore demonstrate that microcystin synthesis becomes advantageous under high light conditions, carbon limitation and elevated temperatures (Jähnichen et al., 2007; Van de Waal et al., 2011; Dziallas and Grossart, 2011).
Proteomic studies comparing the steady-state abundance of proteins in toxic and non-toxic phenotypes came to the conclusion that microcystin production affects the accumulation patterns of enzymes involved in carbon, nitrogen and energy metabolism, as well as in redox control (Zilliges et al., 2011; Alexova et al., 2011; Tonietto et al., 2012). The extracellular glycoprotein MrpC also accumulates differently in microcystin deficient cultures, which might imply a role of microcystin in regulation of colony formation.

The above mentioned studies describe the effects of environmental factors on microcystin production and the differences between toxic and non-toxic strains, without giving any mechanistic explanation for the molecule's exact mode of action. However, electron microscopy of immuno-gold labelled *Microcystis* cells indicate microcystin accumulation around e.g. thylakoids (Young et al., 2005; Gerbersdorf, 2006). This finding already points towards a direct interaction of microcystin with specific components of the cell.

1.10 Microcystin interaction with proteins

Recently, the direct interaction of microcystin with cellular proteins was described (Zilliges, 2007; Zilliges et al., 2011; Ahlert, 2013). The binding partners comprise enzymes involved in carbon and energy metabolism, see figure 1.3. The microcystin-protein interaction was more pronounced under high light conditions and iron limitation, as well as after the addition of hydrogen peroxide (Kehr, 2009; Zilliges et al., 2011). In an attempt to characterize the effect of microcystin binding to proteins, it was shown that the stability of the microcystinylated large RubisCO subunit against proteolysis is higher *in vitro* (Zilliges et al., 2011). A similar effect was recorded for *in vitro* microcystinylated, recombinant phosphoribulokinase (PRK) and the associated CP12 linker protein (Ahlert, 2013).

Table 1.3: Microcystin binding partners that have been identified so far in protein extracts of *Microcystis aeruginosa* PCC 7806 wild-type by Western blot analysis (Zilliges et al., 2011; Ahlert, 2013). n.q., not quantified; n.t., not tested

Protein identity	**Category**	**Differential in WT & Δ*mcyB***	**Microcystin binding *in vitro***
Small subunit of RubisCO	Photosynthesis	Yes	n.t.
Large subunit of RubisCO	Photosynthesis	Yes	Yes
Phosphoribulokinase	Photosynthesis	Yes	Yes
CP12	Photosynthesis	Yes	Yes
Phycocyanin alpha subunit	Photosynthesis	Yes	n.t.
Phycocyanin beta subunit	Photosynthesis	n.q.	n.t.
Allophycocyanin alpha subunit	Photosynthesis	n.q.	n.t.
Glutathione reductase	Biosynthesis	Yes	n.t.

The currently proposed model of microcystin involvement in cellular processes is summarized in figure 1.6.

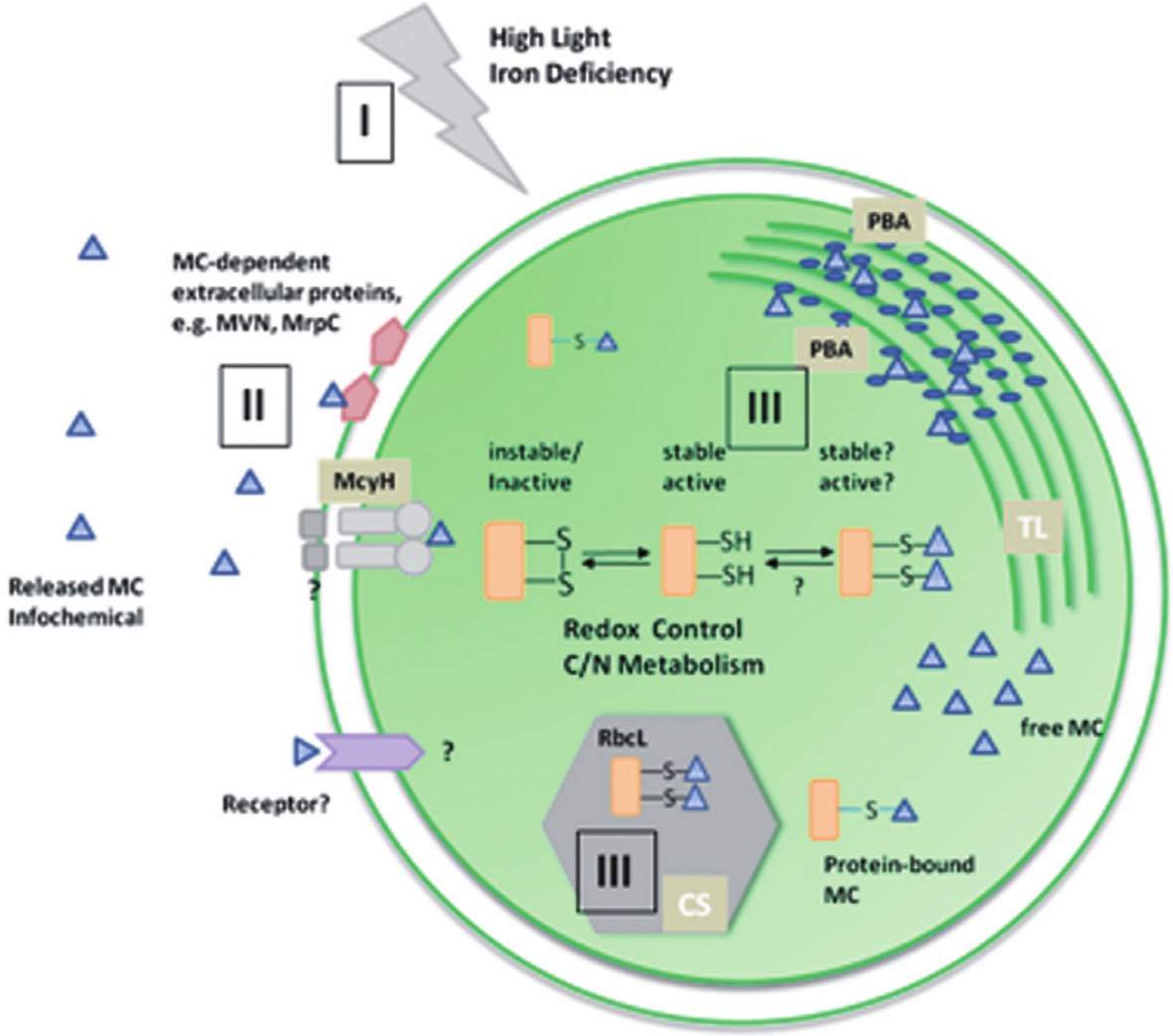

Figure 1.6: Scheme of proposed microcystin functions in *Microcystis aeruginosa*: I) High light and iron limitation stimulate microcystin biosynthesis. II) Some of the microcystin could be exported *via* the ABC transporter McyH. External microcystin, either exported or present due to cell lysis, could act as signal peptide for induction of its own biosynthesis and regulation of extracellular proteins like the glycoprotein MrpC and the lectin MVN, to which it could also bind. III) Parts of intracellular microcystin interact with proteins including phycobilisome antennae proteins (PBA) and the large subunit of Rubisco (RbcL). High light and oxidative stress favour covalent binding to cysteine residues. This binding affects protein stability and could participate in redox regulation of enzyme activity primarily involved in C/N metabolism and redox control. TL, thylakoids; CS, carboxysomes. Figure adopted from (Neilan et al., 2013).

1.11 Aim of the study

According to the currently proposed physiological functions of microcystin, this study aims at further elucidating the involvement of microcystin production in cellular processes of *Microcystis aeruginosa*. Especially its proposed role under putatively stress inducing conditions is addressed. In the first part of this work, the focus is put on high light induced dynamics of microcystin abundances in *Microcystis* cells. The characterization of microcystin-protein interactions is of particular interest.

The second part deals with the impact of high light on cyanobacterial primary metabolism comparing the *Microcystis aeruginosa* 7806 wild-type strain with its microcystin deficient $\Delta mcyB$ mutant and the established model cyanobacterium *Synechocystis* PCC 6803. The consequences of microcystin production on the accumulation of primary metabolites in *Microcystis*, as well as strain-specific differences are of particular interest.

2

On the Significance of Microcystin Conjugate Formation

Most of this chapter's data had recently been published under the title:

"Microcystin production revisited: conjugate formation makes a major contribution"

Sven Meissner[1], Jutta Fastner[2] and Elke Dittmann[1]

[1]Department of Microbiology, Institute of Biochemistry and Biology, University of Potsdam, Golm, Germany.

[2]Federal Environment Agency, Section Drinking Water Treatment and Resource Protection, Berlin, Germany.

Environmental Microbiology, 15(6):1810–1820, 2013

2.1 Abstract

Factors affecting the induction of microcystin production are not well understood. High light stimulates the synthesis of mcy-genes and biosynthetic proteins, whereas its effect on the actual cellular microcystin content appears variable. The recent discovery of microcystin- protein conjugate formation *in vivo* opens a new perspective on the dynamics of microcystin production and its primary role in the producing organisms. This study focused on determining the total amounts of cellular microcystin including the non-extractable, i.e. protein bound fraction. A significant part of the total microcystin appeared to be bound to the otherwise inaccessible protein fraction of *Microcystis* and *Planktothrix* strains. High light triggered a very articulated increase of microcystin content in the protein fraction, but, not in extracts analyzed by LC-MS and ELISA. The formation of conjugates contributed to a significant increase of the total microcystin content under high light conditions. Analysis of five different field samples revealed that neglecting the protein fraction leads to underestimation of total microcystin loads. Fi-

nally, the application of immuno-fluorescence microscopy furthermore allowed the identification of toxic colonies in field samples and indicated different grades of microcystin conjugate formation. The effects of protein microcystinylation, as well as its selectivity towards specific residues, are discussed in detail.

2.2 Introduction

In recent decades, the frequency and magnitude of cyanobacterial mass developments have increased in many parts of the world. Toxin production by cyanobacteria like *Microcystis* fuels the concerns of health- and water authorities. Characterization of the factors that affect microcystin production and figuring out its primary biological role might contribute to the establishment of more effective bloom management strategies.
To find out more about the kinetics of microcystin production and the physiological role it might play for the producing organisms, it is essential to reliably determine the total microcystin amounts present in the cells. Current microcystin quantification techniques comprise liquid chromatography coupled with diode array detectors (LC-DAD), or more sensitive mass spectrometers (LC-MS) (Sivonen and Jones, 1999). *In vitro* inhibition assays with eukaryotic protein phosphatases are used to quantify microcystins according to their toxic potential (Carmichael and An, 1999; Metcalf et al., 2001). Enzyme-linked immunosorbent assays (ELISA), employing highly specific α-microcystin antibodies are commercially available. Another technique invilves oxidative cleavage of the microcystin Adda-moiety to 2-methyl-3-methoxy-4-phenylbutyric acid (MMPB) and its detection by LC-MS or gas chromatography (GC) (Kaya and Sano, 1999). However, the protocols of all the above-mentioned techniques include the microcystin extraction and extensive sample preparation prior to quantification. Consequently, only the free and extractable microcystin fraction is considered for analysis and quantification.
A recent study reports that microcystin binds to proteins of *Microcystis aeruginosa* PCC 7806 *in vivo* and that high light conditions stimulate this effect (Zilliges et al., 2011). Aim of this study thus was to quantitatively assess the impact of changed light

conditions on microcystin-protein interaction and to estimate its significance with regard to the total cellular microcystin pool. To realize this, two immuno-blotting techniques were combined with an established LC-MS method and a commercially available ELISA-kit for microcystin quantification. Low light-adapted cultures of *Microcystis aeruginosa* PCC 7806 and *Microcystis aeruginosa* Nies 843 were exposed to high light, and the microcystin contents were determined in methanol extracts and the methanol-insoluble protein fractions respectively.

Additionally, the phenomenon of microcystin binding to proteins of *Microcystis* was demonstrated to occur also in the natural habitats by analyzing field samples from five different lakes. Finally, immuno-fluorescence microscopy of freshly collected *Microcystis* colonies was employed to differentiate between toxic and non-toxic ecotypes.

2.3 Methods

2.3.1 Cultivation of cyanobacteria

The cyanobacterial strains used in this study were cultured semi-continuously in 1 L Erlenmeyer flasks at 23° C under constant fluorescent light (Philips Master TL-D 58W/ 865) at a photon flux rate of 8 μmol photons $\cdot$ $m^{-2}\cdot$ s^{-1}. Cell cultures were maintained at optical densities (OD_{750}) between 0.3 and 1.0 by regular dilution with fresh BG-11 medium (Rippka et al., 1979). Three independent biological replicates of the strain *Microcystis aeruginosa* PCC 7806 were included in this study. The microcystin deficient PCC 7806 Δ*mcyB* mutant strain (Dittmann et al., 1997) served as control. To draw a more general picture, the microcystin producing cyanobacterial strains *Microcystis aeruginosa* Nies 843 and *Planktothrix agardhii* NIVA-CYA 126 were included in this study as well.

2.3.2 High light experiment

For the highlight experiment, 200 mL cyanobacterial cultures were grown to OD_{750} of 0.8-0.9 and exposed to elevated photon flux rates of 250 μmol photons $\cdot$ $m^{-2}\cdot$ s^{-1}. Samples were taken from low light adapted cultures before the onset of highlight exposition (0 h) and after three hours of highlight (3 h). During the highlight experiment, the temperature was monitored, and the pH of the culture medium was recorded (see table 2.1).

Cells from 50 mL culture samples were collected by centrifugation at 6.000 $\times$ g and RT for five minutes and washed once with water. The washed sample pellets of about 0.5 mL were inactivated by immediately suspending the cells in 1.5 mL methanol and stored at -20° C until further processing.

Table 2.1: Specifications of the high light experiment samples

Strain	**OD_{750}**	**pH 0 h**	**pH 3 h HL**	**ΔpH 0 - 3 h HL**
WT A	0.849	9.47	11.2	1.73
WT B	0.974	9.78	11.09	1.31
WT C	0.876	9.96	11.04	1.08
$\Delta mcyB$	0.698	9.63	10.99	1.36
Nies 843	0.79	9.74	11.03	1.29

2.3.3 Field samples

The field samples were selected from an archive of the Federal Environmental Agency of Germany (Umweltbundesamt, UBA). The samples were taken with a plankton net from five different lakes with cyanobacteria-dominated phytoplankton, see table 2.2. Concentrated samples were lyophilized and stored at -20° C until analysis. For immunofluorescence microscopy (IFM), freshly collected samples from lake Zernsee were used (see 2.3.11).

Table 2.2: Field samples A-E, origin and specifications

Sample	Sampling site	Date	Sample composition
A	Bautzen Reservoir	23.10.1995	*Microcystis sp.*
B	Wannsee	23.08.1995	*Microcystis sp.*
C	Müggelsee	29.07.1996	*Microcystis sp.; Anabaena sp.*
D	Postweiher	22.08.1995	*Microcystis sp.*
E	Schwielowsee	01.07.1996	***Microcystis sp.***; *Anabaena sp.*

2.3.4 Microcystin extraction

All cyanobacterial samples were extracted with 75 % methanol as described by Fastner (Fastner et al., 1998). Briefly, the suspended samples were mechanically treated with an ultrasonic probe (Sonopuls UW 3100 MS72, Bandelin, Germany) for one minute, followed by vigorous shaking for 30 minutes on an orbital shaker. The insoluble material was sedimented by centrifugation at 15.000×g for 5 minutes. The procedure was repeated three times. Cleared extracts from each extraction cycle were pooled and kept at -20° C until analysis. The remaining insoluble fractions were suspended in equal volumes of 100 % methanol and stored at -20° C. Nodularin from samples of *Nodularia spumigena* CCY 9414 (kindly provided by Martin Hagemann) was extracted accordingly after the cells had been harvested by vacuum filtration and inactivated in methanol.

2.3.5 Microcystin quantification by LC-MS

Extracted microcystin was quantified by LC-MS analog to (Spoof et al., 2003), employing an API 5500 QTrap mass spectrometer (AB Sciex, USA) equipped with a turbo-ion spray interface, which was connected to an Agilent 2900 series HPLC system (Agilent Technologies, Waldbronn, Germany). Microcystins were separated at 30° C on a Purospher STAR RP-18 end-capped column with dimensions of 30 × 4 mm, packed with 3 μm particles (Merck, Germany). The mobile phase was composed of A: 0.5 % formic acid and B: 0.5 % formic acid in acetonitrile. A mobile phase gradient was run with

25 % B at 0 minutes, to 70 % B at 10 + 1 minutes. 10 μL of appropriately diluted sample was injected. For the identification and quantification of different microcystin congeners (MCs), standards of [Asp3]-MC-RR; MC-RR; MC-YR; [Asp3]-MC-LR; MC-LR; MC-LW; MC-LF; MC-LA were utilized (Enzo Life Sciences, Germany).

2.3.6 ELISA

The commercial Adda-specific microcystin quantification ELISA was performed according to the manufacturers' protocol (Abraxis LLC, Warminster, PA, USA). Dried cyanobacterial extracts were first dissolved in 100 % methanol and diluted individually with water to concentrations within the recommended range of the assay. The effective methanol concentration of the analyzed samples was $\ll$ 1 %. Photometric data acquisition was acquired with a Varioskan® Flash (Thermo Fisher Scientific Inc. Waltham, MA, USA) plate reader.

2.3.7 Sample preparation for total microcystin quantification

Equal amounts of the pooled extract fraction and the corresponding suspension of insoluble matter were in parallel transferred to fresh tubes each. The extracts were dried in a centrifugal vacuum concentrator and dissolved completely in SDS-PAGE loading buffer (0.5 % SDS; Tris-HCl pH 8.2; 10 % glycerol; 20 mM DTT) by vigorous mixing at RT. Duplicates of a defined microcystin standards were treated equally throughout. The corresponding insoluble material was sedimented by centrifugation, and the methanol was aspirated carefully. Equal volumes of SDS-PAGE loading buffer were added to the air dried pellets. The protein was solubilized by thorough ultrasonication without cooling for three cycles of 30 seconds. All samples were denatured at 85° C for 5 minutes and alkylated with 30 mM iodoacetamide for 10 minutes at RT. Unreacted iodoacetamide was quenched by addition of another 30 mM DTT, and the samples were centrifuged at 13.000×g and RT for 10 minutes.

2.3.8 SDS-PAGE and Western blot analysis

Samples were loaded on 12.5 % poly-acrylamide gels. The Laemmli buffer system was employed for electrophoresis, and the runs were stopped before the migration front escaped the gels. Separated proteins and peptides were transferred from the gels onto Amersham® Hybond-C Extra nitrocellulose membrane (GE Healthcare, USA) using a wet blot electrophoresis apparatus (Protean mini; BioRad, USA) with constantly low currents of 9 mA (∼7 V) overnight. To further support the quantitative binding of proteins and peptides to the membrane and to prevent "blow through", the transfer buffer contained 20 % methanol (Towbin et al., 1979). After electrophoretic transfer, the membranes were rinsed with water and dried completely. Blocking of the membranes was done with 1 % PVP-40 (Polyvinylpyrrolidone, average molecular weight 40 kDa) dissolved in phosphate buffered saline pH=8 and 0.3 % Tween® 20 (PBS-T). The membranes were washed twice with PBS-T, and the primary antibody was applied at a concentration of 1:10.000. The antibodies were allowed to bind their antigen at 4° C for a minimum three hours. After three washing cycles of at least 10 minutes, the HRP-linked secondary antibodies were applied at the same dilution and incubated at 4° C for at least one hour. Thoroughly washed membranes were reacted with SuperSignal® West Pico substrate (Thermo Fisher Scientific Inc. Waltham, MA, USA) and the chemiluminescence signals were recorded with a ChemiDoc™XRS+ Imager (BioRad, USA). Quantification was carried out using the built in Image Lab™software (BioRad, USA).

2.3.9 Dot blot analysis

The samples for Dot blot were the same as used for Western analysis. Excess dodecyl sulfate was removed from the samples by addition of 50 mM dipotassium phosphate (K_2HPO_4) and incubated at 4° C for two hours (Suzuki and Terada, 1988). Insoluble potassium dodecyl sulfate was removed from the solutions by centrifugation at 10.000×g and RT for one minute.

The samples were appropriately diluted with water and transferred to 96 well plates

(black flat bottom, Greiner). 10 % methanol was added to the samples to support protein binding to nitrocellulose membranes. Immobilization of the sample on the membrane was carried out passively. To that end, pinches of nitrocellulose with a diameter of 6 mm were carefully placed in each well containing 100 μL of sample and equilibrated on an orbital shaker at RT for a minimum of 30 minutes. Subsequent treatment of the membrane pinches inside the wells was identical to that of Western blot analysis.

2.3.10 Data analysis and evaluation

For the estimation of the microcystin content in the samples analyzed by Dot blot, duplicates of a microcystin-LR standard dilution series were run parallel to establish a regression curve for the chemiluminescence signal intensity. In Western blot analysis, a dilution series of a microcystin-LR standard was included in each run. Only values within the linear signal intensity range of the regression curve were considered for microcystin quantification in the samples.

To test whether the high light treatment resulted in significant changes of the detected amounts of microcystin in Dot blot-, Western blot- and ELISA samples, a one-sided paired Student's T-test was performed. Null hypothesis, H0: difference of means before and after treatment (3 h – 0 h) = 0; alternative hypothesis H1: difference of means (3 h – 0 h) > 0; confidence interval = 95 %; n = 3. Normal distribution of differences between 0 h and 3 h was tested with the Shapiro-Wilk-test.

2.3.11 Immuno-fluorescence microscopy (IFM)

Freshly collected and concentrated field samples were spotted on sample slides and left to dry on air. Subsequent fixation of the immobilized cells was done with -20° C methanol for 20 minutes and acetone for 1 minute. The fixed samples were equilibrated in PBS (phosphate buffered saline, pH 8) for 5 minutes and further permeabilized enzymatically with freshly prepared lysozyme (2 mg/ mL) in PBS-TX (PBS + 0.3 % Triton® X-100) at RT for 5 minutes. The samples were washed thoroughly with PBS-TX and

subsequently blocked with 1 % PVP-40 in PBS-T (PBS + 0.3 % Tween® 20) at 4° C for at least one hour. Antibodies were applied to thoroughly washed samples in PBS-T at concentrations of 1:500 for anti-microcystin antibody and 1:200 for secondary FITC-labeled antibody at 4° C for a minimum of one hour each. Observation and image acquisition was done with an inverted digital fluorescence microscope (AMG EVOS fl, Peqlab, Erlangen, Germany).

2.3.12 RubisCO purification and analysis

Cells from 1 L culture were harvested by centrifugation at 6.000×g for 5 minutes after high light exposition for three hours. The cell pellet was washed once with water and snap frozen in liquid nitrogen. The samples were kept on ice throughout all following extraction steps. First, the cells were opened successively with mild sonication (Sonopuls UW 3100 MS72, Bandelin, Germany) in BEMP buffer (20 mM bicine, 1 mM EDTA, 20 mM $MgCl_2$, 20 mM $NaHCO_3^-$) + 1 mM freshly added DTT until the supernatant remained almost clear after centrifugation for 20 minutes at 20.000×g. The remaining pellet was further sonicated for another five minutes. The proteins of the resulting supernatant were precipitated with 60 % ammonium sulfate after salting out contaminants with 20 % ammonium sulfate. The protein was again dissolved in BEMP and purified by fast protein liquid chromatography (FPLC) using a Superose® 6 gelfiltration column with 125 mL bed volume (GE Healthcare, USA), connected to an ÄKTAprime plus™system (GE Healthcare, USA). Fractions containing RubisCO were concentrated with centrifugal filters (Amicon® Ultra-50K, Millipore, USA). Blue-native PAGE was performed exactly according to the protocol recommended in (Wittig et al., 2006). For Western Blot analysis of RubisCO, see 2.3.8.

2.4 Results

2.4.1 Microcystin quantification in methanol extracts

To characterize the impact of high light illumination on the actual cellular microcystin loads, two standard techniques for microcystin quantification in cyanobacterial extracts were performed in this study, see figure 2.1. The results of LC-MS did not indicate significant high light induced changes of microcystin concentration in PCC 7806. A change of the two microcystin congeners ratio MC-LR to (D-Asp3)-MC-LR was not observed as well.

The values of microcystin quantification obtained by the ELISA were about 60-70 % higher than those of LC-MS in samples of PCC 7806. A significant light dependent increase of 21.6 % was detected by the ELISA, probably indicating the presence of low molecular weight microcystin conjugates, which were not detected by LC-MS.

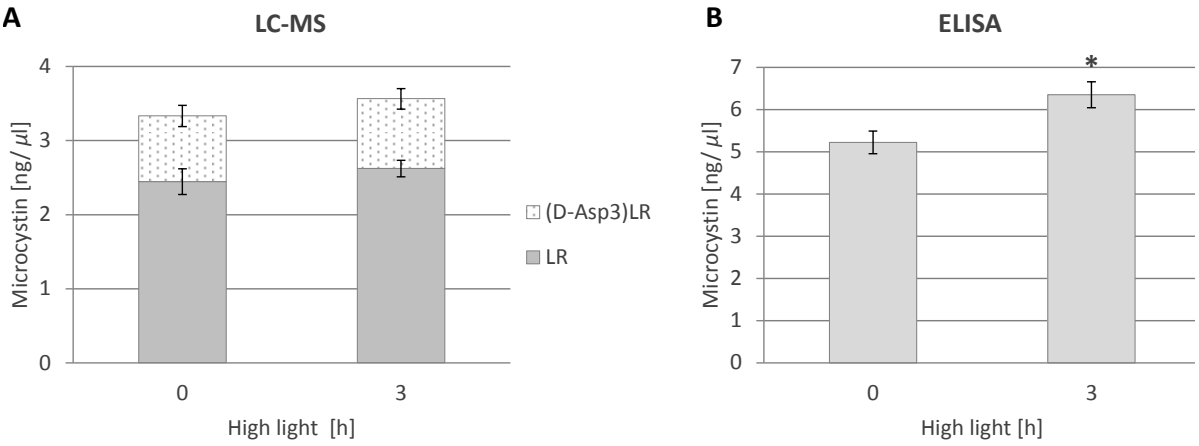

Figure 2.1: Microcystin concentration in methanol extracts of *Microcystis* PCC 7806 wild-type cells from low light adapted cultures before (0 h) and after high light exposition for three hours (3 h). Samples of three independent biological replicates were analyzed by **A:** LC-MS using quantitative standards, and **B:** ELISA commercial kit. Student's t-Test on significance resulted in $^*p = 0.0244$.

2.4.2 Immunological quantification of total cellular microcystin

Methanol extracts of cyanobacteria samples, commonly used for microcystin quantification, contain mainly low molecular weight substances like chlorophyll and small peptides, whereas the methanol-insoluble fractions consist of high molecular weight proteins after extraction. In order to assess the complete cellular microcystin, both fractions were included for membrane-based immunological quantification. To make use of the obtained fluorescence signals from Western- and Dot blot analysis as a quantitative proxy, a microcystin standard was run simultaneously. Figure 2.2 demonstrates the relation between microcystin concentration and the obtained chemiluminescence signal.

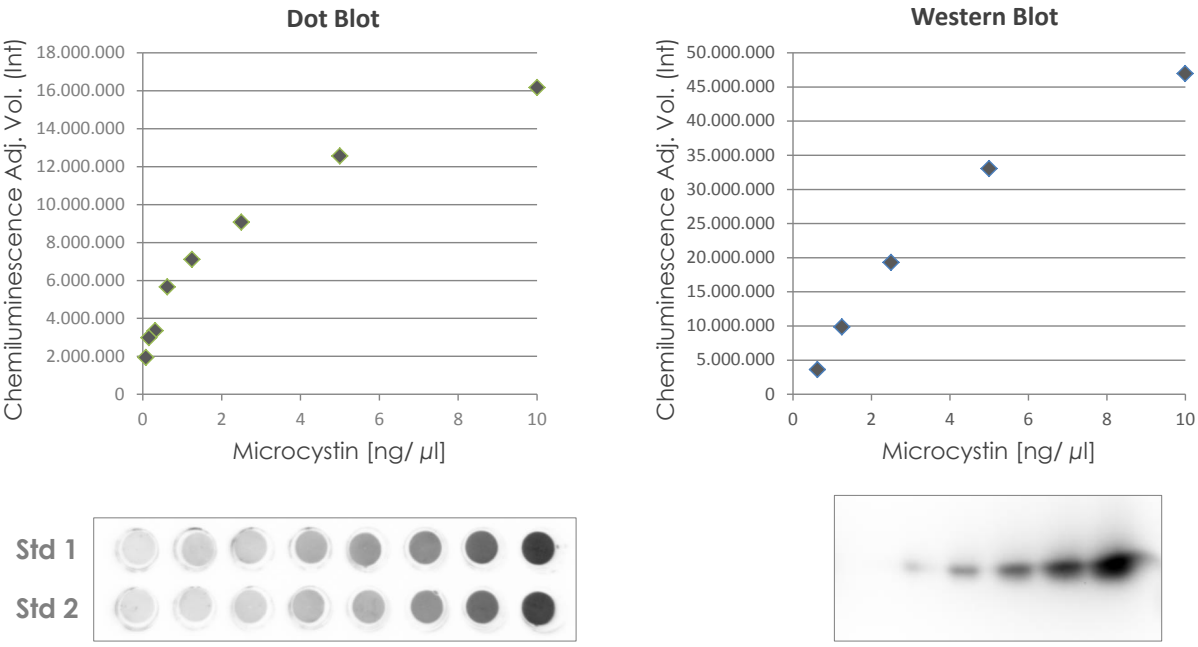

Figure 2.2: Microcystin standard dilution series used to quantify microcystin concentration in biological samples in Western- and Dot blot analysis.

Three independent biological replicates of *Microcystis* PCC 7806 wild were analyzed by membrane-based immunological methods. Figure 2.3 A+B show the results of Western blot analysis. In all three replicates, a high light induced increase of the microcystin-derived signal was detected in the protein fractions (∼55 % increase), whereas the signal

intensity remained constant in the extract fractions. The same samples were subjected to Dot blot analysis as visualized in figure 2.3 C+D. Again, the amount of detected microcystin in the extracts remained unchanged after high light exposition for three hours, whereas the increase of the protein-bound microcystin was even more pronounced (∼3.9-fold increase). No chemiluminescence signals were detected in the samples of the microcystin deficient Δ*mcyB* mutant. However, although the microcystin amounts in the methanol extracts, as determined by Dot blot and Western blot, correlated with those from ELISA and LC-MS, the results should be considered as semi-quantitative due to inherent methodological uncertainties regarding the immobilization of the sample to the membrane.

To draw a more general picture, samples of an identically high light-treated culture of the toxic strain *Microcystis aeruginosa* Nies 843 were processed and analyzed analog to those of the strain PCC 7806. Since no microcystin standards were included, only relative values were obtained for Western- and Dot blot analysis. Figure 2.4 summarizes the results. Analog to the data obtained for PCC 7806, the amount of microcystin in methanol extracts was almost unchanged. The results of LC-MS and the ELISA (A+B) even indicated a slight decrease of extractable microcystin. In marked contrast, the amount of protein-bound microcystin was strongly increased after high light treatment for three hours as became evident by Western blot and Dot blot analysis (2.4 C-F). Initially, 25 % of total cellular microcystin was detected in the methanol-insoluble fraction. After three hours, high light exposition that amount was increased ∼5-fold to then ∼60 % of total cellular microcystin. In total, the microcystin load approximately doubled during that time. Microcystin-protein interaction was more pronounced in Nies 843, which should be further examined in future experiments including more biological replicates.

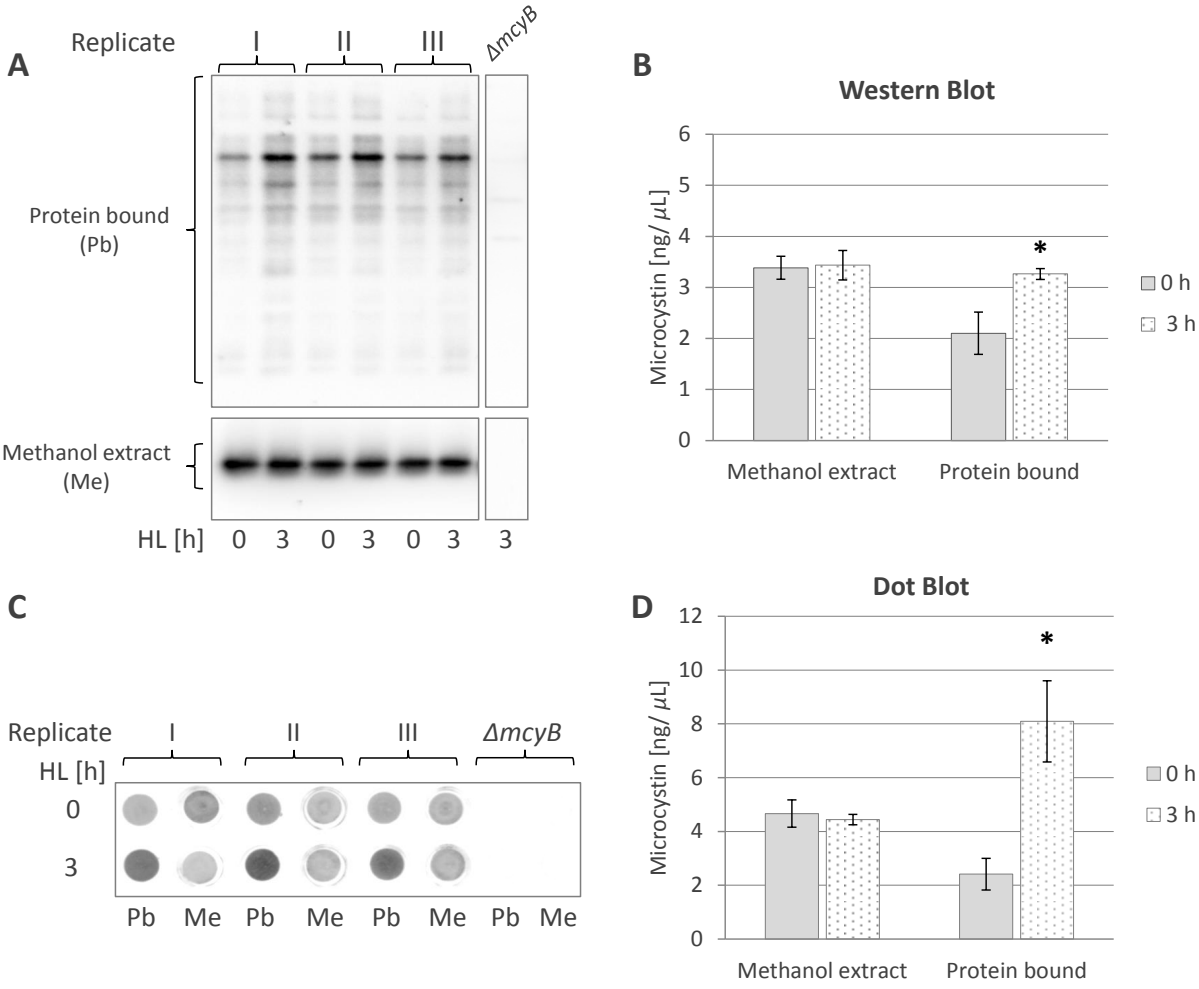

Figure 2.3: Total microcystin quantification by immunological techniques in cells of three independent *Microcystis* PCC 7806 wild-type cultures before (0 h) and after three hours high light exposition (3 h). Samples from a *Microcystis* PCC 7806 $\Delta mcyB$ mutant culture served as control. The determined microcystin quantities were in general agreement with those obtained by LC-MS, see figure 2.2. **A:** Western Blots of methanol insoluble proteins and the corresponding methanol extracts after SDS-PAGE; **C:** Dot Blots of the same samples. **B+D:** Visualization of microcystin quantification data after relation to external microcystin standards, see figure 2.2. $*p = 0.044$ (Western Blot); $*p = 0.0244$ (Dot Blot) according to Student's t-Test of significance.

2.4.3 RbcL is a major target of microcystin interaction

As already became visible in the Western Blots of figures 2.3 A and 2.4 C, the major microcystin signal in the methanol-insoluble fractions derived from protein bands

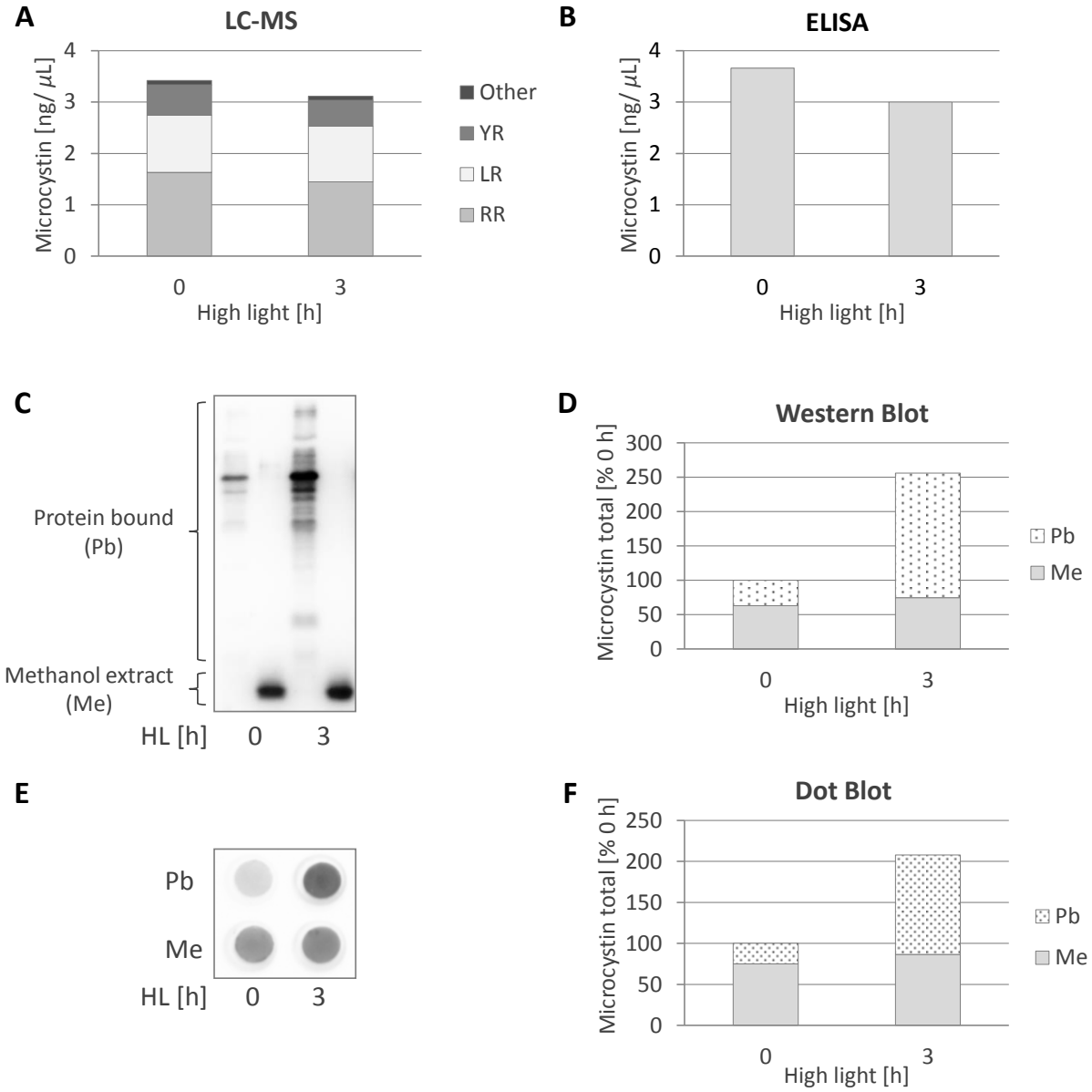

Figure 2.4: Microcystin quantification in samples of *Microcystis aeruginosa* Nies 843 analog to figures 2.1 and 2.3; **A+B:** Microcystin quantification in the methanol extract by LC-MS and ELISA; **C-F:** Immunological determination of the total cellular microcystin content by Western Blot and Dot Blot.

of approximately 50 kDa. Following an attempt to isolate and purify RubisCO from *Microcystis* PCC 7806 wild-type cells after high light exposition revealed that the large subunit of RubisCO was indeed a target for microcystin binding. The extraction procedure implied that the analyzed RubisCO most likely originated from carboxysomes.

Figure 2.5 A illustrates the migration of the 16-mer (L_8S_8) RubisCO enzyme complex in Blue-native PAGE. The same sample was subjected to denaturing SDS-PAGE, followed by Western blot analysis and immunological detection of microcystin, as well as the large RubisCO subunit RbcL (figure 2.5 B). Chemiluminescence signals were detected in both Western blots at the corresponding bands, which confirmed microcystin association with RbcL inside carboxysomes. As became evident from the α-microcystin Western blot, the small RubisCO subunit was not involved in detectable microcystin-protein interactions. The corresponding Coomassie-stained polyacrylamide gel, shown in figure 2.5B, provided a measure of overall RubisCO purity in the analyzed sample.

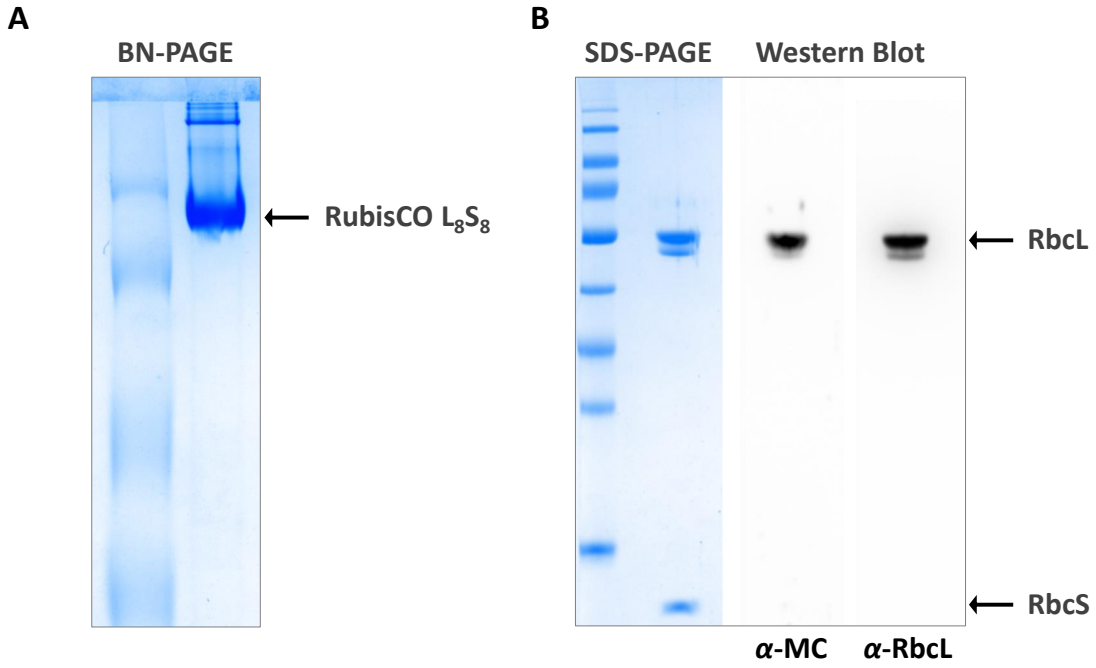

Figure 2.5: Purified RubisCO from high light-treated *Microcystis* PCC 7806 cultures. **A:** Blue-native PAGE of the RubisCO complex consisting of 8 large- and 8 small subunits (L_8S_8) after Coomassie staining. **B:** Denaturing SDS-PAGE of isolated RubisCO; Coomassie-stained gel with protein size marker, as well as RbcL and microcystin detection on the corresponding Western blots. No microcystin signal was detected at RbcS.

2.4.4 Conserved microcystin-protein interaction mechanism

The α, β- unsaturated carbon of the N-methyldehydroalanine moiety of microcystin was shown to bind to thiol groups of cysteines by a Michael type addition mechanism (Runnegar et al., 1995; Zilliges et al., 2011). To clarify whether that mechanism is a unique feature of microcystin and *Microcystis* cells, or if its conserved among other cyanobacteria and even a microcystin related secondary metabolite, protein fractions of *Planktothrix agardhii* NIVA-CYA 126 and *Nodularia spumigena* CCY 9414 were analyzed. Nodularin is a cyclic pentapeptide produced by *Nodularia sp.*. It shares many similarities with microcystin like the Adda-moiety, but it contains N-methyldehydrobutyrine instead of N-methydehydroalanine. Therefore, nodularin theoretically should be able to interact with cysteines *via* Michael addition. The filamentous cyanobacterium *Planktothrix agardhii* NIVA-CYA 126, on the other hand, produces [D-Asp3]-MC-RR and [D-Asp3]-MC-LR, which can also be found in *Microcystis* species.

The proteins of the methanol-insoluble fractions of both strains were separated by SDS-PAGE and electro-blotted to nitrocellulose membranes. The Adda-specific, α-microcystin antibody was used for microcystin and nodularin detection. As illustrated in figure 2.6, both secondary metabolites were present in the insoluble protein fraction after extraction of the cyanobacterial cells. The binding pattern of microcystin in the *P. agardhii* resembled those found in samples of *Microcystis*. The signal of nodularin in the sample of *N. spumigena* was completely different, indicating alternative protein binding partners and probably also a different physiological role of that molecule.

2.4.5 Microcystin quantification in field samples

To test whether conjugate formation of microcystin also occurs in the field and to evaluate the general applicability of the membrane-based microcystin quantification technique, five field samples from different locations were also included in this study, see table 2.2.

LC-MS provided information about the composition of the microcystin pool (figure 2.7

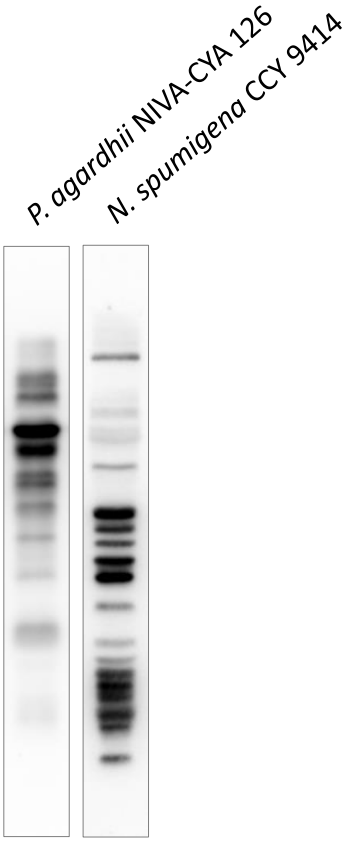

Figure 2.6: Western Blot analysis of methanol-insoluble fractions of *Planktothrix agardhii* NIVA-CYA 126 and *Nodularia spumigena* CCY 9414 cells after methanol extraction. An α-Adda specific microcystin antibody was used.

A). The arginine containing microcystins MC-LR, RR and YR were the dominating congeners in all field samples. The results of the commercial ELISA (figure 2.7 B), which is based on quantitative detection of the Adda moiety present in all microcystins, suggested a higher microcystin load in 4 out of 5 field samples. Non-standard microcystins, as well as low molecular weight- and methanol-soluble conjugates, probably also contributed to the amounts of microcystin detected by the ELISA kit, but were overlooked by LC-MS. Analysis of methanol extracts and methanol-insoluble fractions of the field samples by Dot blot and Western blot (figure 2.7 C-F) underpinned the above described results obtained from analyzing the lab strain samples, see figures 2.3 and 2.4. A significant amount of microcystin apparently was still present in the methanol-insoluble fraction

after extraction. In Dot blot analysis that portion accounted for 37-53 % of the total cellular microcystin. Relative microcystin quantification by Western blot delivered comparable results, although the amount of protein-bound microcystin appeared higher. The methanol-insoluble fractions contained non-cyanobacterial material, which gave the samples a brownish color. Those impurities probably consisted of exo-polysaccharides, humic substances and the like, which caused a smear on the gels and hindered the separation of proteins to distinct bands. However, the results from Western blot and Dot blot analysis were in line with those obtained from LC-MS and ELISA, but they also indicated that a considerable amount of microcystin was neglected by the standard quantification techniques, which focus on extracts only.

2.4.6 Immuno-fluorescence microscopy (IFM)

The same highly specific α-microcystin antibody that was used in Western Blot and Dot blot analysis was also employed to visualize toxic *Microcystis* colonies by IFM in a freshly collected field sample. Figure 2.8 shows the co-occurrence of toxic and non-toxic colonies in a single sample. Since sample preparation for IFM included extraction with organic solvents (see methods 2.3.11), the detected microcystin was most likely part of the not extractable, i.e. protein-bound fraction. The red auto-fluorescence was due to the presence of phycobiliproteins, since the also red-fluorescing chlorophyll was removed from the samples during sample preparation as well.

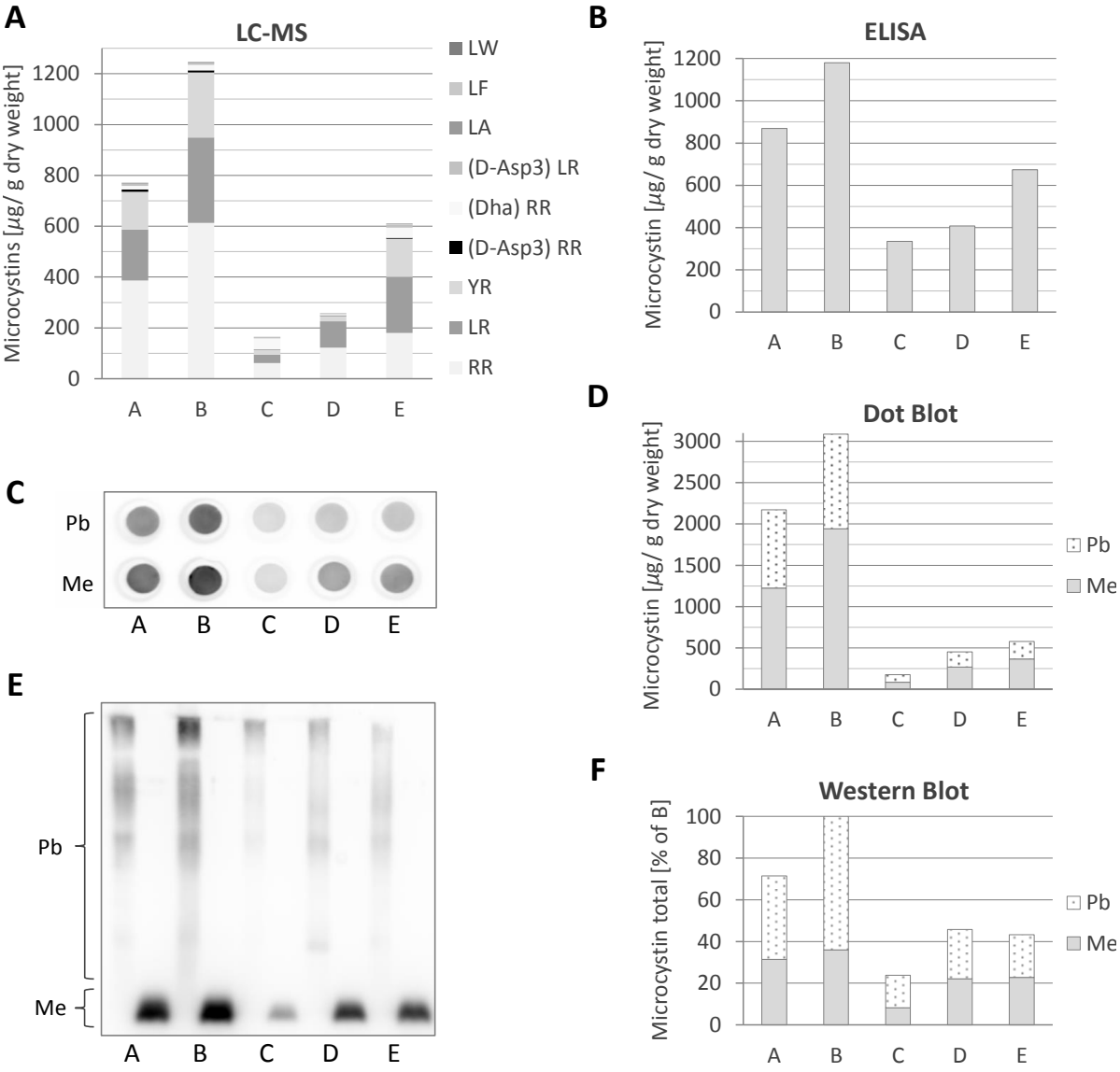

Figure 2.7: Microcystin quantification in field samples A: LC-MS of methanol extracts reflected the concentration and the diversity of microcystin congeners. **B:** The ELISA to quantify microcystin in methanol extracts showed higher microcystin loads in 4 out of 5 field samples. **C-F:** Dot blot and Western blot analysis revealed that a significant portion of the total cellular microcystin remained bound to proteins after extraction.

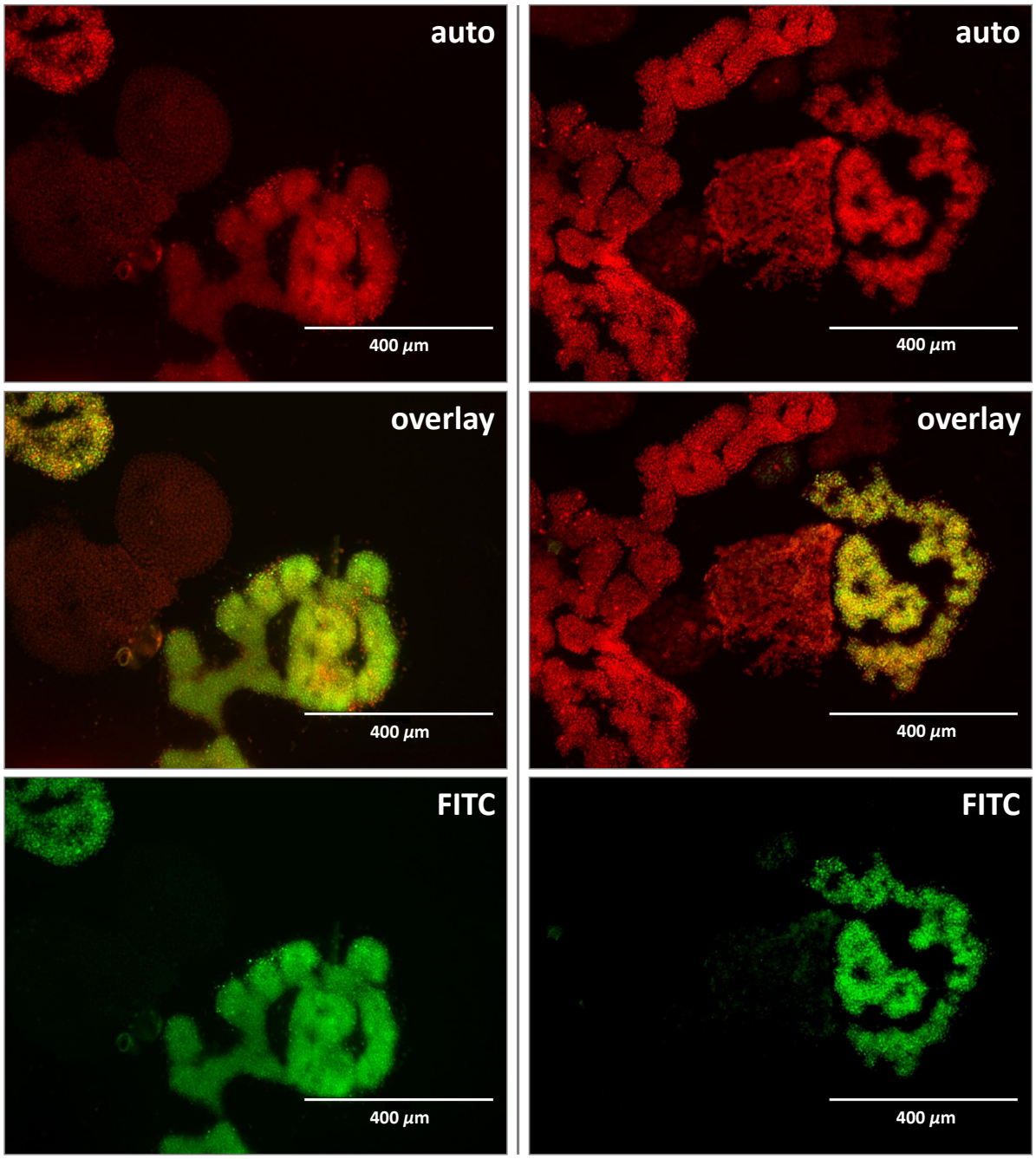

Figure 2.8: Immuno-fluorescence microscopy of field samples. Microcystin-positive colonies can be distinguished from microcystin-negative ones. The upper pictures in each column show the phycobillin-derived autofluorescence of the cyanobacteria. The lower pictures show the FITC-fluorescence signals originating from immunologically labeled microcystin in the samples. The pictures in the middle of each column show the overlays of both fluorescence micrographs.

2.5 Discussion

The dynamics of microcystin production and its interaction with proteins were demonstrated in lab experiments using two toxic *Microcystis* strains. Analysis of purified RubisCO from *Microcystis* cells confirmed that this key enzyme is a major interaction partner for microcystin. Furthermore, Western blot analysis of protein extracts from two other toxic cyanobacterial strains suggested a conserved mode of microcystin interaction with proteins. Field samples of cyanobacteria were also analyzed in this study, to evaluate the applicability of the immuno-blotting techniques for examination of less homogeneous probes and to assess the actual relevance of microcystin-protein interaction in natural cyanobacterial communities. Additionally, immuno-fluorescence microscopy using field samples was employed, to visualize protein-bound microcystin *in situ*.

2.5.1 Membrane-based quantification of total microcystin

None of the applied quantification methods provided a perfect solution for the assessment of the total cellular microcystin loads. The established methods, which focus on microcystin extracts, are highly sensitive and robust, but they do not include the protein-bound fraction. The membrane-based immunological quantification methods described in this study cover the whole cellular microcystin but can only provide a semi-quantitative measure. Nonetheless, the results obtained from Western- and Dot blot analysis of extract samples were in general agreement with those from LC-MS and the commercial ELISA kit.

Protein-blotting methods are intrinsically biased due to binding preferences towards more hydrophobic proteins and peptides and overall limited binding capacities of the membrane. However, the danger of losing especially low molecular weight proteins and peptides during electro-blotting had been overcome by the passive immobilization of the samples in Dot blot approach. A major advantage of the blotting methods was that the proteins were previously denatured, which might support the accessibility of

the antigen for the antibody. Prolonged incubation times and relatively high antibody concentrations might as well supported the detection of protein-bound microcystin in the corresponding samples. Combination of the methods used in this study should have provided a first robust estimate of the indeed biological situation.

2.5.2 Microcystin production is induced by high light

Although the extraction of microcystin was considered as complete, a significant amount of 30-75 % of the total cellular microcystin remained in the methanol-insoluble fraction, depending on the previous treatment. Whereas the amount of extractable microcystin remained almost constant, a clear increase was observed in the protein fraction after high light exposition for three hours. In total, the cellular microcystin load approximately doubled within that time.

Previous studies report high light induced accumulation of mcy-gene transcripts (Kaebernick et al., 2000) and Mcy-proteins involved in microcystin synthesis (Börner and Dittmann, 2005), whereas the determined microcystin concentrations remain vastly unchanged. Another study reports a positive correlation of microcystin content per cell with light intensity under overall light limiting growth conditions and a negative correlation under excessive illumination (Wiedner et al., 2003). The results obtained in this study might help to explain those somewhat contradictory findings and eventually serve as inspiration for new approaches aiming at deciphering the mystery of microcystin production in cyanobacteria.

2.5.3 Microcystin-protein interaction

The toxicity of microcystin is caused by the inhibition of eukaryotic protein phosphatases. The mode of action involves the specific interaction of the microcystin Adda moiety with a hydrophobic groove of protein phosphatases. This non-covalent interaction is responsible for the immediate toxicity within minutes. Subsequent covalent mi-

crocystin binding to specific cysteine residues *via* Michael-type addition is much slower (Pereira et al., 2013). Chemically, the reaction involves ionization of the cysteine thiol to the reactive thiolate by abstraction of the hydrogen by a molecule of water (base), the transfer of a hydrogen from water to the α,β-unsaturated carbonyl group of N-methyl-dehydroalanine (Mdha) and addition of sulfur to the β-carbon of the Mdha moiety of microcystin.

The formation of microcystin-cysteine conjugates is not restricted to eukaryotic protein phosphatases. *In vitro*, the formation of microcystin with cysteine-containing tripeptide glutathione and the free amino acid cysteine by Michael-type addition is carried out under alkaline conditions (pH ∼11.5) in a 5 % potassium carbonate solution (Kondo et al., 1992). It is further suggested that for purposes of microcystin detoxification in eukaryotes, the conjugation of microcystin to glutathione *in vivo* is catalyzed by the enzyme glutathione-S-transferase (GST) at physiological pH (Pflugmacher et al., 1998). To answer the question whether conjugate formation of microcystin with cellular proteins in *Microcystis* is catalyzed enzymatically was not within the scope of this study. However, the interaction of microcystin with cysteine residues of cellular proteins was demonstrated *in vitro* (Zilliges et al., 2011). The binding is abolished by previously blocking either the thiols of the proteins with DTNB or the microcystin Mdha reactive moiety with cysteamine.

A change of the intracellular milieu induced by prolonged exposition to high light most likely boosted microcystin interaction with proteins *in vivo*. The electrostatic environment might provide a selectivity mechanism for the microcystinylation of specific cysteine residues textitvia Michael addition. As outlined above, the thiolate rather than the uncharged thiol of cysteine participates in Michael-type addition. The pK_a of a cysteine's sulfhydryl depends on its electrostatic environment, i.e. the net charge character of the neighboring amino acids, see table 2.3.

Negatively charged amino acids (at neutral pH) increase the pK_a of a proximal cysteine-SH and by that lower the deprotonation tendency of cysteine-SH. Conversely, positively

Table 2.3: pK_a of the cysteine thiol in synthetic peptides; adopted from (Lutolf et al., 2001)

Peptide	**crr**	**rcr**	**cr**	**cys**	**rcd**	**crd**	**cdr**	**cd**	**dcd**	**cdd**
pK_a	8.12	8.22	8.31	8.49	8.50	8.51	8.43	8.57	8.85	8.93

charged amino acids lower the pK_a of a proximal cysteine–SH and support deprotonation to cysteine-S^- at already less basic pH (Lutolf et al., 2001).
High light leads to acidification of thylakoid lumen and alkalinization of the cytoplasm (Falkner et al., 1976). Prolonged exposition to high light might cause imbalances of intracellular pH homeostasis in cyanobacteria. The alkaline cytoplasm in turn could favor deprotonation of pH-sensitive SH-groups and by that facilitate selective microcystin binding to specific cysteines. Figure 2.9 summarizes possible sites of microcystin-protein interaction *via* Michael addition to cysteines, exemplified by the large RubisCO subunit (RbcL). Data from a previous MALDI-MS approach for identification of microcystin binding partners was included as well.

The question about the fate of the conjugated microcystin remains matter of speculation. The thioether bond between Mdha of microcystin and the cysteine thiol is regarded to be irreversible. Enzymatic activity to cleave off protein-bound microcystin would eventually result in a sudden increase of extractable microcystin quota, which was not observed yet. Degradation of microcystin-protein conjugates by general protein turnover might be the most likely scenario.
In principle, microcystin-glutathione and cysteine conjugates showed much weaker toxicity in mice than purely administered microcystin-LR due to increased metabolism and secretion (Ito et al., 2002). The overall toxicological threat connected with numerous freshwater cyanobacteria is caused by the free and extractable, i.e. reactive microcystin, which is reliably detected by the established quantification techniques. Hence, adaptations of current risk-assessment protocols might not be necessary. For the biological understanding of toxic cyanobacteria, however, future studies should include the protein-bound microcystin fraction, which had been neglected from analysis so far.

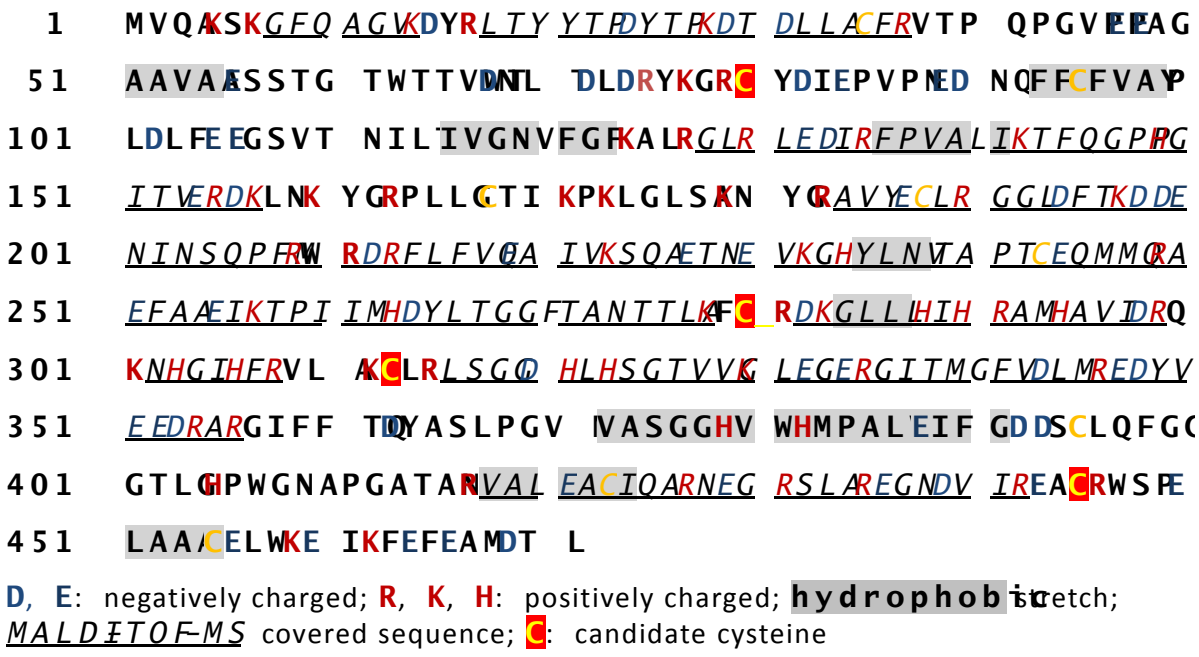

Figure 2.9: RbcL primary structure with highlighted: charged amino acids at neutral pH, stretches of hydrophobic amino acids probably buried inside the enzyme complex, sequence fragments covered in a previous study (MALDI-MS by S. Mikkat, University of Rostock), cysteine residues possibly interacting with microcystin. Note that the previous MALDI-MS approach covered 51 % of the RbcL sequence, including 5 out of 12 cysteines, but none of the proposed candidate cysteines.

2.5.4 Biological implications

The results from the experiments performed in the laboratory indicated that microcystin interaction with proteins was triggered by a shift from low- to high light illumination in two different toxic *Microcystis* strains. At their habitats, cyanobacteria are exposed to fluctuating environmental conditions. Especially extreme high light intensities at the water surface might pose a challenge to the organism. Thus, a major aim of this study was to test whether microcystin conjugate formation can also be observed in the field. Although it could not be figured out to what environmental conditions the field samples were exposed before they were collected, the detection of a significant amount of total cellular microcystin in the insoluble protein fraction underlined the relevance of the phe-

nomenon as such for toxic cyanobacteria at their natural habitat.

As previously reported and confirmed in this study, the large RubisCO subunit (RbcL) in a major target for microcystinylation (Zilliges et al., 2011; Meissner et al., 2013). The effects resulting from microcystin-protein interactions are not well understood yet. An experiment focusing on the stability of RbcL in cell extracts of *Microcystis* show that the microcystinylated form is more resistant against proteolysis by the serine protease subtilisin (Zilliges et al., 2011). The same effect was also observed for phosphoribulokinase (PRK), another enzyme participating in carbon fixation *via* the CBB (Christine Ahlert, Master thesis). Microcystinylated, recombinant PRK of *Microcystis* PCC 7806 was less susceptible towards degradation by subtilisin than the non-microcystinylated control *in vitro*.

Studies on RubisCO from the green algae *Chlamydomonas reinhardtii* report that the enzyme's turnover rate is increased under oxidizing conditions (Marin-Navarro and Moreno, 2003). Oxidation of the protein thiols leads to the formation of disulphide bridges between specific cysteine residues, which in turn induced a conformational change of the whole protein. As a consequence, an otherwise hidden loop of RbcL becomes accessible for proteolysis by subtilisin. Following cleavage at that specific site, the RubisCO L_8S_8 holoenzyme complex disassembles, and the subunits are degraded completely.

Another study on *Synechocystis* PCC 6803 RubisCO reports dissociation of the hexadecameric enzyme complex into single subunits upon oxidation and disulfide formation between conserved cysteines, but without the additional action of a protease (Marcus et al., 2003). However, in both studies the dissociation of the holoenzyme was prevented by alkylation of the cysteine thiols prior to oxidation. Thus, it might be speculated that microcystinylation of specific cysteine residues might stabilize a stable structure of the RubisCO L_8S_8 complex under oxidizing conditions. Interestingly, a decline of enzyme activity upon microcystinylation was neither observed for RubisCO (carboxylase activity) in cell extracts nor for recombinant PRK *in vitro* (Christine Ahlert, Master thesis). Alkylation of the accessible cysteines with iodoacetate leads to a decrease of RubisCO activity in *Synechocystis* PCC 6803 (Marcus et al., 2003).

Another aspect of protein microcystinylation during high light might be the protection of essential cysteine residues against random carbonylation by various reactive substances. For instance, lipid peroxidation occurs under oxidative stress conditions and induces the accumulation of e.g. 4-hydroxynonenal (HNE) as degradation product (Madian and Regnier, 2010). HNE is an α,β-unsaturated hydroxyalkenal with the potential to from protein adducts *via* Michael addition to the amino acids cysteine $\gg$ histidine $>$ lysine, with possibly adverse effects on enzyme activity (Doorn and Petersen, 2002; Dalle-Donne et al., 2006). HNE modifications are considered as a general marker for oxidative stress and can be detected in cyanobacteria (Allahverdiyeva et al., 2013), see 2.10.

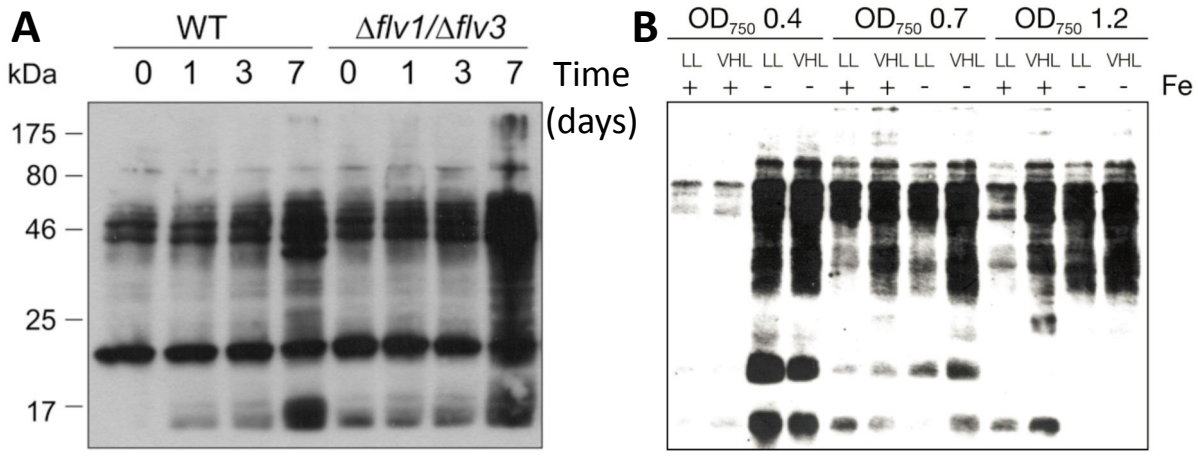

Figure 2.10: Carbonylation *vs.* microcystinylation of cyanobacterial proteins *in vivo*, A: OxyBlot™(Millipore, USA) of cell extracts from *Synechocystis* WT and a flavodiiron protein 1/3 (Δ*flv1*/Δ*flv3*) double-mutant after exposition to fluctuating light conditions for the indicated time (days). The blot shows protein-HNE adducts as general indicator for oxidative stress, figure from the supplement of (Allahverdiyeva et al., 2013). **B:** Anti-microcystin Western blot of *Microcystis* PCC 7806 WT cell extracts from culture samples taken at different optical densities. High light (VHL = 500 μmol photons $\cdot$ $m^{-2}\cdot$ s^{-1}) and iron limitation (-Fe) strongly induced microcystin-protein interaction, figure from (Kehr, 2009). The optical resemblance between A and B might indicate similar binding characteristics to proteins of microcystin and HNE.

Adduction of microcystin and HNE to proteins share the same mechanism. A physiolog-

ical role of microcystin to prevent random alkylation of critical cysteines during episodes of oxidative stress appears likely.

Microcystin binding to proteins was also observed for the genus *Planktothrix*. Nodularin, which might be considered as a minimalistic type of microcystin, was found to bind to proteins of the producing organism *Nodularia* as well. Microcystinylated proteins was also detected in field samples, which further underlined the general relevance of the phenomenon. Thus, the specific binding of microcystin to proteins might be an ancient type of post-translational modification to stabilize enzymes to keep the metabolic machinery intact under critical environmental conditions.

2.5.5 Immuno-fluorescence detection of toxic colonies

The application of immuno-fluorescence based methods to detect toxic phenotypes could provide a valuable tool to characterize the composition of the cyanobacterial community. In this study, the microcystin specific fluorescence signals allowed the differentiation between toxic and non-toxic colonies in a field sample. Sample preparation for IFM includes the extraction of microcystin during fixation and membrane permeabilization with methanol and acetone. Thus, the detected FITC signals most probably were derived from the not extractable-, protein-bound microcystin fraction. The differing fluorescence intensities between individual colonies furthermore suggested non-uniform relevance of microcystin interaction with proteins and could also indicate differences between the observed specimens concerning their recent environmental past.

Many non-microcystin producing phenotypes harbor mcy-genes and the genome copy number of potentially toxic genotypes can differ between single strains and even during different growth phases (Kurmayer and Kutzenberger, 2003). Hence, immuno-fluorescence methods could be used for evaluation and complementation of RT-PCR based approaches for assessing potential threats connected with cyanobacterial toxins in the field and might help to elucidate a possible ecological role of microcystin-protein interaction.

2.5.6 Open questions

Still there are many open questions concerning microcystin-protein interactions. In future studies, the exact microcystin binding residues of cellular proteins have to be determined, which would allow closer characterization of the microcystinylation mechanism and its possible effects. So far, mass spectrometric attempts (MALDI-MS) failed to tackle that issue successfully. The use of enriched protein- or peptide fractions as well as alternative ionization strategies such as, e.g. electron spray ionization (ESI), might be the key to identify microcystinylated fragments. Finally, further fragmentation of the peptides and analysis of the fragments by MS/MS might supply unambiguous evidence for the mode and specificity of microcystin-protein interaction.

The questions about microcystin involvement on regulating enzyme activities and its impact on the general metabolism of *Microcystis aeruginosa* are addressed in the following chapter.

3

The Metabolic Adaptation of *Microcystis* to High Light is Affected by Microcystin and Broadly Different in *Synechocystis*

Most of this chapter's data had recently been published under the title:

"Metabolomic analysis indicates a pivotal role of the hepatotoxin microcystin in high light adaptation of *Microcystis*"

Sven Meissner[1], Dirk Steinhauser[2] and Elke Dittmann[1]

[1]Department of Microbiology, Institute of Biochemistry and Biology, University of Potsdam, Golm, Germany.

[2]Max Planck Institute of Molecular Plant Physiology, Potsdam-Golm, Germany

Environmental Microbiology, 2014

3.1 Abstract

Recent studies suggest beneficial effects of microcystin production under high light intensities and inorganic carbon limitation. In this study, the metabolic response to elevated light conditions was studied in the microcystin producing cyanobacterium *Microcystis aeruginosa* PCC 7806, its microcystin deficient Δ*mcyB* mutant strain and the widely used model cyanobacterium *Synechocystis* PCC 6803. A comprehensive GC/MS-based metabolomics study was conducted and combined with quantification of storage compounds and estimation of net photosynthetic activity. The obtained dataset revealed differences between *Microcystis* wild-type and the Δ*mcyB* mutant strain concerning photorespiration and the accumulation of general stress related metabolites. Huge differences between *Microcystis* and *Synechocystis* in terms of resource utilization and storage under high light conditions became evident as well. This study provides new insights into the metabolic diversity of cyanobacteria, the specific lifestyle of bloom-forming *Microcystsis* and the role of microcystin.

3.2 Introduction

Microcystis is one of the major species frequently involved in freshwater cyanobacterial blooms often culminating in the formation of floating scums. Survival and proliferation in such habitats implies the existence of efficient adaptations to resist sharp physico-chemical gradients and strong diurnal shifts of inorganic carbon availability and oxygen concentration due to photosynthetic activity at daytime and respiration in the night. Especially the resistance to very high light conditions at the water surface might pose a major threat. Several studies report advantageous effects of microcystin production under carbon limitation (Jähnichen et al., 2007) and prolonged exposition to high light (Kardinaal et al., 2007; Van de Waal et al., 2011; Zilliges et al., 2011). Microcystin was also found to have an impact on the transcriptome and the proteome of the producing organism (Zilliges et al., 2011; Tonietto et al., 2012). Another feature of microcystin is its ability to bind directly to proteins *in vivo* and by that modulate the stability of enzyme complexes (Zilliges et al., 2011) and possibly also their functionality. Thus, involvement of microcystin in regulating the activity of enzymes of the primary metabolism in *Microcystis* might be anticipated but remains elusive yet.

To tackle that question, the impact of a light intensity change from low to high on the metabolism of cyanobacteria was examined. The metabolic dynamics of the toxic *Microcystis* strain PCC 7806 wild-type were compared with those of the microcystin deficient mutant PCC 7806 $\Delta mcyB$. For means of interspecies comparison and to put the gained information into context with already published metabolomic studies, a widely used model cyanobacterium *Synechocystis* PCC 6803 was also included in this study. The measurement of glycogen and cyanophycin accumulation in the cells, as well as parameters such as oxygen evolution and pH in the medium, were included to characterize net photosynthetic activity of the different genotypes. The GC/MS metabolomic approach followed in this study provided snapshots of the metabolic constitution of the low light adapted cells before and after exposition to elevated light intensity for one hour and three hours respectively.

3.3 Methods

3.3.1 Strains and cultivation

Each of the strains *Microcystis aeruginosa* PCC 7806, $\Delta mcyB$ (Dittmann et al., 1997) and *Synechocystis* PCC 6803 were cultured in 5 independent biological replicates. Semi-continuous cultures of about 100 mL were grown in 0.5 L Erlenmeyer flasks and maintained at optical densities (OD_{750}) between 0.3 and 0.9 by regular dilution with fresh BG-11 medium (Rippka et al., 1979). The strains were cultured at 25° C without external aeration or permanent shaking under constant fluorescent light (Philips Master TL-D 58W/ 865) with a photon flux rate of 15 μmol photons $\cdot$ $m^{-2}\cdot$ s^{-1} .

The biovolume was calculated by multiplying the cell number present at a certain OD_{750} with the strain-specific average cell volume. Cell numbers were determined by counting cells in a Thoma chamber (0.0025 mm^2 grids, 0.01 mm depth) with the help of a digital microscope (AMG EVOS fl, Peqlab, Erlangen, Germany) and ImageJ analysis software (Rasband WS. ImageJ, U.S. National Institutes of Health, Bethesda, Maryland, USA). Cell diameters were determined with the above-mentioned microscope as well. Cell volumes were calculated assuming a spherical shape of the cells.

Table 3.1: Biovolume: Cell diameter, cell number at $OD_{750} = 1$ and corresponding biovolumes for *M. aeruginosa* PCC 7806 and *Synechocystis* PCC 6803

Strain	**Diameter [μm]**	**Cells $\cdot$ $mL^{-1}\cdot$ OD^{-1}**	**Biovolume [$\mu L \cdot mL^{-1}\cdot OD^{-1}$]**
PCC 7806	3.39	$6.69 \cdot 10^7$	1.36
PCC 6803	2.35	$2.04 \cdot 10^8$	1.39

3.3.2 High light exposition

A shift from light limitation to carbon limitation, with all accompanying secondary effects, was intended to trigger physiological reactions and adaptations, which might also

be relevant in the field during cyanobacterial mass developments. Intentionally, buffering substances, as well as supplementation with excess inorganic carbon were excluded from the growth medium.

For the experiments, the cultures were grown to optical densities of 0.7 (0.96 ± 0.06 μL cells/ 1 mL culture). The light intensity was elevated from 15 to 250 μmol photons · m^{-2}· s^{-1}. Photon flux rate was measured with a LI-250A light meter and a spherical sensor (LI-COR® Biosciences, USA). Oxygen concentration and pH of the cultures were determined with a PCE-PHD 1 probe (PCE Deutschland GmbH, Meschede, Germany). The temperature remained constant at 25° C during the time of exposition.

3.3.3 Glycogen quantification

For glycogen quantification, samples were taken from three independent cultures of each strain. Cells from 1 mL culture were collected by centrifugation at each time point and immediately fixed in ethanol. The ethanol was discarded by pelleting the samples in a centrifuge and careful aspiration of the liquid. All samples were dried completely on air. The glycogen of each sample was hydrolyzed to glucose in 100 μL 3.5 % sulfuric acid for 40 minutes at 100° C. For colorimetric determination of the glucose content, 1 mL of 6 % (v/v) *o*-toluidine in acetic acid was added to each hydrolysate and incubated for another 7 minutes at 100° C. Subsequently the samples were cooled on ice for 5 minutes and centrifuged briefly at room temperature. The reaction product had an absorption maximum at 635 nm, which was measured with a bench top photometer (Applied Science) under a fume hood. A calibration curve was established for quantification in parallel with the help of identically processed glycogen standards.

3.3.4 Estimation of cyanophycin content

Three independent replicates of each low light adapted strain were sampled after 0, 1, 2 and 3 hours of high light exposition. Cyanophycin was extracted according to the protocol of (Simon and Weathers, 1976). Cells from 10 mL culture were washed once

with water and stored -20° C until further processing on the same day. The cells were re-suspended in water containing 0.5 % Triton X-100 and extracted by shaking at 4° C overnight. *Synechocystis* samples required further mechanical treatment on a cell mill (Retsch, Germany) for 15 minutes. The samples were centrifuged at 20.000×g and 4° C for 30 minutes. The pellets were washed with water three times. Cyanophycin was dissolved in 0.1 M HCl at RT on a shaker for 1 hour. The samples were cleared by centrifugation, and the obtained extracts were analyzed by SDS-PAGE. For the estimation of the cyanophycin content the Coomassie stain intensity of the diffuse band between 25 and 35 kDa was quantified using Image Lab™software (BioRad, USA).

3.3.5 Electron microscopy

To prevent artifacts due to collapse of gas vesicles during centrifugation, the cells from 2 mL culture were collected by fast vacuum filtration (Krall et al., 2009). Immediately after collection, the cells were suspended in 100 μL 100 mM sodium cacodylate buffer pH 7.0 containing 2.5 % glutaraldehyde and 2 % formaldehyde for fixation at RT for 1h and at 4° C overnight. Subsequently, the cells were embedded in 1.5 % low melting agarose (Sieve GP, Biozym, Oldendorf, Germany) and immediately spread on microscopy sample slides. After solidification of the agarose, cubes of less than 1 mm^3 were cut, transferred into fresh 1.5 mL tubes and washed 3 times for 10 minutes in 100 mM sodium cacodylate buffer. The samples were post-fixed at RT for 90 minutes with 2 % OsO_4 in 100 mM sodium cacodylate buffer and subsequently washed in water. Dehydration was done in a graded ethanol series and acetone. The specimens were embedded in Agar low viscosity resin (Agar Scientific Elektron Technology UK Ltd, Stansted, United Kingdom). Ultra-thin sections were stained with uranyl acetate, as well as lead citrate. Imaging was carried out on a Philips CM100 transmission electron microscope operating at 100 kV. Electron microscopy was conducted in cooperation with Prof. Dr. Otto Baumann, Potsdam University, Golm, Germany.

3.3.6 Sample preparation for GC/MS

Cells from cyanobacterial cultures at optical densities of 0.7 were harvested by fast vacuum filtration under the corresponding light conditions of the experiment (Krall et al., 2009). Durapore® PVDF hydrophilic filters with a diameter of 25 mm and a pore size of 0.45 μm (Millipore, USA) were used. After aspiration of the medium, the filters with adhering cells were rapidly transferred to fresh 1.5 mL microcentrifuge tubes and frozen in liquid nitrogen immediately. The samples were stored at -80° C until metabolite extraction. In total, samples of five independent biological replicates of each of the three genotypes, taken at 3 different time points were analyzed. The analytical background was assessed with the help of five extraction blanks i.e. filters without adhering cells that were identically processed as follows.

Metabolite extraction was done by a one-step extraction procedure as described in (Huege et al., 2011). In short, 1 mL of $\leq$ -15° C cold 90 % (v/v) methanol extraction solution supplemented with 0.8 μg/ mL U-^{13}C-sorbitol [1] was added to the frozen samples, followed by immediate vortexing for 1 minute. Subsequently, the samples were further extracted in an ice-cooled bath-type sonicator 2 times for 5 minutes, as well as vigorous shaking by an orbital shaker for another 90 minutes at 4° C. The filters were removed carefully from the tubes and the extracts centrifuged at 10.000×g and 4 ° C for 5 minutes. From the extracts, a fraction of 900 μL was transferred to fresh 1.5 mL tubes and subsequently dried in a vacuum concentrator at RT in the dark. The samples were stored at -20° C for a maximum of one week until analysis.

Extracellular metabolites were also analyzed. To that end, the spent medium of 2 mL culture samples was cleared from cells by centrifugation at 10.000×g and 4° C for 5 minutes. 1.5 mL of the medium was transferred to fresh tubes and centrifuged as above to exclude any cell transfer. Finally, 750 μL of the cleared supernatant was again transferred to fresh tubes and dried in a vacuum concentrator as described above.

Metabolite analysis was carried out according to an established protocol for the quan-

[1] U-^{13}C-sorbitol served as internal analytical standard for assessment of extraction variability

tification of metabolites from cyanobacterial extracts including various classes of small molecules such as sugars, sugar alcohols, organic acids, amino acids and nucleosides, as well as various lipophilic substances (Krall et al., 2009; Huege et al., 2011).
Metabolite derivatization and GC-EI-TOF-MS analysis with m/z acquisition of 85–750 were performed as described (Huege et al., 2011). A mixture of fatty acid methyl esters (FAMEs) was included during derivatization and used as internal marker system to adjust the retention index (RI) for chromatographic retention time variation (Krall et al., 2009).

3.3.7 GC/MS data processing and analysis

GC/MS data was processed and analyzed by Dr. Dirk Steinhauser (Max-Planck-Institute, Golm, Germany). Non-targeted alignment of chromatograms was followed by curating of the aligned peaks to obtain a targeted peak library of low redundancy for ultimate peak extraction and quantification. The obtained dataset comprised 45 sample profiles with 501 peaks and a total of 2082 (9.23 %) missing values. The compounds were identified by using reference compound libraries of commercially available standards (Kopka et al., 2005; Krall et al., 2009; Huege et al., 2011).

3.3.8 Statistical analyses and visualization

Data analysis was performed by D. Dirk Steinhauser (Max-Planck-Institute, Golm, Germany) according to (Sokal and Rohlf, 1995) and (Legendre and Legendre, 1998) using R 3.0.2 (R Development Core Team, 2013). Hierarchical cluster analysis (HCA) with average linkage clustering was used to draw cluster trees. The number of supported clusters was estimated using gap statistic (Tibshirani et al., 2001). Factors for two-way ANOVA were genotype, treatment (as time) and genotype-treatment interaction. Mean differences were estimated with Tukey's HSD method, and the p-values were corrected by Benjamini–Yekutieli correction (Benjamini and Yekutieli, 2001).

3.4 Results

3.4.1 High light, oxygen evolution and medium pH

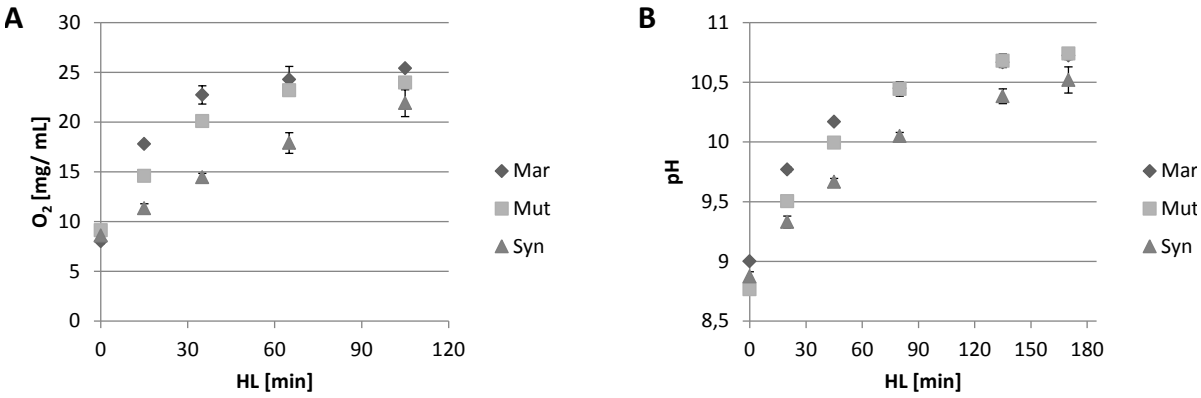

Figure 3.1: Net photosynthesis of three independent cultures of each cyanobacterial strain under high light **A:** Oxygen evolution; **B:** pH dynamics in the culture medium after the onset of high light illumination. Whiskers indicate the standard deviation from the means in each diagram.

Oxygen evolution served as a direct proxy of net photosynthetic activity during the first half of the experiment. Initially, the oxygen concentration of light limited cultures was in equilibrium with the atmosphere, which indicated that the light intensity was close to the photosynthetic compensation point. Highlight illumination led to oxygen over-saturation of the culture medium. The steepest increase was observed in wild-type *Microcystis* cultures. Oxygen evolution in the *Microcystis* $\Delta mcyB$ mutant cultures was significantly lower than in the cultures of the wild-type during the first 15 minutes of the experiment and was even more lagging behind in the cultures of *Synechocystis*. For p-values of significance test, see table 3.3. Since oxygen escaped steadily from the cultures into the atmosphere, only the first three values could serve as a measure for net photosynthesis. However, the pH as an indirect measure for the CO_2 uptake from the medium by cyanobacterial cells might also roughly reflect net photosynthesis. Indeed, the increase of pH behaved proportionally to oxygen evolution in all three strains. *Microcystis* wild-type cultures again showed the significantly steepest increase during the first

45 minutes of the high light treatment followed by Δ*mcyB* mutant- and *Synechocystis* cultures.

3.4.2 High light induced metabolic differences between strains

The above described differences already suggested strain-specific metabolic traits. The heat map of figure 3.2 shows those 193 metabolites, which were present in all cyanobacterial strains and which accumulated significantly different in at least one of the tested-, low light adapted genotypes after exposition of the respective cultures to high light for one hour [T1], or for three hours [T3]. The biggest cluster comprised those metabolites, which accumulated in a similar fashion in all three genotypes (cluster A, n=68), indicating a conserved response to high light illumination. Among the identified metabolites were mainly amino acids, as well as compounds of the CBB and the TCA. However, for many other metabolites, species specific changes were detected. Metabolites, which accumulated specifically in *Synechocystis*, but were vastly unchanged in *Microcystis* comprised metabolites of the clusters B (specific decrease, n=8) and F (specific increase, n=46). Cluster F includes the amino acids glycine, arginine, proline, glutamine and norleucine, which did not accumulate significantly different in *Microcystis* cultures under high light.

Several metabolites accumulated specifically in both *Microcystis aeruginosa* genotypes, as visualized in cluster D (specific increase, n=32) and G (specific decrease, n=2). Most remarkably, high light illumination led to specific accumulation of a number of metabolites only in *Microcystis* wild-type cells (cluster C, n=34), but neither in the *Microcystis* Δ*mcyB* mutant genotype, nor in *Synechocystis* cells. Although the metabolites of this cluster, except 1,3-dihydroxyacetone, could not be classified yet, a substantial impact of microcystin production on the metabolism of *Microcystis* might be anticipated.

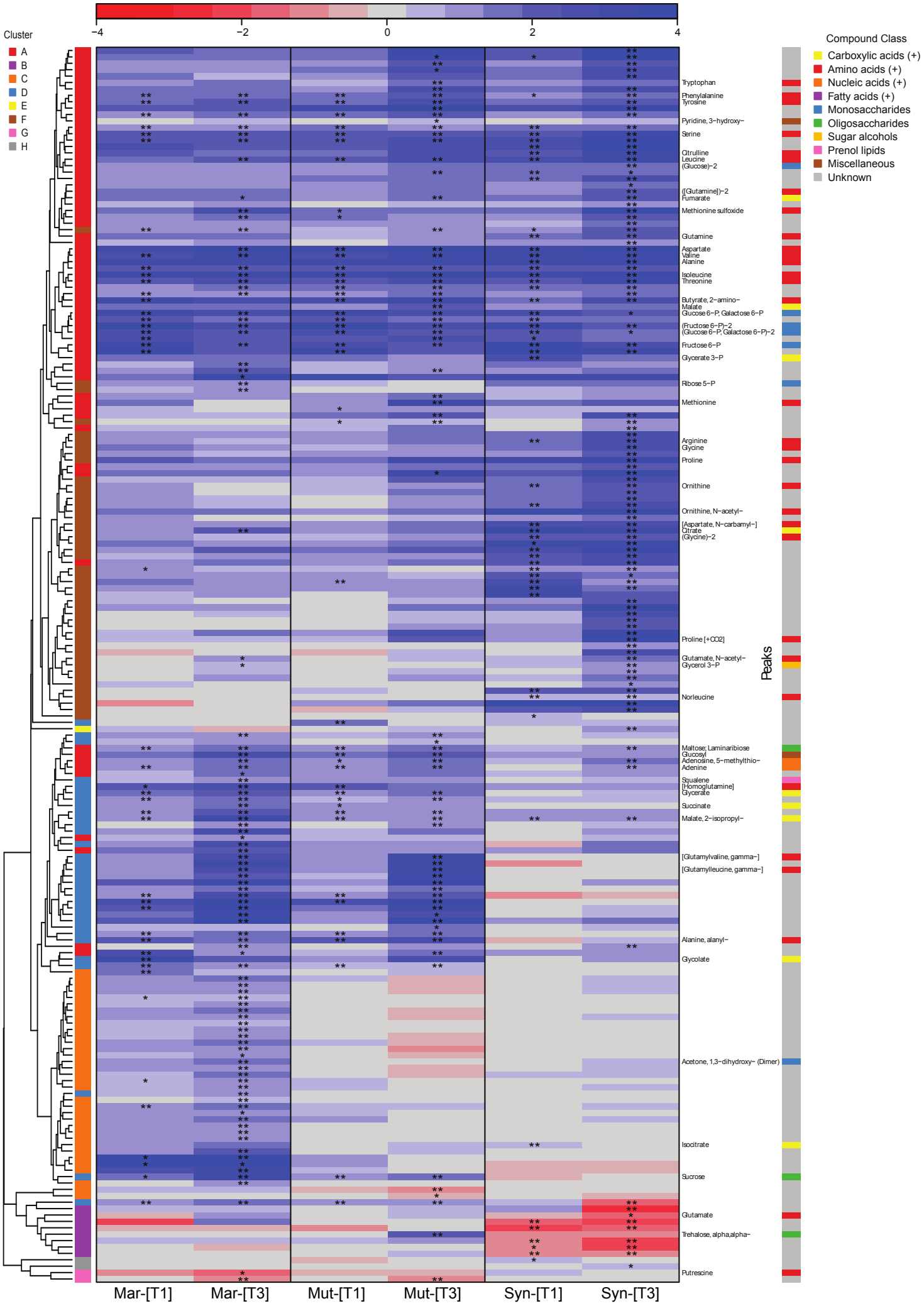
Cluster
A
B
C
D
E
F
G
H
−4
−2
0
2
4
Compound Class
Carboxylic acids (+)
Amino acids (+)
Nucleic acids (+)
Fatty acids (+)
Monosaccharides
Oligosaccharides
Sugar alcohols
Prenol lipids
Miscellaneous
Unknown
Tryptophan
Phenylalanine
Tyrosine
Pyridine, 3−hydroxy−
Serine
Citrulline
Leucine
(Glucose)−2
([Glutamine])−2
Fumarate
Methionine sulfoxide
Glutamine
Aspartate
Valine
Alanine
Isoleucine
Threonine
Butyrate, 2−amino−
Malate
Glucose 6−P; Galactose 6−P
(Fructose 6−P)−2
(Glucose 6−P; Galactose 6−P)−2
Fructose 6−P
Glycerate 3−P
Ribose 5−P
Methionine
Arginine
Glycine
Proline
Ornithine
Ornithine, N−acetyl−
[Aspartate, N−carbamyl−]
Citrate
(Glycine)−2
Proline [+CO2]
Glutamate, N−acetyl−
Glycerol 3−P
Norleucine
Maltose; Laminaribiose
Glucosyl
Adenosine, 5−methylthio−
Adenine
Squalene
[Homoglutamine]
Glycerate
Succinate
Malate, 2−isopropyl−
[Glutamylvaline, gamma−]
[Glutamylleucine, gamma−]
Alanine, alanyl−
Glycolate
Acetone, 1,3−dihydroxy− (Dimer)
Isocitrate
Sucrose
Glutamate
Trehalose, alpha,alpha−
Putrescine
Peaks
Mar-[T1]
Mar-[T3]
Mut-[T1]
Mut-[T3]
Syn-[T1]
Syn-[T3]

Figure 3.2: Cluster tree and heat map visualization of the 193 peaks with a significant light dependent change in at least one genotype. The color coded scale above the heat map represents a measure for log2-fold changes of means after high exposition of low light adapted cells after 1 hour [T1] and after 3 hours [T3]. The genotypes are denoted as Mar: *Microcystis* PCC 7806 wild-type; Mut *Microcystis* 7806 Δ*mcyB* mutant; Syn: *Synechocystis* PCC 6803. Significant changes as determined by Tukey's HSD method are marked with asterisks: *$p \leq 0.05$ and **$p \leq 0.01$. Names of identified metabolites are right beside the heat map. Substance classes are color encoded by the neighbouring bar at the right side. Clusters of the color coded hierarchical cluster tree on the left separates metabolite groups with specific accumulation patterns. Cluster A summarizes substances with a similar light dependent accumulation pattern across all genotypes. Clusters F and B indicate *Synechocystis* PCC 6803 specific responses not present in either of both *Microcystis* PCC 7806 genotypes. Cluster D denotes responses conserved in both *Microcystis* PCC 7806 genotypes but not in *Synechocystis* PCC 6803. Cluster C indicates responses unique for only the *Microcystis* wild-type but not for any of the other genotypes.

Mar vs. Mut

To better figure out the impact of microcystin production on the metabolome of *Microcxystis*, data of *Synechocystis* was excluded from the analysis. In total, 85 out of the 501 metabolites (17 %) accumulated significantly different in *Microcystis* wild-type (Mar) and the Δ*mcyB* mutant strain (Mut) upon high light illumination, as illustrated in the sub-heatmap and cluster tree shown in figure 3.3. Most of the differences between the two genotypes became apparent after three hours of high light exposition.

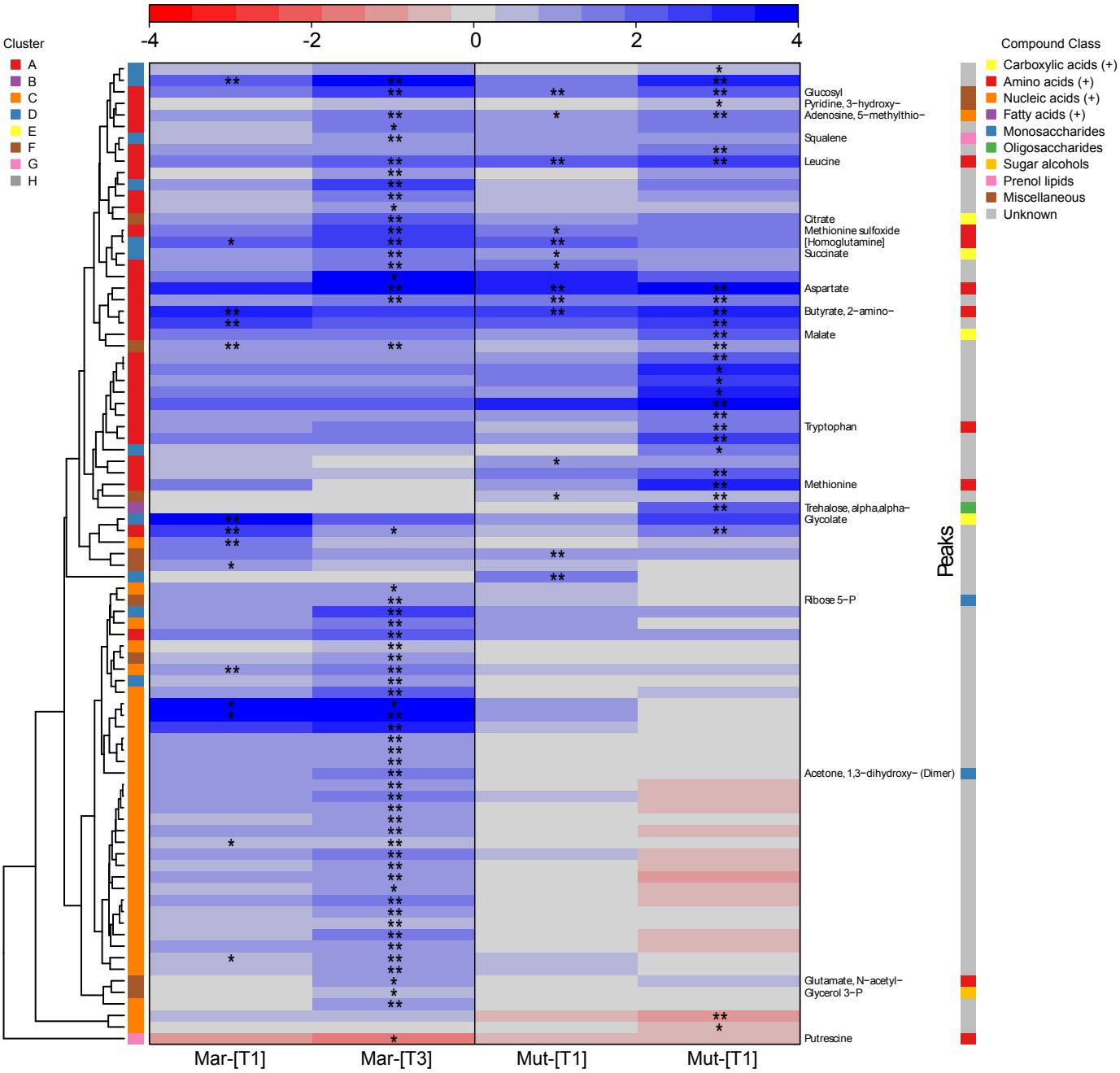

Figure 3.3: Cluster tree and heat map visualization of 85 peaks showing significant high light induced differences between *Microcystis aeruginosa* PCC 7806 wild-type (Mar) and the microcystin deficient Δ*mcyB* mutant strain (Mut) after one hour [T1] and after three hours [T3]. The scale of log2-fold changes to initially low light adapted cells is placed above the heat map. Asterisks denote significant changes according to Tukey's HSD with *$p \leq 0.05$ and **$p \leq 0.01$. At the right side are the metabolite names of annotated peaks and the bar gives the chemical class as explained in the top-right legend. Metabolites were separated into groups according to their accumulation pattern and visualized on the as color coded hierarchical cluster tree on the left.

3.4.3 Central carbon pathway metabolites

Intermediates, especially those of the Calvin-Benson-Bassham cycle (CBB), are denoted by rather small pool sizes and fast turnover rates. Accordingly, the following bar diagrams represent steady state levels of metabolite concentrations under the applied conditions at the sampling time points. They do not reflect fluxes of e.g. carbon through specific metabolic routes, but rather indicate metabolite accumulation due to rate-limiting reactions (bottlenecks), overall up- or downshift of the utilization loads of certain pathways, as well as accumulation of stable intermediates for purposes of e.g. cell homoeostasis, or storage.

The concentration of the CBB pathway intermediates was overall strongly increased 3-4-fold the initial values in all three strains after one hour of high light exposition. Interestingly, the levels of ribulose-5-phosphate (R5P) in *Synechocystis* were constantly about 3-4 times lower than those in the *Microcystis* strains. After three hours of illumination, the concentration of most CCB intermediates had dropped again to 2-3 times the initial levels. Glucose-6-phosphate (G6P), which links the CBB and glycogen synthesis, showed essentially similar temporal dynamics. A clear difference between *Microcystis* and *Synechocystis* was found in phosphoenolpyruvate (PEP) and pyruvate levels. Whereas *Microcystis* showed decreasing PEP concentrations after one hour of high light, the PEP and pyruvate levels in *Synechocystis* rose. The overall dynamics of PEP and pyruvate in *Synechocystis* were comparable to those of CBB intermediates and G6P, which might indicate channeling of assimilated carbon from the CBB towards the TCA. Indeed, citrate and isocitrate showed similar temporal dynamics. In contrast, PEP concentrations declined and pyruvate remained constant in *Microcystis* after one hour of high light.

The most surprising discovery of the metabolic study was that *Microcystis* samples only contained almost undetectable amounts of isocitrate under the conditions of the experiment. The almost undetectable levels of isocitrate might imply that *Microcystis* synthesizes 2-oxoglutarate (2-OG) in an alternative manner, at least during illumina-

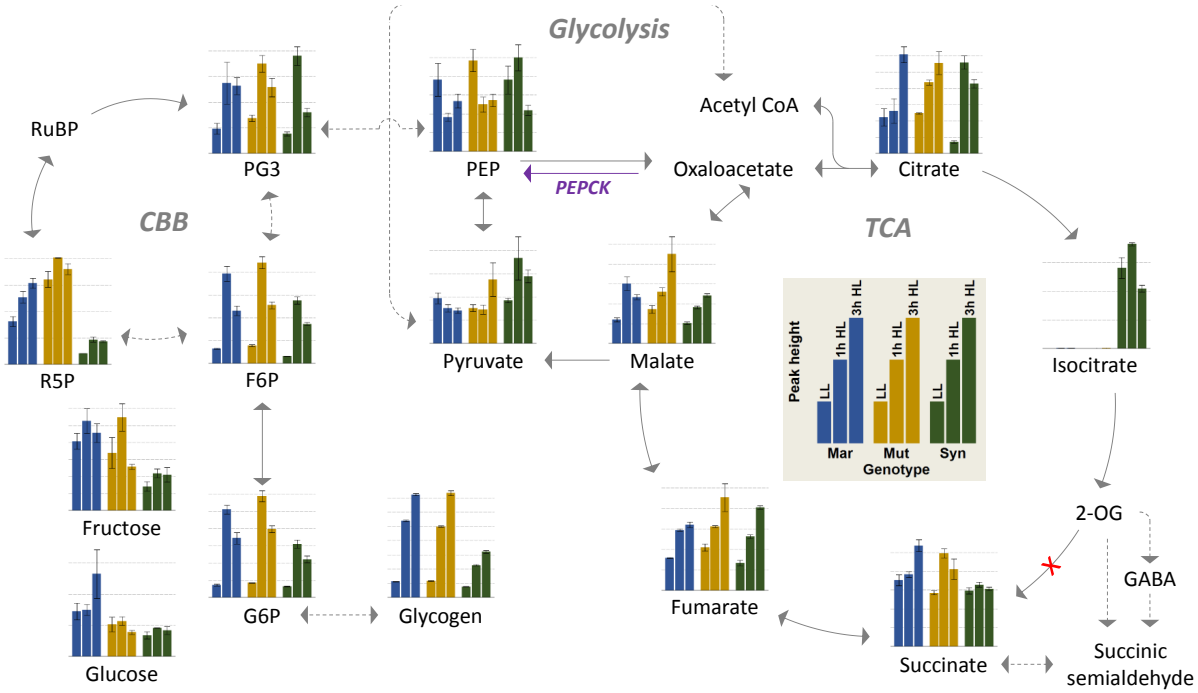

Figure 3.4: Impact of high light on the central carbon metabolism; The scheme comprises barplots of the measured metabolites involved in the Calvin-Benson-Bessham cycle (CBB), glycolysis, and tri-carbonic acid metabolism (TCA), as well as tightly connected compounds. The proposed shunts to close the TCA-cycle *via* succinic semialdehyde are also included. The *Microcystis* specific enzyme PEPcarboxykinase is highlighted in purple. RuBP, ribulose-1,5-bisphosphate; PG3, 3-phosphoglycerate; PEP, phospho*enol*pyruvate; 2-OG, 2-oxoglutarate; a diagram explaining the barplots can be found inside the TCA.

tion. Alternatively, it might be inferred that isocitrate turnover is extremely fast and the pool size is very low, or that its synthesis is down-regulated to very low levels in *Microcystis*, but not in *Synechocystis* under the conditions of the experiment.

The overall dynamics of C-4 intermediates in all three strains and citrate in *Microcystis*, differed from those of the CBB in that their levels increased during the whole three hours of high light exposition. Only in 7806 WT, the malate levels behaved like CBB intermediates and might point towards the involvement of microcystin in carbon shuffling between malate and CBB during prolonged high light illumination.

3.4.4 Amino acids

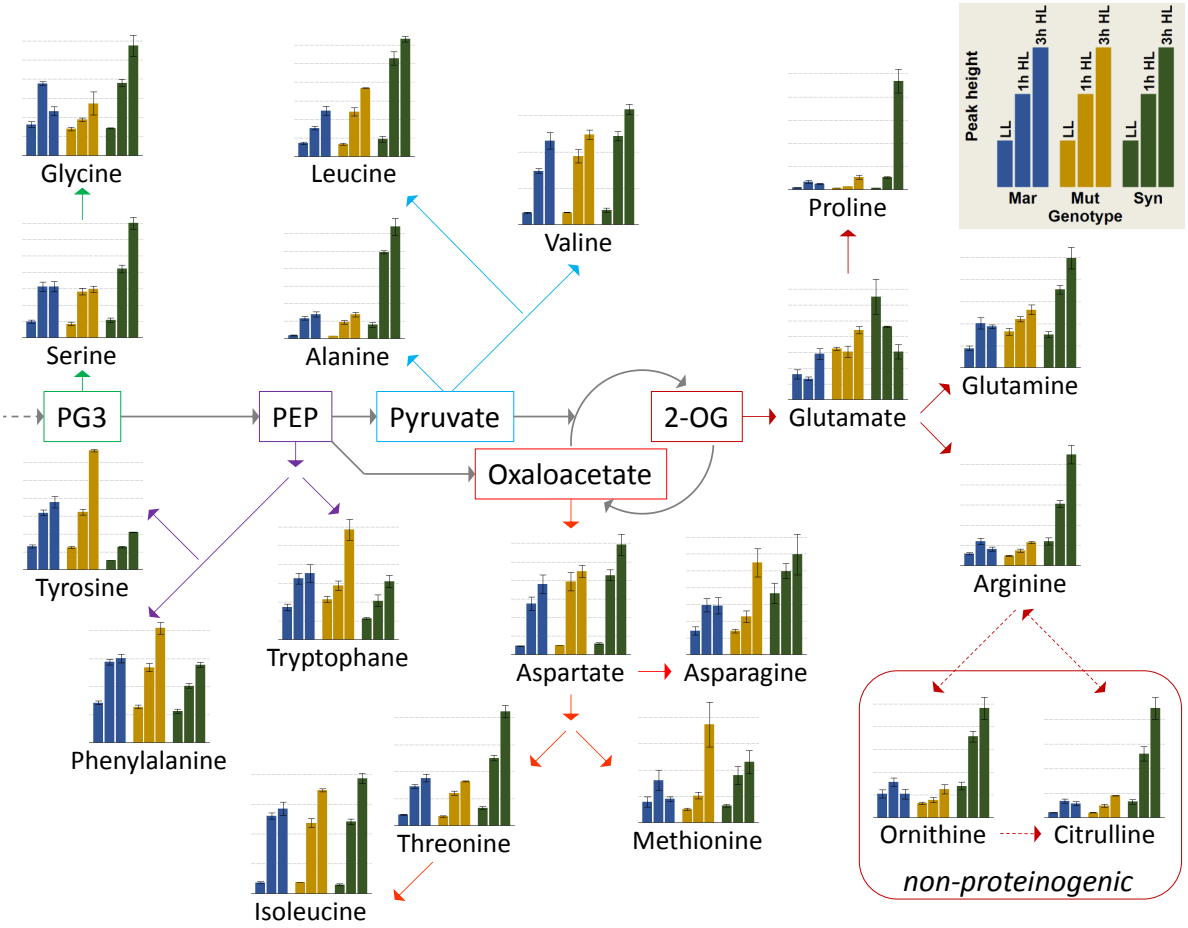

Figure 3.5: Amino acid accumulation during high light exposition and their proposed metabolic origins. The description of the bar-plots can be found at the upper right corner. PG3, 3-phosphoglycerate; PEP, phospho*enol*pyruvate; 2-OG, 2-oxoglutarate

During high light exposition, the accumulation of most amino acids was increased in all strains, as visualized in figure 3.5. However, some substantial and species-specific differences became apparent with regard to groups of amino acids deriving from distinct precursor metabolites. Serine and glycine levels were stronger increased in *Synechocystis*, probably indicating a higher utilization rate of 3-phosphoglycerate. Though, both amino acids could also originate from photorespiration, which will be presented later in section 3.6. Levels of amino acids synthesized from PEP were in general more increased in *Microcystis* cultures, especially in those of the microcystin deficient $\Delta mcyB$

mutant. The accumulation of pyruvate derived alanine and leucine, but not valine was more pronounced in *Synechocystis* cultures. Amino acids of the aspartate family showed strong increases, which might indicate a connection to active β-carboxylation of PEP by PEPcarboxylase utilizing bicarbonate to form the precursor metabolite oxaloacetate.
The strongest species-specific differences were observed for 2-oxoglutarate derived amino acids. Whereas the levels of those amino acids were almost unaffected in both *Microcystis* genotypes, a pronounced increase became evident in the samples of *Synechocystis*. Only the glutamate concentration declined from initially high levels. It seems likely that the synthesis of glutamate could not keep pace with its further rate of utilization into related amino acids, as well as in photorespiration 3.6.
The almost constant levels of 2-oxoglutarate related amino acids found in *Microcystis* cells are probably connected with the above reported absence of isocitrate, (see 3.4) and might further indicate rather low involvement of an oxidative TCA metabolism during illumination. In sharp contrast, *Synechocystis* appeared to channel lots of assimilates from the CBB towards the TCA for synthesis 2-OG and the derived amino acids.

3.4.5 Photorespiration

Photorespiration is a result of the RubisCO-oxygenase activity, which is favored under conditions of low carbon-to-oxygen ratios during illumination. The immediate products of RuBP oxygenation are one molecule of PG3 and one molecule of 2-Phosphoglycolate (2PG). 2PG is a potent inhibitor of the glycolytic enzymes triosephosphate isomerase and phosphofructokinase in plants (Anderson, 1971; Kelly and Latzko, 1976) and thus needs to be metabolised quickly. Cyanobacteria possess highly effective carbon concentrating mechanisms, which are supposed to effectively restrict 2PG formation to basal levels under standard conditions (see 1.2).

In this study the first measured photorespiratory intermediate was glycolate, see figure 3.6. In *Microcystis* wild-type cells, an 8-fold increase of glycolate was detected after one

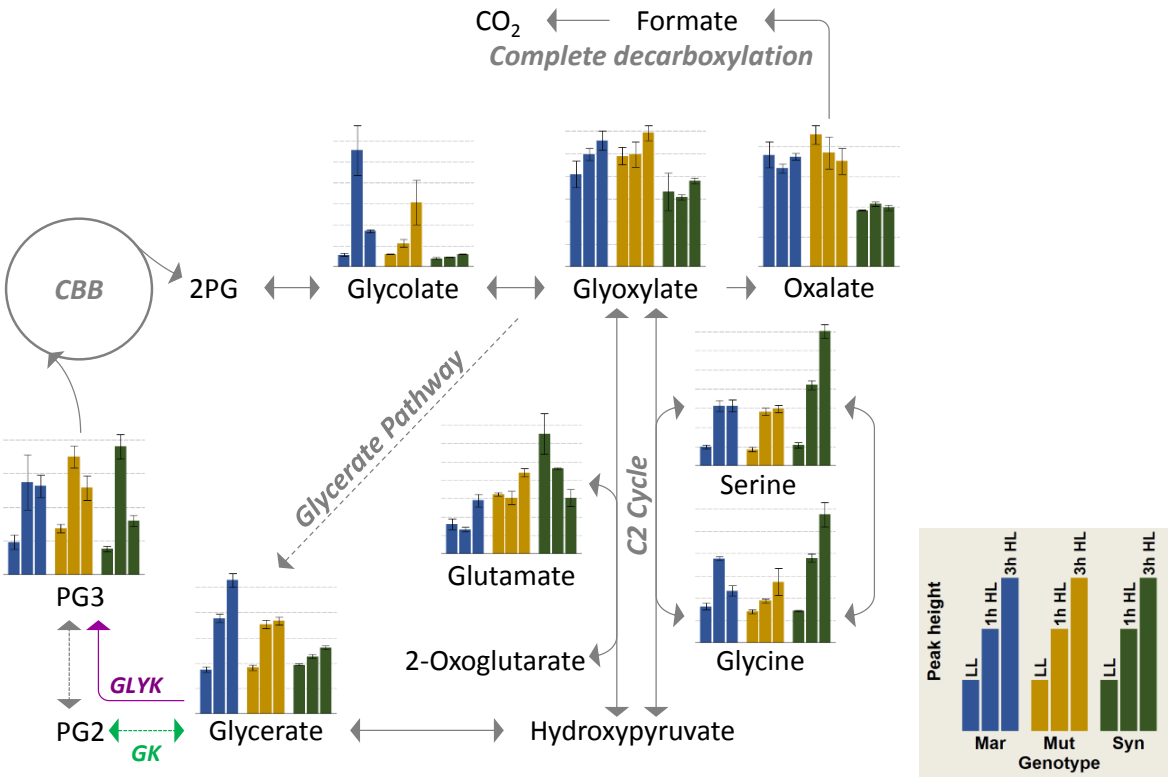

Figure 3.6: Photorespiration: Routes of the RuBP-oxygenation product 2-phosphoglycolate (2PG) metabolism and associated metabolites. The description of the bar-plots is displayed at the lower right corner.

hour of high light exposition. Interestingly, the amount of glycolate had declined again to values of about 3-fold the initial concentration after three hours of high light. In the Δ*mcyB* mutant, the glycolate concentration was only moderately increased after one hour, but steadily continued to rise to 4-fold the initial value after three hours of high light exposition.

From all of the other measured metabolites, only glycerate could serve as an additional indicator for high light-induced photorespiratory activity in *Microcystis*. Here, the values steadily increased in *Microcystis* wild-type 2.5-fold and 2-fold in the Δ*mcyB* mutant. It might be worth noting that the *Microcystis* genome encodes for a plant-type D3-glycerate kinase (GLYK), which directly catalyzes the phosphorylation of glycerate to 3-phosphoglycerate (PG3). In *Synechocystis* on the other hand, the conversion of glycerate to PG3 requires the concerted action of a class I glycerate kinase (GK) and a

phosphoglycerate mutase. The presence of GLYK could indicate a higher relevance of PG3 regeneration *via* the glycerate pathway in *Microcystis*.

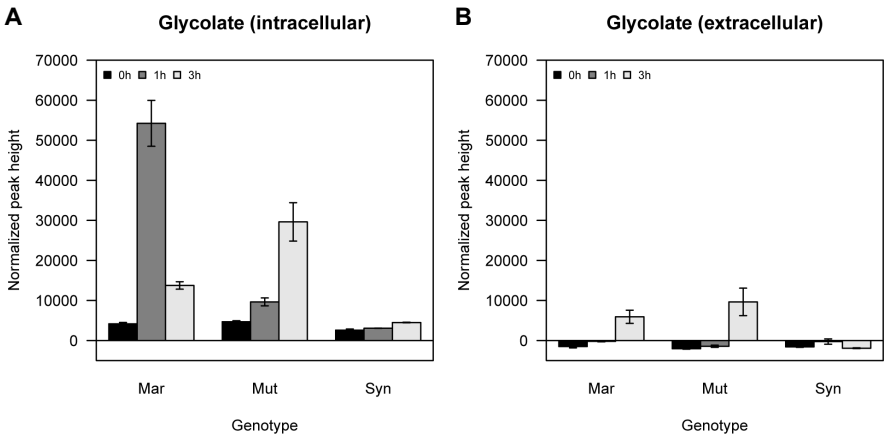

Figure 3.7: Glycolate accumulation inside the cells, A and in the culture medium , B of *Microcystis* wild-type (Mar), Δ*mcyB* mutant (Mut) and *Synechocystis* (Syn) cultures during high light exposition.

Interestingly, some of the produced glycolate was also found in the medium of *Microcystis* cultures after three hours of high light, which indicated secretion of at least parts of the photorespiratory intermediate, see figure 3.7. However, the relatively high intracellular amounts in *Microcystis* wild-type after one hour and the comparably low extracellular amounts occurring only after three hours of high light indicated metabolism of most of the produced glycolate by the cells.

Synechocystis cells showed only indirect signs of photorespiration during the entire time of high light exposition. Although not unequivocally assignable to photorespiratory metabolism, the decline of glutamate levels, as well as the increase of serine and glycine concentrations could eventually hint towards active glyoxylate processing to hydroxypyruvate *via* the plant like C2 oxidative photosynthetic carbon cycle. However, the measured intracellular glycolate levels remained at a constantly low level, and none of it was found excreted into the medium, see figure 3.7. Either the photorespiratory machin-

ery of *Synechocystis* was running so extremely efficient that no glycolate and glyoxylate built up or the oxygenation of RuBP was efficiently suppressed under the applied high light conditions in *Synechocystis*.

3.4.6 Compatible solutes

Compatible solutes are protective substances that have stabilizing effects on cell components and are reported to be synthesized in response to general stress (Klähn and Hagemann, 2011). The *Microcystis* mutant strain accumulated highest levels of the compatible solutes sucrose and trehalose, see figure 3.8. Prolonged high light exposition further increased their concentrations. The loss of microcystin synthesis eventually caused metabolic imbalances, which in turn led to elevated stress levels in the *Microcystis* mutant under the experimental conditions.

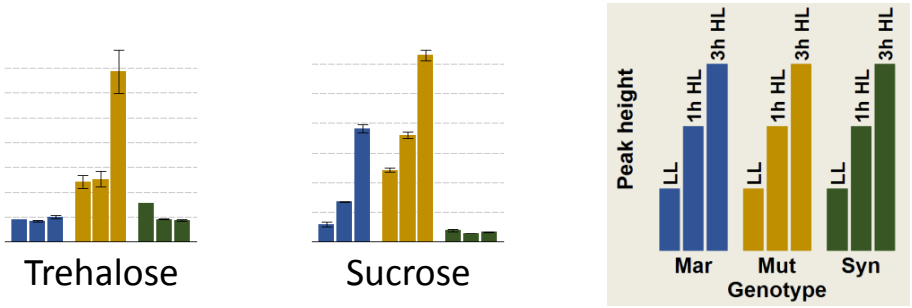

Figure 3.8: Compatible solutes -Accumulation of sucrose and trehalose might indicated a general stress response, most pronounced in *Microcystis* mutant cells. The description of the bar-plots is displayed at the right.

3.4.7 Quantification of storage compounds

Since metabolite fluxes could not be determined, it is indispensable to quantify the end products of photosynthesis to estimate the main metabolic routes indirectly. The electron micrographs of figure 3.9 show representative cells of the three cyanobacteria

strains before and after three hours of high light exposition. *Microcystis* cells were densely packed with coarse glycogen granules (Gg), which occupied almost all available space in the cytoplasm and between thylakoids. Though to a lower extent, *Synechocystis* also showed accumulation of glycogen granules, which were fine and did not cover the whole cytoplasmic space. The inclusions only visible in *Synechocystis* high light samples probably represent cyanophycin granules (Cp), for comparison see (Li et al., 2001). Interestingly, cells of the PCC 7806 $\Delta mcyB$ mutant appeared to possess higher numbers of gas vesicles than the wild-type (not systematically determined).

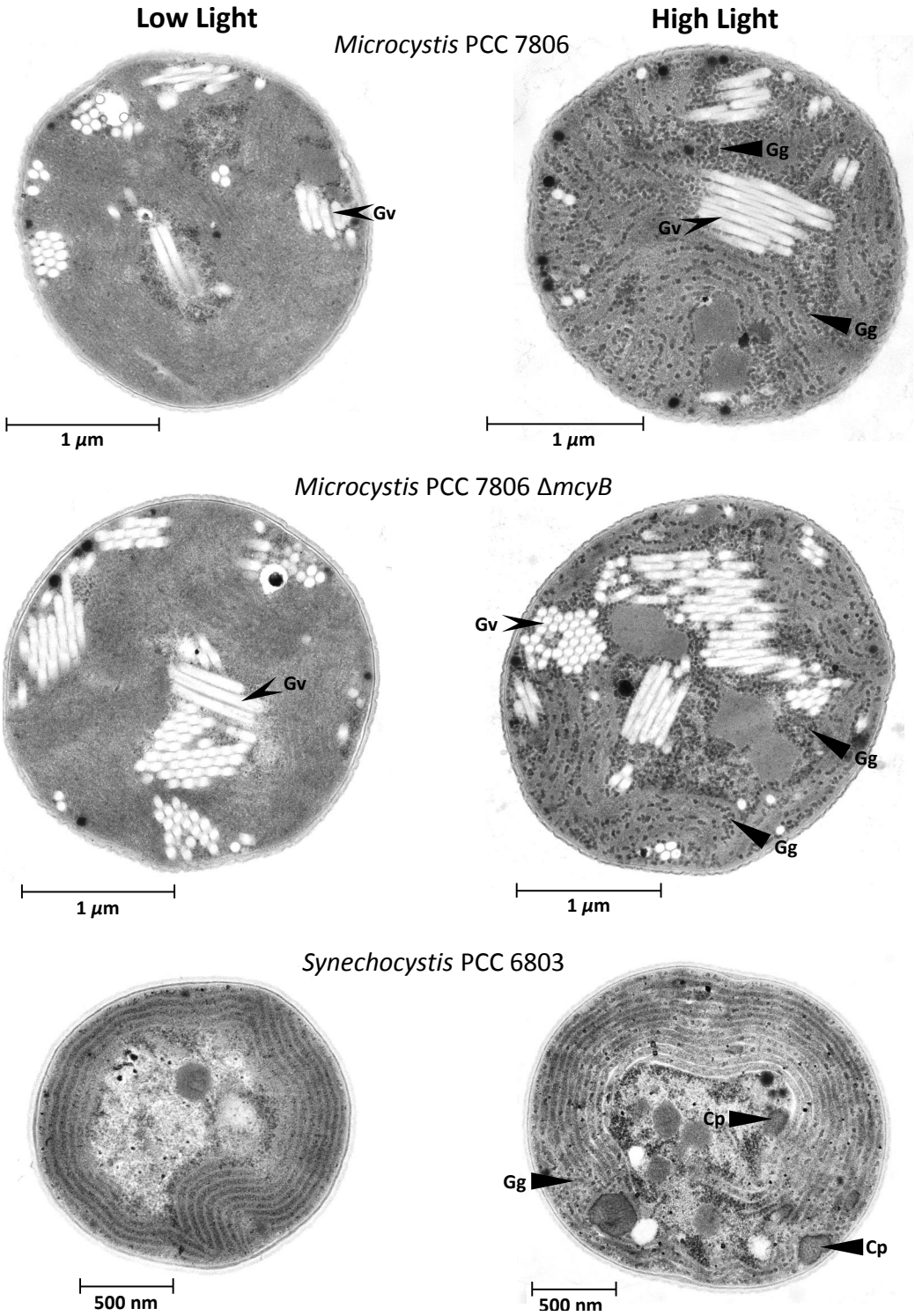

Figure 3.9: Electron microscopy of cells before (left) and after high light exposition for three hours (right); Gg, Glycogen granules; Gv, Gas vesicles; Cp, Cyanophycin; pictures were taken by Prof. Dr. Otto Baumann, Potsdam University.

Glycogen is supposed to be the main storage compound of reduced carbon in cyanobacteria. Thus, it was used as a relative measure to estimate the overall net photosynthetic activity of the cyanobacterial strains *via* the Calvin-Benson-Bassham cycle under the conditions of the experiment.

Figure 3.10 shows that the glycogen levels in all three strains were low in the beginning. Over the whole time of the experiment, glycogen levels increased in all strains, which indicates no absolute inorganic carbon depletion even after three hours of high light exposition. Both *Microcystis* strains showed about two times higher total glycogen accumulation per biovolume than *Synechocystis*. Although not tested significant (see table 3.5), the *Microcystis* wild-type accumulated slightly more glycogen than the microcystin deficient mutant during the first 90 minutes, which in turn accumulated more glycogen during the second half of the experiment. Interestingly, all three strains accumulated glycogen with a higher rate during the first 90 minutes and continued at a lower rate for the following 90 minutes. Note that glycogen accounted for about 8.5 % of the fresh weight in *Microcystis* and for about 4 % in *Synechocystis* at the end of the experiment.

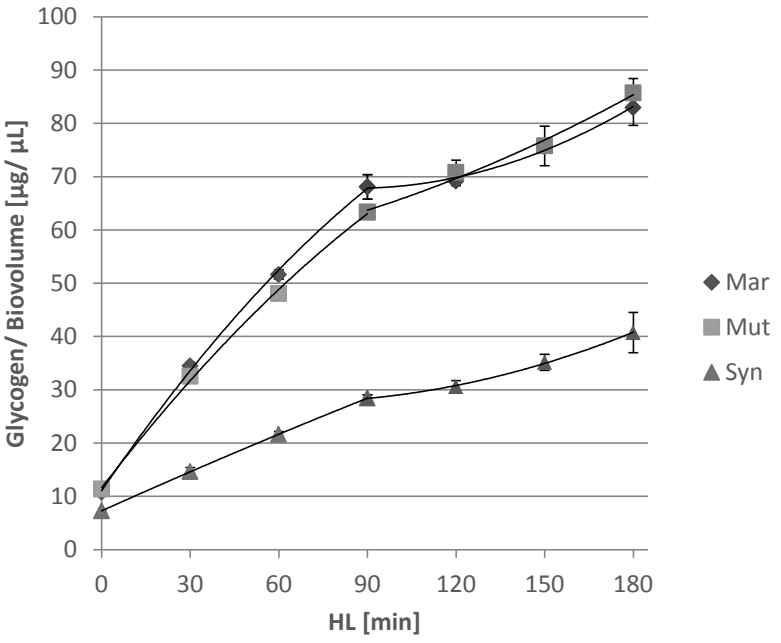

Figure 3.10: Glycogen accumulation per biovolume in cells of the cyanobacterial strains during high light exposition for three hours.

Cyanophycin, a polypeptide consisting of the two amino acids arginine and aspartate, is another typical storage compound of cyanobacteria. Granules of that copolymer became visible in electron micrographs of high light treated *Synechocystis* cells, but not in those of *Microcystis*, see 3.9. Relative determination of cyanophycin accumulation during high light exposition indeed revealed strain-specific differences. *Synechocystis* strongly accumulated cyanophycin, whereas both *Microcystis* genotypes did not, see figure 3.11 and supplement figure 3.14. In *Synechocystis* cyanophycin accumulated in a sigmoid fashion with the strongest increase between two and three hours under high light, which coincides with the decline of glycogen accumulation. In contrast, the cyanophycin content in both *Microcystis* genotypes declined during the first hour of the experiment and increased again to approximately the initial values within the following two hours. Please note that the bar diagram in figure 3.11 represents only relative cyanophycin concentrations. Considering the original Coomassie-stained gel of *Synechocystis* shown in figure 3.11 B) it became apparent that the low light adapted cells initially lacked almost any cyanophycin.

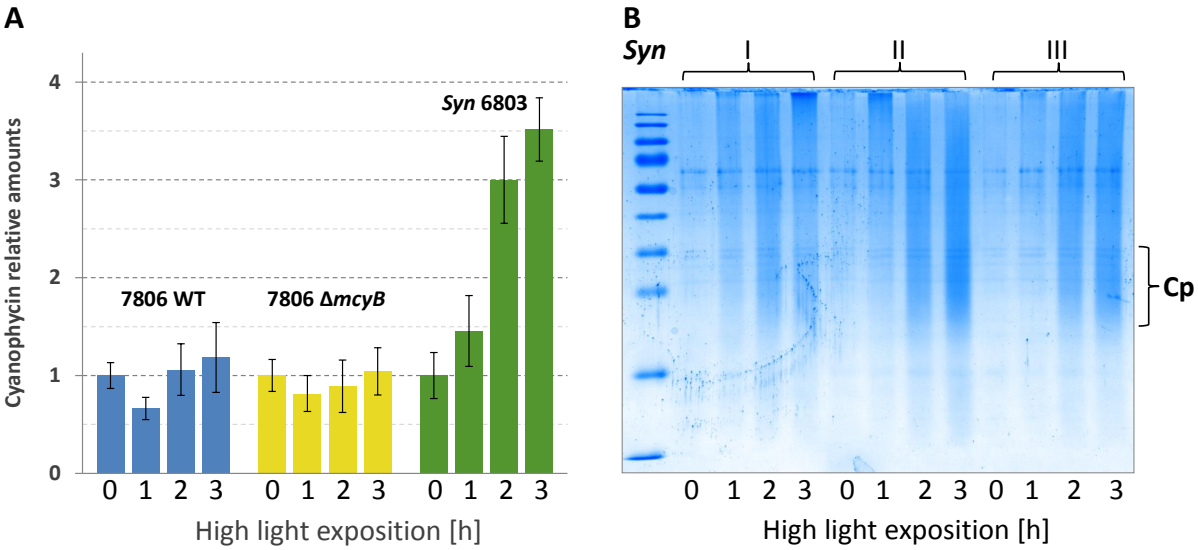

Figure 3.11: Cyanophycin: A, Relative accumulation upon high light illumination. Error bars indicate the standard deviation from the mean of three replicates each. **B,** Coomassie-stained gel of *Synechocystis* extracts from three replicates (I-III); Cp, cyanophycin smear area used for relative quantification. For gels of *Microcystis* extracts, see 3.14.

3.5 Discussion

This study aimed at characterizing the cyanobacterial metabolism under changing light conditions. For the first time, the *Microcystis aeruginosa* PCC 7806 wild-type and its Δ*mcyB* mutant strain was included in a metabolomics analysis and compared with the established model cyanobacterium *Synechocystis* PCC 6803. Valuable information about the role of microcystin in *Microcystis*, as well as conserved and strain-specific metabolic features was gained. The experimental set-up was chosen with the intention to simulate conditions as they might also be encountered at the natural habitat of *Microcystis*. A shift from low to high light directly increased photosynthesis rates of the cells and lead to marked changes of dependent secondary parameters, such as culture pH, oxygen concentration and inorganic carbon availability, which most likely had an impact on cyanobacterial adaptation processes during the experiment. The dynamics of those parameters might have been restricted by e.g. including pH buffering substances in the medium, blow out the produced oxygen by external aeration and by the supplementation of the cultures with additional sodium bicarbonate or CO_2 as source for inorganic carbon. However, all this artificial and never complete manipulations were intentionally excluded for the price of not knowing which exact parameter triggered what effect, but for the benefit of obtaining a more general and probably more representative picture of cyanobacterial adaptations as they might also be expected to take place in the field.

3.5.1 High light experiment

As intended, the onset of high light illumination triggered a marked increase of dissolved oxygen and the pH in the culture medium of all strains. *Microcystis* and *Synechocystis* showed distinct differences in photosynthetic activity and accumulation patterns of central carbon pathway intermediates, amino acids and storage compounds. Also, photorespiration seems to be of higher relevance in *Microcystis* under the conditions of the

experiment. A clear impact of microcystin on the metabolism of *Microcystis* to high light conditions, and its accompanying secondary effects might be inferred from the collected data.

3.5.2 Net photosynthetic activity

In this experiment oxygen evolution and glycogen accumulation served as a direct measure for net photosynthetic activity. Low initial glycogen contents, as well as oxygen concentrations in equilibrium with the atmosphere, indicated light limitation under the standard culture conditions before elevating the light intensity. During high light exposition the pH values correlated proportional with oxygen evolution and therefore could serve as an additional proxy for net photosynthesis; i.e. CO_2 or proton uptake, for the complete duration of the experiment.

Net photosynthesis was clearly lower in cultures of *Synechocystis*, which was reflected by comparably low glycogen content of the cells and moderate oxygen evolution. The capacity of the *Microcystis* strains to produce glycogen was significantly higher, which might indicate specific capabilities due to the original life style of the species.

In the field, *Microcystis* species regularly participate in cyanobacterial mass developments. Under those conditions, it might be of fundamental importance for the cells to harbor machinery that utilizes inorganic carbon as fast as possible and to store it in a reduced form as glycogen. *Microcystis* species synthesize gas-filled vesicles and usually form macroscopic colonies. The interplay with the assimilate ballast lets them actively migrate between different layers of the water column (Reynolds et al., 1987). In theory, low ballast of reduced carbon and lowered turgor would let colonies quickly rise to the water surface for utilization of light energy and inorganic carbon. Floating colonies could acquire CO2 directly at the water-atmosphere interface. Conversely, high ballast of reduced carbon and increased turgor would let them sink to deeper layers, where the availability of inorganic nutrients is higher. Note that the glycogen content accounted for about 8.5 % of the fresh weight in *Microcystis* after three hours exposition to high

light. The elevated levels of compatible solutes, especially in the *Microcystis* Δ*mcyB* mutant, might also suggest an adaptation to increase the turgor for reversal of buoyancy (Reynolds et al., 1987).

In contrast, *Synechocystis* has a different lifestyle in that this species does not participate in the formation of cyanobacterial mass developments. The cells do not possess gas vesicles, and the formation of buoyant colonies was not reported yet. The original habitat of *Synechocystis* therefore might have favored a different strategy when sudden changes of light intensities are encountered by the organism.

In general, all three tested genotypes accumulated glycogen throughout the experiment, indicating neither severe photoinhibition nor net carbon loss due to photorespiration during the three hours of high light illumination. Interestingly, all strains showed a pronounced simultaneous decline of the glycogen accumulation rate after 90 minutes, which might indicate a general adaptation to the light conditions of the experiment. Depletion of Ci and limitation of glycogen accumulation to the rate of CO2 diffusing into the medium might explain that phenomenon. This conclusion is in line with the only moderate pH increase between 90 and 180 minutes of high light exposition.

An important aspect of *Microcystis* species is their ability to produce various secondary metabolites with often yet unknown functions. In the case of microcystin, as one of the most intensely studied cyanobacterial secondary metabolites, a significant role in physiological adaptation becomes more and more evident, which is also reflected by the differences observed in this study between the two *Microcystis* strains PCC 7806 wild-type and its microcystin deficient Δ*mcyB* mutant. Oxygen evolution was significantly lower in the Δ*mcyB* mutant during the first minutes after the shift from low- to high light, see table 3.3. Also, the steeper pH increase in the medium and faster glycogen accumulation point towards a specific function in inorganic carbon acquisition during adaptation to increased light intensities.

In previous studies it was shown that microcystin can bind to proteins (Zilliges et al., 2011), see also chapter 2 of this work. It binds covalently to thiol groups of cysteines

and by that lowers the susceptibility of proteins towards proteolytic digest. Especially the change of light conditions from low to high supports the interaction of microcystin with cellular proteins, with the large subunit of the carbon fixing enzyme RubisCO as one of the major targets.
The question about whether or not microcystin production has an impact on enzyme activities was the motivation for conducting the metabolomics approach discussed in the following.

3.5.3 High light exposition revealed strain specific metabolic differences

The heat map 3.2 provided a representative estimate of the differential metabolite accumulation in the three strains used in this study after transfer of the cultures to high light. From a total of 501 peaks detected in each of the 45 chromatograms, 193 showed significant light-induced changes in at least one of the three strains. About one-third (n=68) of the 193 variable peaks represented substances, which accumulated in all three strains simultaneously, indicating a conserved cyanobacterial reaction triggered by a shift from low- to high light. The remaining two-thirds (125) of accumulated non-uniformly in the three strains. About 28 % of the 193 light dependent metabolites were specifically changed only in *Synechocystis*, 18 % in both *Microcystis* strains, but not in *Synechocystis* and another 18 % were only changed in the microcystin producing *Microcystis* wild-type. Despite not knowing the exact identity of many of the detected compounds it might be concluded that:

1. High light changed the metabolic constitution of all strains
2. The metabolomic changes were species specific
3. Microcystin production influenced the metabolism of *Microcystis*

3.5.4 Central carbon pathway metabolites

High light exposition triggered a sharp increase of most measured CBB intermediates in all tested strains after one hour. This finding appears plausible, since it was assumed that the cultures were grown under light limiting conditions just above the light compensation point, which was also reflected by low initial oxygen concentrations and low glycogen contents. However, the onset of high light illumination presumably triggered the activation of key CBB enzymes and the accumulation of CBB intermediates. During the first minutes of high light illumination, the so-called induction period, most of the existing triose phosphates and newly assimilated carbon are used to build up intermediates for acceleration of the CBB. After one hour of high light exposition, the amount of the measured CBB intermediates might reflect the maximum capacity of the cycle in the tested genotypes. The observed decrease of CBB intermediates after three hours of high light might be explained by general down-regulation of the cycle due to the limitation by inorganic carbon. However, still, the concentrations of CBB intermediates in the cells were about 2-3 times higher at that time as they were in light-limited cultures.

The general accumulation pattern of CBB intermediates was not observed for ribose-5-phosphate (R5P), which additionally accumulated about three times higher in *Microcystis* cultures. However, R5P is also strongly involved in the synthesis of nucleotides, co-enzymes and proteins. For that reason, the observed concentrations of R5P could not exclusively be linked to its role as CBB intermediate but indicated strong strain-specific differences not explainable yet.

Metabolites involved in glycolysis showed non-uniform accumulation patterns. PEP levels declined from comparably high initial concentrations in both *Microcystis* genotypes but were elevated in *Synechocystis* after one hour of high light exposition. At the end of the experiment, the PEP levels were highly similar in all three strains. Pronounced channeling of assimilates from the CBB towards TCA might be assumed for *Synechocystis*, since the accumulation pattern of PEP resembled that of CBB intermediates, as well as those of citrate and isocitrate. The glycolytic formation of pyruvate yielding addi-

tional ATP, as well as channeling of assimilates towards citrate, is probably suppressed in *Microcystis* in the light. The different accumulation patterns of 2-oxoglutarate derived amino acids in both species further supported this assumption, see 3.5.7.

3.5.5 TCA metabolism

The very low levels of detected isocitrate in both *Microcystis* strains was highly unexpected and had never been reported for cyanobacteria before. Both species harbor the same set of respective genes. Hence, a *Microcystis*-specific regulation of isocitrate synthesis and/ or metabolism might be inferred. In general, cyanobacteria do not perform TCA metabolism in the appearance of the classical TCA-cycle, as present in e.g. aerobic heterotrophs since the enzyme complex of 2-oxoglutarate dehydrogenase is absent. Huge efforts have been undertaken to find enzyme candidates in cyanobacteria to bridge the missing step of the cycle. Recently, 2-oxoglutarate dehydrogenase and succinic semialdehyde dehydrogenase were finally figured out as most promising candidates (Zhang and Bryant, 2011). An alternative route from 2-oxoglutarate over γ-aminobutyric acid (GABA) and succinic semialdehyde to succinate was described. To what extent a closed TCA cycle is required for photoautotrophic growth remains to be clarified in the future. However, the relatively low levels of isocitrate in *Microcystis* might even challenge the assumption that 2-OG is produced *via* decarboxylation of isocitrate by the enzyme isocitrate dehydrogenase, although present. It might be proposed that the oxidative reactions of the TCA, which yield additional ATP and NADH, were mostly down-regulated during illumination. Nonetheless, even under light limiting conditions [T0] almost no detectable isocitrate was present in *Microcystis* cells, which might indeed indicate a strain-specific peculiarity.

Alternatively, the pool size of isocitrate could have been smaller in *Microcystis*. The conversion of citrate to 2-oxoglutarate *via cis*-aconitate and isocitrate by aconitase and isocitrate dehydrogenase were possibly carried out in a very condensed way. For exam-

ple, the formation of a functional complex including both enzymes could also explain the very little amounts of detectable isocitrate that were present in *Microcystis* cells.
If citrate was indeed not further metabolized to isocitrate in *Microcystis*, it appears almost certain that the TCA-cycle metabolites malate, fumarate and succinate originated mainly from β-carboxylation of PEP to form oxaloacetate by the action of PEPcarboxylase. From an energetic perspective, it generally appears favorable also for *Synechocystis* to employ these parts of the TCA mainly in a reductive fashion, to regenerate ADP and NADP for maintaining high photosynthetic activity. Additionally, carbon fixation by PEPcarboxylase utilizes bicarbonate with high affinity and is not bothered with (undesirable) competing reactivity like RubisCO at low CO_2 : O_2 ratios.
PEPcarboxylase is an essential enzyme in cyanobacteria (Luinenburg and Coleman, 1990). Significant amounts of inorganic carbon are primarily fixed by PEP carboxylation (Young et al., 2011). The observed accumulation of oxaloacetate-derived metabolites and amino acids could suggest that the action of PEPcarboxylase becomes even more relevant in situations of high photosynthetic activity marked by high oxygen concentrations and CO_2 deprivation.

3.5.6 Cyanobacterial C4 characteristics

The above discussed primary carbon fixation *via* PEP carboxylation is a common feature among certain vascular land plants employing the C4- or crassulacean acid metabolism (CAM) to concentrate CO_2 around RubisCO. It might be speculated that cyanobacteria also employ at least parts of that type of carbon concentrating mechanism. Flux analysis experiments in *Synechocystis* PCC 6803 already showed a substantial flow of carbon from malate towards pyruvate (Yang et al., 2002; Young et al., 2011), characteristic for C4-type plants. Mutants of *Synechocystis* PCC 6803 with knocked out malic enzyme were also shown to grow much slower than the wild-type under constant illumination (Bricker et al., 2004).
Besides the very effective utilization of bicarbonate by PEPcase, a positive side effect

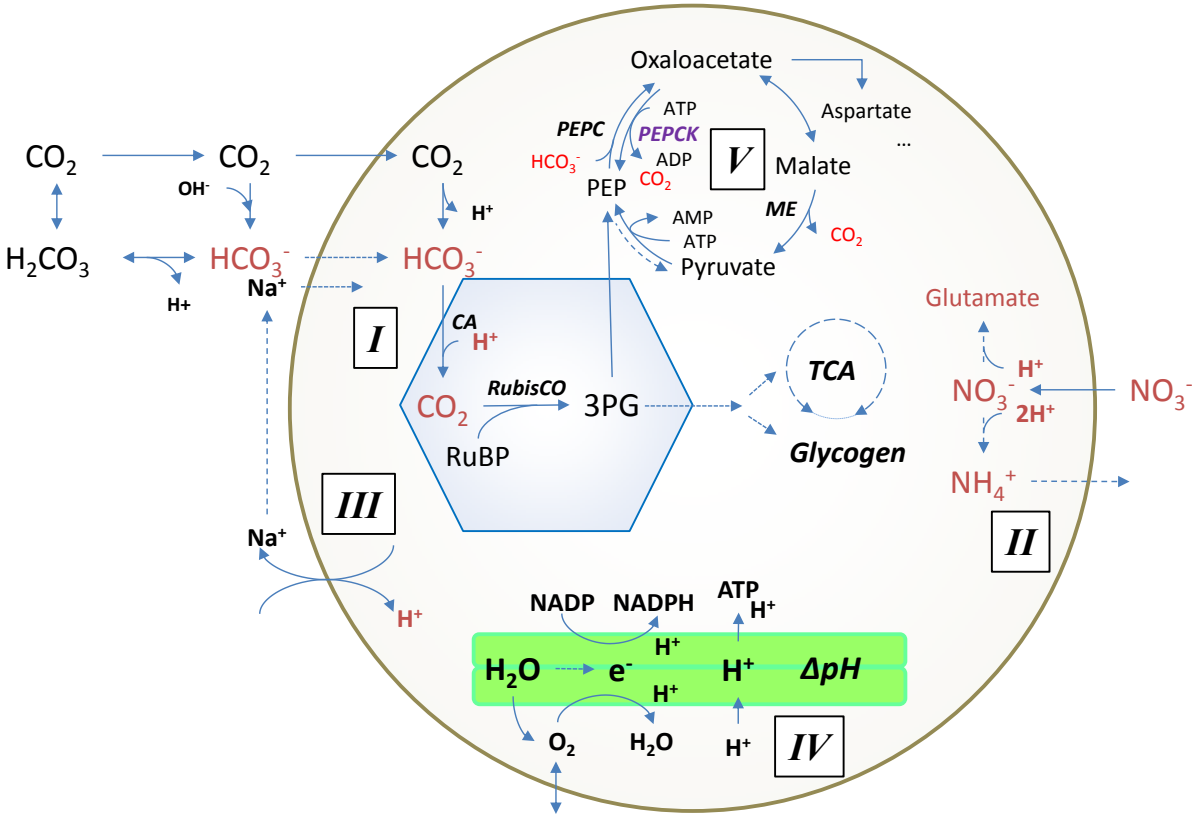

Figure 3.12: Scheme of selected metabolic features affecting the intracellular pH during photosynthesis: ***[I]*** denotes the assimilation of bicarbonate from the surrounding medium, which requires equimolar amounts of protons, i.e. pH_{in} balancing. ***[II]*** illustrates nitrate import and reduction. Assimilation of nitrate *via* ammonium into glutamate requires one balancing proton, excretion of ammonium two. ***[III]*** shows proton import from the medium in exchange with sodium ions. ***[IV]*** illustrates the pH-neutral light energy metabolism and redox control by oxygen reduction to water. ***[V]*** highlights the direct bicarbonate assimilation route *via* PEP-carboxylation and the synthesis of organic acids for pH_{in} balancing. Metabolic cycling *via* malate and pyruvate for means of dissipation of excess energy might be inferred as well (Young et al., 2011; Nogales et al., 2012). Direct pyruvate synthesis from PEP is broadly suppressed in the light (You et al., 2014).

of that C4-type carbon concentration would be the temporal accumulation of organic acids, which might positively contribute to maintaining cellular pH homoeostasis during episodes of high light illumination, see 3.12. Since bicarbonate is one of the main inorganic carbon sources for autotrophic cyanobacterial growth, the need for effective

pH regulation appears inevitable. Nitrate reduction to ammonium and its utilization in amino acid synthesis also requires equimolar amounts of protons, see equation 3.1. Balancing of the cytoplasmic pH is probably achieved by the concerted action of proton import from the medium *via* e.g. Na^+/ H^+ antiporters (Miller et al., 1984; Billini et al., 2008) and probably also by the synthesis and accumulation of molecules with a high pH buffering capacity such as organic acids like malate, fumarate and also citrate, as was observed in this study.

A discriminating feature between the cyanobacterial species is the presence of the enzyme PEPcarboxykinase (PEPCK) in the genome of *Microcystis* PCC 7806. This enzyme directly catalyzes the reaction from oxaloacetate back to PEP with the help of only one molecule ATP, releasing CO_2 and ADP. Compared to the regeneration of PEP from malate by the action of malic enzyme $NADP^+$ and pyruvate-phosphate dikinase, which *in summa* requires 2 ATP (AMP + PP_i is released), the action of PEPCK theoretically saves 50 % of the energy.
Carbon fixation for e.g. carbohydrate synthesis mutually depends on RuBP carboxylation by RubisCO. Thus, the presence of PEPCK could indicate a higher relevance of temporal C4-metabolites accumulation in bloom-forming *Microcystis*. The efficient conversion of e.g. malate to PEP and CO_2 *via* oxaloacetate might be advantageous in supporting RuBP carboxylation after a change from CO_2 limiting conditions and excess light to moderate illumination. Interestingly, PEPCK is also encoded in the genomes of confirmed alkalophils and cyanobacteria living in dense mats, where bicarbonate can be assumed to be the major source of inorganic carbon.

3.5.7 Amino acid metabolism

The onset of high light illumination triggered a pronounced accumulation of most amino acids in all tested strains. The experimental set-up did not allow statements about the exact origin of the measured amino acids. Hence, it can not be distinguished, whether

Table 3.2: PEPCK distribution among cyanobacterial species; selection of *Microcystis* PCC 7806 homologues according to BLASTp (http://blast.ncbi.nlm.nih.gov/Blast)

Strain	Habitat	Accession
Coleofasciculus sp. PCC 7420	microbial mats	WP_006104302
Geitlerinema sp. PCC 7407	mats on different substrates	YP_007108527
Cyanothece sp. PCC 7822	rice fields	YP_003890568
Pleurocapsa sp. PCC 7327	alkaline lakes	YP_007083253
Oscillatoria acuminata PCC 6304	mats on different substrates	YP_007088744
Arthrospira platensis Nies-39	alkalophilic, (sub)tropical	YP_005068380

the observed accumulation of amino acids was due to proteolytic degradation of proteins or *de novo* synthesis. However, the apparent accumulation of cyanophycin granules in *Synechocystis* rather point towards net amino acid and peptide synthesis (Kolodny et al., 2006).

Of the primarily 3-phosphoglycerate derived amino acids serine and glycine, a stronger high light induced increase was observed in *Synechocystis* cells. Though, both amino acids could also be products of the C2 photorespiratory cycle, which might has a higher relevance in *Synechocystis*. Amino acids originating from PEP accumulated most in cells of the *Microcystis* $\Delta mcyB$ mutant, which might imply a regulatory role of microcystin in certain biosynthesis steps of those amino acids. Pyruvate-derived amino acids, especially alanine and leucine accumulated stronger in *Synechocystis*.

Taking into account the proposed flow of carbon from PEPcarboxylation to oxaloacetate *via* malate and the malic enzyme back to pyruvate (Young et al., 2011), it appeared plausible that the associated amino acids accumulated due to this type of carbon cycling in *Synechocystis*. *Microcystis* on the other hand employs the enzyme PEPCK and therefore might accumulate higher amounts of PEP derived amino acids originating from oxaloacetate.

Amino acids of the aspartate family increasingly accumulated in all three strains during high light exposition, probably underlining the importance of PEP carboxylation in cyanobacteria. PEPC activity is regarded to be essential in cyanobacteria (Luinenburg

and Coleman, 1990). For methionine, the strongest increase was observed in the Δ*mcyB* *Microcystis* mutant, which again suggests an active role of microcystin in regulating amino acid metabolism.

Much stronger accumulation was observed for 2-oxoglutarate derived amino acids in *Synechocystis*. Especially the levels of proline and arginine, as well as the arginine-associated and non-proteinogenic amino acids ornithine and citrulline were significantly more abundant in *Synechocystis*. As already discussed above (see also 3.5.6), the data might suggest that *Microcystis* probably did not fuel TCA metabolism *via* PEP towards isocitrate and 2-oxoglutarate, at least not during illumination.

Aspects of nitrate reduction

Nitrate is the main nitrogen source in the culture medium used in this experiment. Its reduction to ammonium requires huge amounts of energy and probably take part in balancing the flow of reducing power derived from the photosystems. For eukaryotic algae, the reduction of nitrate to ammonium and even its excretion was described under carbon limitation (Azuara and Aparicio, 1983). Excretion of ammonium was also reported for filamentous, nitrogen-fixing cyanobacteria, which constitutively produce heterocysts (Ploug et al., 2011). The observation that *Synechocystis* resists relatively high ammonium concentrations in the growth medium, which are otherwise toxic for eukaryotic photoautotrophs may underlines the importance of nitrate reduction under certain conditions (Dai et al., 2014).

$$
\begin{aligned}
&NO_3^- + H_2O + 8\ \{H\} \longrightarrow NH_4^+ + 2\ H_2O + 2\ OH^- \\
&NH_4^+ + \text{2-OG} + 2\ \{H\} \longrightarrow \text{Glutamate} + H_2O + H^+ \\
&\text{---} \\
&NO_3^- + \text{2-OG} + 10\ \{H\} \longrightarrow \text{Glutamate} + 3\ H_2O + OH^-
\end{aligned}
\tag{3.1}
$$

The pronounced accumulation of amino acids especially in *Synechocystis* and, though to a lesser extent also in *Microcystis*, point towards high relevance of nitrate reduction in cyanobacteria under the conditions of the experiment. Nitrate reduction and subsequent assimilation involve equimolar proton uptake (Kohl and Nicklisch, 1988). Thus, the pH increase in the culture medium might in part be attributed to nitrate reduction, see equation 3.1 (adopted from (Kohl and Nicklisch, 1988)) and figure 3.13 and 3.12.

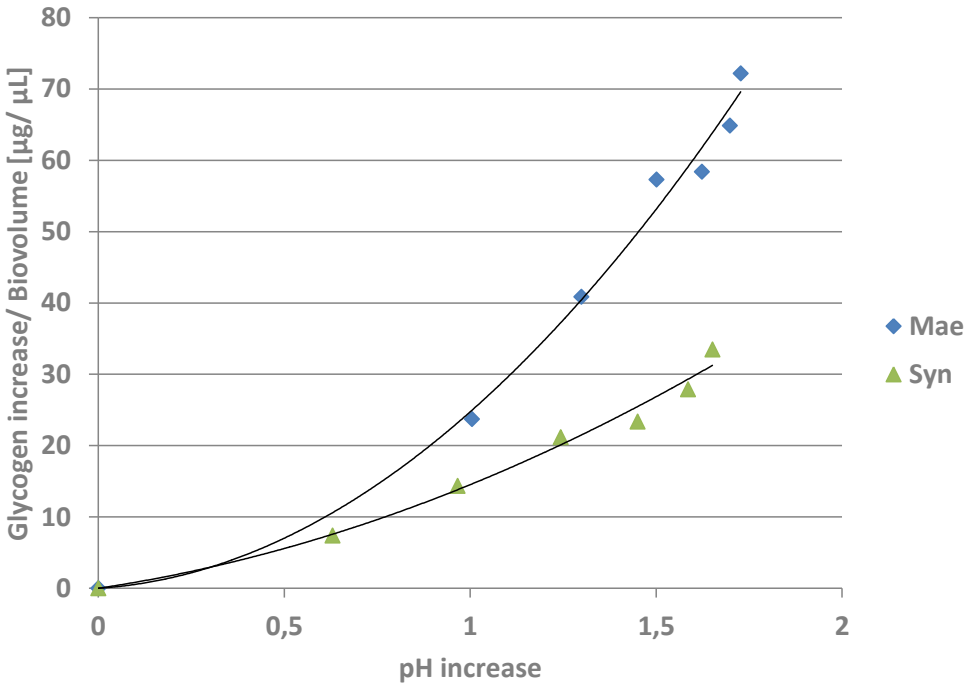

Figure 3.13: Glycogen accumulation over pH increase: The amount of glycogen in *Synechocystis* (Syn) increased only about 50 % of that in *Microcystis* (Mae), whereas the pH increase was almost similar. Less C_i was transformed to glycogen, but higher rates of nitrate assimilation and cyanophycin synthesis probably drove the pH increase in *Synechocystis* to equally high values.

During high light exposition, *Microcystis* and *Synechocystis* showed almost similar pH increases in the medium, whereas the contents of glycogen and cyanophycin differed substantially between both species. *Microcystis* obviously utilized mainly inorganic carbon for glycogen synthesis that drove the increase of the medium pH. Of course, cyanophycin accumulation also requires C_i assimilation. However, substantially higher rates of ni-

trate reduction must be assumed for *Synechocystis*, which contributed to the elevation of the pH in the medium accordingly.

3.5.8 Photorespiration

Under normal conditions, cyanobacteria employ an array of mechanisms to channel excess light energy reaching the cells towards manifold directions, e.g. non-photochemical quenching (NPQ) (Bailey and Grossman, 2008) and photoreduction of oxygen to water (Hackenberg et al., 2009; Allahverdiyeva et al., 2011), as well as metabolic cycling (Young et al., 2011; Nogales et al., 2012) and nitrate reduction, to prevent damage and to maintain favorable intracellular conditions for the production of biomass. In that context, photorespiration must not be thought of as primarily faulty and wasteful metabolic burden, since it is an integral part of the energy channeling network in oxygenic photosynthesis (Tolbert, 1997) and eventually contributes to optimal biosynthesis efficiency of e.g. serine and glycine (Knoop et al., 2010).

Photorespiration in the strict sense, i.e. net oxygen consumption and mobilization of stored carbon for oxidation, was not observed in any of the tested strains, see 3.10. In a broader sense, photorespiration was observed as changed accumulation patterns of metabolites involved in the regeneration of 3-phosphoglycerate from 2-phosphoglycolate. Of all detected and identified metabolites, which were directly assignable to photorespiration, only glycolate showed a significant intracellular increase in *Microcystis* PCC 7806 WT after one hour highlight and after three hours in the $\Delta mcyB$ mutant. Also, excretion of glycolate was observed in both *Microcystis* strains after three hours but not in *Synechocystis*. The intracellular glycolate levels of *Synechocystis* remained constant during the experiment as well, indicating that either photorespiration was running highly efficient, or that detectable photorespiration possibly did not occur at all in that strain under the applied light conditions.

The discrepancy between the dynamics of intracellular glycolate levels and the directly following photorespiratory intermediate glyoxylate in *Microcystis* might be explained by

fundamentally different concentrations of both metabolites under low light conditions. The initially higher concentration of glyoxylate could also indicate metabolic origins different from glycolate. During highlight, the additional glyoxylate produced from glycolate as a direct product of RuBP oxygenation eventually contributed only relatively little to the overall bigger glyoxylate pool. (Knoop et al., 2010) suggested that in cyanobacteria glyoxylate could serve as sole precursor for glycine, serine and cysteine synthesis instead of 3-phosphoglycerate. Thus, a certain level of photorespiration was probably also realized under low light to fuel glyoxylate production. The relatively strong increase of glycolate in *Microcystis* wild-type after one hour could point towards an imbalance of the photorespiratory metabolism directly after elevation of the light intensity, which was overcome after three hours. In cells of the *Microcystis* mutant glycolate levels were not as much increased as in the wild-type after one hour, but after three hours. It would be interesting to see, what happens if the cells were further exposed to high light.

Although not unequivocally attributable to photorespiration, the levels of glycerate in *Microcystis* might indicate regeneration of PG3 *via* the glycerate pathway, especially in the microcystin producing *Microcystis* wild-type. The involvement of the C2 photorespiratory cycle in *Microcystis* might be suggested as well since the accumulation pattern of glycine generally reflected that of glycolate. The presence of a plant-like D3-glycerate kinase could underline an overall higher relevance of PG3 regeneration in *Microcystis* than in *Synechocystis*.

Despite the fact that no significant increase of glycolate levels were detected in *Synechocystis*, the accumulation of serine and glycine could eventually hint towards active photorespiration *via* the C2 cycle. Interestingly, the levels of both amino acids showed the same accumulation pattern in *Synechocystis* as e.g. glutamine and arginine, whose production also involved glutamate. Taken together, it appears likely that the glyoxylate mutually produced by oxygenation of RuBP during photosynthesis indeed served as alternative precursor for glycine and serine synthesis in the tested cyanobacterial strains as proposed by (Knoop et al., 2010).

Glycolate excretion

After three hours both *Microcystis* genotypes had excreted glycolate into the medium, which indicated that parts of the RuBP oxygenation product was not regenerated to PG3 by the cells. Glycolate excretion could eventually be attributed to the specific lifestyle of *Microcystis*. In general, autotrophic phytoplankton benefits from a rich heterotrophic bacterial community for means of re-mineralization of organic matter (Kühl et al., 1996; Kirkwood et al., 2006). Heterotrophs growing on macroscopic colonies in turn are better protected against grazing by zooplankton and benefit from cyanobacterial exudates as source of reduced carbon. Thus, for colony-forming *Microcystis* exudation of e.g. glycolate does not imply complete loss of carbon. High water temperature and low concentrations of N and P limits bacterial growth efficiency (Del Giorgio and Cole, 1998). Under bloom conditions, most of the nutrients (N, P) are fixed as biomass, which means that most of the exudate reduced carbon cannot be utilized by heterotrophs for biomass formation and is again mainly lost by respiration CO_2. The formation of colonies by cyanobacteria could eventually establish a spatially restricted closed bacterial loop so that carbon once acquired effectively remains therein (Tchernov et al., 2003). Accordingly, non-colony forming species like *Synechocystis* would restrict DOC exudation and total loss of carbon.

3.5.9 Conclusions

GC/MS analysis revealed a number of metabolites whose accumulation was affected by microcystin production. Interestingly, many of the respective differences between the *Microcystis* strains were unique for the wild-type, which made the microcystin deficient mutant appear more similar to the control strain *Synechocystis*. Unfortunately, most of those metabolites were unknowns, which limited the number of conclusions that could be drawn from the dataset. However, among the differentially accumulating metabolites in the two *Microcystis* genotypes were several amino acids, the compatible solutes su-

crose and trehalose as well as glycogen and glycolate. The differences in glycolate and glycogen accumulation during the first hour of the experiment might indicate an overall higher initial activity of RubisCO in the microcystin producing wild-type in both directions. During the following two hours of the experiment glycolate accumulated stronger in the microcystin deficient mutant cultures and the glycogen contents of both *Microcystis* genotypes were leveled out as well. It was previously shown that microcystin binds mainly to RubisCO especially during prolonged high light exposition and by that stabilizes the enzyme (Zilliges et al., 2011). It might be speculated that microcystinylation has an activity-modulating effect on RubisCO in both directions and by that eventually plays a role in fine-tuning of the carbon metabolism in *Microcystis* under changing conditions. Together with the elevated levels of stress related compatible solutes in the microcystin deficient *Microcystis* mutant these findings support the hypothesis that microcystin is indeed involved in the regulation of the primary metabolism and by that could contribute to the reported competitive advantage of microcystin producing *Microcystis* genotypes under high light (Zilliges et al., 2011) and carbon limitation (Jähnichen et al., 2007; Van de Waal et al., 2011).

Biotechnological aspects

The data obtained throughout this study support the notion that cyanobacterial species differ substantially in utilizing assimilates. Including *Synechocystis* in this study revealed strain specific metabolic responses to the same experimental conditions. High light exposition of low light adapted cells triggered strain-specific responses, which was reflected by the non-uniform accumulation pattern of many key metabolites. The differences between the two species became most obvious in the very low levels of isocitrate in *Microcystis* cells and the varied accumulation of 2-OG derived amino acids. Furthermore, photorespiration seems of lower relevance in *Synechocystis* under the applied conditions. Remarkably, neither the described capability of *Microcystis* to accumulate glycogen to about 8.5 % the fresh weight, nor the feature of *Synechocystis* to strongly accumulate cyanophycin within only three hours of elevated light exposition had been re-

ported before and would probably not have been observed under constant lab conditions. Although sharing essentially the same primary-metabolic features, different cyanobacteria species obviously follow distinct strategies to accumulate and store assimilates. Hence, metabolomic screening of available strains at changing growth conditions could accelerate the development of strategies for the profitable use of cyanobacteria as source of renewable energy or for the production of base products of the chemical industry.

3.5.10 Limitations and perspectives

Metabolomics is one of the currently most exciting scientific fields, which will contribute strongly to the understanding of the living world. Compared to other widely used –omics approaches, metabolomics is probably the most direct way to examine the effects of environmental stimuli on an organism. Transcriptomics, for example, cannot give least evidence for the amount of gene products due to e.g. posttranscriptional modification events, whereas proteomics cannot provide information about e.g. actual enzyme activities. Metabolomics, on the other hand, directly displays the impact of environmental stimuli on an organism's constitution and can provide straight information about the adaptation of an organism. However, stable metabolite quantities do not imply an unchanged utilization ballast of the respective pathway. For example, increased flux velocities through a metabolic route yielding in accumulation of storage metabolites or finally growth are not necessary represented.
Prerequisites for valid and reproducible metabolome analysis are optimized sampling procedures, robust extraction protocols as well as sensitive and versatile metabolite identification and quantification facilities. Not less important are thorough data processing and profound statistical analysis.

One of the major shortcomings of this metabolomic study was the inability to determine the absolute amounts of metabolites, as well as metabolic fluxes. Thus, some of the conclusions drawn from the existing dataset concerning, e.g. the extent of PEP-

carboxylation and C4-characteristics of cyanobacteria are rather speculative and require additional evidence. The most fundamental limitation of the metabolomics approach followed in this study laid in the incomplete metabolite library, which covered only 104 out of 501 detected metabolites. Consequently, the extension of metabolite libraries is most urgently needed. The application of structure elucidating nuclear magnetic resonance (NMR) in metabolomic analysis of cyanobacteria could further help to figure out, which metabolites are present.

Bioinformatics of the post-genomic era can give valuable information on possible metabolic routes to be expected in an organism. Today, many of the proposed cyanobacterial metabolic pathways are hypothetical, and even the existence of basic routes lack experimental evidence. The combination of metabolic flux analysis with untargeted transcriptomics and robust biochemical characterization of candidate enzymes might help to close the yet persisting gaps of the cyanobacterial metabolic network in the near future. For example, to solve the isocitrate conundrum of *Microcystis*, enzyme assays in cell extracts aiming at the conversion steps from citrate to 2-oxoglutarate might yield a convincing explanation. The general TCA metabolism might also be examined by pulse-chase analysis with C^{13}-labeled/ unlabeled substrates.

Additionally, this metabolomics study focused on the effects of high light treatment on low light adapted cells. Additionally, metabolites not present in each of the strains were not considered for analysis. Thus, the existing dataset should be further examined to figure out general strain-specific differences apart from those induced by treatment with high light.

The glycogen concentration served as a measure for net photosynthesis and suggested overall higher rates for *Microcystis*, which was in line with the observed oxygen evolution. However, glycogen was not the only storage compound in *Synechocystis*. Nitrate reduction to ammonium also triggers pH increase 3.5.7, but not oxygen evolution. It thus was concluded that *Synechocystis* channeled more energy towards amino acid, protein

as well as cyanophycin synthesis, whereas *Microcystis* produced more carbohydrates. To get a general estimate about how effective light energy and nutrients are channeled under the experimental conditions, all of the known storage compounds including poly-β-hydroxyalkanoate might be quantified as well. Alternatively, the dynamics of the cell's elemental composition could be analyzed and compared. Calorimetry and determination of the C, O, H, N, S, P, (Fe) content in cyanobacteria cells might yield valuable information about their general assimilation and adaptation strategies.

Finally, the effect of microcystinylation on the activity of selected enzymes such as RubisCO should be analyzed *in vitro*. The activity of enzymes in $\Delta mcyB$ mutant extracts could be measure with and without previous microcystinylation. The combination with a targeted GC/MS- or LC/MS-based analysis would eventually even allow the determination of the RubisCO oxygenase activity.

Appendix

Tables of estimated p-values using the Tukey's HSD test for differences of means comparing *Microcystis aeruginosa* PCC 7806 (Mar) with the $\Delta mcyB$ mutant (Mut) or with *Synechocystis* PCC 6803 (Syn) at the corresponding time points, p-value ≤ 0.05 in bold

Table 3.3: Oxygen evolutuion upon high light exposition

$\mathbf{t}_{min}$	**0**	**15**	**35**	65	105
Mar *vs.* Mut	0.98499	**0.02679**	0.12952	0.98884	0.89269
Mar *vs.* Syn	0.99999	$\mathbf{6.18 \cdot 10^{-7}}$	$\mathbf{2.79 \cdot 10^{-9}}$	$\mathbf{8.48 \cdot 10^{-7}}$	**0.01065**

Table 3.4: pH dynamics upon high light exposition:

$\mathbf{t}_{min}$	**0**	**20**	**45**	**80**	**135**	**175**
Mar *vs.* Mut	**0.00049**	$\mathbf{4.81 \cdot 10^{-5}}$	**0.02015**	1	1	1
Mar *vs.* Syn	**0.27769**	$\mathbf{4.82 \cdot 10^{-10}}$	$\mathbf{1.13 \cdot 10^{-11}}$	$\mathbf{5.89 \cdot 10^{-9}}$	$\mathbf{1.51 \cdot 10^{-5}}$	**0.00369**

Table 3.5: Glycogen accumulation upon high light exposition

t_{min}	**0**	**30**	**60**	**90**	**120**	**150**	**180**
Mar *vs.* Mut	1	0.999	0.797	0.319	1	1	0.999
Mar *vs.* Syn	0.919	$\mathbf{1.25{\cdot}10^{-11}}$	$\mathbf{1.06{\cdot}10^{-12}}$	$\mathbf{1.06{\cdot}10^{-12}}$	$\mathbf{1.06{\cdot}10^{-12}}$	$\mathbf{1.06{\cdot}10^{-12}}$	$\mathbf{1.06{\cdot}10^{-12}}$

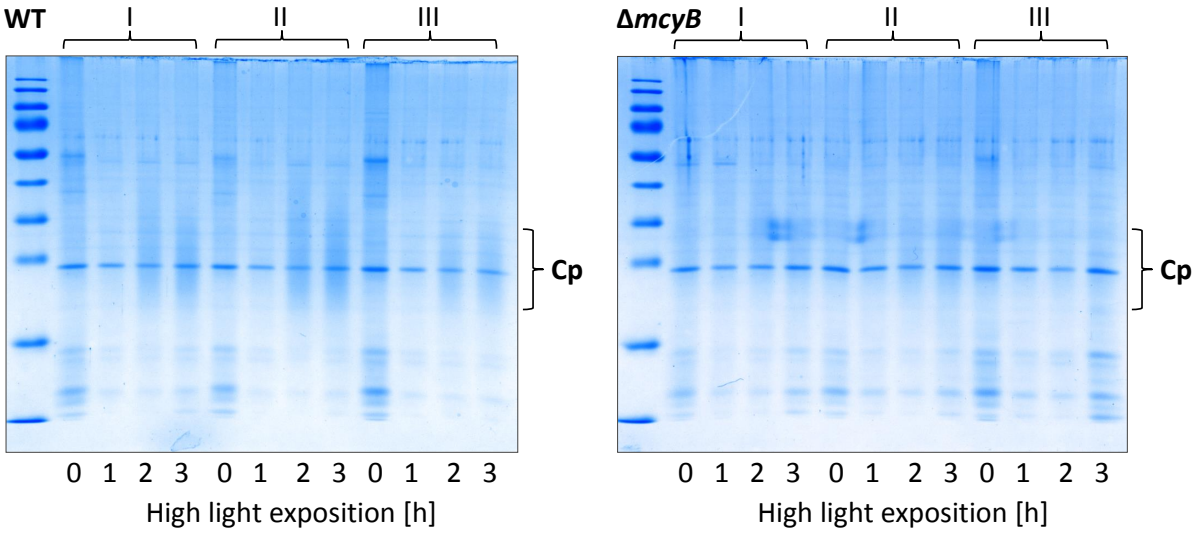

Figure 3.14: Cyanophycin accumulation in three replicates (I-III) of both *Microcystis* genotypes upon high light illumination; Coomassie-stained gels used for relative quantification, see figure 3.11.

4

General Discussion & Outlook

The two previous chapters treated two aspects of microcystin production in *Microcystis* under changing light conditions separately that are mutually connected with each other. Hence, the intention of this final chapter is to provide a synthesis of the drawn conclusions and to give a brief outlook on current- and future studies focusing on the relation between microcystin and pH.

4.1 Ecological aspects of microcystin production

The ancestor of all today's potentially toxic cyanobacteria had the ability to produce microcystin (Rantala et al., 2004). It might be speculated that microcystin synthesis once had been a mutual prerequisite for those cyanobacteria under the ancient environmental conditions. The co-occurrence of toxic and non-toxic strains today might be the consequence of a lowered selection pressure that once favored microcystin producing phenotypes. Thus, the question arises, whether microcystin production is still relevant, at least temporarily or whether it is completely dispensable and just a relic.
However, considering the high overall cost of microcystin synthesis and the maintenance of the genes involved most probably imply a still significant biological role. The co-occurrence of toxic and non-toxic strains might also imply a certain threshold for a trade-off between the cost of microcystin production and its beneficial effects today. It might be argued that microcystin production enables the corresponding phenotypes to occupy sub-niches within chemotypically heterogeneous *Microcystis* communities.

4.2 High light and microcystin

Microcystin production is probably induced by changes of the energy and nutrient status of the cell (Kaebernick et al., 2000; Straub et al., 2011; Humbert et al., 2013). This finding is in line with the observation that the global transcription regulator Ntca binds to the microcystin promoter in *Microcystis* PCC 7806 (Ginn et al., 2010). NtcA is supposed to orchestrate nitrogen uptake and its incorporation into carbon skeletons according to the energy and nutrient status of the cell. Corresponding genes putatively regulated by NtcA furthermore comprise components of the carbon concentrating mechanism (CCM), RubisCO, proteins of photosystem II and I, as well as NADH dehydrogenases, thioredoxin and iron stress-induced protein (Su et al., 2005). Iron also plays a pivotal role in adjusting the cellular redox balance (Helman et al., 2003; Allahverdiyeva et al., 2013).

Association of the transcription factor Fur (ferric uptake regulator) with the promoter region of mcy-genes (Sevilla et al., 2008) furthermore suggests a relation of microcystin to factors connected with high photosynthetic activity such as the cytoplasmic pH.
The results of the metabolomics study point towards the same direction. High light induced the significantly different metabolite accumulation patterns in toxic and nontoxic *Microcystis* PCC 7806.

4.3 Microcystin and high pH

Energization of the photosynthetic apparatus in the light establishes a chemiosmotic pH gradient across the thylakoid membrane, leading to marked alkalinization of the cytoplasm. During illumination the cytoplasmic pH is around 8, which is reflected by the maximum activities of RubisCO and cyanophycin synthetase at around pH 8.2. The cytoplasmic pH could eventually be much higher, when the external medium pH exceeds values greater than 10. Cyanobacteria assimilate significant amounts of the anionic compounds nitrate and bicarbonate during photosynthesis, which implies the existence of effective mechanisms to maintain intracellular pH homeostasis. Otherwise, the cells must have evolved adaptations to tolerate high intracellular pH, at least temporarily.
In the lab, the shift of cultures from low to high light-induced microcystin production and its interaction with proteins. Results of a first experiment using the pH indicator and vital stain Neutral red indeed suggested a pronounced increase of intracellular pH under prolonged high light exposition in *Microcystis*, see figure 4.1. The mechanism of microcystin covalent binding to proteins *in vivo* probably depends on the cytoplasmic pH, see 2.3 and role of microcystin in stabilizing proteins against proteolysis had been demonstrated earlier (Zilliges et al., 2011). However, effects of protein microcystinylation such as protection against e.g. random carbonylation or against damage caused by non-physiologically high pH as well as enzyme-activity modulating properties might be anticipated but need further examination.

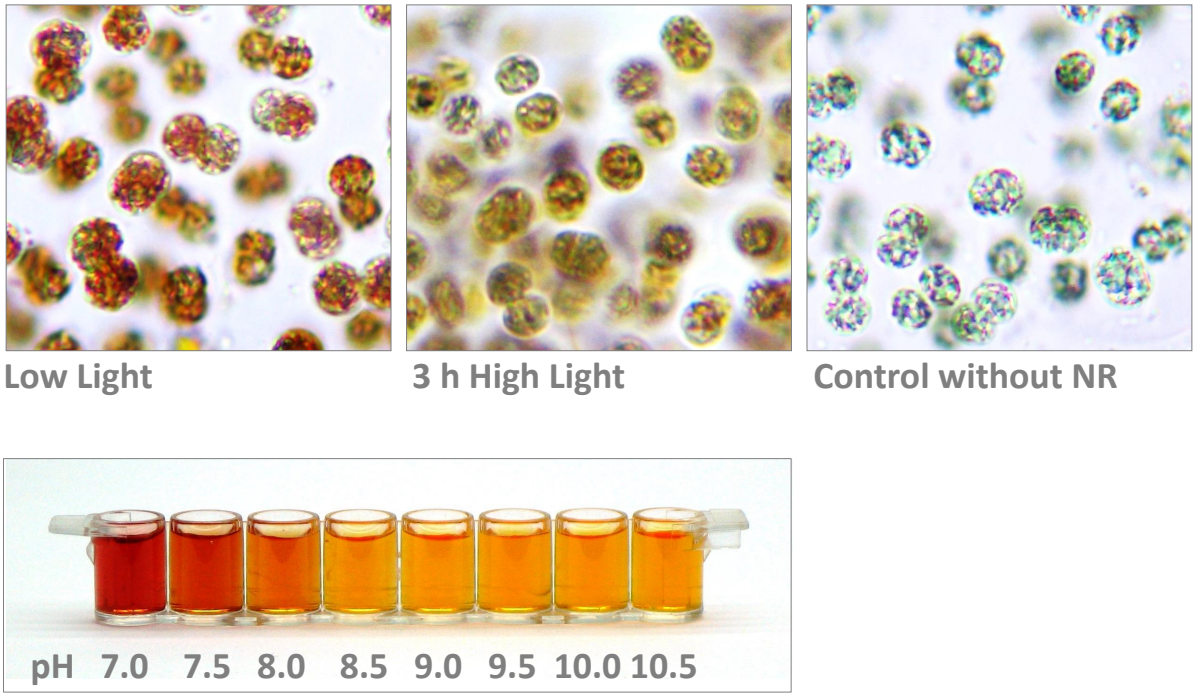

Figure 4.1: Intracellular pH: A *Microcystis* culture was exposed to high light conditions for 3 hours, mixed 1:20 with a 1 % Neutral red BG 11 solution and incubated for 10 minutes before observation. Cells from a low light adapted culture were treated equally. Unstained cells served as control. Under low light conditions the intracellular pH appears to be around 7 or lower. The yellow colour of Neutral red indicates elevated cytoplasmic pH above $\geq$ 8.5 after high light exposition. Figure from (Meissner et al., 2014).

4.4 Sodium depletion phenotype

The strain-specific differences in terms of medium pH increase and glycogen accumulation presented in figure 3.13 were the initial motivation to grow *Synechocystis* PCC 6803, the microcystin producing strain *Microcystis aeruginosa* PCC 7806 and the deficient $\Delta mcyB$ mutant in sodium depleted BG-11 medium under standard low light conditions. Sodium is needed for bicarbonate uptake, which requires HCO_3^-/ Na^+ symport (Kaplan et al., 1984) and pH balancing that involves Na^+/ H^+ antiporters. Both components are encoded in a single gene cluster suggesting their concerted action (San-

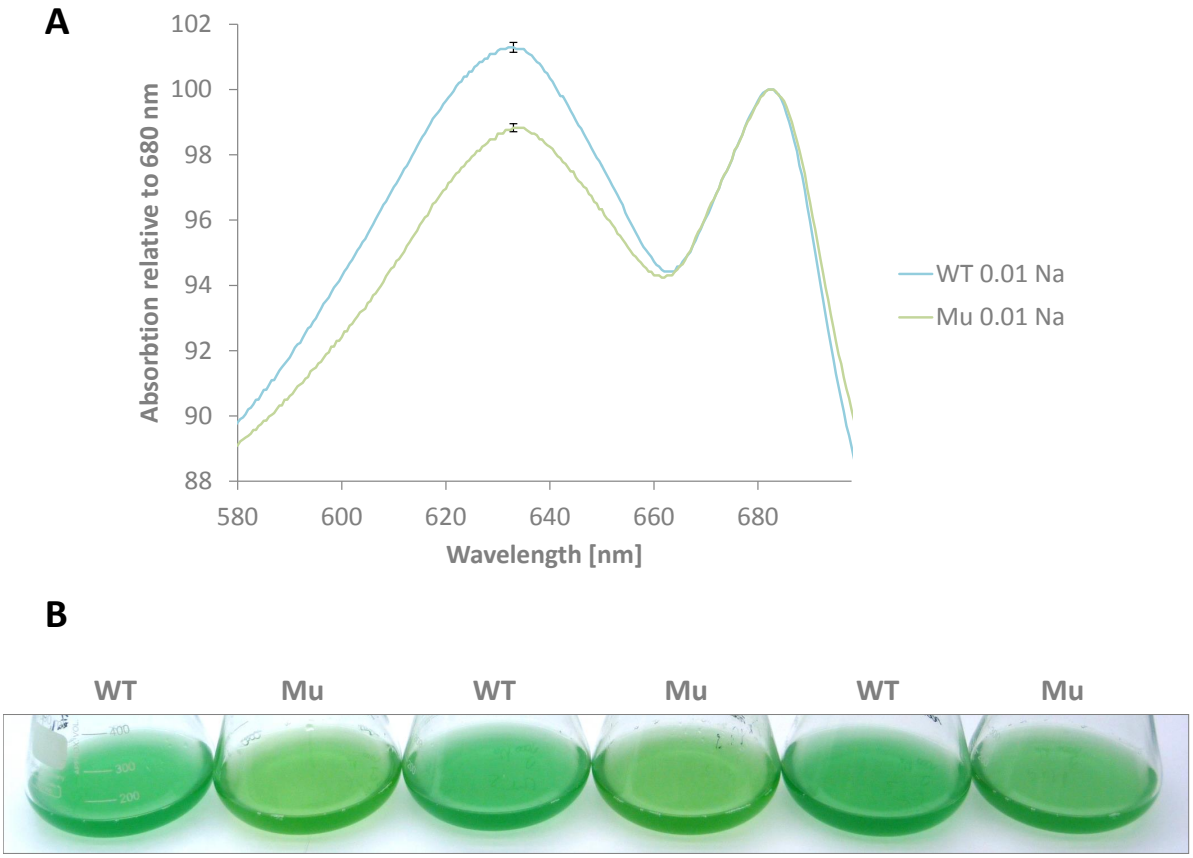

Figure 4.2: Impact of sodium depletion, A: illustrates the absorption spectra of *Microcystis* PCC 7806 wild-type (WT) and the microcystin deficient Δ*mcyB* mutant (Mu) grown at 1 % of the usual sodium concentration. **B:** is a photograph of the respective cultures.

drini et al., 2014).

Sodium deprivation repeatedly induced pronounced phenotypic differences between the *Microcystis* wild-type and the Δ*mcyB* mutant, see figure 4.2. The ratio between PS-II accessory phycobiliproteins (632 nm) and chlorophyll a (680 nm) was reduced in the Δ*mcyB* mutant but not in the wild-type. Two out of three *Synechocystis* culture replicates obviously did not survive the low sodium content in the medium and could not be analyzed further.

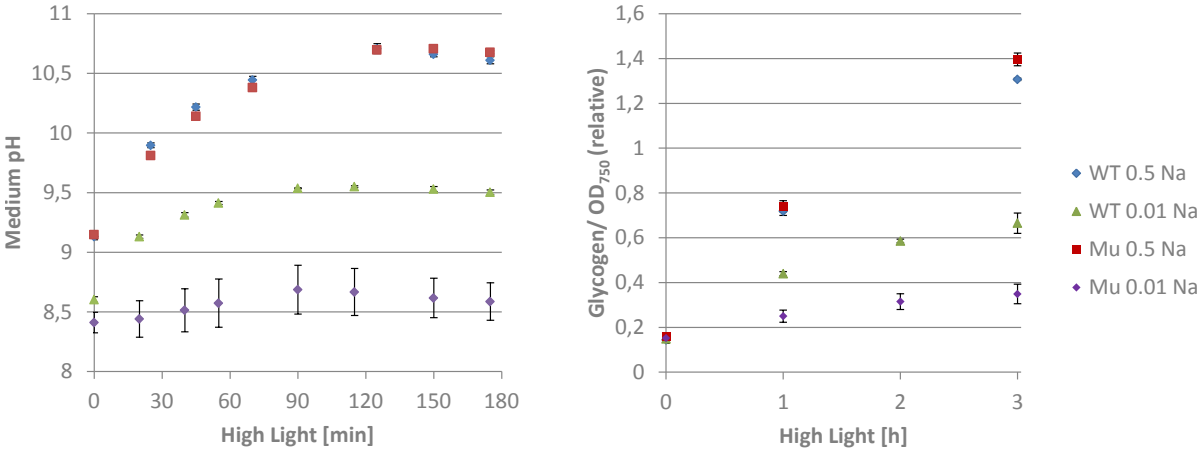

Figure 4.3: High light and sodium depletion: The Δ*mcyB* mutant (Mu) showed less photosynthetic activity at 1 % of the usual sodium concentration as reflected by lower pH increase in the medium and less glycogen accumulation when compared to the wild-type (WT). 50 % sodium concentration had no detectable impact on either strain.

High light exposition of the sodium depleted cultures indicated a higher photosynthetic activity in the wild-type, as became visible by higher amounts of stored glycogen and the increase of the medium pH, see figure 4.3.

In which way microcystin was involved in phenotype induction remains the matter of future research. However, elevated microcystin production and higher growth rates of the *Microcystis* PCC 7806 wild-type compared to the deficient Δ*mcyB* mutant under sodium depletion were already reported (Jähnichen et al., 2007). Whether the microcystin dependent sodium depletion phenotype is primarily caused by C_i limitation due to impairment of Na^+/ HCO_3^- symport (Jähnichen et al., 2007) or Na^+/ H^+ antiport for maintaining pH homeostasis has to be clarified.

Bibliography

Ahlert, C. (2013). Microcystin-einfluss auf proteine des calvin-benson-zyklus. Master's thesis, University of Potsdam.

Alexova, R., Haynes, P. A., Ferrari, B. C., and Neilan, B. A. (2011). Comparative protein expression in different strains of the bloom-forming cyanobacterium microcystis aeruginosa. *Molecular and Cellular Proteomics*, 10(9).

Alfonso, M., Perewoska, I., and Kirilovsky, D. (2001). Redox control of ntca gene expression in synechocystis sp. pcc 6803. nitrogen availability and electron transport regulate the levels of the ntca protein. *Plant Physiology*, 125(2):969–981.

Allahverdiyeva, Y., Ermakova, M., Eisenhut, M., Zhang, P., Richaud, P., Hagemann, M., Cournac, L., and Aro, E.-M. (2011). Interplay between flavodiiron proteins and photorespiration in synechocystis sp. pcc 6803. *Journal of Biological Chemistry*, 286(27):24007–24014.

Allahverdiyeva, Y., Mustila, H., Ermakova, M., Bersanini, L., Richaud, P., Ajlani, G., Battchikova, N., Cournac, L., and Aro, E.-M. (2013). Flavodiiron proteins flv1 and flv3 enable cyanobacterial growth and photosynthesis under fluctuating light. *Proceedings of the National Academy of Sciences*.

Anderson, L. E. (1971). Chloroplast and cytoplasmic enzymes ii. pea leaf triose phos-

phate isomerases. *Biochimica et Biophysica Acta (BBA) - Enzymology*, 235(1):237 – 244.

Azuara, M. P. and Aparicio, P. J. (1983). In vivo blue-light activation of chlamydomonas reinhardii nitrate reductase. *Plant Physiology*, 71(2):286–290.

Bailey, S. and Grossman, A. (2008). Photoprotection in cyanobacteria: Regulation of light harvesting. *Photochemistry and Photobiology*, 84(6):1410–1420.

Benjamini, Y. and Yekutieli, D. (2001). The control of the false discovery rate in multiple testing under dependency. *Annals of statistics*, pages 1165–1188.

Bersanini, L., Battchikova, N., Jokel, M., Rehman, A., Vass, I., Allahverdiyeva, Y., and Aro, E.-M. (2014). Flavodiiron protein flv2/flv4-related photoprotective mechanism dissipates excitation pressure of psii in cooperation with phycobilisomes in cyanobacteria. *Plant Physiology*, 164(2):805–818.

Billini, M., Stamatakis, K., and Sophianopoulou, V. (2008). Two members of a network of putative na+/h+ antiporters are involved in salt and ph tolerance of the freshwater cyanobacterium synechococcus elongatus. *Journal of Bacteriology*, 190(19):6318–6329.

Börner, T. and Dittmann, E. (2005). Molecular biology of cyanobacterial toxins. In Huisman, J., Matthijs, H. C. P., and Visser, P. M., editors, *Harmful Cyanobacteria*, volume 3 of *Aquatic Ecology Series*, pages 25–40. Springer Netherlands.

Briand, J. F., Jacquet, S., Bernard, C., and Humbert, J. F. (2003). Health hazards for terrestrial vertebrates from toxic cyanobacteria in surface water ecosystems. *Veterinary Research*, 34(4):361–377.

Bricker, T. M., Zhang, S., Laborde, S. M., Mayer, P. R., Frankel, L. K., and Moroney, J. V. (2004). The malic enzyme is required for optimal photoautotrophic growth of synechocystis sp. strain pcc 6803 under continuous light but not under a diurnal light regimen. *Journal of Bacteriology*, 186(23):8144–8148.

Carmichael, W. W. and An, J. (1999). Using an enzyme linked immunosorbent assay (elisa) and a protein phosphatase inhibition assay (ppia) for the detection of microcystins and nodularins. *Natural Toxins*, 7(6):377–385.

Christiansen, G., Kurmayer, R., Liu, Q., and Börner, T. (2006). Transposons inactivate biosynthesis of the nonribosomal peptide microcystin in naturally occurring planktothrix spp. *Applied and Environmental Microbiology*, 72(1):117–123.

Christiansen, G., Molitor, C., Philmus, B., and Kurmayer, R. (2008). Nontoxic strains of cyanobacteria are the result of major gene deletion events induced by a transposable element. *Molecular Biology and Evolution*, 25(8):1695–1704.

Dai, G.-Z., Qiu, B.-S., and Forchhammer, K. (2014). Ammonium tolerance in the cyanobacterium synechocystis sp. strain pcc 6803 and the role of the psba multigene family. *Plant, Cell and Environment*, 37(4):840–851.

Dalle-Donne, I., Aldini, G., Carini, M., Colombo, R., Rossi, R., and Milzani, A. (2006). Protein carbonylation, cellular dysfunction, and disease progression. *Journal of cellular and molecular medicine*, 10(2):389–406.

Del Giorgio, P. A. and Cole, J. J. (1998). Bacterial growth efficiency in natural aquatic systems. *Annual Review of Ecology and Systematics*, 29(1):503–541.

DeVries, S. E., Galey, F. D., Namikoshi, M., and Woo, J. C. (1993). Clinical and pathologic findings of blue-green algae (microcystis aeruginosa) intoxication in a dog. *Journal of Veterinary Diagnostic Investigation*, 5(3):403–408.

Dittmann, E., Fewer, D. P., and Neilan, B. A. (2013). Cyanobacterial toxins: biosynthetic routes and evolutionary roots. *FEMS Microbiology Reviews*, 37(1):23–43.

Dittmann, E., Neilan, B. A., Erhard, M., vonDohren, H., and Borner, T. (1997). Insertional mutagenesis of a peptide synthetase gene that is responsible for hepatotoxin production in the cyanobacterium microcystis aeruginosa pcc 7806. *Molecular Microbiology*, 26(4):779–787.

Dokulil, M. and Teubner, K. (2000). Cyanobacterial dominance in lakes. *Hydrobiologia*, 438(1-3):1–12.

Doorn, J. A. and Petersen, D. R. (2002). Covalent modification of amino acid nucleophiles by the lipid peroxidation products 4-hydroxy-2-nonenal and 4-oxo-2-nonenal. *Chemical Research in Toxicology*, 15(11):1445–1450. PMID: 12437335.

Dunn, I. G. (1967). Diurnal fluctuations of physicochemical conditions in a shallow tropical pond. *Limnology and Oceanography*, 12(1):pp. 151–154.

Dziallas, C. and Grossart, H.-P. (2011). Increasing oxygen radicals and water temperature select for toxic microcystis sp. *PLoS ONE*, 6(9):e25569.

Eriksson, J. E., Gronberg, L., Nygard, S., Slotte, J. P., and Meriluoto, J. A. O. (1990a). Hepatocellular uptake of h-3 dihydromicrocystin-lr, a cyclic peptide toxin. *Biochimica Et Biophysica Acta*, 1025(1):60–66.

Eriksson, J. E., Toivola, D., Meriluoto, J. A. O., Karaki, H., Han, Y. G., and Hartshorne, D. (1990b). Hepatocyte deformation induced by cyanobacterial toxins reflects inhibition of protein phosphatases. *Biochemical and Biophysical Research Communications*, 173(3):1347–1353.

Falkner, G., Horner, F., Werdan, K., and Heldt, H. W. (1976). ph changes in the cytoplasm of the blue-green alga anacystis nidulans caused by light-dependent proton flux into the thylakoid space. *Plant Physiology*, 58(6):717–718.

Fastner, J., Flieger, I., and Neumann, U. (1998). Optimised extraction of microcystins from field samples - a comparison of different solvents and procedures. *Water Research*, 32(10):3177–3181.

Fewer, D. P., Halinen, K., Sipari, H., Bernardova, K., Manttari, M., Eronen, E., and Sivonen, K. (2011). Non-autonomous transposable elements associated with inactivation of microcystin gene clusters in strains of the genus anabaena isolated from the baltic sea. *Environmental Microbiology Reports*, 3(2):189–194.

Francis, G. (1878). Poisonous australian lake. *Nature*, 18:11–12. Letters to Editor.

Gerbersdorf, S. U. (2006). An advanced technique for immuno-labelling of microcystins in cryosectioned cells of microcystis aeruginosa pcc 7806 (cyanobacteria): Implementations of an experiment with varying light scenarios and culture densities. *Toxicon*, 47(2):218 – 228.

Ginn, H. P., Pearson, L. A., and Neilan, B. A. (2010). Ntca from microcystis aeruginosa pcc 7806 is autoregulatory and binds to the microcystin promoter. *Applied and Environmental Microbiology*, 76(13):4362–4368.

Hackenberg, C., Engelhardt, A., Matthijs, H., Wittink, F., Bauwe, H., Kaplan, A., and Hagemann, M. (2009). Photorespiratory 2-phosphoglycolate metabolism and photoreduction of o2 cooperate in high-light acclimation of synechocystis sp. strain pcc 6803. *Planta*, 230(4):625–637.

Havens, K. E. (2008). Cyanobacteria blooms: effects on aquatic ecosystems. In Hudnell, H., editor, *Cyanobacterial Harmful Algal Blooms: State of the Science and Research Needs*, volume 619 of *Advances in Experimental Medicine and Biology*, pages 733–747. Springer New York.

Helman, Y., Tchernov, D., Reinhold, L., Shibata, M., Ogawa, T., Schwarz, R., Ohad, I., and Kaplan, A. (2003). Genes encoding a-type flavoproteins are essential for photoreduction of o2 in cyanobacteria. *Current Biology*, 13(3):230 – 235.

Hoiczyk, E. and Hansel, A. (2000). Cyanobacterial cell walls: News from an unusual prokaryotic envelope. *Journal of Bacteriology*, 182(5):1191–1199.

Huege, J., Krall, L., Steinhauser, M.-C., Giavalisco, P., Rippka, R., de Marsac, N. T., and Steinhauser, D. (2011). Sample amount alternatives for data adjustment in comparative cyanobacterial metabolomics. *Analytical and bioanalytical chemistry*, 399(10):3503–3517.

Huisman, J., Sharples, J., Stroom, J. M., Visser, P. M., Kardinaal, W. E. A., Verspagen, J. M. H., and Sommeijer, B. (2004). Changes in turbulent mixing shift competition for light between phytoplankton species. *Ecology*, 65(4):2960–2970.

Humbert, J.-F., Barbe, V., Latifi, A., Gugger, M., Calteau, A., Coursin, T., Lajus, A., Castelli, V., Oztas, S., Samson, G., Longin, C., Medigue, C., and de Marsac, N. T. (2013). A tribute to disorder in the genome of the bloom-forming freshwater cyanobacterium <italic>microcystis aeruginosa</italic>. *PLoS ONE*, 8(8):e70747.

Ito, E., Takai, A., Kondo, F., Masui, H., Imanishi, S., and ichi Harada, K. (2002). Comparison of protein phosphatase inhibitory activity and apparent toxicity of microcystins and related compounds. *Toxicon*, 40(7):1017 – 1025.

Jähnichen, S., Ihle, T., Petzoldt, T., and Benndorf, J. (2007). Impact of inorganic carbon availability on microcystin production by microcystis aeruginosa pcc 7806. *Applied and Environmental Microbiology*, 73(21):6994–7002.

Jochimsen, E. M., Carmichael, W. W., An, J., Cardo, D. M., Cookson, S. T., Holmes, C. E., Antunes, M. B., de Melo Filho, D. A., Lyra, T. M., Barreto, V. S. T., Azevedo, S. M., and Jarvis, W. R. (1998). Liver failure and death after exposure to microcystins at a hemodialysis center in brazil. *New England Journal of Medicine*, 338(13):873–878.

Jöhnk, K. D., Huisman, J., Sharples, J., Sommeijer, B., Visser, P. M., and Stroom, J. M. (2008). Summer heatwaves promote blooms of harmful cyanobacteria. *Global Change Biology*, 14(3):495–512.

Kaebernick, M., Neilan, B. A., Börner, T., and Dittmann, E. (2000). Light and the transcriptional response of the microcystin biosynthesis gene cluster. *Applied and Environmental Microbiology*, 66(8):3387–3392.

Kaebernick, M., Rohrlack, T., Christoffersen, K., and Neilan, B. A. (2001). A spontaneous mutant of microcystin biosynthesis: genetic characterization and effect on daphnia. *Environmental Microbiology*, 3(11):669–679.

Kaplan, A., Volokita, M., Zenvirth, D., and Reinhold, L. (1984). An essential role for sodium in the bicarbonate transporting system of the cyanobacterium anabaena variabilis. *FEBS Letters*, 176(1):166 – 168.

Kardinaal, W. E. A., Tonk, L., Janse, I., Hol, S., Slot, P., Huisman, J., and Visser, P. M. (2007). Competition for light between toxic and nontoxic strains of the harmful cyanobacterium microcystis. *Applied and Environmental Microbiology*, 73(9):2939–2946.

Kaya, K. and Sano, T. (1999). Total microcystin determination using erythro-2-methyl-3-(methoxy-d3)-4-phenylbutyric acid (mmpb-d3) as the internal standard as the internal standard. *Analytica Chimica Acta*, 386(1):107–112.

Kehr, J. (2009). *Characterisation of the lectin microvirin from Microcystis aeruginosa PCC 7806 and new insights into the role of microcystin*. PhD thesis.

Kelly, G. and Latzko, E. (1976). Inhibition of spinach-leaf phosphofructokinase by 2-phosphoglycollate. *{FEBS} Letters*, 68(1):55 – 58.

Kinney, J., Axen, S., and Kerfeld, C. (2011). Comparative analysis of carboxysome shell proteins. *Photosynthesis Research*, 109(1-3):21–32.

Kirkwood, A., Nalewajko, C., and Fulthorpe, R. (2006). The effects of cyanobacterial exudates on bacterial growth and biodegradation of organic contaminants. *Microbial Ecology*, 51(1):4–12.

Klähn, S. and Hagemann, M. (2011). Compatible solute biosynthesis in cyanobacteria. *Environmental Microbiology*, 13(3):551–562.

Knoop, H., Zilliges, Y., Lockau, W., and Steuer, R. (2010). The metabolic network of synechocystis sp. pcc 6803: Systemic properties of autotrophic growth. *Plant Physiology*, 154(1):410–422.

Kohl, J.-G. and Nicklisch, A. (1988). Ökophysiologie der algen. *Akademie- Verlag Berlin*.

Kolodny, N. H., Bauer, D., Bryce, K., Klucevsek, K., Lane, A., Medeiros, L., Mercer, W., Moin, S., Park, D., Petersen, J., Wright, J., Yuen, C., Wolfson, A. J., and Allen, M. M. (2006). Effect of nitrogen source on cyanophycin synthesis in synechocystis sp. strain pcc 6308. *Journal of Bacteriology*, 188(3):934–940.

Komarek, J. and Anagnostidis, K. (1998). In *Suesswasserflora von Mitteleuropa; Bd. 19 Cyanoprocaryota Teil 1 Croococcales*. Gustav Fischer Verlag Jena.

Kondo, F., Ikai, Y., Oka, H., Okumura, M., Ishikawa, N., Harada, K., Matsuura, K., Murata, H., and Suzuki, M. (1992). Formation, characterization, and toxicity of the glutathione and cysteine conjugates of toxic heptapeptide microcystins. *Chemical Research in Toxicology*, 5(5):591–596.

Kopka, J., Schauer, N., Krueger, S., Birkemeyer, C., Usadel, B., Bergmüller, E., Dörmann, P., Weckwerth, W., Gibon, Y., Stitt, M., et al. (2005). The golm metabolome database. *Bioinformatics*, 21(8):1635–1638.

Krall, L., Huege, J., Catchpole, G., Steinhauser, D., and Willmitzer, L. (2009). Assessment of sampling strategies for gas chromatography–mass spectrometry (gc–ms) based metabolomics of cyanobacteria. *Journal of Chromatography B*, 877(27):2952–2960.

Kühl, M., Glud, R. N., Ploug, H., and Ramsing, N. B. (1996). Microenvironmental control of photosynthesis and photosynthesis-coupled respiration in an epilithic cyanobacterial biofilm1. *Journal of Phycology*, 32(5):799–812.

Kurmayer, R. and Kutzenberger, T. (2003). Application of real-time pcr for quantification of microcystin genotypes in a population of the toxic cyanobacterium microcystis sp. *Applied and Environmental Microbiology*, 69(11):6723–6730.

Latifi, A., Ruiz, M., and Zhang, C.-C. (2009). Oxidative stress in cyanobacteria. *FEMS Microbiology Reviews*, 33(2):258–278.

Le Ai Nguyen, V., Tanabe, Y., Matsuura, H., Kaya, K., and Watanabe, M. M. (2012). Morphological, biochemical and phylogenetic assessments of water-bloom-forming

tropical morphospecies of microcystis (chroococcales, cyanobacteria). *Phycological Research*, 60(3):208–222.

Legendre, P. and Legendre, L. (1998). *Numerical ecology*. Elsevier.

Li, H., Sherman, D. M., Bao, S., and Sherman, L. A. (2001). Pattern of cyanophycin accumulation in nitrogen-fixing and non-nitrogen-fixing cyanobacteria. *Archives of microbiology*, 176(1-2):9–18.

Luinenburg, I. and Coleman, J. (1990). A requirement for phosphoenolpyruvate carboxylase in the cyanobacterium synechococcus pcc 7942. *Archives of Microbiology*, 154(5):471–474.

Lutolf, M. P., Tirelli, N., Cerritelli, S., Cavalli, L., and Hubbell, J. A. (2001). Systematic modulation of michael-type reactivity of thiols through the use of charged amino acids. *Bioconjugate Chemistry*, 12(6):1051–1056.

Lyons, T. W., Reinhard, C. T., and Planavsky, N. J. (2014). The rise of oxygen in earth/'s early ocean and atmosphere. *Nature*, 506(7488):307–315.

Madian, A. G. and Regnier, F. E. (2010). Proteomic identification of carbonylated proteins and their oxidation sites. *Journal of Proteome Research*, 9(8):3766–3780.

Marcus, Y., Altman-Gueta, H., Finkler, A., and Gurevitz, M. (2003). Dual role of cysteine 172 in redox regulation of ribulose 1,5-bisphosphate carboxylase/oxygenase activity and degradation. *Journal of Bacteriology*, 185(5):1509–1517.

Marcus, Y., Berry, J., and Pierce, J. (1992). Photosynthesis and photorespiration in a mutant of the cyanobacterium synechocystis pcc 6803 lacking carboxysomes. *Planta*, 187(4):511–516.

Marin-Navarro, J. and Moreno, J. (2003). Modification of the proteolytic fragmentation pattern upon oxidation of cysteines from ribulose 1,5-bisphosphate carboxylase/oxygenase. *Biochemistry*, 42(50):14930–14938.

Meissner, S., Fastner, J., and Dittmann, E. (2013). Microcystin production revisited: conjugate formation makes a major contribution. *Environmental Microbiology*, 15(6):1810–1820.

Meissner, S., Steinhauser, D., and Dittmann, E. (2014). Metabolomic analysis indicates a pivotal role of the hepatotoxin microcystin in high light adaptation of microcystis. *Environmental Microbiology*, pages n/a–n/a.

Metcalf, J. S., Bell, S. G., and Codd, G. A. (2001). Colorimetric immuno-protein phosphatase inhibition assay for specific detection of microcystins and nodularins of cyanobacteria. *Applied and Environmental Microbiology*, 67(2):904–909.

Miller, A. G., Turpin, D. H., and Canvin, D. T. (1984). Na+ requirement for growth, photosynthesis, and ph regulation in the alkalotolerant cyanobacterium synechococcus leopoliensis. *Journal of Bacteriology*, 159(1):100–106.

Muller-Navarra, D. C., Brett, M. T., Park, S., Chandra, S., Ballantyne, A. P., Zorita, E., and Goldman, C. R. (2004). Unsaturated fatty acid content in seston and trophodynamic coupling in lakes. *Nature*, 427(6969):69–72.

Nakagawa, M., Takamura, Y., and Yagi, O. (1987). Isolation and characterization of the slime from a cyanobacterium, microcystis-aeruginosa k-3a. *Agricultural and Biological Chemistry*, 51(2):329–337.

Neilan, B. A., Pearson, L. A., Muenchhoff, J., Moffitt, M. C., and Dittmann, E. (2013). Environmental conditions that influence toxin biosynthesis in cyanobacteria. *Environmental Microbiology*, 15(5):1239–1253.

Nogales, J., Gudmundsson, S., Knight, E. M., Palsson, B. O., and Thiele, I. (2012). Detailing the optimality of photosynthesis in cyanobacteria through systems biology analysis. *Proceedings of the National Academy of Sciences*, 109(7):2678–2683.

Otsuka, S., Suda, S., Shibata, S., Oyaizu, H., Matsumoto, S., and Watanabe, M. M. (2001). A proposal for the unification of five species of the cyanobacterial genus

microcystis kützing ex lemmermann 1907 under the rules of the bacteriological code. *International Journal of Systematic and Evolutionary Microbiology*, 51(3):873–9.

Paerl, H. W. and Huisman, J. (2008). Blooms like it hot. *Science*, 320(5872):57–58.

Paerl, H. W. and Otten, T. G. (2013). Harmful cyanobacterial blooms: Causes, consequences, and controls. *Microbial Ecology*, 65(4):995–1010.

Paerl, H. W. and Ustach, J. F. (1982). Blue-green-algal scums - an explanation for their occurrence during fresh-water blooms. *Limnology and Oceanography*, 27(2):212–217.

Pereira, S. R., Vasconcelos, V. M., and Antunes, A. (2013). Computational study of the covalent bonding of microcystins to cysteine residues - a reaction involved in the inhibition of the ppp family of protein phosphatases. *FEBS Journal*, 280(2):674–680.

Pflugmacher, S., Wiegand, C., Oberemm, A., Beattie, K. A., Krause, E., Codd, G. A., and Steinberg, C. E. (1998). Identification of an enzymatically formed glutathione conjugate of the cyanobacterial hepatotoxin microcystin-lr: the first step of detoxication. *Biochimica et Biophysica Acta (BBA) - General Subjects*, 1425(3):527 – 533.

Ploug, H., Adam, B., Musat, N., Kalvelage, T., Lavik, G., Wolf-Gladrow, D., and Kuypers, M. M. M. (2011). Carbon, nitrogen and o2 fluxes associated with the cyanobacterium *Nodularia spumigena* in the baltic sea. *ISME J*, 5(9):1549–1558.

Price, G. (2011). Inorganic carbon transporters of the cyanobacterial co2 concentrating mechanism. *Photosynthesis Research*, 109(1-3):47–57.

Price, G. D., Badger, M. R., Woodger, F. J., and Long, B. M. (2008). Advances in understanding the cyanobacterial co2-concentrating-mechanism (ccm): functional components, ci transporters, diversity, genetic regulation and prospects for engineering into plants. *Journal of Experimental Botany*, 59(7):1441–1461.

Rantala, A., Fewer, D. P., Hisbergues, M., Rouhiainen, L., Vaitomaa, J., Börner, T., and Sivonen, K. (2004). Phylogenetic evidence for the early evolution of microcystin

synthesis. *Proceedings of the National Academy of Sciences of the United States of America*, 101(2):568–573.

Reynolds, C. S., Oliver, R. L., and Walsby, A. E. (1987). Cyanobacterial dominance: The role of buoyancy regulation in dynamic lake environments. *New Zealand Journal of Marine and Freshwater Research*, 21(3):379–390.

Rippka, R., Deruelles, J., Waterbury, J. B., Herdman, M., and Stanier, R. Y. (1979). Generic assignments, strain histories and properties of pure cultures of cyanobacteria. *Journal of General Microbiology*, 111(1):1–61.

Rohrlack, T., Dittmann, E., Borner, T., and Christoffersen, K. (2001). Effects of cell-bound microcystins on survival and feeding of daphnia spp. *Applied and Environmental Microbiology*, 67(8):3523–3529.

Rohrlack, T., Dittmann, E., Henning, M., Börner, T., and Kohl, J.-G. (1999). Role of microcystins in poisoning and food ingestion inhibition of daphnia galeata caused by the cyanobacterium microcystis aeruginosa. *Applied and Environmental Microbiology*, 65(2):737–739.

Runnegar, M., Berndt, N., Kong, S. M., Lee, E. Y. C., and Zhang, L. F. (1995). In-vivo and in-vitro binding of microcystin to protein phosphatase-1 and phosphatase-2a. *Biochemical and Biophysical Research Communications*, 216(1):162–169.

Sandrini, G., Matthijs, H. C. P., Verspagen, J. M. H., Muyzer, G., and Huisman, J. (2014). Genetic diversity of inorganic carbon uptake systems causes variation in co2 response of the cyanobacterium microcystis. *ISME J*, 8(3):589–600.

Schatz, D., Keren, Y., Vardi, A., Sukenik, A., Carmeli, S., Borner, T., Dittmann, E., and Kaplan, A. (2007). Towards clarification of the biological role of microcystins, a family of cyanobacterial toxins. *Environmental Microbiology*, 9(4):965–970.

Sevilla, E., Martin-Luna, B., Vela, L., Bes, M. T., Fillat, M. F., and Peleato, M. L.

(2008). Iron availability affects mcyd expression and microcystin-lr synthesis in microcystis aeruginosa pcc7806. *Environmental Microbiology*, 10(10):2476–2483.

Simon, R. D. and Weathers, P. (1976). Determination of the structure of the novel polypeptide containing aspartic acid and arginine which is found in cyanobacteria. *Biochimica et Biophysica Acta (BBA) - Protein Structure*, 420(1):165 – 176.

Sivonen, K. and Jones, G. (1999). Chapter 3. cyanobacterial toxins. In Chorus, I. and Bartram, J., editors, *Toxic cyanobacteria in water- A guide to their public health consequences, monitoring and management*. UNESCO, WHO and UNEP by E&FN Spon.

Sokal, R. and Rohlf, F. (1995). *Biometry: the principles and practice of statistics in biological research.* W.H. Freeman and Company, New York.

Sommer, U., Adrian, R., De Senerpont Domis, L., Elser, J. J., Gaedke, U., Ibelings, B., Jeppesen, E., Luerling, M., Molinero, J. C., Mooij, W. M., van Donk, E., and Winder, M. (2012). Beyond the plankton ecology group (peg) model: Mechanisms driving plankton succession. *Annual Review of Ecology, Evolution, and Systematics*, 43(1):429–448.

Spoof, L., Vesterkvist, P., Lindholm, T., and Meriluoto, J. (2003). Screening for cyanobacterial hepatotoxins, microcystins and nodularin in environmental water samples by reversed-phase liquid chromatography-electrospray ionisation mass spectrometry. *J Chromatogr A*, 1020(1):105–119.

Stewart, I., Seawright, A., and Shaw, G. (2008). Cyanobacterial poisoning in livestock, wild mammals and birds â€“ an overview. In Hudnell, H., editor, *Cyanobacterial Harmful Algal Blooms: State of the Science and Research Needs*, volume 619 of *Advances in Experimental Medicine and Biology*, pages 613–637. Springer New York.

Straub, C., Quillardet, P., Vergalli, J., de Marsac, N. T., and Humbert, J.-F. (2011). A day in the life of <italic>microcystis aeruginosa</italic> strain pcc 7806 as revealed by a transcriptomic analysis. *PLoS ONE*, 6(1):e16208.

Su, Z., Olman, V., Mao, F., and Xu, Y. (2005). Comparative genomics analysis of ntca regulons in cyanobacteria: regulation of nitrogen assimilation and its coupling to photosynthesis. *Nucleic Acids Research*, 33(16):5156–5171.

Suzuki, H. and Terada, T. (1988). Removal of dodecyl sulfate from protein solution. *Analytical Biochemistry*, 172(1):259 – 263.

Tanigawa, R., Shirokane, M., Maeda, S.-i., Omata, T., Tanaka, K., and Takahashi, H. (2002). Transcriptional activation of ntca-dependent promoters of synechococcus sp. pcc 7942 by 2-oxoglutarate in vitro. *Proceedings of the National Academy of Sciences*, 99(7):4251–4255.

Tchernov, D., Silverman, J., Luz, B., Reinhold, L., and Kaplan, A. (2003). Massive light-dependent cycling of inorganic carbon between oxygenic photosynthetic microorganisms and their surroundings. *Photosynthesis Research*, 77(2-3):95–103.

Thomas, R. H. and Walsby, A. E. (1986). The effect of temperature on recovery of buoyancy by microcystis. *Journal of General Microbiology*, 132(6):1665–1672.

Tibshirani, R., Walther, G., and Hastie, T. (2001). Estimating the number of clusters in a data set via the gap statistic. *Journal of the Royal Statistical Society: Series B (Statistical Methodology)*, 63(2):411–423.

Tillett, D., Dittmann, E., Erhard, M., von Dohren, H., Borner, T., and Neilan, B. A. (2000). Structural organization of microcystin biosynthesis in microcystis aeruginosa pcc7806: an integrated peptide-polyketide synthetase system. *Chemistry & Biology*, 7(10):753–764.

Toivola, D. M., Eriksson, J. E., and Brautigan, D. L. (1994). Identification of protein phosphatase 2a as the primary target for microcystin-1r in rat-liver homogenates. *Febs Letters*, 344(2-3):175–180.

Tolbert, N. E. (1997). The c2 oxidative photosynthetic carbon cycle. *Annual Review of Plant Physiology and Plant Molecular Biology*, 48(1):1–25. PMID: 15012254.

Tonietto, A., Petriz, B., Araujo, W., Mehta, A., Magalhaes, B., and Franco, O. (2012). Comparative proteomics between natural microcystis isolates with a focus on microcystin synthesis. *Proteome Science*, 10(1):38.

Towbin, H., Staehelin, T., and Gordon, J. (1979). Electrophoretic transfer of proteins from polyacrylamide gels to nitrocellulose sheets: procedure and some applications. *Proceedings of the National Academy of Sciences*, 76(9):4350–4354.

Usher, K. M., Bergman, B., and Raven, J. A. (2007). Exploring cyanobacterial mutualisms. *Annual Review of Ecology Evolution and Systematics*, 38:255–273.

Van de Waal, D. B., Verspagen, J. M., Finke, J. F., Vournazou, V., Immers, A. K., Kardinaal, W. E. A., Tonk, L., Becker, S., Van Donk, E., Visser, P. M., and Huisman, J. (2011). Reversal in competitive dominance of a toxic versus non-toxic cyanobacterium in response to rising co2. *ISME J*, 5(9):1438 – 1450.

Vazquez-Bermudez, M. F., Herrero, A., and Flores, E. (2002). 2-oxoglutarate increases the binding affinity of the ntca (nitrogen control) transcription factor for the synechococcus glna promoter. *FEBS Letters*, 512(1-3):71 – 74.

Via-Ordorika, L., Fastner, J., Kurmayer, R., Hisbergues, M., Dittmann, E., Komarek, J., Erhard, M., and Chorus, I. (2004). Distribution of microcystin-producing and non-microcystin-producing microcystis sp in european freshwater bodies: Detection of microcystins and microcystin genes in individual colonies. *Systematic and Applied Microbiology*, 27(5):592–602.

Whitton, B. A., Ward, D. M., Castenholz, R. W., Miller, S. R., Stal, L. J., Paerl, H. W., Oliver, R. L., David P. Hamilton, J. D. B., Ganf, G. G., Sejnohova, L., Marsalek, B., Cristiana Callieri, G. C., Stockner, J. G., Pentecost, A., Whitton, B. A., Albertano, P., Chunxiang Hu, K. G., Vincent, W. F., Quesada, A., Quesada, A., and Oren, A. (2012). Part 1, environments. In Whitton, B. A., editor, *Ecology of Cyanobacteria II*, pages 39–427. Springer Netherlands.

Wiedner, C., Visser, P. M., Fastner, J., Metcalf, J. S., Codd, G. A., and Mur, L. R. (2003). Effects of light on the microcystin content of microcystis strain pcc 7806. *Applied and Environmental Microbiology*, 69(3):1475–1481.

Wittig, I., Braun, H.-P., and Schagger, H. (2006). Blue native page. *Nat. Protocols*, 1(1):1754–2189.

Yang, C., Hua, Q., and Shimizu, K. (2002). Metabolic flux analysis in synechocystis using isotope distribution from 13c-labeled glucose. *Metabolic Engineering*, 4(3):202 – 216.

You, L., Berla, B., He, L., Pakrasi, H. B., and Tang, Y. J. (2014). 13c-mfa delineates the photomixotrophic metabolism of synechocystis sp. pcc 6803 under light- and carbon-sufficient conditions. *Biotechnology Journal*, 9(5):684–692.

Young, F. M., Thomson, C., Metcalf, J. S., Lucocq, J. M., and Codd, G. A. (2005). Immunogold localisation of microcystins in cryosectioned cells of microcystis. *Journal of Structural Biology*, 151(2):208 – 214.

Young, J. D., Shastri, A. A., Stephanopoulos, G., and Morgan, J. A. (2011). Mapping photoautotrophic metabolism with isotopically nonstationary 13c flux analysis. *Metabolic Engineering*, 13(6):656 – 665.

Zhang, S. and Bryant, D. A. (2011). The tricarboxylic acid cycle in cyanobacteria. *Science*, 334(6062):1551–1553.

Zilliges, Y. (2007). *Molekulare Funktionsanalyse von Microcystin in Microcystis aeruginosa PCC 7806*. PhD thesis.

Zilliges, Y., Kehr, J.-C., Meissner, S., Ishida, K., Mikkat, S., Hagemann, M., Kaplan, A., Börner, T., and Dittmann, E. (2011). The cyanobacterial hepatotoxin microcystin binds to proteins and increases the fitness of *Microcystis* under oxidative stress conditions. *PLoS ONE*, 6(3):e17615.

Appendix

Metabolomic data summary

Mass Spectral Feature (MSF)			Metabolite Information	Normalized signal intensities																																												
				No. of observations (counts)									Mean average									Standard error : $SE = s/\sqrt{n}$									Coefficient of variation (CV) [%]								
#	M/Z	RI Time (avg) [s]	Metabolite	Mar-[T0]	Mar-[T1]	Mar-[T3]	Mut-[T0]	Mut-[T1]	Mut-[T3]	Syn-[T0]	Syn-[T1]	Syn-[T3]	Mar-[T0]	Mar-[T1]	Mar-[T3]	Mut-[T0]	Mut-[T1]	Mut-[T3]	Syn-[T0]	Syn-[T1]	Syn-[T3]	Mar-[T0]	Mar-[T1]	Mar-[T3]	Mut-[T0]	Mut-[T1]	Mut-[T3]	Syn-[T0]	Syn-[T1]	Syn-[T3]	Mar-[T0]	Mar-[T1]	Mar-[T3]	Mut-[T0]	Mut-[T1]	Mut-[T3]	Syn-[T0]	Syn-[T1]	Syn-[T3]
1	160	186,26	Glyoxylate	5	5	4	5	4	4	4	5	5	2046	2481	2787	2446	2483	2956	1657	1534	1900	296	139	210	194	284	170	412	60	65	32,3	12,5	15,1	17,7	22,9	11,5	49,8	8,8	7,6
2	126	187,4	_	4	5	4	5	4	4	4	5	5	1020	607	601	1267	820	1066	2365	1539	1781	255	82	65	76	68	197	241	183	212	50	30,2	21,8	13,3	16,5	36,9	20,4	26,6	26,6
3	117	189,48	Lactate	5	5	4	5	4	4	4	5	5	1199730	1261725	1114915	1022239	1047326	908754	844506	912326	935120	23462	43391	41362	81226	58577	75349	32192	84054	62727	4,4	7,7	7,4	17,8	11,2	16,6	7,6	20,6	15
4	89	189,6	_	4	5	4	4	4	4	4	5	5	6815	5989	5959	4919	6532	5867	5515	3324	4773	1703	766	1334	376	505	689	872	454	611	50	28,6	44,8	15,3	15,5	23,5	31,6	30,5	28,6
5	85	194,17	_	3	5	4	5	4	4	4	4	5	2454	2885	2543	2462	2604	2245	2251	2110	2168	19	131	138	152	96	26	106	61	85	1,4	10,2	10,9	13,8	7,4	2,3	9,5	5,7	8,7
6	101	195,32	_	5	5	4	5	5	5	5	5	5	4482	3288	4875	3662	5502	7351	4389	3049	3257	1269	359	1019	353	810	2120	724	523	540	63,3	24,4	41,8	21,5	32,9	64,5	36,9	38,3	37
7	161	203,25	_	5	5	5	5	5	4	4	5	5	8594	8577	10070	9961	10047	10762	9531	9615	9564	557	475	720	146	506	212	171	268	91	14,5	12,4	16	3,3	11,3	3,9	3,6	6,2	2,1
8	152	204,41	Pyridine, 2-hydroxy-	5	5	5	5	5	5	5	5	5	38221	40698	56578	44646	51152	61580	28946	42061	44362	1915	3251	2477	1619	6094	8427	2861	1312	907	11,2	17,9	9,8	8,1	26,6	30,6	22,1	7	4,6
9	245	204,88	_	5	5	5	5	4	4	4	4	5	829	1296	1865	634	783	1021	572	601	596	129	173	654	19	78	253	43	6	32	34,9	29,9	78,4	6,7	20	49,5	14,9	2	11,9
10	144	206,06	_	4	4	5	5	4	5	4	5	5	443	561	496	438	476	595	508	789	1499	18	10	43	10	13	46	20	128	269	8,2	3,5	19,3	5,2	5,3	17,1	7,9	36,1	40,1
11	177	206,27	Glycolate	5	5	4	3	5	5	5	5	5	5645	55438	17003	5969	11166	30517	3991	4606	5978	692	12058	738	79	1935	10608	448	111	138	27,4	48,6	8,7	2,3	38,7	77,7	25,1	5,4	5,2
12	116	208,48	Alanine	5	5	5	3	5	5	5	4	5	37372	233895	277969	30683	187491	276318	158634	986768	1276464	4371	18738	30975	322	20696	27350	24490	15759	98170	26,2	17,9	24,9	1,8	24,7	22,1	34,5	3,2	17,2
13	110	212,46	_	5	5	4	5	5	5	5	4	5	800	585	664	1395	1277	2394	1613	1290	1783	65	45	20	168	262	669	187	33	248	18	17,3	6	27	45,9	62,5	25,9	5,2	31,1
14	89	216,65	_	5	5	5	5	5	5	5	5	5	4360	4417	4488	4641	4426	3451	3546	4241	3888	452	266	249	259	398	425	85	430	295	23,2	13,4	12,4	12,5	20,1	27,5	5,3	22,7	17
15	174	222,35	Pyruvate	5	5	5	5	5	5	5	5	3	3506	3278	3200	3126	3239	6346	2942	6165	5232	420	331	267	348	429	1681	163	1616	88	26,8	22,5	18,7	24,9	29,6	59,2	12,4	58,6	2,9
16	102	227,96	Glycine	5	4	5	5	4	5	4	5	5	2541	4060	3377	2471	2952	4384	2679	8643	8436	328	356	394	127	260	725	168	1572	744	28,9	17,6	26,1	11,5	17,6	37	12,6	40,7	19,7
17	153	228,44	_	5	4	5	5	5	5	5	5	4	1269	1118	1326	1352	1246	1051	780	1109	796	215	19	207	116	162	60	88	140	65	37,9	3,5	34,8	19,2	29	12,7	25,1	28,2	16,2
18	140	233,99	_	5	5	4	5	5	5	3	5	5	48168	48274	50604	53502	52591	77189	45754	44822	47157	7165	2676	1720	2648	4566	19058	628	3595	3430	33,3	12,4	6,8	11,1	19,4	55,2	2,4	17,9	16,3
19	174	234,62	_	5	5	3	5	4	5	4	5	5	1289	1383	1540	1377	1440	1503	1146	1279	1269	112	141	8	97	76	192	65	69	73	19,5	22,8	0,9	15,7	10,5	28,5	11,3	12,1	12,8
20	177	245,83	_	5	5	5	5	5	3	5	5	3	3270	4141	4067	3436	3765	3472	2801	3017	3171	129	141	231	61	214	9	248	33	9	8,8	7,6	12,7	4	12,7	0,4	19,8	2,4	0,5
21	130	248,86	Butyrate, 2-amino-	4	5	5	4	5	5	5	5	5	1024	6584	4437	1216	5387	8526	3038	8437	13736	10	497	514	7	474	699	460	356	748	1,9	16,9	25,9	1,2	19,7	18,3	33,9	9,4	12,2
22	89	253,49	_	5	3	5	3	4	5	5	4	5	3066	3958	4116	3131	3649	2938	2064	3535	3739	264	14	578	40	489	385	223	192	698	19,2	0,6	31,4	2,2	26,8	29,3	24,1	10,8	41,7
23	184	254,45	_	5	5	5	5	4	5	4	5	5	1716	1828	1883	1917	1711	3189	1443	1601	1635	230	57	219	232	119	860	187	89	98	29,9	6,9	25,9	27,1	13,9	60,3	25,9	12,4	13,4
24	116	254,62	_	5	5	5	5	4	4	4	5	5	3089	3622	3732	2732	2772	2855	2124	2613	2901	403	123	498	278	158	560	247	219	246	29,1	7,6	29,8	22,7	11,4	39,3	23,3	18,7	18,9
25	104	260,76	_	5	5	5	5	5	5	5	5	5	3935	3292	3500	3675	3869	4114	2723	3191	3155	599	296	413	317	569	427	282	185	185	34	20,1	26,4	19,3	32,9	23,2	23,2	12,9	13,1
26	147	264,46	Oxalate	5	5	5	5	5	5	4	5	4	37186	32676	36590	43837	37873	35071	18715	20856	19633	4289	1507	1098	3171	5298	4335	276	704	923	25,8	10,3	6,7	16,2	31,3	27,6	2,9	7,5	9,4
27	144	271,67	Valine	5	5	5	4	5	5	5	5	5	16425	73705	115307	16925	93929	123912	19914	121682	158497	1161	3683	10994	393	9154	6199	2720	6632	7308	15,8	11,2	21,3	4,6	21,8	11,2	30,5	12,2	10,3
28	131	273,85	_	5	4	5	5	5	5	4	5	5	720	992	934	636	1356	1852	703	938	2903	124	32	159	46	208	120	56	52	117	38,4	6,4	38	16,1	34,2	14,5	15,8	12,5	9
29	140	275,46	Acetate	5	5	4	5	5	5	5	5	5	3245	2088	1841	3149	2470	7644	1631	2279	1955	474	92	141	383	353	3521	221	242	214	32,6	9,9	15,4	27,2	32	103	30,3	23,7	24,4
30	120	280,02	_	5	5	4	5	5	5	5	4	5	904	749	736	1296	977	1240	1380	1431	1422	66	46	45	68	102	105	127	52	117	16,3	13,6	12,3	11,8	20,9	18,9	20,6	7,2	18,3
31	152	282,79	Pyridine, 3-hydroxy-	5	5	5	5	4	4	5	5	5	5096	5654	6545	5793	6860	7642	3954	4639	4909	267	141	360	181	118	451	243	149	155	11,7	5,6	12,3	7	3,4	11,8	13,7	7,2	7
32	140	286,66	_	5	5	5	5	4	5	4	5	5	1385	1302	1853	1668	1863	1919	930	1038	1209	106	106	99	56	54	278	26	83	61	17,1	18,3	12	7,4	5,8	32,3	5,5	17,8	11,2
33	125	287,52	_	4	5	5	5	5	4	5	5	5	78463	82486	81581	75093	68135	70770	63753	70112	66418	1655	3568	4530	2427	1944	831	4805	1980	3606	4,2	9,7	12,4	7,2	6,4	2,3	16,9	6,3	12,1
34	89	288,01	_	5	5	4	5	5	5	5	5	5	15365	17601	12730	14703	13802	12242	8316	7667	9645	1090	829	145	878	1006	902	384	471	541	15,9	10,5	2,3	13,4	16,3	16,5	10,3	13,7	12,5
35	103	288,79	_	5	5	5	4	5	5	4	5	3	751	1443	1583	1880	1326	2127	507	714	1122	45	211	164	127	106	422	7	47	5	13,3	32,7	23,1	13,5	17,9	44,4	2,9	14,6	0,7
36	144	289,12	_	4	5	5	5	5	5	5	5	5	411	2294	1443	430	1569	1959	1195	5164	11647	12	196	163	18	135	202	126	251	671	5,8	19,1	25,3	9,4	19,2	23,1	23,5	10,9	12,9
37	205	291,9	Glycerol	5	5	5	5	5	5	5	5	5	344959	375945	354100	357132	355381	332221	206598	218496	241190	8239	15206	11767	3922	19937	15471	18168	7299	9294	5,3	9	7,4	2,5	12,5	10,4	19,7	7,5	8,6
38	241	299,54	_	4	5	5	5	5	5	5	4	5	1539	2186	1990	1769	2223	2078	1528	2794	2440	32	87	70	60	104	70	89	36	106	4,2	8,9	7,8	7,6	10,5	7,6	13	2,6	9,7
39	158	304,98	Leucine	5	5	5	5	5	3	5	5	4	7184	15352	24692	6777	24199	36800	9371	52725	63096	720	890	2395	541	2227	131	1454	3610	1595	22,4	13	21,7	17,8	20,6	0,6	34,7	15,3	5,1
40	117	305,92	_	5	4	5	4	5	5	5	5	5	11750	10840	12445	13322	16577	13149	9097	8063	8884	1677	251	867	43	2062	973	1064	846	1099	31,9	4,6	15,6	0,7	27,8	16,5	26,1	23,5	27,7
41	228	306,44	_	5	4	5	5	5	5	5	5	5	1089	949	1194	1012	1213	1452	946	804	938	194	70	187	83	158	133	138	125	119	39,7	14,7	35	18,4	29	20,5	32,5	34,7	28,2
42	166	308,41	_	5	5	3	5	5	5	5	5	5	1926	1577	1375	1470	1564	3858	1112	1623	1036	423	163	14	66	134	1432	145	245	77	49,1	23,1	1,7	10	19,1	83	29,2	33,8	16,6
43	198	309,12	_	5	5	5	5	4	5	4	4	5	1232	820	749	1011	1040	4670	809	859	838	224	58	108	115	125	2082	68	55	98	40,6	15,9	32,1	25,5	24,1	99,7	16,8	12,9	26,2
44	89	309,79	_	5	5	5	5	5	3	4	5	5	2542	2819	3110	2685	2930	2394	2406	2199	2205	129	171	182	121	136	11	23	71	81	11,3	13,5	13,1	10,1	10,4	0,8	1,9	7,2	8,2
45	103	312,64	Acetone, 1,3-dihydroxy- (Dimer)	4	5	5	5	5	5	4	5	5	1388	2504	3473	1771	1533	1546	479	554	642	37	479	409	285	103	137	50	34	17	5,3	42,7	26,3	36	15	19,8	23,3	13,9	5,8
46	151	313,55	_	5	5	5	5	5	5	4	5	5	1135	1147	1616	1247	1519	2408	942	1166	1220	144	117	256	97	208	466	63	168	172	28,3	22,7	35,4	17,4	30,6	43,3	13,3	32,3	31,5
47	158	318,91	Isoleucine	5	5	5	4	5	4	5	5	5	7555	51995	56964	7759	47391	69257	6169	48290	77331	560	2035	4526	126	2995	1083	665	1854	3524	16,6	8,8	17,8	3,3	14,1	3,1	24,1	8,6	10,2
48	110	319,47	_	5	4	5	5	5	5	4	5	5	6029	24774	11442	5110	6604	12414	6029	11301	8778	822	588	1200	265	504	1627	208	441	375	30,5	4,7	23,5	11,6	17,1	29,3	6,9	8,7	9,5
49	117	322,35	Caprylate	5	5	5	5	5	5	4	3	5	5445	5623	5540	5591	5727	5624	4496	4674	5027	421	266	217	154	236	251	139	25	188	17,3	10,6	8,8	6,2	9,2	10	6,2	0,9	8,3
50	174	322,31	_	5	5	5	5	4	4	4	5	4	1784	2540	2981	1941	2124	1965	1206	1394	1341	271	541	376	211	235	409	142	113	93	33,9	47,6	28,2	24,3	22,1	41,6	23,5	18,2	13,8
51	124	323,09	_	5	5	5	5	4	5	3	5	5	1768	2474	4211	3095	4047	4858	1428	2876	2798	203	328	331	240	69	487	10	110	57	25,7	29,7	17,6	17,4	3,4	22,4	1,2	8,6	4,5
52	219	324,48	_	5	5	5	5	5	5	2	4	5	710	1012	1461	575	764	1275	472	415	453	29	63	69	8	37	115	40	13	17	9	14	10,5	3,1	10,7	20,1	11,9	6,3	8,4
53	174	325,01	Glycine	5	3	4	5	4	5	3	4	5	32653	75588	46680	27962	37640	54628	28655	75785	115054	3132	1816	4319	2052	1939	12113	438	3758	11078	21,4	4,2	18,5	16,4	10,3	49,6	2,6	9,9	21,5
54	299	333	Orthophosphate	5	5	5	5	5	5	5	5	5	319248	351760	303546	395091	450819	419540	197784	268721	289688	26709	9765	24081	12595	9482	10779	10985	21391	18171	18,7	6,2	17,7	7,1	4,7	5,7	12,4	17,8	14
55	100	333,52	_	5	5	5	5	5	5	5	5	4	3812	4248	4868	4388	4738	3793	2546	2964	2946	226	154	217	174	203	253	81	119	33	13,3	8,1	10	8,8	9,6	14,9	7,1	9	2,3
56	158	336,03	Norleucine	0	2	1	0	0	3	4	5	5		394	398			472	9514	12991	12697		26				55	273	678	531		9,3				20,2	5,7	11,7	9,4
57	85	338,44	_	5	5	4	5	4	5	5	5	5	2094	2128	1935	1858	1631	2171	2011	2156	3964	247	155	52	82	26	130	190	152	117	26,4	16,3	5,4	9,8	3,2	13,4	21,1	15,7	6,6
58	142	338,55	Proline	5	5	4	5	3	5	5	5	5	4494	17508	12430	3781	7573	27112	3928	26636	234013	815	3403	1089	336	40	4254	412	1522	25895	40,6	43,5	17,5	19,9	0,9	35,1	23,4	12,8	24,7
59	171	341,14	Urea	5	4	4	3	5	5	5	5	5	466385	501060	452457	454810	480456	407383	320587	408357	414043	52515	8820	13614	2030	31563	23551	12769	25448	17842	25,2	3,5	6	0,8	14,7	12,9	8,9	13,9	9,6
60	103	344,48	Glycerate	5	5	5	5	5	5	3	5	5	3493	7561	10555	3643	7056	7342	3875	4530	5229	223	326	559	221	330	296	66	168	143	14,3	9,6	11,8	13,5	10,5	9	3	8,3	6,1
61	117	344,82	_	5	5	5	5	5	5	5	5	5	2890	5716	7609	5376	6407	6990	2545	2876	3350	236	149	421	294	357	191	89	73	93	18,3	5,8	12,4	12,2	12,4	6,1	7,8	5,6	6,2
62	116	345,34	_	5	5	5	5	5	5	5	5	4	20572	26664	23758	41818	43155	45253	1688	1666	1276	2774	939	2225	2451	5185	3393	404	207	143	30,1	7,9	20,9	13,1	26,9	16,8	53,5	27,7	22,5
63	129	347,51	_	5	5	5	5	5	5	3	4	5	2432	3071	2921	2908	2972	2394	1541	1331	1469	177	125	163	210	237	191	7	91	86	16,3	9,1	12,5	16,2	17,8	17,8	0,7	13,6	13
64	105	348,23	Benzoate	5	5	4	5	5	5	5	5	5	11717	11449	11852	10680	12169	10686	9026	8836	9818	740	296	195	351	1091	457	480	443	338	14,1	5,8	3,3	7,3	20	9,6	11,9	11,2	7,7
65	240	356,94	_	5	4	5	5	5	5	4	5	5	1499	1976	1808	1598	1559	1459	1136	1504	1325	93	57	70	72	191	227	70	104	102	13,9	5,7	8,6	10,1	27,3	34,8	12,3	15,5	17,2
66	204	357,22	Serine	5	5	5	5	5	4	5	5	5	19894	62510	62300	16664	56341	59152	21447	84231	140063	2013	5397	6341	2186	4147	3705	2878	4608	7535	22,6	19,3	22,8	29,3	16,5	12,5	30	12,2	12
67	217	361,29	_	5	5	5	5	5	5	4	4	5	1338	1340	1369	1983	1878	1939	471	448	452	63	77	41	56	103	114	17	20	20	10,5	12,9	6,8	6,3	12,3	13,1	7,3	8,7	10,1
68	144	362,2	_	5	4	5	4	3	4	5	5	5	1569	3193	16498	1170	8222	4151	1488	8750	9225	354	780	5165	94	308	1147	181	1524	1778	50,5	48,8	70	16	6,5	55,2	27,1	38,9	43,1
69	228	363,04	_	2	4	4	5	4	4	4	4	5	1411	883	938	672	896	2110	754	755	735	524	159	148	57	179	712	99	140	107	52,5	36,1	31,6	19	40	67,5	26,3	37,2	32,4

Mass Spectral Feature (MSF)			Metabolite Information	Normalized signal intensities																																			
				No. of observations (counts)									Mean average									Standard error : $SE = s/\sqrt{n}$									Coefficient of variation (CV) [%]								
#	M/Z	RI Time (avg) [s]	Metabolite	Mar-[T0]	Mar-[T1]	Mar-[T3]	Mut-[T0]	Mut-[T1]	Mut-[T3]	Syn-[T0]	Syn-[T1]	Syn-[T3]	Mar-[T0]	Mar-[T1]	Mar-[T3]	Mut-[T0]	Mut-[T1]	Mut-[T3]	Syn-[T0]	Syn-[T1]	Syn-[T3]	Mar-[T0]	Mar-[T1]	Mar-[T3]	Mut-[T0]	Mut-[T1]	Mut-[T3]	Syn-[T0]	Syn-[T1]	Syn-[T3]	Mar-[T0]	Mar-[T1]	Mar-[T3]	Mut-[T0]	Mut-[T1]	Mut-[T3]	Syn-[T0]	Syn-[T1]	Syn-[T3]
73	110	370,34	_	5	5	4	5	4	5	5	5	5	1844	1339	1123	1324	1997	1540	1673	1279	1588	509	364	125	152	352	284	379	246	276	61,7	60,7	22,3	25,7	35,3	41,2	50,7	43	38,8
74	241	370,44	_	5	5	5	5	5	5	5	5	5	1327	1689	2311	2008	1998	3521	2625	3859	4778	100	159	104	150	167	339	525	275	250	16,9	21	10,1	16,6	18,7	21,5	44,7	15,9	11,7
75	245	370,9	Fumarate	4	5	4	5	4	5	5	5	5	2833	6770	7372	4311	7056	10547	2145	4397	7340	153	349	285	381	93	1622	210	227	227	10,8	11,5	7,7	19,8	2,6	34,4	21,9	11,6	6,9
76	156	371,59	_	4	4	4	5	4	4	5	5	5	1947	2262	3718	2720	2832	2954	2358	2011	2296	193	137	353	329	129	156	161	189	130	19,8	12,1	19	27	9,1	10,6	15,3	21	12,7
77	234	372,16	_	5	5	5	4	5	5	5	5	5	925	14580	16501	810	1207	868	901	992	776	151	4048	3704	38	200	137	124	100	66	36,4	62,1	50,2	9,3	37	35,4	30,6	22,6	19
78	158	372,37	_	1	4	4	0	3	2	1	5	5	645	880	1416		735	1612	665	1169	14302		45	196		82	871		139	1076		10,3	27,7		19,2	76,4		26,6	16,8
79	157	373,37	_	5	5	5	5	5	5	5	5	5	3909	3465	3736	3502	3821	5633	3053	2936	3064	665	265	491	122	504	1298	280	344	338	38	17,1	29,4	7,8	29,5	51,5	20,5	26,2	24,7
80	156	374,32	Pipecolate	5	5	5	5	5	5	5	5	5	6833	9454	8187	4013	4639	5137	6197	6107	5842	748	467	785	673	656	472	423	672	436	24,5	11	21,4	37,5	31,6	20,6	15,3	24,6	16,7
81	170	374,68	_	5	4	5	5	4	5	4	5	5	1131	1299	1410	1365	1498	1306	777	1126	975	107	32	68	55	90	111	86	31	37	21,2	4,9	10,8	8,9	12	18,9	22	6,2	8,5
82	89	375,99	_	5	5	5	5	5	5	5	5	5	1335	1615	1440	1360	1355	1302	798	940	1260	95	84	56	49	55	75	58	39	39	15,9	11,6	8,8	8	9	12,8	16,1	9,3	6,9
83	103	383,71	_	5	5	5	5	5	5	2	4	5	42423	36594	28027	37464	34415	25471	540	521	484	1241	1149	1201	1256	941	671	84	20	46	6,5	7	9,6	7,5	6,1	5,9	22,1	7,6	21
84	136	386,29	Nicotinate	5	4	4	5	5	5	4	5	5	1626	1499	1375	1475	1601	1539	1018	1416	1444	293	76	142	88	205	122	47	139	118	40,3	10,2	20,7	13,3	28,6	17,7	9,1	22	18,3
85	103	388,94	_	5	3	5	4	4	5	4	5	5	2056	3312	3652	2135	2812	3167	1964	2856	5889	53	14	80	22	26	121	63	87	266	5,8	0,7	4,9	2,1	1,8	8,5	6,4	6,8	10,1
86	217	389,43	_	5	5	5	5	5	5	3	3	3	1174	1108	1189	1724	1627	1670	427	409	452	56	67	31	43	99	77	29	18	15	10,7	13,5	5,8	5,6	13,5	10,3	11,7	7,7	5,6
87	99	391,87	Uracil	5	5	4	4	5	5	5	5	5	5702	7162	8205	6626	7823	8545	6775	4907	6277	1307	483	379	170	1083	936	805	919	889	51,2	15,1	9,2	5,1	31	24,5	26,6	41,9	31,7
88	130	392,29	_	5	5	4	5	5	5	5	5	5	1086	1606	2083	993	1708	2523	1038	2606	2216	112	151	115	21	102	150	102	345	173	23	21,1	11,1	4,7	13,3	13,3	22	29,6	17,4
89	117	393,2	_	3	5	5	5	5	5	4	5	5	661	1099	1156	856	1225	1416	694	881	1668	8	44	65	38	93	62	12	123	267	2,2	8,9	12,6	9,8	17	9,8	3,5	31,3	35,8
90	100	393,52	_	5	4	5	5	4	4	5	5	5	6172	7381	6197	5908	6457	13897	3948	4640	8006	1037	373	1269	1816	977	3077	403	707	550	37,6	10,1	45,8	68,7	30,3	44,3	22,8	34,1	15,3
91	103	393,67	_	5	4	5	4	4	4	4	5	5	1557	1553	1595	1427	1699	1948	529	591	787	36	8	35	18	13	75	32	30	18	5,2	1	4,9	2,6	1,5	7,7	12	11,5	5
92	86	393,95	_	4	5	5	5	4	5	5	5	4	723	1088	973	927	768	1397	1344	1086	1303	25	125	132	115	51	308	112	16	27	6,9	25,7	30,4	27,7	13,3	49,2	18,5	3,3	4,2
93	103	397,43	_	5	5	5	4	5	5	5	5	5	1375	5744	7813	1233	1484	1391	1532	1204	1140	104	617	2242	52	185	179	177	90	102	16,8	24	64,2	8,5	27,9	28,8	25,9	16,7	20
94	117	397,96	_	5	5	5	5	5	5	5	5	5	1609	1793	1925	1844	1771	1673	1526	1514	1343	202	122	164	147	225	167	276	166	137	28,1	15,2	19,1	17,9	28,4	22,3	40,4	24,6	22,8
95	196	401,73	_	5	5	5	5	5	5	5	5	5	10738	11767	14570	13429	15194	14986	6586	5927	7815	1016	594	1356	1097	605	1175	552	573	706	21,1	11,3	20,8	18,3	8,9	17,5	18,7	21,6	20,2
96	102	403,93	_	5	5	5	4	3	4	3	4	5	21538	802387	767909	17586	31223	18947	28644	23928	21117	2373	194823	198536	1922	1023	3985	228	2080	2529	24,6	54,3	57,8	21,9	5,7	42,1	1,4	17,4	26,8
97	218	406,18	_	5	4	5	4	5	4	4	5	5	647	1496	2576	913	1439	1579	729	1095	1970	54	300	469	21	163	49	71	107	156	18,7	40,1	40,7	4,7	25,4	6,1	19,6	21,8	17,8
98	269	406,24	_	3	5	5	5	5	5	4	5	4	799	1099	1164	1080	1102	1473	1092	1158	1407	10	76	43	130	117	139	36	116	26	2,2	15,5	8,3	26,9	23,7	21,1	6,7	22,4	3,6
99	97	407,83	_	4	2	4	5	4	4	1	1	1	469	651	539	1126	1036	1445	427	381	398	35	53	36	266	167	70				15,1	11,4	13,2	52,9	32,3	9,6			
100	217	408,4	Erythritol	5	4	5	5	5	4	4	5	5	2302	2823	3284	2419	2800	2310	2157	2602	2589	333	200	283	151	244	25	24	139	125	32,3	14,2	19,3	14	19,5	2,1	2,2	11,9	10,8
101	117	411,07	_	5	4	5	5	5	5	5	4	5	2975	3857	3967	3488	3687	3082	2916	2986	3157	212	145	137	176	200	138	127	62	132	15,9	7,5	7,7	11,3	12,2	10	9,8	4,1	9,4
102	99	411,5	_	4	5	5	4	5	5	5	5	5	1248	1471	1673	1202	1262	1257	875	870	908	27	87	45	5	43	83	39	29	32	4,4	13,2	6	0,8	7,6	14,8	9,9	7,3	7,9
103	133	414,58	_	5	5	4	5	5	4	3	4	2	890	839	732	1819	1064	1204	466	467	464	166	63	53	227	203	198	39	27	72	41,6	16,9	14,4	27,9	42,6	32,8	14,3	11,4	21,9
104	196	414,82	_	5	5	4	5	4	3	3	4	3	3145	2769	3505	561	514	559	464	451	424	581	261	46	47	57	59	47	12	30	41,3	21,1	2,6	18,8	22,2	18,1	17,7	5,1	12,2
105	85	416,23	_	5	5	5	5	4	5	5	3	5	5364	5993	5375	4862	4228	5945	5606	4729	5340	843	627	583	273	44	626	712	87	422	35,1	23,4	24,3	12,6	2,1	23,5	28,4	3,2	17,7
106	143	417,36	_	5	4	4	5	5	4	5	5	4	1088	1155	1427	4971	3997	6618	774	627	715	257	115	159	1400	714	368	60	84	63	52,8	19,9	22,3	63	39,9	11,1	17,4	30	17,5
107	117	418,97	_	4	5	5	3	5	5	5	5	5	869	1198	1301	764	1001	2990	1099	1022	1280	167	212	130	4	135	983	153	196	210	38,5	39,5	22,4	0,9	30	73,5	31,1	43	36,7
108	146	420,9	_	4	5	5	5	4	4	2	3	3	583	900	811	5094	4405	5995	391	428	442	47	215	131	1410	243	340	26	30	54	16	53,3	36	61,9	11	11,3	9,4	12	21,3
109	159	422,33	_	4	5	5	5	4	5	3	2	3	1771	3541	3867	2092	3851	4362	417	420	444	78	141	134	86	56	185	19	2	37	8,9	8,9	7,7	9,2	2,9	9,5	7,8	0,6	14,4
110	113	422,79	Thymine	5	5	5	5	5	5	5	4	3	2367	2201	2920	2547	2732	3006	2951	2662	2751	65	142	198	118	201	215	211	44	5	6,2	14,4	15,1	10,4	16,4	16	16	3,3	0,3
111	115	425,13	_	5	3	5	5	5	5	5	5	5	872	760	937	1267	848	937	1371	1088	1097	50	9	51	55	59	121	82	54	53	12,8	2	12,1	9,6	15,4	28,8	13,4	11,2	10,7
112	159	425,37	_	5	4	5	5	5	5	4	5	5	1047	1025	1288	1000	1010	1820	1800	1835	2262	144	68	62	34	79	318	15	82	139	30,7	13,3	10,7	7,6	17,4	39,1	1,6	10	13,7
113	143	427,91	_	5	4	5	5	5	5	5	5	5	2100	2046	2270	2072	2407	3172	1415	1210	1340	394	84	205	87	95	499	159	132	144	41,9	8,2	20,2	9,4	8,8	35,2	25	24,3	24
114	194	429,02	_	5	5	5	3	5	5	5	5	5	2336	2907	3664	2628	3411	3340	1154	1191	1557	152	126	255	30	187	334	95	70	108	14,6	9,7	15,6	2	12,3	22,3	18,4	13,2	15,5
115	117	430,48	Decanoate	5	5	5	5	5	5	5	5	3	7477	7806	8452	7790	8163	8012	6595	6771	7866	367	288	373	105	195	169	220	208	31	11	8,2	9,9	3	5,3	4,7	7,5	6,9	0,7
116	88	433,73	_	5	5	5	5	5	5	4	5	4	5470	5750	7028	3782	3821	3817	631	492	545	696	623	1004	215	221	266	135	35	54	28,5	24,2	31,9	12,7	12,9	15,6	42,8	15,7	19,9
117	140	433,81	_	5	5	4	5	5	5	5	5	5	2168	1743	1533	1835	2138	1754	1720	1432	1584	375	187	172	106	303	266	446	194	262	38,7	24	22,5	12,9	31,7	33,9	57,9	30,4	36,9
118	89	433,94	_	5	5	5	5	5	4	1	3	2	1908	1998	2180	2261	1855	2699	739	580	532	276	138	299	301	319	68		73	75	32,3	15,4	30,7	29,7	38,5	5		21,9	19,9
119	143	434,37	_	5	5	5	5	5	4	4	3	3	1261	1466	1392	3965	3189	5304	460	502	522	307	193	227	998	510	293	33	16	42	54,4	29,4	36,4	56,3	35,7	11	14,4	5,3	14
120	232	435,93	_	5	4	4	4	5	5	4	4	5	526	1716	1142	410	1159	3539	1468	5659	16631	35	117	104	15	224	889	44	337	2166	14,8	13,6	18,2	7,3	43,2	56,2	6	11,9	29,1
121	143	436,86	_	5	5	5	4	5	5	5	5	5	1258	1294	1318	1765	1775	2650	797	778	915	253	126	169	337	161	401	86	87	76	45	21,8	28,7	38,2	20,3	33,8	24,1	25,1	18,6
122	100	437,63	_	4	5	5	5	5	5	4	4	0	1696	2281	2287	2006	1937	2832	1873	3098		132	47	141	136	174	328	49	216		15,6	4,6	13,7	15,2	20,1	25,9	5,2	13,9	
123	146	440,02	_	5	5	5	5	3	5	5	4	5	4268	4435	5201	40085	29978	38001	1065	1619	1359	907	1243	966	10351	1685	6655	73	104	272	47,5	62,7	41,6	57,7	9,7	39,2	15,3	12,8	44,7
124	88	440,35	_	4	5	5	4	4	4	2	3	3	2251	2653	2953	2037	2267	2520	477	404	418	64	250	214	41	48	38	93	14	27	5,7	21,1	16,2	4	4,2	3	27,5	5,8	11,4
125	133	440,72	Malate	5	4	4	5	5	5	5	5	5	2141	5902	5336	3532	5854	10444	1635	3055	4394	172	356	288	416	466	2099	86	122	157	17,9	12,1	10,8	26,4	17,8	44,9	11,8	8,9	8
126	218	442,18	_	5	5	4	4	5	5	5	5	3	772	1678	1087	521	999	1937	931	2258	3833	65	165	48	17	87	428	69	426	79	18,7	22	8,9	6,4	19,4	49,4	16,5	42,2	3,6
127	292	442,33	_	5	4	4	4	5	4	4	5	5	763	1340	2121	571	1248	1793	545	953	1503	29	29	101	5	41	53	13	63	105	8,5	4,3	9,5	1,9	7,4	5,9	4,8	14,8	15,6
128	85	442,87	_	5	5	5	4	4	4	5	5	5	4423	4968	4446	4120	3692	4866	4957	4135	4802	721	545	435	66	56	247	653	314	370	36,4	24,5	21,9	3,2	3	10,1	29,5	17	17,2
129	146	450,06	_	5	5	5	5	5	5	5	5	5	2746	3097	2689	3248	3654	4638	624	618	631	219	117	246	139	299	466	43	58	53	17,9	8,4	20,4	9,6	18,3	22,5	15,4	20,9	18,7
130	133	450,2	_	5	4	5	3	5	3	5	5	5	2768	2815	2970	3068	3647	4768	2095	1530	1967	601	261	562	49	510	61	281	438	434	48,6	18,5	42,3	2,8	31,2	2,2	30	64,1	49,4
131	131	450,31	_	5	5	5	5	5	4	5	5	5	2008	2583	2534	2297	2636	2944	1459	1377	1558	150	115	202	52	162	52	80	54	64	16,7	10	17,8	5	13,7	3,5	12,3	8,7	9,2
132	217	451,69	_	4	5	5	5	4	3	5	5	5	2224	4253	9753	3262	5301	11552	3228	2232	2406	82	401	261	123	39	115	108	62	46	7,3	21,1	6	8,5	1,5	1,7	7,5	6,2	4,3
133	100	452,45	_	5	5	5	5	4	4	5	5	5	2150	3537	2966	2333	2578	3303	3168	6679	11249	184	320	288	102	57	137	259	1282	2164	19,1	20,2	21,7	9,7	4,4	8,3	18,3	42,9	43
134	243	453,88	_	4	4	4	5	4	4	4	4	2	1484	1482	1498	1440	1497	1492	1403	1560	1747	78	15	38	104	62	41	67	45	40	10,5	2	5,1	16,2	8,2	5,6	9,6	5,7	3,2
135	151	454,96	_	5	5	4	5	4	4	4	5	5	1427	1642	1593	1739	1865	1848	570	585	576	43	71	57	84	50	198	8	21	23	6,8	9,7	7,1	10,8	5,4	21,4	2,9	8,1	9,1
136	255	455,28	_	5	5	4	5	4	4	4	5	5	8714	10308	11895	10528	10230	11726	10389	8751	9617	2131	620	875	989	671	693	547	1471	1171	54,7	13,5	14,7	21	13,1	11,8	10,5	37,6	27,2
137	232	457,17	Aspartate	5	5	5	3	5	5	5	5	5	23618	137407	189585	25983	196365	224635	30385	213787	295870	1027	18239	24796	223	24828	16867	1691	14578	28754	9,7	29,7	29,2	1,5	28,3	16,8	12,4	15,2	21,7
138	170	457,41	_	5	5	5	5	5	5	5	5	5	625	1105	1365	634	1414	1587	709	1491	1912	33	86	135	25	134	82	24	78	136	11,9	17,4	22,1	8,8	21,2	11,5	7,7	11,7	16
139	159	458,85	_	4	4	4	5	4	4	4	1	1	874	1178	1333	2450	2062	2585	742	1085	1237	19	99	26	530	278	294	4			4,4	16,8	3,9	48,4	26,9	22,7	1,1		
140	156	464,26	_	0	0	1	1	2	2	5	5	5			385	375	373	380	2336	2214	2138					5	3	272	257	286					1,9	1,2	26	25,9	29,9
141	146	464,33	_	5	4	5	5	5	5	4	5	5	2426	2628	3048	4357	4546	5124	497	532	573	259	108	332	262	399	338	34	45	48	23,9	8,2	24,4	13,4	19,6	14,7	13,7	18,9	18,7

Mass Spectral Feature (MSF)			Metabolite Information	Normalized signal intensities																																			
				No. of observations (counts)									Mean average									Standard error : $SE = s/\sqrt{n}$									Coefficient of variation (CV) [%]								
#	M/Z	RI Time (avg) [s]	Metabolite	Mar-[T0]	Mar-[T1]	Mar-[T3]	Mut-[T0]	Mut-[T1]	Mut-[T3]	Syn-[T0]	Syn-[T1]	Syn-[T3]	Mar-[T0]	Mar-[T1]	Mar-[T3]	Mut-[T0]	Mut-[T1]	Mut-[T3]	Syn-[T0]	Syn-[T1]	Syn-[T3]	Mar-[T0]	Mar-[T1]	Mar-[T3]	Mut-[T0]	Mut-[T1]	Mut-[T3]	Syn-[T0]	Syn-[T1]	Syn-[T3]	Mar-[T0]	Mar-[T1]	Mar-[T3]	Mut-[T0]	Mut-[T1]	Mut-[T3]	Syn-[T0]	Syn-[T1]	Syn-[T3]
145	146	467,91	_	5	5	5	5	5	5	2	2	5	650	785	724	2183	1828	2135	404	398	471	55	65	52	520	252	251	19	6	23	18,8	18,4	16,1	53,2	30,9	26,3	6,6	2	11
146	155	468,78	_	5	5	5	4	5	4	5	5	5	1832	3220	3641	2346	3682	4835	3134	4972	8548	264	446	835	69	869	94	415	1214	1522	32,3	30,9	51,3	5,9	52,8	3,9	29,6	54,6	39,8
147	217	469,64	_	3	5	4	2	5	5	4	4	5	891	1393	1897	1217	1681	1954	615	766	773	69	46	36	178	77	30	13	32	28	13,3	7,4	3,7	20,7	10,3	3,4	4,3	8,4	8,2
148	204	470,22	_	5	5	5	5	3	5	2	4	2	1660	1765	2073	10994	8186	10476	439	587	622	261	365	241	2768	298	1601	35	81	106	35,1	46,3	26	56,3	6,3	34,2	11,3	27,4	24,2
149	111	470,7	Adipate	5	5	4	5	4	4	4	5	5	3066	3578	3422	3213	4649	3326	2514	3082	3761	182	171	113	295	237	620	105	244	623	13,3	10,7	6,6	20,5	10,2	37,3	8,4	17,7	37
150	133	473,17	_	5	5	3	5	4	5	5	5	5	912	1377	2843	1236	1833	1812	714	1049	1060	68	54	38	51	27	113	35	46	26	16,6	8,8	2,3	9,2	2,9	14	10,8	9,8	5,5
151	157	473,37	Malate, 2-isopropyl-	3	4	3	5	5	4	4	5	4	411	744	2673	438	845	851	519	858	849	9	7	15	10	31	28	17	35	10	3,8	2	1	5,3	8,2	6,5	6,7	9,2	2,3
152	128	474,22	Methionine	5	5	4	5	4	5	5	5	5	1565	3222	1791	1023	2045	7424	1286	3581	4594	398	761	166	93	255	1704	99	684	877	56,8	52,8	18,5	20,2	25	51,3	17,2	42,7	42,7
153	137	476,36	_	5	5	5	4	5	5	4	5	5	1105	1250	1248	1355	1439	1574	991	943	990	70	42	77	9	79	131	17	83	62	14,2	7,5	13,8	1,4	12,3	18,6	3,4	19,7	13,9
154	100	477,64	_	4	4	4	5	4	4	0	2	1	835	1199	2685	729	1232	1553		1318	1474	117	347	538	145	293	327		136		28	57,8	40,1	44,6	47,6	42,1		14,6	
155	207	482,14	_	4	5	4	5	5	5	5	4	3	1150	1474	1661	1340	1407	1521	1150	1233	1335	33	150	17	67	44	103	48	31	6	5,8	22,7	2	11,1	7	15,1	9,3	5	0,7
156	146	482,76	_	5	5	4	5	4	5	5	5	5	3950	2949	2243	3359	3057	9022	1192	1198	852	1024	242	71	173	93	3116	140	201	90	58	18,4	6,3	11,5	6,1	77,2	26,3	37,5	23,7
157	217	483,53	_	5	5	5	5	5	5	5	5	5	2119	2443	2386	3095	3177	3694	1107	1027	1166	306	150	298	310	187	256	94	130	133	32,3	13,7	27,9	22,4	13,1	15,5	19	28,2	25,6
158	118	486,97	_	5	5	5	5	5	5	4	3	5	5267	5953	5696	3879	3743	4812	3386	2878	1846	293	713	603	209	370	419	123	36	110	12,4	26,8	23,7	12	22,1	19,5	7,2	2,2	13,3
159	142	490,55	Arginine	5	5	5	5	5	4	5	5	5	3005	6006	4118	2472	3686	5773	5981	15277	27461	281	734	509	125	375	251	900	914	2317	20,9	27,3	27,6	11,3	22,8	8,7	33,6	13,4	18,9
160	116	490,81	_	4	5	5	3	5	4	3	5	5	631	998	1025	426	1113	987	678	1877	3017	43	111	162	32	114	109	155	92	151	13,6	24,9	35,4	13,1	22,9	22	39,5	11	11,2
161	170	491,51	[Homoglutamine]	5	5	5	5	5	5	4	5	5	570	2010	3186	649	2146	1822	418	676	828	52	226	176	33	149	437	5	39	40	20,2	25,2	12,4	11,3	15,5	53,6	2,2	12,9	10,9
162	103	492,76	_	5	5	5	5	5	5	4	4	5	2722	2559	3040	5116	4705	4411	635	484	508	124	110	205	329	535	483	121	11	40	10,2	9,6	15,1	14,4	25,4	24,5	38,2	4,5	17,6
163	199	493,12	_	5	5	5	5	5	5	5	5	5	1425	1235	1415	1267	1584	2273	1001	971	998	318	138	263	63	206	433	110	134	127	49,8	25	41,5	11,1	29,1	42,6	24,5	30,9	28,4
164	100	494,25	_	5	5	5	5	5	5	5	5	5	1034	2339	2680	1135	1948	5189	1051	2289	5316	156	437	484	68	261	520	89	381	714	33,8	41,8	40,4	13,4	30	22,4	19	37,2	30
165	195	495,2	_	5	5	4	3	5	4	5	5	5	1234	2048	4077	2395	3269	4528	1060	2092	2163	189	363	329	39	277	65	41	139	132	34,3	39,7	16,1	2,8	18,9	2,9	8,5	14,8	13,7
166	112	495,6	_	3	4	5	2	5	5	4	5	5	431	533	544	412	534	1259	508	1211	2128	15	24	51	2	64	244	25	137	252	6,2	9,1	21	0,8	26,8	43,3	9,7	25,3	26,5
167	171	496,04	_	5	5	5	5	4	5	4	5	5	962	1348	1263	813	1118	1098	762	606	654	101	57	241	103	68	112	101	34	23	23,4	9,4	42,7	28,3	12,2	22,7	26,4	12,6	7,9
168	175	497,03	_	5	4	5	5	5	4	5	5	5	892	1112	2146	995	1472	2225	976	1202	1674	136	48	370	67	185	61	96	153	166	34,1	8,7	38,6	15	28	5,5	22	28,5	22,2
169	117	498,61	_	4	5	5	3	4	4	5	5	5	609	1193	1865	573	1342	1824	1093	4463	13679	23	73	215	22	182	272	119	148	1067	7,4	13,6	25,8	6,7	27,1	29,8	24,3	7,4	17,4
170	112	498,7	_	4	4	3	5	5	5	4	5	5	527	928	807	500	796	1752	616	1045	2241	48	48	21	17	88	351	19	108	188	18	10,4	4,4	7,6	24,7	44,8	6	23	18,7
171	177	500,22	_	5	5	5	5	5	5	5	5	5	1273	1576	1793	1369	1502	3170	1661	1715	2207	76	144	108	37	34	716	75	132	134	13,2	20,4	13,4	6	5	50,5	10,1	17,2	13,5
172	103	500,64	_	4	5	5	5	5	4	5	5	5	1863	2505	2349	2535	2754	2626	1304	2411	3091	40	241	231	310	376	48	82	165	818	4,3	21,5	22	27,4	30,5	3,6	14	15,3	59,1
173	217	500,79	Ribose (; Ribulose)	5	5	4	5	5	5	4	4	5	1556	1914	1917	2318	2397	2650	581	816	796	65	156	36	63	206	73	55	37	22	9,3	18,2	3,7	6	19,2	6,2	18,9	9,2	6,1
174	103	502,32	_	5	5	5	5	5	3	5	4	5	2303	3507	4148	3715	3523	2887	1962	2067	2571	202	329	265	297	150	15	138	84	100	19,6	21	14,3	17,9	9,5	0,9	15,8	8,1	8,7
175	123	505,51	_	5	4	4	3	5	5	5	5	5	1457	1568	2113	1459	1716	3122	2007	1794	2216	196	76	28	7	113	584	37	206	233	30	9,7	2,6	0,8	14,7	41,8	4,1	25,6	23,5
176	156	506,62	Pyroglutamate	5	5	5	5	5	5	5	5	5	345870	265499	589268	437493	543183	681657	1263073	675622	689996	66553	22658	130801	45439	105515	40583	161529	116522	94457	43	19,1	49,6	23,2	43,4	13,3	28,6	38,6	30,6
177	128	507,76	Glutamate	5	5	5	4	5	4	5	4	5	161382	132660	289716	323471	303524	440491	652039	461718	303714	29644	10381	34711	8545	35326	23727	111579	4179	46335	41,1	17,5	26,8	5,3	26	10,8	38,3	1,8	34,1
178	217	510,63	_	4	5	5	5	5	5	1	5	4	5571	5437	6823	10196	8863	9487	469	635	573	93	428	228	333	249	616		82	34	3,4	17,6	7,5	7,3	6,3	14,5		28,9	11,7
179	255	510,68	_	4	3	4	5	3	5	5	5	5	1626	1701	1954	1888	1788	2427	2134	1673	1762	185	7	115	208	26	307	87	285	192	22,7	0,8	11,7	24,6	2,5	28,3	9,2	38,1	24,4
180	146	510,9	_	4	5	5	5	5	3	2	5	5	526	603	767	1392	1222	1546	466	433	433	8	27	45	206	161	8	42	15	17	3,1	10,2	13,2	33,1	29,4	0,9	12,6	7,8	8,7
181	100	512,79	_	4	5	5	4	4	4	3	4	5	820	889	667	852	841	960	2409	1333	701	127	82	80	43	100	135	374	189	62	30,9	20,5	26,7	10	23,8	28,1	26,9	28,4	19,8
182	179	515,21	Nicotinamide	4	3	5	5	4	5	4	4	5	15410	17187	18104	23688	23462	22366	1435	2287	1895	201	72	819	911	444	2184	156	76	154	2,6	0,7	10,1	8,6	3,8	21,8	21,8	6,7	18,2
183	129	516,65	_	5	5	4	5	5	5	4	5	4	23467	28415	32560	28718	29958	25374	24383	24960	27071	1439	1410	267	900	252	1742	402	1647	146	13,7	11,1	1,6	7	1,9	15,4	3,3	14,8	1,1
184	174	517,17	Putrescine	4	4	5	5	3	5	5	5	4	3548	2506	1572	3448	2809	2601	2287	2809	2139	614	292	114	383	15	206	132	308	27	34,6	23,3	16,2	24,9	0,9	17,7	12,9	24,5	2,5
185	117	518,8	_	4	5	5	5	5	5	5	5	5	1828	2280	3044	1677	1816	1955	1619	1636	1903	18	78	45	75	73	44	54	81	51	2	7,6	3,3	10	9	5	7,4	11,1	6
186	205	518,88	_	5	5	5	5	5	5	5	4	5	872	986	1564	800	895	1268	916	982	1147	18	62	80	38	40	34	25	14	40	4,5	14,1	11,4	10,7	10	6	6	2,8	7,8
187	100	519,19	_	5	5	4	3	4	4	4	4	5	651	502	516	744	467	664	2512	844	1047	72	28	23	12	49	45	186	168	147	24,8	12,6	8,8	2,7	20,9	13,6	14,8	39,7	31,4
188	140	520,21	_	5	5	5	5	4	5	4	5	5	536	609	704	573	669	730	494	697	2005	9	16	44	17	34	84	9	37	123	3,8	5,9	14	6,8	10	25,7	3,7	11,7	13,7
189	182	520,3	_	5	4	5	5	5	5	5	4	5	1647	2091	2460	2023	2121	1605	1534	1565	1584	121	36	120	99	218	117	53	35	54	16,5	3,4	10,9	10,9	23	16,3	7,8	4,5	7,7
190	85	520,46	_	5	5	5	5	4	5	5	3	5	3723	4216	3737	3596	3237	4576	4364	3589	3912	647	431	423	259	80	618	629	46	313	38,9	22,8	25,3	16,1	4,9	30,2	32,3	2,2	17,9
191	328	521,45	_	2	5	4	0	4	5	2	4	5	418	470	687		491	829	407	538	2387	11	37	179		46	134	9	97	800	3,7	17,4	52,2		18,7	36,2	3	35,9	74,9
192	117	521,87	_	4	5	5	5	5	5	4	4	4	1472	1972	2419	1878	2041	1959	838	1115	1390	35	53	86	106	93	120	8	34	25	4,7	6	8	12,6	10,2	13,7	1,9	6,1	3,6
193	102	522,75	_	5	5	5	5	5	5	5	4	5	3171	3305	3981	2428	2261	2508	651	777	938	261	164	139	63	63	111	31	4	59	18,4	11,1	7,8	5,8	6,2	9,9	10,8	0,9	14
194	173	523,26	_	3	5	5	5	4	5	5	5	5	1838	2011	2143	2124	2026	2165	1307	1297	1508	10	80	115	78	47	146	127	47	153	1	8,9	12	8,2	4,6	15,1	21,7	8,2	22,7
195	200	524,39	_	5	5	4	5	5	4	4	5	5	548	795	601	518	587	646	708	1069	1590	24	46	39	37	50	52	33	137	255	9,8	12,9	13,1	15,9	18,9	15,9	9,2	28,6	35,9
196	100	525,47	_	5	4	5	5	5	5	2	5	5	716	1274	1185	494	1087	2551	1265	2626	5768	97	59	266	33	203	646	284	138	400	30,4	9,3	50,3	15,1	41,8	56,6	31,7	11,8	15,5
197	133	527,36	Phosphoenolpyruvate	5	5	5	5	5	5	5	5	5	1679	940	1474	2457	1344	1505	1509	2065	986	359	106	218	305	221	185	262	257	113	47,8	25,3	33,1	27,8	36,8	27,5	38,8	27,8	25,5
198	142	527,62	_	4	4	5	4	4	4	5	5	5	996	625	6076	2792	2840	1061	1235	1148	828	299	107	2735	415	695	509	213	213	101	60	34,3	100,7	29,7	49	96,1	38,6	41,5	27,3
199	195	527,67	_	3	5	5	4	5	5	5	5	5	1244	1091	1308	1282	1366	1330	958	1006	937	4	73	128	17	112	63	95	45	75	0,6	15	22	2,7	18,4	10,6	22,2	10,1	18
200	117	527,9	Dodecanoate	5	4	5	3	5	5	5	5	5	7473	5601	7305	7242	7169	7127	5272	4968	4934	529	150	163	4	321	370	102	240	92	15,8	5,3	5	0,1	10	11,6	4,3	10,8	4,2
201	100	528,06	_	5	5	5	5	5	5	5	4	5	1162	1613	2346	2129	2190	2949	2148	4056	3612	182	237	425	232	245	216	428	167	809	35	32,9	40,5	24,4	25	16,4	44,6	8,3	50,1
202	111	528,07	_	5	5	5	5	5	5	5	3	5	1345	1194	1302	1358	1441	1416	1253	1135	1224	152	81	84	61	45	103	89	7	109	25,2	15,1	14,4	10	6,9	16,2	15,9	1	19,9
203	288	529,81	_	5	5	5	3	5	5	4	5	4	413	659	518	435	473	687	573	1597	2470	13	24	44	16	21	117	25	291	126	6,8	8,2	19,1	6,4	10	38	8,9	40,7	10,2
204	98	529,93	_	5	5	5	5	5	5	4	5	5	1629	3653	4178	1580	2723	10602	2014	7800	23594	80	322	863	173	395	3256	63	929	1376	10,9	19,7	46,2	24,4	32,5	68,7	6,3	26,6	13
205	128	530,08	Glutamine	4	5	5	5	5	5	4	5	5	690	1564	1414	925	1398	1972	1107	1910	3468	17	122	209	81	139	178	67	201	289	4,8	17,4	33,1	19,6	22,2	20,1	12,1	23,5	18,6
206	116	530,15	Alanine, alanyl-	5	5	5	5	5	5	5	5	5	4448	15565	10255	3244	10148	14250	1804	1311	2373	465	867	524	147	273	1052	120	48	70	23,4	12,4	11,4	10,1	6	16,5	14,8	8,1	6,6
207	218	531,09	Phenylalanine	5	5	4	5	5	5	5	5	4	2851	5772	6019	2561	5383	8194	2256	4069	5557	134	195	314	121	297	430	136	163	193	10,5	7,6	10,4	10,6	12,3	11,7	13,5	8,9	6,9
208	103	531,27	_	5	4	5	5	5	5	4	5	0	994	1807	2129	1102	1684	2045	990	1254		57	82	82	63	84	64	25	41		12,8	9,1	8,6	12,8	11,2	7	5,1	7,4	
209	101	533,06	_	4	4	5	5	5	5	0	0	0	3772	3709	4927	2241	2099	2247				124	65	447	99	203	185				6,6	3,5	20,3	9,9	21,7	18,4			
210	156	533,75	_	5	4	5	5	5	5	5	5	5	2426	2468	3185	2274	2712	3468	2647	2238	3079	604	108	575	294	412	173	120	338	394	55,7	8,7	40,4	28,9	34	11,2	10,1	33,7	28,6
211	142	533,85	Proline [+CO2]	5	4	3	5	5	5	5	5	5	1004	1222	1276	898	1088	2762	947	1523	10812	205	31	27	86	88	643	32	272	1870	45,7	5,1	3,7	21,4	18,1	52	7,6	39,9	38,7
212	85	534,93	_	5	5	5	5	5	4	5	5	5	3556	3640	3397	3880	3940	5668	3276	2823	3246	755	317	314	112	512	137	597	90	237	47,5	19,5	20,7	6,4	29,1	4,8	40,7	7,1	16,3
213	117	536,07	_	4	5	5	5	5	5	0	0	1	2754	2283	2999	1916	1647	1834			502	47	77	297	76	102	91				3,4	7,6	22,1	8,8	13,8	11,1			

Mass Spectral Feature (MSF)			Metabolite Information	Normalized signal intensities: No. of observations (counts)									Mean average									Standard error : $SE = s/\sqrt{n}$									Coefficient of variation (CV) [%]								
#	M/Z	RI Time (avg) [s]	Metabolite	Mar-[T0]	Mar-[T1]	Mar-[T3]	Mut-[T0]	Mut-[T1]	Mut-[T3]	Syn-[T0]	Syn-[T1]	Syn-[T3]	Mar-[T0]	Mar-[T1]	Mar-[T3]	Mut-[T0]	Mut-[T1]	Mut-[T3]	Syn-[T0]	Syn-[T1]	Syn-[T3]	Mar-[T0]	Mar-[T1]	Mar-[T3]	Mut-[T0]	Mut-[T1]	Mut-[T3]	Syn-[T0]	Syn-[T1]	Syn-[T3]	Mar-[T0]	Mar-[T1]	Mar-[T3]	Mut-[T0]	Mut-[T1]	Mut-[T3]	Syn-[T0]	Syn-[T1]	Syn-[T3]
217	157	541,84	_	5	5	5	5	5	3	5	5	5	3802	4149	4353	4672	5046	5113	4465	4081	4287	451	250	409	204	228	47	113	248	252	26,5	13,5	21	9,8	10,1	1,6	5,7	13,6	13,2
218	89	542,39	_	4	5	5	5	5	5	3	5	5	864	1212	1297	1192	1414	1625	1248	1709	2199	26	94	78	54	79	84	7	41	78	5,9	17,4	13,4	10,1	12,5	11,6	1	5,4	7,9
219	85	543,44	_	5	5	5	5	4	4	5	5	5	3026	3307	2920	2855	2517	3177	3527	2900	3079	517	350	322	200	75	168	465	213	272	38,2	23,7	24,6	15,7	5,9	10,6	29,5	16,4	19,8
220	204	548,63	_	5	5	4	5	5	4	4	5	5	1371	1777	1599	989	1781	1731	1223	1617	1536	143	59	55	57	80	105	205	125	150	23,3	7,4	6,9	12,8	10,1	12,2	33,6	17,3	21,8
221	129	549,83	_	5	4	5	5	4	5	4	5	5	1010	1542	1871	1014	1426	1904	1077	1124	1447	98	28	108	44	16	113	69	87	97	21,7	3,6	12,9	9,7	2,3	13,3	12,7	17,3	15
222	116	549,94	Asparagine	5	5	5	5	5	5	5	5	5	1429	2954	2914	1411	2269	5479	3658	4976	5970	251	398	493	99	351	842	604	448	1217	39,3	30,1	37,8	15,7	34,6	34,4	36,9	20,1	45,6
223	98	549,97	_	5	4	5	5	5	4	5	5	5	508	633	714	503	608	830	2597	2605	1566	18	11	88	16	65	20	418	116	160	7,9	3,4	27,5	7	23,8	4,9	35,9	10	22,8
224	112	550,33	_	5	4	5	5	5	5	4	4	5	4082	1902	4620	3626	3642	2839	1447	1361	1138	955	211	1106	466	1158	603	97	186	105	52,3	22,2	53,5	28,8	71,1	47,5	13,5	27,3	20,6
225	243	555,76	Glycerol 2-P	5	4	5	5	5	5	5	5	5	1151	1119	1251	1150	1247	1377	1245	1023	1221	57	35	23	36	58	73	99	71	34	11,1	6,3	4,1	7	10,4	11,8	17,8	15,6	6,3
226	101	556,05	_	5	5	5	5	5	5	4	5	5	1547	1634	1863	1652	1781	1799	1483	1406	1592	67	91	48	43	62	91	77	33	11	9,7	12,5	5,8	5,9	7,8	11,3	10,4	5,2	1,5
227	156	556,19	_	5	5	4	5	5	5	5	5	5	2252	2324	2996	9114	7387	9995	1867	2446	2273	413	446	142	1882	1264	1134	165	106	362	41,1	42,9	9,5	46,2	38,3	25,4	19,7	9,7	35,6
228	125	556,34	_	5	5	5	5	5	5	5	5	5	1171	1527	1834	1185	1470	2385	1105	1104	1286	168	208	129	36	110	482	52	69	62	32,1	30,4	15,7	6,8	16,7	45,2	10,4	14,1	10,7
229	204	556,42	_	5	4	5	5	5	5	4	5	5	1752	1837	2337	1776	2354	2159	1988	1990	1995	105	18	51	117	152	66	372	81	76	13,4	2	4,9	14,7	14,4	6,9	37,4	9,1	8,5
230	99	558,73	_	5	5	5	4	5	5	5	5	5	1668	2547	3166	2015	2737	2174	1162	1190	1242	175	284	370	65	269	214	46	61	56	23,5	24,9	26,1	6,4	22	22	8,9	11,4	10,2
231	217	560,45	Glucosyl	5	5	5	5	5	5	5	5	5	4610	10454	20853	6207	16520	22512	6274	11287	11396	567	722	967	299	1394	1873	309	1252	632	27,5	15,5	10,4	10,8	18,9	18,6	11	24,8	12,4
232	142	570,43	Ornithine	5	5	5	5	5	5	5	5	5	10437	15632	10416	6322	7747	12516	13946	35666	48009	1792	1750	2184	492	1126	1989	1759	2423	4959	38,4	25	46,9	17,4	32,5	35,5	28,2	15,2	23,1
233	299	573,9	Glycerol 3-P	4	5	5	5	5	5	4	5	5	103654	99617	130379	110051	111197	122579	91566	112929	143967	3871	5080	3217	3639	4865	5010	1559	1630	2371	7,5	11,4	5,5	7,4	9,8	9,1	3,4	3,2	3,7
234	214	575,93	_	4	5	4	5	4	5	4	5	5	475	815	784	588	636	1517	644	1477	10484	25	92	97	54	28	277	48	82	903	10,5	25,1	24,7	20,6	8,8	40,8	14,7	12,4	19,2
235	111	576,33	_	5	5	4	4	5	5	5	5	5	2005	2352	2861	1870	2173	4363	2355	2108	2965	407	311	59	26	90	766	153	313	357	45,4	29,5	4,1	2,8	9,2	39,3	14,5	33,1	26,9
236	142	577,01	_	4	5	5	4	5	5	5	5	5	579	989	737	520	799	1007	941	1492	3248	72	59	103	22	56	131	108	343	561	25	13,4	31,3	8,4	15,7	29,2	25,6	51,4	38,6
237	103	578,95	Fructose	4	5	4	5	5	4	5	5	5	20314	26294	22786	16953	27403	12860	7067	10929	10459	2301	3656	2734	4532	4028	782	1440	1244	2115	22,7	31,1	24	59,8	32,9	12,2	45,5	25,5	45,2
238	156	579,99	Glutamate, N-acetyl-	5	5	5	5	5	4	5	4	5	3055	3135	5083	4480	4512	5361	1949	2631	4383	526	433	306	191	334	97	251	16	168	38,5	30,9	13,5	9,5	16,5	3,6	28,8	1,2	8,6
239	85	580,6	_	5	5	5	5	4	4	5	5	5	7082	7118	6412	5540	4994	7426	1024	922	966	1462	796	778	234	324	313	68	25	78	46,1	25	27,1	9,5	13	8,4	14,9	6,1	18
240	205	581,54	_	4	5	4	5	5	5	5	4	5	729	830	655	2949	3132	1779	701	950	1294	59	103	25	1027	1023	386	74	28	53	16,1	27,7	7,5	77,9	73	48,5	23,5	5,9	9,2
241	117	581,88	_	5	2	4	5	4	5	5	5	5	1170	1215	1462	2499	3276	1507	1014	1306	1543	142	104	228	819	1001	239	89	103	25	27,1	12,1	31,2	73,3	61,1	35,4	19,5	17,7	3,6
242	104	582,11	_	5	4	5	5	5	5	5	5	5	1860	1613	2627	2056	2354	1872	1488	1662	1583	235	111	545	163	302	230	36	85	70	28,3	13,7	46,4	17,7	28,7	27,5	5,4	11,5	9,9
243	247	583,35	_	5	5	5	5	5	4	4	5	5	540	1767	1381	550	1833	1388	498	1292	1031	36	141	37	17	102	58	13	154	46	15	17,8	5,9	6,8	12,5	8,4	5,4	26,7	9,9
244	299	586,83	_	5	4	5	5	5	4	5	5	4	908	952	1118	1731	1742	1511	537	642	653	55	25	132	320	348	120	40	36	18	13,6	5,3	26,4	41,3	44,7	15,9	16,8	12,4	5,5
245	205	587,27	Sorbitol	4	5	5	4	3	5	5	5	3	31147	32326	37641	30187	30392	27542	26211	26976	25950	3096	2311	2199	649	347	1382	2110	1455	111	19,9	16	13,1	4,3	2	11,2	18	12,1	0,7
246	128	588,06	_	5	5	5	5	5	5	4	5	5	1420	2445	3712	1526	3148	2852	1127	1704	4047	144	159	244	17	193	452	12	147	240	22,7	14,6	14,7	2,5	13,7	35,4	2,1	19,3	13,2
247	160	590,08	Glucose	5	5	5	5	5	5	5	3	5	7244	7462	13225	5164	5693	3888	3378	4582	4182	1362	870	3939	1150	668	334	585	51	634	42,1	26,1	66,6	49,8	26,2	19,2	38,7	1,9	33,9
248	265	591,55	_	5	5	4	4	5	3	4	3	5	1411	2402	4060	1618	1628	2262	591	653	569	371	229	148	47	171	7	107	22	60	58,8	21,3	7,3	5,8	23,4	0,5	36,1	5,8	23,8
249	273	592,46	Citrate	5	5	5	4	4	4	5	5	5	9858	14264	35280	12735	24736	28544	2817	23204	19343	2268	4093	2948	140	794	1616	331	1831	993	51,4	64,2	18,7	2,2	6,4	11,3	26,3	17,6	11,5
250	197	594,67	_	5	5	4	5	4	5	4	5	5	1440	1144	957	1080	1060	1073	967	873	809	136	128	35	86	65	99	88	73	81	21,1	25,1	7,4	17,9	12,3	20,7	18,2	18,6	22,4
251	123	595,49	_	5	5	5	4	5	5	5	5	5	1185	1353	1365	1422	1518	1703	1183	1010	1108	128	74	133	33	93	141	36	127	84	24,2	12,3	21,8	4,7	13,7	18,5	6,8	28,1	16,9
252	273	597,44	Isocitrate	4	4	4	4	3	4	5	5	4	517	969	1355	692	804	845	109017	150925	98705	52	175	372	63	39	53	12398	3436	1417	20,2	36,1	55	18,1	8,5	12,6	25,4	5,1	2,9
253	156	598,09	Glutamine	5	5	5	5	5	5	5	5	5	17704	40195	37322	32663	44117	52647	30037	70957	99692	2152	5181	1701	3025	2410	4408	2670	4071	9846	27,2	28,8	10,2	20,7	12,2	18,7	19,9	12,8	22,1
254	96	598,75	_	5	5	5	5	5	5	3	5	5	1403	5512	5160	830	5158	12478	2087	11023	21115	297	870	1145	113	1525	3069	260	816	949	47,4	35,3	49,6	30,5	66,1	55	21,6	16,5	10,1
255	205	598,7	Glucose	5	5	5	5	5	5	5	3	4	1497	2200	2935	1206	1932	2671	1758	4037	4809	199	201	621	121	184	447	92	50	82	29,7	20,4	47,3	22,4	21,3	37,4	11,8	2,1	3,4
256	121	600,01	_	5	5	5	5	4	5	5	5	5	7356	8340	8470	9446	9709	11323	6949	6545	6489	291	229	276	197	86	1056	302	488	230	8,9	6,1	7,3	4,7	1,8	20,9	9,7	16,7	7,9
257	140	601,06	_	5	4	5	5	5	5	5	5	5	2129	675	4271	3585	3611	3660	7847	2888	2350	748	109	901	178	780	642	974	172	179	78,5	32,2	47,2	11,1	48,3	39,2	27,8	13,3	17
258	117	601,35	_	5	5	3	5	5	5	5	5	5	122474	176116	187609	128805	166816	164568	143593	112407	135536	25262	30136	3104	13700	23863	27912	13710	18564	19000	46,1	38,3	2,9	23,8	32	37,9	21,3	36,9	31,3
259	156	602,88	_	5	5	4	5	5	5	5	5	4	802	596	1603	1031	1253	1306	3229	1328	1461	143	46	360	96	248	117	723	263	153	39,8	17,4	44,9	20,9	44,2	20	50,1	44,3	20,9
260	299	605,24	Glycerate 3-P	5	5	5	5	5	5	5	5	5	4848	13706	13133	6880	17492	12893	3831	19023	8011	1086	4050	1601	620	1618	1831	386	1828	843	50,1	66,1	27,3	20,2	20,7	31,8	22,5	21,5	23,5
261	95	605,68	_	5	4	4	5	5	5	5	5	5	88633	98315	96982	100313	99853	100242	103519	104091	103165	7415	877	2355	2181	4323	3275	1765	1446	4372	18,7	1,8	4,9	4,9	9,7	7,3	3,8	3,1	9,5
262	157	605,82	Citrulline	4	5	5	5	5	3	5	5	5	2153	6803	5760	2073	4908	9013	6533	25991	44536	77	829	792	141	708	53	902	2863	4560	7,1	27,2	30,8	15,2	32,3	1	30,9	24,6	22,9
263	119	609,44	_	5	5	3	5	5	5	5	5	4	3028	3403	2839	2542	3110	2192	3974	3761	2861	446	510	63	214	367	270	549	364	241	32,9	33,5	3,8	18,8	26,4	27,6	30,9	21,6	16,9
264	85	613	_	5	5	4	5	4	5	5	3	5	1764	1757	1589	1700	1363	1965	1856	1647	1809	156	140	78	63	73	154	131	36	117	19,8	17,8	9,8	8,3	10,6	17,5	15,8	3,8	14,4
265	217	613,69	_	0	0	0	0	2	1	0	5	4					533	501		1282	1379					25			10	12					6,6			1,7	1,7
266	156	615,12	_	4	5	5	5	5	5	4	5	5	4675	5748	5688	4348	5893	8626	40379	21190	13675	505	555	963	415	990	963	996	874	845	21,6	21,6	37,8	21,3	37,6	24,9	4,9	9,2	13,8
267	205	615,28	_	4	5	4	5	5	5	5	5	3	8952	8969	12606	11410	9201	8295	6238	7017	6679	1484	747	479	537	451	381	122	484	17	33,2	18,6	7,6	10,5	10,9	10,3	4,4	15,4	0,4
268	117	615,99	Tetradecanoate	4	5	5	5	5	5	5	5	5	42759	44019	49863	48961	51708	52924	41633	43299	46645	2901	2135	1781	525	1669	1093	1140	383	906	13,6	10,8	8	2,4	7,2	4,6	6,1	2	4,3
269	197	616,74	_	5	5	4	5	4	5	4	5	4	1498	1268	1094	1166	1177	1195	956	874	714	142	161	49	144	107	160	134	112	34	21,2	28,4	8,9	27,6	18,1	29,8	28	28,7	9,6
270	217	617,12	_	5	5	5	5	5	5	5	5	5	926	2688	3447	1068	3368	3914	680	2302	2427	26	36	79	64	90	213	21	85	51	6,4	3	5,1	13,4	6	12,2	6,8	8,3	4,7
271	95	618,86	_	5	5	4	4	5	5	5	5	5	20247	21802	21278	21896	22009	22511	22876	22121	22327	2297	736	492	199	956	802	324	516	1128	25,4	7,5	4,6	1,8	9,7	8	3,2	5,2	11,3
272	197	619,14	_	5	3	4	5	4	5	5	4	4	1953	1566	1180	1395	1442	1382	1151	850	846	211	43	60	193	117	213	177	74	33	24,1	4,8	10,2	31	16,2	34,5	34,3	17,5	7,9
273	197	622,93	_	5	5	4	5	4	5	4	4	5	1498	1205	964	1105	1083	1089	944	712	702	146	147	73	164	97	168	148	42	81	21,9	27,3	15,1	33,2	18	34,5	31,3	11,8	25,9
274	85	624,45	Nonadecane	5	5	5	5	4	5	4	5	5	4526	4725	3972	2570	2109	3363	615	584	559	992	383	395	265	147	302	50	33	30	49	18,1	22,2	23,1	13,9	20,1	16,4	12,5	12,1
275	294	624,56	_	3	5	5	4	5	5	4	5	5	940	1036	1261	1278	1476	1609	498	589	602	8	56	46	34	51	204	14	18	14	1,5	12	8,1	5,2	7,7	28,4	5,5	6,6	5,3
276	204	624,83	_	5	5	5	5	5	5	5	5	5	877	1081	1253	1074	1277	1469	722	775	851	44	26	59	49	27	124	32	58	50	11,2	5,3	10,6	10,2	4,7	18,9	9,8	16,6	13,2
277	103	626,03	_	5	4	5	5	5	4	5	5	5	1132	1290	1897	939	1104	1334	1565	1533	2689	117	22	99	62	48	16	63	62	122	23,1	3,5	11,6	14,8	9,8	2,3	9	9,1	10,2
278	100	626,88	[Aspartate, N-carbamyl-]	5	5	5	5	5	5	5	5	5	703	1246	1402	789	1379	1592	681	3453	2779	69	67	164	38	111	66	31	488	342	21,9	11,9	26,2	10,7	17,9	9,3	10,3	31,6	27,5
279	95	627,01	_	5	4	4	5	5	5	5	5	5	30183	32645	31282	33145	33016	33836	35172	33715	33110	3527	375	784	764	1453	1283	173	454	1740	26,1	2,3	5	5,2	9,8	8,5	1,1	3	11,8
280	197	628,4	_	5	5	4	5	4	5	5	5	5	1887	1549	1368	1486	1579	1643	1157	1062	974	187	148	34	163	84	140	141	127	89	22,2	21,3	4,9	24,6	10,7	19	27,2	26,6	20,5
281	143	628,46	_	5	5	5	5	4	5	5	5	5	1508	1489	1472	1492	1639	2097	939	805	855	243	100	99	61	30	242	58	68	60	36	15	15,1	9,2	3,6	25,8	13,8	18,9	15,6
282	204	630,93	_	5	5	5	5	4	5	4	5	5	2190	2154	3166	1147	1386	2012	1760	2309	2536	427	187	758	107	53	280	176	206	266	43,5	19,4	53,5	20,8	7,6	31,1	20	19,9	23,5
283	194	632,11	_	5	5	5	5	5	5	5	5	5	1438	1623	1877	1632	2041	2113	1381	1165	1282	251	148	198	103	139	226	110	120	136	39	20,4	23,6	14,1	15,2	23,9	17,8	23	23,7
284	100	632,26	_	5	5	5	5	5	5	5	4	5	1686	2488	2551	1530	2572	3002	1117	1106	1449	241	285	386	54	316	258	85	24	84	32	25,6	33,9	7,9	27,4	19,2	16,9	4,3	12,9
285	156	632,62	[Glutamate, N-acetyl-]	5	5	5	5	5	5	5	5	5	2408	1920	3216	3217	2905	3012	1097	1818	2428	628	271	530	258	516	356	145	257	334	58,3	31,5	36,8	17,9	39,7	26,4	29,5	31,6	30,8

Mass Spectral Feature (MSF)			Metabolite Information	Normalized signal intensities																																	
				No. of observations (counts)									Mean average									Standard error : $SE = s/\sqrt{n}$									Coefficient of variation (CV) [%]								
#	M/Z	RI Time (avg) [s]	Metabolite	Mar-[T0]	Mar-[T1]	Mar-[T3]	Mut-[T0]	Mut-[T1]	Mut-[T3]	Syn-[T0]	Syn-[T1]	Syn-[T3]	Mar-[T0]	Mar-[T1]	Mar-[T3]	Mut-[T0]	Mut-[T1]	Mut-[T3]	Syn-[T0]	Syn-[T1]	Syn-[T3]	Mar-[T0]	Mar-[T1]	Mar-[T3]	Mut-[T0]	Mut-[T1]	Mut-[T3]	Syn-[T0]	Syn-[T1]	Syn-[T3]	Mar-[T0]	Mar-[T1]	Mar-[T3]	Mut-[T0]	Mut-[T1]	Mut-[T3]	Syn-[T0]	Syn-[T1]	Syn-[T3]
289	102	639,07	_	2	5	2	0	1	3	4	5	5	440	457	392		465	640	576	818	2150	40	24	26			144	60	58	96	12,9	11,9	9,4			38,9	20,8	15,9	9,9
290	133	639,84	_	5	4	3	5	5	5	5	5	3	1024	1202	1229	1333	1481	1565	828	767	935	66	31	12	186	152	193	53	59	8	14,4	5,2	1,7	31,1	23	27,5	14,3	17	1,6
291	117	640,11	_	5	5	5	5	5	5	5	5	5	6844	7622	8643	12477	13497	15029	5363	4148	4694	478	716	691	3146	3042	3327	321	441	287	15,6	21	17,9	56,4	50,4	49,5	13,4	23,8	13,7
292	128	643,12	Methionine sulfoxide	5	4	5	5	5	5	5	5	5	1334	3772	5659	1690	4690	4125	741	2073	6189	197	198	450	40	323	754	36	309	523	33	10,5	17,8	5,3	15,4	40,9	10,9	33,4	18,9
293	117	645,38	_	3	5	5	5	5	5	5	5	5	4594	3942	4775	6707	6588	6735	3447	3244	3255	35	91	222	868	947	923	143	70	77	1,3	5,2	10,4	28,9	32,2	30,6	9,3	4,9	5,3
294	299	646,86	Hexadecan-1-ol	5	5	3	5	5	5	5	5	5	1504	1557	1662	1776	1987	1778	1534	1469	1509	51	71	1	77	127	42	21	64	50	7,5	10,1	0,1	9,6	14,3	5,3	3	9,7	7,4
295	174	647,91	_	4	5	4	1	4	5	5	5	5	961	1298	1146	734	1004	1593	2656	2348	5106	124	89	101		36	333	336	151	562	25,7	15,2	17,7		7,2	46,7	28,3	14,4	24,6
296	152	651,84	_	5	5	5	3	5	5	4	3	3	39715	41770	39310	17836	18800	19507	448	393	427	1972	2225	2098	185	2149	1527	52	9	19	11,1	11,9	11,9	1,8	25,6	17,5	23,3	3,9	7,8
297	89	652,1	_	3	5	5	5	4	4	5	5	5	1021	1001	1244	780	789	959	1130	1315	1779	1	40	52	12	57	45	68	28	82	0,2	8,9	9,3	3,4	14,5	9,3	13,4	4,8	10,3
298	171	652,17	_	5	5	5	4	5	4	5	5	5	1016	1394	1818	1057	1385	936	1090	1182	1463	31	143	143	23	106	66	21	79	63	6,8	22,9	17,5	4,3	17,2	14	4,3	15	9,6
299	103	653,89	_	3	5	5	5	5	4	4	5	4	1765	2391	6761	1670	6783	1360	854	824	1144	140	782	1710	275	2131	516	65	18	72	13,7	73,1	56,6	36,8	70,3	75,8	15,3	5	12,6
300	156	654,47	_	5	5	5	5	5	5	4	5	5	1454	2349	6398	2077	2923	5099	504	559	794	235	424	1506	164	301	616	44	72	38	36,1	40,3	52,6	17,6	23	27	17,3	28,7	10,6
301	117	657,26	Pentadecanoate	5	5	4	5	4	5	5	5	5	5709	6005	5847	6463	7701	7497	5471	4681	6427	261	283	78	504	399	571	448	327	737	10,2	10,6	2,7	17,5	10,4	17	18,3	15,6	25,6
302	218	658,17	Tyrosine	5	5	5	5	5	4	3	5	3	13188	31886	37772	12579	32279	66743	5299	12661	21021	864	1617	3168	572	1535	839	58	377	105	14,6	11,3	18,8	10,2	10,6	2,5	1,9	6,7	0,9
303	87	660,53	_	5	5	5	5	5	5	4	4	5	1010	1697	2026	1315	1586	1016	771	824	1022	55	174	201	80	162	139	35	35	54	12,2	23	22,2	13,6	22,9	30,7	9,1	8,5	11,9
304	128	662,22	_	4	5	5	5	4	5	5	3	5	512	801	852	574	928	874	640	4219	1685	56	105	84	36	48	121	83	52	252	21,7	29,4	22,1	14,1	10,4	30,9	28,9	2,1	33,5
305	103	663,47	_	4	5	5	5	5	5	5	5	5	439	652	824	595	807	910	2105	2474	2454	31	27	44	33	53	60	65	51	97	13,9	9,2	12	12,5	14,7	14,9	6,9	4,6	8,8
306	128	666,82	_	5	2	4	4	5	2	0	1	1	521	1028	2212	614	1202	920		371	1172	72	251	137	112	312	383				31	34,5	12,4	36,5	58	58,9			
307	179	669,03	_	4	5	4	5	5	5	4	5	4	786	1186	1206	865	1400	2196	597	843	953	51	43	55	38	153	349	16	48	9	13	8	9,1	9,9	24,4	35,5	5,3	12,6	1,9
308	124	671,12	_	5	5	5	3	5	5	5	5	5	912	923	1098	907	997	2171	764	910	972	36	87	93	8	80	573	30	31	32	8,9	21,2	18,8	1,6	17,9	59	8,6	7,5	7,4
309	205	673,92	_	5	5	5	4	5	5	5	5	5	640	1073	1108	515	1041	976	658	1332	1689	37	35	49	9	41	39	57	35	31	13	7,2	9,9	3,5	8,9	8,9	19,2	5,9	4,1
310	103	676,52	_	5	5	5	4	5	5	3	5	5	561	1599	1891	468	1552	1960	386	2115	3203	30	45	143	18	50	117	6	64	122	12,1	6,3	16,9	7,6	7,3	13,3	2,7	6,8	8,5
311	96	677,88	_	3	2	4	5	4	5	5	5	4	1066	365	1426	1109	1284	729	1445	817	519	267	1	385	136	366	46	304	114	58	43,4	0,3	53,9	27,5	57	14,1	47,1	31,3	22,5
312	264	679,44	Adenine	4	5	5	5	5	5	4	5	5	3156	5145	8915	3753	5847	10533	3182	3729	6221	77	191	256	111	316	276	121	162	145	4,9	8,3	6,4	6,6	12,1	5,9	7,6	9,7	5,2
313	142	680,07	_	0	4	4	0	1	4	1	5	5		460	413		377	566	384	1203	2146		29	2			58		89	219		12,7	1,1			20,6		16,6	22,9
314	117	680,12	_	5	5	5	5	5	5	5	5	5	1298	1422	1589	2247	2427	2435	659	669	1142	148	90	151	519	572	455	32	62	198	25,5	14,2	21,3	51,7	52,7	41,8	11	20,6	38,7
315	97	680,43	_	5	5	4	5	5	3	5	5	5	1247	1445	1394	1555	1449	1619	1111	1070	1058	240	27	28	50	124	17	57	39	82	43	4,2	4	7,2	19,1	1,8	11,5	8,1	17,2
316	104	682,33	_	5	5	4	5	5	5	3	4	4	7081	5358	5061	14801	12760	12181	845	685	525	2034	568	548	1966	2808	1600	152	59	36	64,2	23,7	21,7	29,7	49,2	29,4	31,1	17,2	13,6
317	142	682,58	_	5	5	5	5	5	4	4	5	5	453	891	744	464	678	1162	889	2452	4261	35	84	98	8	97	163	95	364	481	17,3	21,1	29,4	4	31,9	28	21,4	33,2	25,3
318	101	682,72	_	5	5	5	5	5	5	5	4	4	1206	1667	1786	1388	1496	1114	973	950	1211	79	233	105	90	169	104	49	14	47	14,7	31,2	13,1	14,5	25,3	20,9	11,1	2,9	7,8
319	99	684,89	_	5	5	5	5	5	4	4	5	5	57836	111642	121938	73261	92045	56346	44193	38275	43463	7868	14661	18308	7087	12699	2768	581	5036	2756	30,4	29,4	33,6	21,6	30,9	9,8	2,6	29,4	14,2
320	156	685,24	_	5	5	3	2	5	4	2	5	5	441	1406	3862	431	1085	3156	492	476	627	24	126	70	16	78	133	50	36	62	12	20	3,1	5,4	16	8,4	14,4	16,9	21,9
321	128	688,45	_	5	4	5	5	3	4	4	5	5	1847	3347	10735	1369	2159	9083	1378	972	1473	114	121	1303	58	20	239	39	37	92	13,8	7,2	27,1	9,4	1,6	5,3	5,7	8,6	14
322	115	688,58	_	5	5	5	4	5	3	5	4	5	974	1224	1951	1408	1596	2582	704	604	752	200	105	310	35	154	30	104	67	86	46	19,1	35,5	5	21,5	2	33	22,3	25,6
323	160	689,21	_	0	5	4	0	4	5	0	5	5		565	750		518	691		2807	1416		57	140		33	65		776	289		22,7	37,2		12,8	21		61,8	45,6
324	103	690,4	_	5	5	5	5	5	5	5	3	4	1306	1363	1467	2196	2026	1992	872	779	642	203	146	203	355	472	463	89	6	15	34,8	24	30,9	36,1	52,1	52	22,8	1,3	4,6
325	167	690,71	_	5	5	4	4	5	5	4	5	5	1253	1939	917	1547	1411	3078	754	975	725	255	446	91	164	241	477	94	69	55	45,4	51,4	19,9	21,2	38,1	34,7	25,1	15,9	16,9
326	110	692,26	_	5	4	5	5	5	5	4	3	5	1025	2323	1298	1241	1355	1494	578	492	542	59	79	52	81	53	139	101	33	37	12,9	6,8	9	14,5	8,8	20,8	35,1	11,7	15,4
327	149	694,2	_	5	4	5	5	5	5	5	5	5	11675	9565	10824	10010	12756	11014	8748	7430	6443	954	366	1728	1126	1207	1451	1137	685	242	18,3	7,7	35,7	25,2	21,2	29,5	29,1	20,6	8,4
328	174	694,54	Ornithine, N-acetyl-	5	4	5	5	5	5	1	4	5	890	2493	1801	929	1723	1997	382	3920	8343	95	63	167	188	179	254		145	860	23,7	5	20,8	45,2	23,3	28,4		7,4	23
329	311	695,68	Hexadecenoate, 9Z-	5	5	5	5	5	3	5	5	5	1485	1673	1687	1618	1818	2059	2389	1772	1876	234	244	282	78	123	35	192	210	193	35,3	32,6	37,4	10,8	15,1	2,9	18	26,5	23
330	117	696,78	Hexadecanoate	5	3	5	4	5	4	4	5	5	582460	651785	615180	543669	652301	681473	602871	485645	541128	114359	4250	61435	12348	62389	34613	29978	61165	56464	43,9	1,1	22,3	4,5	21,4	10,2	9,9	28,2	23,3
331	169	698,48	_	5	5	5	5	5	5	5	5	5	1134	1170	1335	1144	1111	1119	1259	1619	1454	73	45	20	25	38	37	90	55	32	14,5	8,6	3,4	4,9	7,6	7,3	15,9	7,5	4,9
332	94	699,56	_	5	5	5	3	5	5	1	2	3	1323	1315	1182	989	861	816	427	397	462	108	32	62	6	48	28		28	51	18,2	5,4	11,6	1,1	12,4	7,7		10,1	19,1
333	102	700,03	_	5	5	5	5	4	5	5	4	5	1887	2107	1925	2112	2001	2054	1679	1596	1737	212	126	58	58	45	162	93	6	81	25,2	13,4	6,8	6,1	4,5	17,6	12,4	0,8	10,4
334	128	701,88	_	5	5	5	4	5	4	4	5	5	443	652	1613	488	677	3267	567	483	513	12	10	259	18	56	162	27	24	10	6,3	3,3	35,9	7,2	18,6	9,9	9,4	11	4,2
335	138	703,93	_	5	5	5	5	3	5	5	5	5	1120	1062	1850	1412	1491	1525	1661	1272	1306	166	119	301	62	20	112	164	74	72	33,1	25	36,4	9,8	2,3	16,4	22,1	13	12,2
336	299	704,5	Ribose 5-P	5	5	5	5	3	5	4	5	5	1624	2549	3071	3218	4032	3612	422	946	866	188	217	192	298	17	210	8	90	33	25,8	19,1	14	20,7	0,7	13	3,7	21,2	8,6
337	174	708,59	_	5	5	5	5	5	5	4	5	5	926	1683	1770	883	1546	1890	785	1173	1659	47	115	153	10	103	89	4	42	51	11,4	15,2	19,3	2,4	14,9	10,6	1,1	8,1	6,9
338	128	710,1	_	5	5	5	5	5	5	4	5	3	964	3645	7680	751	1304	11146	563	515	838	74	385	1214	38	101	1041	21	30	6	17,2	23,6	35,3	11,3	17,4	20,9	7,5	13,1	1,1
339	156	712,18	_	5	5	5	4	5	5	4	4	4	809	3902	12205	671	2914	9447	455	434	532	60	186	408	16	397	188	21	13	29	16,5	10,7	7,5	4,6	30,4	4,5	9,3	6,1	11
340	141	718,8	_	4	5	5	5	5	5	0	0	0	1105	1080	1109	2458	2111	1919				144	148	173	269	373	163				26	30,7	35	24,5	39,5	19			
341	117	718,9	_	5	4	5	5	5	5	4	5	5	2680	2957	3232	3188	3711	3717	2326	2283	2572	175	125	212	154	274	499	193	216	118	14,6	8,5	14,7	10,8	16,5	30	16,6	21,1	10,2
342	116	723,79	_	5	5	4	5	5	5	4	5	4	1914	2859	1575	1683	1927	2481	676	822	988	499	361	125	176	70	280	25	44	11	58,3	28,2	15,9	23,4	8,1	25,2	7,2	11,9	2,2
343	156	724,08	_	5	5	5	3	4	5	5	5	4	1514	2260	1428	1174	1440	2655	1370	2922	4534	241	194	128	21	179	353	186	477	381	35,6	19,2	20	3,2	24,8	29,7	30,3	36,5	16,8
344	97	724,33	_	5	5	5	4	5	4	4	5	5	1682	1949	2035	1593	1827	2048	2505	2646	2722	59	97	106	6	59	26	21	69	44	7,8	11,1	11,6	0,8	7,2	2,5	1,7	5,8	3,6
345	103	726,83	_	5	5	5	5	5	5	4	5	4	924	988	801	1113	1728	1002	904	607	541	51	75	45	95	183	90	315	67	18	12,2	17	12,4	19	23,6	20,1	69,7	24,7	6,7
346	143	733,23	Phytol	5	5	5	5	3	5	5	5	4	138071	152573	153367	150736	150307	160199	135227	137885	158874	2567	4256	4722	2809	501	1556	7614	10347	992	4,2	6,2	6,9	4,2	0,6	2,2	12,6	16,8	1,2
347	204	733,39	_	5	4	4	5	4	5	4	3	5	995	548	888	584	1064	1259	20666	166711	604727	319	90	193	96	192	376	479	2786	61168	71,6	33	43,5	36,9	36,1	66,7	4,6	2,9	22,6
348	197	735,84	_	5	5	4	5	4	5	4	5	5	790	1663	1249	997	1327	1299	553	644	623	36	59	8	52	16	36	16	10	15	10,2	8	1,2	11,7	2,3	6,2	5,8	3,4	5,4
349	156	735,79	_	5	5	5	5	5	5	5	5	5	717	1229	1962	698	1023	1697	1105	3575	5365	87	39	103	59	20	236	126	440	731	27	7,1	11,7	18,7	4,4	31	25,4	27,5	30,5
350	103	737,25	_	4	4	4	5	5	5	5	5	4	1767	2416	1382	1483	1650	1930	4960	5584	7357	257	195	42	52	52	152	109	77	231	29,1	16,1	6,1	7,8	7,1	17,6	4,9	3,1	6,3
351	149	738,57	_	4	5	5	4	3	5	5	5	5	6225	7206	6995	7194	8841	8339	4698	4655	4885	179	542	190	192	100	866	340	144	73	5,7	16,8	6,1	5,3	2	23,2	16,2	6,9	3,3
352	267	739,25	Urocanate	5	5	4	5	4	3	4	5	5	1646	2529	1269	1657	1414	2753	998	998	1109	295	404	95	196	56	57	47	87	170	40,1	35,7	15	26,5	7,9	3,6	9,5	19,6	34,2
353	174	741,43	_	4	5	3	1	3	5	5	5	5	443	401	455	435	441	518	1915	1117	968	13	7	26		15	36	221	49	42	6	3,8	10		5,9	15,4	25,8	9,8	9,6
354	217	746,87	_	5	5	5	5	5	5	4	5	5	561	677	684	607	712	723	1150	1460	1290	22	21	13	15	35	43	87	66	89	8,7	6,9	4,2	5,5	10,9	13,1	15,1	10,1	15,4
355	183	748,32	_	5	5	4	5	5	5	5	5	5	8006	11861	12045	20850	20864	24642	1382	1545	1317	1625	828	693	1819	1428	2291	373	245	293	45,4	15,6	11,5	19,5	15,3	20,8	60,3	35,5	49,8
356	124	751,17	_	5	5	5	5	5	5	5	5	5	2317	2407	2644	2910	3113	3516	1182	1390	1447	175	266	222	184	267	495	37	68	111	16,9	24,7	18,8	14,1	19,2	31,5	6,9	10,9	17,2
357	204	751,57	_	5	5	5	5	5	5	5	5	5	34584	42369	11986	9422	12744	21625	50262	49602	50084	12095	7768	2037	553	1904	3902	2031	2387	1809	78,2	41	38	13,1	33,4	40,3	9	10,8	8,1

Mass Spectral Feature (MSF) / Metabolite Information / Normalized signal intensities — No. of observations (counts)

#	M/Z	RI Time (avg) [s]	Metabolite	Mar-[T0]	Mar-[T1]	Mar-[T3]	Mut-[T0]	Mut-[T1]	Mut-[T3]	Syn-[T0]	Syn-[T1]	Syn-[T3]
361	97	761,68	_	4	5	5	4	5	5	5	5	5
362	98	762,04	_	5	5	5	4	4	5	5	5	5
363	131	763,53	_	0	1	1	0	0	1	5	5	5
364	103	766,6	Fructose 6-P	5	5	5	5	5	5	5	5	5
365	117	768	Octadecenoic acid, n-(Z)	5	5	5	5	5	4	4	5	5
366	217	768,41	Fructose 6-P	4	5	4	5	5	3	5	5	5
367	204	769,51	_	5	4	5	5	5	5	5	5	5
368	91	769,58	[Linolenate, gamma-]	5	5	5	5	5	5	5	5	5
369	339	770,61	_	5	4	5	5	5	4	4	5	5
370	117	770,93	Stearate	5	4	5	5	5	4	4	5	5
371	95	771,63	[Linolenate, alpha-]	5	5	5	5	5	5	4	5	5
372	322	771,82	_	5	5	5	3	4	5	0	2	1
373	160	773,09	Glucose 6-P; Galactose 6-P	5	5	5	5	5	5	5	5	5
374	102	775,03	_	5	4	5	5	5	5	5	5	5
375	156	776,97	[Glutamylleucine, gamma-]	5	5	5	5	5	4	5	5	5
376	299	779,67	Glucose 6-P; Galactose 6-P	5	5	4	5	5	5	5	4	5
377	146	785,24	_	4	5	4	4	5	3	4	5	5
378	156	785,38	_	5	5	5	5	5	5	5	5	5
379	318	789,69	_	5	5	5	5	5	5	5	5	4
380	202	790,53	Tryptophan	5	5	5	5	5	5	4	5	5
381	103	790,9	_	5	4	5	3	5	5	5	4	5
382	116	790,98	_	5	5	5	5	5	5	4	5	3
383	169	794,33	_	5	5	5	5	5	5	0	1	2
384	146	795,92	_	5	5	5	5	5	5	0	0	0
385	299	802,01	_	5	5	5	5	5	5	4	5	5
386	146	802,92	_	5	5	5	5	5	5	0	2	2
387	146	808,86	_	5	5	4	5	5	5	2	1	1
388	174	809,86	_	5	3	5	4	5	5	2	1	5
389	156	809,95	_	5	3	5	3	5	5	5	5	5
390	95	811,66	_	5	5	5	5	4	5	5	5	5
391	103	813,36	_	5	4	5	5	5	5	5	5	4
392	146	813,78	_	5	5	5	5	5	5	0	0	0
393	129	816,44	_	5	5	5	5	5	5	3	1	1
394	103	818,63	_	5	5	5	5	5	4	0	0	0
395	146	819,86	_	5	5	3	5	5	5	2	1	1
396	117	822,79	_	5	3	5	5	5	5	5	5	5
397	85	823,3	_	5	4	5	5	5	4	4	5	5
398	146	823,71	_	5	5	5	5	5	4	0	0	0
399	204	826,87	_	5	5	4	5	5	5	4	5	4
400	146	828,55	_	5	5	5	5	5	4	2	2	2
401	189	831,18	_	5	5	5	5	5	5	5	5	5
402	361	840,54	Sucrose	5	4	4	5	5	5	5	4	5
403	387	841,55	_	5	5	5	5	5	4	5	5	5
404	160	843,34	_	2	5	5	5	5	5	4	5	5
405	131	848,49	_	5	5	5	5	5	5	5	5	5
406	202	848,65	_	5	4	5	5	5	5	5	4	5
407	247	849,9	_	5	5	5	5	5	5	0	0	0
408	132	851,69	_	5	5	5	5	5	5	5	5	5
409	100	855,21	_	5	5	5	4	4	5	5	5	5
410	99	855,23	_	5	5	5	4	5	5	5	4	5
411	173	857,15	_	5	5	5	5	5	5	3	5	5
412	85	859,88	_	5	4	5	5	4	5	5	5	5
413	409	860,2	_	5	5	5	5	3	5	0	0	0
414	101	860,42	_	5	5	5	5	5	5	5	5	5
415	99	866,08	_	5	5	5	5	5	5	5	4	5
416	204	869,96	Maltose; Laminaribiose	4	4	5	5	4	5	4	5	5
417	129	870,38	_	5	4	4	5	4	4	4	5	5
418	99	872,76	_	5	4	5	5	5	5	4	2	4
419	115	873,13	_	5	5	5	5	5	5	5	4	5
420	202	873,26	_	5	4	5	5	5	5	5	4	5
421	191	875,92	Trehalose, alpha,alpha-	1	4	4	5	5	5	1	2	2
422	173	877,28	_	5	5	5	5	5	5	3	5	5
423	129	881	_	5	5	5	5	4	4	4	5	5
424	109	887,04	_	5	5	5	5	5	4	5	5	5
425	133	887,38	_	5	4	3	5	4	5	5	5	4
426	239	887,67	_	5	4	5	5	5	4	5	5	5
427	99	890,57	_	4	4	5	5	5	5	4	4	5
428	204	906,44	_	4	3	5	4	5	5	5	5	3
429	103	915,42	_	5	5	5	5	5	5	3	0	2

Normalized signal intensities — Mean average

#	Mar-[T0]	Mar-[T1]	Mar-[T3]	Mut-[T0]	Mut-[T1]	Mut-[T3]	Syn-[T0]	Syn-[T1]	Syn-[T3]
361	1997	2020	2031	2183	2117	2300	1932	1860	1789
362	1286	1398	1517	1432	1345	1904	1573	1478	1606
363		394	367			381	2441	2006	2278
364	1295	7859	4621	1575	8843	5104	638	5504	3458
365	35040	41129	31645	26365	31885	34045	25121	24115	26331
366	460	4535	2380	525	5246	2648	576	3721	2177
367	1220	1497	1397	782	1032	1851	1817	1595	2070
368	30660	36153	24353	23330	26577	35232	21198	17279	16461
369	1973	2171	1941	1982	2160	2469	1449	1406	1523
370	120487	139738	129553	120856	143552	148666	96968	95568	104253
371	38746	45648	35985	32502	36377	46692	31741	28837	30201
372	2239	2202	2177	1651	1256	1674		381	365
373	3635	25515	17216	4230	29424	19823	3219	15491	11083
374	1940	2325	2203	2103	2539	2527	1732	1879	1946
375	627	895	3118	685	1061	4564	550	523	581
376	733	4068	2483	805	4340	3109	674	2233	1788
377	3020	3196	3774	3481	3625	4307	3129	2391	3088
378	1623	5860	15117	1661	2818	15444	656	940	1440
379	3165	3216	4100	4289	4732	5042	652	646	702
380	1725	3247	3520	2138	2871	5840	1135	2070	3092
381	3502	5599	6515	4876	5280	3823	3202	3343	3835
382	3156	4898	4368	3800	4058	4044	2434	3209	2861
383	996	791	1129	1700	1789	2053		382	395
384	43408	44804	48133	78164	83703	79730			
385	613	2645	2003	499	1947	2624	884	2817	2249
386	16643	17371	18262	30885	32276	30361		388	382
387	1814	1723	2034	2311	2507	3317	683	535	456
388	543	436	459	655	471	817	384	378	2055
389	1054	2396	6187	1519	2320	6644	648	758	771
390	2086	2037	1996	2450	2285	2640	1887	1924	1972
391	1415	1816	1783	2134	1729	1441	753	715	657
392	1761	1995	2041	3446	2884	2762			
393	4446	3897	4269	5136	5767	8940	472	420	396
394	4629	4618	4644	6853	6305	5639			
395	2181	2450	2422	4988	4545	4548	381	372	364
396	1615	1851	2380	1700	2008	1693	1696	1486	1554
397	2877	2987	3294	3369	3492	3124	2896	2947	3119
398	1080	1199	1278	2044	1791	1507			
399	2080	2069	1973	2897	2752	2671	473	542	408
400	3409	3855	4089	6975	5851	5276	435	413	442
401	1125	1173	1614	1307	1451	1095	996	957	940
402	11849	27215	76468	48350	72145	125808	7790	5680	6813
403	846	8089	3172	1016	7960	3401	861	10770	5088
404	369	784	578	456	886	663	424	2132	837
405	1712	1369	1494	2110	1905	1454	974	1473	1039
406	2809	4358	5063	4095	4735	3402	1919	2129	2338
407	1686	1681	1824	2738	2690	2862			
408	1981	3741	3964	2574	3234	2133	1067	936	1016
409	836	1012	1254	1333	1295	1514	1040	1512	1592
410	5041	6700	7167	5933	7101	5644	4443	4524	5061
411	1007	1564	1903	1186	1353	1144	1023	1063	1138
412	2198	2443	2610	2553	2804	2546	2040	2167	2207
413	1699	2172	1122	720	650	956			
414	1091	1325	1629	1834	1488	2495	1676	2566	2858
415	4355	6910	8028	5629	6210	3979	2598	2483	2931
416	665	1221	1808	673	1328	1807	765	936	1453
417	3709	5004	4805	4421	4596	5256	4075	3962	4126
418	11150	13188	13266	4835	4358	4415	431	422	422
419	2604	3432	3582	2159	2362	1882	1026	1051	1181
420	2975	4613	5326	4163	4900	3356	2076	2233	2527
421	449	424	500	1204	1262	3429	783	460	432
422	1403	2188	2597	1551	1771	1487	1483	1446	1609
423	3667	4538	3477	3742	3959	4202	3569	3537	3537
424	8017	10208	11586	9325	10486	8138	7333	7662	7875
425	934	1146	1324	1080	1268	990	790	892	850
426	855	1147	1402	1046	1193	821	753	818	842
427	856	1261	1834	1120	1430	845	796	795	865
428	26134	25552	26174	30561	29587	28570	19222	33302	18074
429	10603	11533	11919	16134	15200	15921	378		757

Normalized signal intensities — Standard error : $SE = s/\sqrt{n}$

#	Mar-[T0]	Mar-[T1]	Mar-[T3]	Mut-[T0]	Mut-[T1]	Mut-[T3]	Syn-[T0]	Syn-[T1]	Syn-[T3]
361	25	86	135	28	205	151	271	98	84
362	125	29	40	23	34	93	98	75	88
363							79	198	139
364	49	663	407	72	520	287	23	317	141
365	7783	3643	2494	2346	3452	2167	1799	3071	3002
366	11	425	136	15	246	13	61	127	97
367	251	113	148	39	106	263	98	115	168
368	7288	3429	2620	1643	2424	4541	2531	2597	3060
369	313	92	105	169	199	139	64	164	153
370	11739	3444	3734	2408	6280	5180	4122	4308	4903
371	7850	4048	2948	1702	3185	5924	1557	3284	3572
372	181	204	255	21	52	141		6	
373	260	1260	1671	61	1620	1043	120	1208	1002
374	66	46	107	74	77	66	11	45	47
375	33	77	233	40	81	487	34	29	32
376	35	236	152	11	257	161	31	66	167
377	665	384	211	170	640	73	98	651	579
378	151	545	1171	91	350	2275	25	49	119
379	327	330	334	1154	1290	1430	31	24	10
380	171	287	469	174	250	570	44	305	336
381	187	276	728	21	320	346	136	46	91
382	386	328	420	115	289	490	206	260	29
383	143	35	121	80	205	239			20
384	1076	1059	1229	1308	1332	1884			
385	63	309	182	36	301	488	19	243	127
386	600	166	493	701	420	914		6	3
387	156	49	88	311	292	445	171		
388	45	35	19	14	37	82	2		195
389	227	39	1415	10	249	828	42	91	60
390	94	85	65	108	43	158	96	77	67
391	132	32	139	56	110	113	54	40	25
392	186	81	75	229	266	187			
393	718	247	424	863	875	1464	61		
394	581	364	438	392	666	270			
395	129	74	14	216	236	253	7		
396	174	39	120	125	199	192	170	92	87
397	136	57	67	28	133	113	76	29	121
398	100	18	65	105	113	51			
399	32	47	62	111	149	114	84	21	17
400	386	155	199	418	551	207	4	1	11
401	127	56	56	80	107	128	53	68	34
402	1490	288	2744	1439	2232	3756	1006	118	292
403	53	836	335	9	478	50	37	609	262
404	2	25	16	12	26	22	19	125	31
405	187	161	208	402	412	123	105	351	105
406	225	109	309	242	380	380	67	51	109
407	98	73	46	78	168	96			
408	250	432	606	272	488	256	66	109	68
409	69	89	78	19	10	137	178	117	195
410	214	309	177	60	345	407	80	60	32
411	83	98	168	98	21	57	16	93	63
412	101	35	50	56	64	160	76	24	58
413	234	221	31	37	3	35			
414	116	229	181	96	107	280	490	320	526
415	700	739	1363	372	701	491	225	288	443
416	14	14	92	58	14	81	68	33	48
417	639	120	242	331	177	207	273	406	310
418	1071	531	850	355	203	484	24	1	15
419	149	58	183	117	185	117	20	34	15
420	228	172	313	259	409	341	49	28	120
421		13	27	130	153	438		13	18
422	129	152	232	145	47	43	18	124	76
423	479	223	326	209	298	297	211	218	206
424	315	740	388	220	633	69	156	190	135
425	25	38	5	39	48	82	63	73	15
426	32	51	75	40	86	25	35	53	43
427	13	47	205	58	187	83	7	34	62
428	9912	217	3578	2294	8309	5673	2555	9167	551
429	539	272	402	561	445	541	4		14

Normalized signal intensities — Coefficient of variation (CV) [%]

#	Mar-[T0]	Mar-[T1]	Mar-[T3]	Mut-[T0]	Mut-[T1]	Mut-[T3]	Syn-[T0]	Syn-[T1]	Syn-[T3]
361	2,5	9,5	14,8	2,6	21,7	14,6	31,3	11,8	10,5
362	21,8	4,6	5,9	3,2	5,1	10,9	13,9	11,3	12,3
363							7,3	22	13,6
364	8,4	18,9	19,7	10,3	13,1	12,6	8	12,9	9,1
365	49,7	19,8	17,6	19,9	24,2	12,7	14,3	28,5	25,5
366	4,9	20,9	11,4	6,3	10,5	0,8	23,8	7,7	9,9
367	46	15	23,6	11	22,9	31,7	12,1	16,2	18,1
368	53,2	21,2	24,1	15,7	20,4	28,8	26,7	33,6	41,6
369	35,5	8,4	12,1	19,1	20,6	11,3	8,8	26,1	22,4
370	21,8	4,9	6,4	4,5	9,8	7	8,5	10,1	10,5
371	45,3	19,8	18,3	11,7	19,6	28,4	9,8	25,5	26,4
372	18	20,7	26,1	2,2	8,3	18,8		2,4	
373	16	11	21,7	3,2	12,3	11,8	8,4	17,4	20,2
374	7,6	3,9	10,9	7,8	6,8	5,9	1,5	5,3	5,4
375	11,8	19,1	16,7	13,1	17,1	21,4	14	12,5	12,5
376	10,6	13	12,3	3,2	13,3	11,6	10,2	5,9	20,9
377	44	26,9	11,2	9,8	39,5	2,9	6,3	60,8	42
378	20,8	20,8	17,3	12,2	27,8	32,9	8,3	11,7	18,4
379	23,1	23	18,2	60,1	61	63,4	10,7	8,2	2,8
380	22,2	19,8	29,8	18,2	19,5	21,8	7,7	33	24,3
381	11,9	9,9	25	0,7	13,6	20,3	9,5	2,7	5,3
382	27,3	15	21,5	6,7	15,9	27,1	16,9	18,1	1,8
383	32,2	9,9	23,9	10,5	25,7	26			7,1
384	5,5	5,3	5,7	3,7	3,6	5,3			
385	22,9	26,1	20,3	16,2	34,5	41,6	4,2	19,3	12,6
386	8,1	2,1	6	5,1	2,9	6,7		2	1
387	19,2	6,4	8,6	30,1	26	30	35,5		
388	18,6	14,1	9,4	4,2	17,5	22,5	0,6		21,2
389	48,1	2,9	51,1	1,1	24	27,9	14,4	26,8	17,3
390	10	9,3	7,3	9,9	3,8	13,4	11,4	8,9	7,6
391	20,8	3,5	17,4	5,8	14,3	17,5	16	12,4	7,7
392	23,6	9	8,2	14,9	20,6	15,2			
393	36,1	14,2	22,2	37,6	33,9	36,6	22,2		
394	28,1	17,6	21,1	12,8	23,6	9,6			
395	13,2	6,8	1	9,7	11,6	12,4	2,8		
396	24	3,7	11,3	16,4	22,2	25,4	22,4	13,8	12,4
397	10,6	3,8	4,6	1,8	8,5	7,2	5,3	2,2	8,6
398	20,8	3,4	11,4	11,5	14,1	6,8			
399	3,4	5,1	6,3	8,5	12,1	9,5	35,3	8,6	8,5
400	25,3	9	10,9	13,4	21,1	7,8	1,3	0,2	3,6
401	25,1	10,7	7,7	13,7	16,4	26,2	11,9	15,8	8,2
402	28,1	2,1	7,2	6,7	6,9	6,7	28,9	4,1	9,6
403	14	23,1	23,6	2,1	13,4	3	9,5	12,6	11,5
404	0,7	7,2	6,3	5,9	6,7	7,4	9,1	13,1	8,4
405	24,4	26,3	31,1	42,6	48,3	18,8	24,2	53,3	22,5
406	17,9	5	13,7	13,2	17,9	24,9	7,8	4,8	10,4
407	13	9,7	5,6	6,3	14	7,5			
408	28,2	25,8	34,2	23,6	33,8	26,9	13,9	26	15,1
409	18,4	19,7	13,9	2,8	1,6	20,2	38,2	17,3	27,3
410	9,5	10,3	5,5	2	10,9	16,1	4	2,7	1,4
411	18,5	13,9	19,7	18,4	3,4	11,1	2,8	19,5	12,4
412	10,3	2,8	4,3	4,9	4,6	14	8,3	2,5	5,9
413	30,8	22,7	6,1	11,5	0,9	8,3			
414	23,7	38,6	24,8	11,7	16,1	25,1	65,4	27,9	41,1
415	36	23,9	38	14,8	25,2	27,6	19,3	23,2	33,8
416	4,3	2,3	11,4	19,2	2	10	17,7	7,8	7,4
417	38,5	4,8	10,1	16,7	7,7	7,9	13,4	22,9	16,8
418	21,5	8	14,3	16,4	10,4	24,5	11,1	0,3	7,2
419	12,8	3,7	11,4	12,2	17,5	13,8	4,4	6,5	2,9
420	17,1	7,5	13,1	13,9	18,7	22,7	5,2	2,5	10,6
421		6	10,7	24,1	27,2	28,6		3,8	5,9
422	20,5	15,5	20	20,9	5,9	6,5	2,1	19,2	10,6
423	29,2	11	20,9	12,5	15,1	14,1	11,8	13,8	13,1
424	8,8	16,2	7,5	5,3	13,5	1,7	4,8	5,6	3,8
425	5,9	6,7	0,6	8,1	7,5	18,6	17,9	18,2	3,6
426	8,5	8,8	12	8,5	16,2	6,2	10,4	14,5	11,3
427	3,1	7,4	25	11,6	29,3	21,9	1,7	8,6	16,1
428	75,9	1,5	30,6	15	62,8	44,4	29,7	61,5	5,3
429	11,4	5,3	7,5	7,8	6,5	7,6	2		2,7

Mass Spectral Feature (MSF)			Metabolite Information	No. of observations (counts)									Normalized signal intensities: Mean average									Standard error : $SE = s/\sqrt{n}$									Coefficient of variation (CV) [%]								
#	M/Z	RI Time (avg) [s]	Metabolite	Mar-[T0]	Mar-[T1]	Mar-[T3]	Mut-[T0]	Mut-[T1]	Mut-[T3]	Syn-[T0]	Syn-[T1]	Syn-[T3]	Mar-[T0]	Mar-[T1]	Mar-[T3]	Mut-[T0]	Mut-[T1]	Mut-[T3]	Syn-[T0]	Syn-[T1]	Syn-[T3]	Mar-[T0]	Mar-[T1]	Mar-[T3]	Mut-[T0]	Mut-[T1]	Mut-[T3]	Syn-[T0]	Syn-[T1]	Syn-[T3]	Mar-[T0]	Mar-[T1]	Mar-[T3]	Mut-[T0]	Mut-[T1]	Mut-[T3]	Syn-[T0]	Syn-[T1]	Syn-[T3]
433	149	926,68	_	4	4	5	5	4	5	5	4	5	4198	4904	6177	4231	6181	3975	3872	4212	4350	84	288	649	217	748	195	247	208	242	4	11,8	23,5	11,5	24,2	10,9	14,3	9,9	12,4
434	204	927,27	_	4	3	4	5	5	5	4	5	5	1269	1518	2000	1134	1090	1036	12558	12701	13412	173	371	246	209	41	137	424	963	871	27,3	42,3	24,6	41,1	8,3	29,5	6,8	17	14,5
435	91	930,08	_	5	4	5	4	5	5	5	5	4	1586	1252	2124	1118	11134	1843	1141	1585	1240	208	138	239	30	5055	225	105	273	73	29,3	22	25,2	5,4	101,5	27,3	20,6	38,5	11,8
436	103	931,46	_	5	5	5	5	4	4	4	5	5	1704	1763	1737	1777	1816	1944	1632	1630	1740	138	70	81	34	82	28	20	63	49	18,1	8,9	10,4	4,3	9	2,9	2,5	8,6	6,3
437	103	935,28	_	5	5	5	5	5	5	5	5	5	1338	1128	1250	1125	1416	1782	2599	2343	2708	338	196	236	139	218	337	252	239	254	56,5	38,8	42,2	27,7	34,4	42,2	21,7	22,8	21
438	111	935,55	_	2	2	3	2	2	3	5	5	5	398	397	408	406	454	405	3670	3844	4368	25	28	22	14	41	16	157	117	99	9	10	9,3	4,8	12,7	6,8	9,6	6,8	5,1
439	129	942,09	_	5	4	4	5	5	3	4	5	5	3255	3403	3288	3185	3726	3993	2554	2278	2571	494	80	49	125	317	50	83	226	237	33,9	4,7	3	8,8	19	2,2	6,5	22,2	20,6
440	103	942,07	_	4	5	5	5	5	5	4	5	5	2030	2228	2103	2450	2554	2940	1272	1191	1248	38	85	88	144	264	248	40	43	61	3,8	8,6	9,4	13,1	23,1	18,8	6,3	8,1	10,9
441	111	945,63	_	0	0	1	0	0	1	5	5	5			366			379	1242	1337	1491							54	42	36							9,7	7,1	5,3
442	101	956,67	_	4	4	4	5	5	5	0	1	2	1954	2061	2169	3014	3004	2888		449	445	173	81	118	106	115	90			5	17,7	7,9	10,9	7,9	8,5	6,9			1,7
443	146	956,78	_	4	5	5	5	5	5	0	0	0	9076	9583	10480	18772	18909	18369				63	202	349	953	957	1063				1,4	4,7	7,4	11,4	11,3	12,9			
444	146	964,5	_	5	5	4	5	5	5	0	0	0	4303	4251	4666	8454	8312	8066				128	81	75	389	523	415				6,7	4,3	3,2	10,3	14,1	11,5			
445	103	964,88	_	5	4	5	5	5	5	5	5	5	4155	4111	5073	7513	7211	7175	1298	944	1067	592	97	447	625	1010	364	205	162	164	31,8	4,7	19,7	18,6	31,3	11,3	35,4	38,5	34,3
446	204	969,81	_	5	5	5	5	5	5	5	5	5	905	928	1310	955	965	926	6146	6452	5948	151	235	295	156	41	109	262	267	177	37,3	56,5	50,3	36,6	9,5	26,3	9,5	9,3	6,7
447	103	969,82	_	5	4	5	5	5	5	5	5	5	1238	1279	1474	1407	1544	1408	2834	2933	2717	164	32	155	127	252	137	102	116	86	29,7	4,9	23,5	20,2	36,4	21,7	8	8,8	7,1
448	141	973,16	_	5	5	5	5	5	4	5	4	5	1479	2362	2730	1985	2332	1331	1347	1338	1562	82	207	201	75	242	60	46	47	65	12,3	19,6	16,4	8,5	23,2	9	7,7	6,9	9,3
449	100	975,11	_	4	4	5	5	5	5	0	0	0	947	1439	2549	985	1422	1090				119	120	390	56	198	239				25,1	16,7	34,2	12,8	31,2	49			
450	91	975,98	_	4	5	5	4	5	5	5	5	4	2418	2660	3766	2060	22678	3131	2018	2909	2243	154	735	482	43	10489	432	203	563	156	12,7	61,8	28,6	4,2	103,4	30,8	22,5	43,3	13,9
451	88	977,6	_	5	5	5	5	5	5	0	0	0	3225	4063	2852	1017	1268	2241				447	396	372	186	204	467				31	21,8	29,1	41	36	46,6			
452	95	979,52	Squalene	5	5	5	5	5	3	4	4	5	1752	2182	2798	1073	1560	1966	864	767	1165	59	213	199	43	112	8	53	30	114	7,5	21,8	15,9	8,9	16	0,7	12,3	7,9	21,8
453	204	982,79	_	5	5	5	5	5	5	5	5	5	28612	34224	15104	6671	9102	15683	55638	56134	56437	7508	5458	1490	424	1384	2638	2714	2277	3248	58,7	35,7	22,1	14,2	34	37,6	10,9	9,1	12,9
454	89	983,6	_	5	5	5	5	5	5	4	5	5	2790	2134	2339	4200	4086	4490	1636	1674	1678	299	96	96	224	369	566	95	69	77	23,9	10,1	9,2	11,9	20,2	28,2	11,6	9,2	10,2
455	146	988,99	_	5	5	4	5	5	5	4	5	4	2400	1699	1897	2743	2821	3003	481	431	639	365	52	60	136	113	312	38	15	218	34	6,8	6,3	11,1	8,9	23,2	15,8	7,7	68,1
456	236	994,66	Adenosine, 5-methylthio-	5	5	5	5	5	5	5	5	5	1377	1977	3367	1626	2489	4113	1033	1274	2084	93	118	245	98	79	139	51	88	100	15	13,4	16,2	13,5	7,1	7,6	11,1	15,4	10,8
457	169	995,73	Uridine-5 P (; UDP; UTP)	4	5	4	5	4	5	5	5	4	1208	1839	2008	2228	1869	2764	1066	2230	1221	193	279	265	332	320	483	218	691	76	32	33,9	26,4	33,3	34,2	39,1	45,7	69,3	12,4
458	204	998,62	_	1	1	4	3	2	3	5	5	4	464	636	620	448	439	436	11581	13280	10720			48	34	39	37	733	828	110			15,5	13	12,6	14,7	14,2	13,9	2,1
459	97	998,85	_	0	2	5	2	3	4	4	5	5		468	463	375	377	493	616	836	2158		10	19	2	6	41	38	71	296		2,9	8,9	0,6	2,9	16,6	12,2	19,1	30,7
460	103	1007,09	_	5	5	5	5	4	4	5	5	5	579	614	591	587	632	602	1578	1824	2084	13	21	29	9	11	6	57	99	198	5	7,8	10,9	3,4	3,3	2	8	12,2	21,3
461	204	1007,52	_	3	3	4	4	3	3	5	5	5	432	519	710	424	503	428	3425	4242	5655	26	74	44	22	13	21	134	489	974	10,5	24,5	12,4	10,4	4,6	8,6	8,8	25,8	38,5
462	99	1022,66	_	1	5	5	2	5	4	4	5	4	377	504	684	374	551	604	564	1748	2498		31	72	5	32	46	77	256	208		13,9	23,6	1,8	13	15,3	27,2	32,8	16,6
463	156	1049,59	_	4	5	4	5	4	5	4	5	4	2786	3438	2234	1998	1775	1196	2725	3067	1603	88	466	92	366	29	140	705	642	131	6,3	30,3	8,2	41	3,3	26,2	51,7	46,8	16,3
464	179	1051,8	_	3	2	2	5	4	5	0	0	0	411	470	440	1360	1303	1281				11	20	28	277	233	158				4,8	6,1	9,1	45,6	35,8	27,6			
465	85	1055,4	_	5	5	4	3	5	5	5	5	5	2272	2292	2288	2572	2543	2545	2051	2322	2202	104	48	89	17	189	69	59	107	100	10,3	4,6	7,8	1,1	16,7	6,1	6,4	10,3	10,1
466	114	1061,39	_	5	5	5	5	5	5	4	5	4	1170	1509	1797	1423	1472	1252	1165	1284	1333	30	77	145	45	58	36	17	52	13	5,7	11,4	18	7,1	8,8	6,4	2,9	9	2
467	169	1064,77	Guanosine 5-P (; GDP; GTP)	5	5	4	5	5	5	4	5	4	1404	1252	1148	1681	1662	1629	601	1688	856	455	198	140	237	532	215	67	441	119	72,5	35,4	24,4	31,5	71,6	29,4	22,1	58,4	27,9
468	237	1070,78	Tocopherol, alpha-	3	5	5	5	5	5	5	5	5	6415	5381	5500	4506	4193	4457	6719	6699	6288	20	704	403	230	232	77	434	218	338	0,5	29,3	16,4	11,4	12,4	3,9	14,4	7,3	12
469	174	1071,85	_	0	0	0	0	0	0	5	5	5							3647	4967	4118							420	257	108							25,8	11,6	5,8
470	204	1074,68	_	5	5	5	5	5	5	3	5	3	1048	1506	1897	1604	1708	1513	1076	1183	1187	22	93	204	40	74	79	10	115	8	4,7	13,8	24	5,6	9,6	11,6	1,6	21,8	1,2
471	114	1074,76	_	5	5	5	4	5	5	5	5	5	1836	2925	3888	2381	2579	1885	1975	2248	2225	107	205	500	64	209	154	127	321	197	13	15,7	28,7	5,4	18,1	18,3	14,4	32	19,8
472	117	1074,9	_	5	5	5	5	5	5	4	3	4	966	1329	1465	1304	1283	1204	1031	1119	1109	111	46	181	70	90	109	73	3	26	25,8	7,8	27,6	11,9	15,6	20,3	14,2	0,5	4,6
473	174	1081,69	_	0	0	2	0	0	0	5	5	5			402				5238	6331	5822			18				631	724	362			6,2				27	25,6	13,9
474	204	1083,16	_	5	5	5	4	4	5	1	0	2	681	812	547	2219	2281	2947	437		480	63	46	11	53	22	279			37	20,6	12,7	4,6	4,7	1,9	21,2			10,9
475	179	1086,71	_	5	5	5	5	5	4	5	5	5	915	1047	848	1214	1162	1411	712	730	738	125	78	70	125	87	22	90	111	90	30,5	16,6	18,6	23	16,8	3,1	28,3	34	27,3
476	99	1089,53	_	5	5	5	5	5	5	4	5	4	434	477	509	963	2104	1109	454	540	554	23	41	58	74	234	98	32	37	58	11,9	19,2	25,7	17,2	24,9	19,8	14,2	15,3	20,8
477	113	1093,22	_	5	5	5	4	4	5	5	5	5	2242	3234	4142	2876	2619	2042	2146	2837	2474	260	154	712	70	133	184	206	514	346	25,9	10,6	38,4	4,9	10,2	20,1	21,5	40,5	31,3
478	113	1098,45	_	5	5	5	5	5	5	5	5	5	1092	1508	2320	1551	1589	1114	1027	1285	1357	104	30	325	59	154	96	69	172	136	21,3	4,4	31,3	8,5	21,7	19,3	15	30	22,3
479	204	1118,68	_	5	5	5	5	5	4	5	5	5	23756	27505	21039	18577	21866	23320	17168	13672	15244	3111	1519	1449	788	1693	1212	1695	2027	1448	29,3	12,3	15,4	9,5	17,3	10,4	22,1	33,2	21,2
480	204	1128,02	Isomaltotriose	5	5	5	3	4	5	5	3	5	93588	122498	51931	51248	57210	81947	17645	16289	25175	19208	11762	2865	746	2469	8021	1447	487	1049	45,9	21,5	12,3	2,5	8,6	21,9	18,3	5,2	9,3
481	297	1145,88	Phylloquinone	5	5	5	5	5	5	4	5	5	1318	1322	1267	1471	1408	1302	1393	1624	1604	134	158	140	117	208	118	122	181	234	22,8	26,8	24,6	17,7	33	20,3	17,5	24,9	32,7
482	596	1150,42	_	5	4	5	5	4	5	5	5	5	1483	1574	1522	1645	1490	1599	1540	1712	1570	66	21	37	55	41	91	128	49	81	10	2,6	5,4	7,4	5,4	12,8	18,5	6,4	11,6
483	97	1152	_	4	4	5	5	5	5	3	1	2	1343	1441	1836	2239	2379	2242	496	416	413	87	92	289	731	868	634	107		7	12,9	12,7	35,2	73	81,6	63,3	37,4		2,4
484	204	1163,23	_	5	5	5	5	5	5	4	5	5	3047	3689	2230	2539	2802	3324	1346	1209	1437	341	311	58	160	213	329	53	92	40	25	18,9	5,8	14,1	17	22,1	7,9	17,1	6,2
485	204	1165,79	_	5	5	5	4	5	5	4	5	5	2053	2395	1609	1798	1849	2257	1013	1152	1169	224	183	55	64	146	116	45	57	34	24,4	17,1	7,6	7,1	17,7	11,5	8,8	11,1	6,6
486	204	1171,85	_	5	4	5	4	5	5	4	3	2	8855	9953	5263	4264	5840	7668	795	1033	1238	1749	976	440	269	678	742	108	218	45	44,2	19,6	18,7	12,6	25,9	21,6	27,2	36,6	5,1
487	93	1173,55	_	5	5	5	3	5	5	5	5	4	4296	4788	3067	3093	3512	3570	1951	2154	2259	581	433	247	25	301	244	104	195	33	30,2	20,2	18	1,4	19,2	15,3	11,9	20,3	2,9
488	204	1173,92	_	5	5	5	5	5	5	5	5	5	11172	14881	5919	9026	11350	11873	3239	4267	5819	2123	1940	463	2022	2384	1745	395	693	372	42,5	29,1	17,5	50,1	47	32,9	27,2	36,3	14,3
489	204	1175,92	_	5	5	5	4	5	5	5	5	5	17286	21061	9613	8748	12265	15557	2685	3316	4824	3610	2655	915	729	1760	1734	237	533	325	46,7	28,2	21,3	16,7	32,1	24,9	19,7	36	15,1
490	91	1201,3	_	5	5	5	5	5	5	5	5	5	3141	3222	3425	3601	3272	2875	2554	2896	2767	309	204	376	246	387	250	265	406	332	22	14,2	24,5	15,3	26,4	19,4	23,2	31,3	26,8
491	131	1207,92	_	5	4	4	5	5	4	5	5	5	2011	1746	2164	1989	2466	1770	2593	1864	2182	221	82	64	141	317	475	425	219	302	24,6	9,4	5,9	15,9	28,7	53,7	36,7	26,3	30,9
492	131	1218,77	_	5	4	5	4	5	5	5	5	5	2634	2659	2495	6672	6444	6633	11951	12446	12194	142	35	130	66	253	262	630	907	619	12	2,6	11,6	2	8,8	8,8	11,8	16,3	11,3
493	103	1218,93	_	5	5	4	5	5	5	4	5	4	1532	1486	1311	1832	1787	1780	722	813	850	228	88	140	259	332	282	25	59	9	33,3	13,2	21,4	31,7	41,5	35,4	6,9	16,3	2,1
494	95	1234,25	_	5	5	5	5	5	5	5	5	5	15783	24069	33245	19773	23140	15516	14419	16190	16154	2007	1695	5578	855	2582	1549	2215	3106	2100	28,4	15,7	37,5	9,7	25	22,3	34,3	42,9	29,1
495	129	1237,84	_	5	5	5	5	5	5	5	5	5	1349	1288	1430	1094	1337	1189	1841	2038	1849	220	78	136	125	398	218	362	240	252	36,5	13,6	21,2	25,6	66,5	41	44	26,4	30,4
496	204	1266,5	_	5	5	5	5	4	4	4	5	5	4295	4675	3860	4580	4239	5215	4245	3752	3725	836	376	433	505	294	130	442	618	497	43,6	18	25,1	24,6	13,9	5	20,8	36,8	29,8
497	145	1282,44	_	5	5	4	5	5	5	5	5	5	1098	2554	1234	974	3124	1500	568	2473	1622	188	396	110	71	572	152	57	566	288	38,4	34,7	17,8	16,4	40,9	22,7	22,6	51,2	39,7
498	129	1283,24	_	5	5	4	3	5	5	4	5	5	7696	9756	5258	5249	9494	7645	2497	7409	5583	1315	1471	298	60	1656	902	193	1522	805	38,2	33,7	11,3	2	39	26,4	15,4	45,9	32,3
499	204	1283,7	_	5	5	3	5	5	5	5	5	5	6947	7698	4517	4801	5645	7759	3248	2619	2872	1118	1005	41	285	589	1100	531	344	301	36	29,2	1,6	13,3	23,3	31,7	36,5	29,4	23,4
500	129	1289	_	4	5	4	5	5	5	5	5	4	4191	4221	3213	4477	4423	4194	3711	4822	2965	1016	728	460	664	1083	601	1179	1213	406	48,5	38,6	28,7	33,2	54,8	32	71	56,2	27,4
501	87	1308,95	_	5	5	4	5	5	4	4	5	4	2263	1760	1462	2152	1964	1575	1420	2298	1526	562	277	142	251	398	83	132	573	197	55,5	35,2	19,4	26,1	45,3	10,5	18,6	55,7	25,8

Mass Spectral Feature			Metabolite Information		2-Way ANOVA (Variance Analysis)			TukeyHSD - Tukey Honest Significant Differences (differences between the means)																			
					p.value (adjusted using BY)			p.value (adjusted using Benjamini, Hochberg, and Yekutieli method (BY))																			
								Genotype (G)			Timepoint (T)			(Mar vs. Mut) × T			(Mar vs. Syn) × T			Mar × T			Mut × T			Syn × T		
#	M/Z	Retention [s]	Metabolite	Class	Genotype (G)	Timepoint / Treatment (T)	G × T	Mut-Mar	Syn-Mar	Syn-Mut	T0-T1	T0-T3	T1-T3	Mar:0-Mut:0	Mar:1-Mut:1	Mar:3-Mut:3	Mar:0-Syn:0	Mar:1-Syn:1	Mar:3-Syn:3	Mar:0-Mar:1	Mar:0-Mar:3	Mar:1-Mar:3	Mut:0-Mut:1	Mut:0-Mut:3	Mut:1-Mut:3	Syn:0-Syn:1	Syn:0-Syn:3	Syn:1-Syn:3
					0,05	0,05	0,05	0,05	0,05	0,05	0,05	0,05	0,05	0,05	0,05	0,05	0,05	0,05	0,05	0,05	0,05	0,05	0,05	0,05	0,05	0,05	0,05	0,05
1	160	186,26	Glyoxylate	Carboxylic acids	0,0003	0,3174	1	1	0,0102	0,0006	1	0,3457	1	1	1	1	1	1	1	1	1	1	1	1	1	1	1	1
2	126	187,4	_	Unknown	1E-07	0,0189	1	0,9395	2E-07	8E-05	0,0314	0,3213	1	1	1	1	0,0122	0,1184	0,0118	1	1	1	1	1	1	1	1	1
3	117	189,48	Lactate	Carboxylic acids	5E-05	1	1	0,0254	5E-05	1	1	1	1	1	1	1	0,3191	0,0966	1	1	1	1	1	1	1	1	1	1
4	89	189,6	_	Unknown	0,3624	1	1	1	0,4216	1	1	1	1	1	1	1	1	1	1	1	1	1	1	1	1	1	1	1
5	85	194,17	_	Unknown	0,0005	0,764	1	0,8717	0,0004	0,1535	1	1	1	1	1	1	1	0,0144	1	1	1	1	1	1	1	1	1	1
6	101	195,32	_	Unknown	0,5097	1	1	1	1	0,5139	1	1	1	1	1	1	1	1	1	1	1	1	1	1	1	1	1	1
7	161	203,25	_	Unknown	0,0731	0,6999	1	0,1412	1	1	1	1	1	1	1	1	1	1	1	1	1	1	1	1	1	1	1	1
8	152	204,41	Pyridine, 2-hydroxy-	Miscellaneous	0,0053	0,0009	1	1	0,9846	0,0041	1	0,0006	0,3738	1	1	1	1	1	1	1	1	1	1	1	1	1	1	1
9	245	204,88	_	Unknown	0,0421	0,9433	1	0,8784	0,0508	1	1	0,9101	1	1	1	1	1	1	0,4253	1	1	1	1	1	1	1	1	1
10	144	206,06	_	Unknown	0,0001	0,0104	0,0246	1	0,0009	0,0007	1	0,0096	0,437	1	1	1	1	1	0,0002	1	1	1	1	1	1	1	0,001	0,0849
11	177	206,27	Glycolate	Carboxylic acids	0,0023	0,0276	0,0019	1	0,002	0,3135	0,0448	0,3728	1	1	0,0134	1	1	0,0004	1	0,0015	1	0,1437	1	1	1	1	1	1
12	116	208,48	Alanine	Amino acids	7E-18	4E-15	3E-10	1	5E-12	4E-12	7E-11	6E-12	0,0081	1	1	1	1	2E-10	9E-12	1	0,1183	1	1	0,4774	1	7E-11	1E-11	0,0439
13	110	212,46	_	Unknown	0,0018	0,6526	1	0,0104	0,0168	1	1	1	0,911	1	1	0,1658	1	1	1	1	1	1	1	1	1	1	1	1
14	89	216,65	_	Unknown	1	1	1	1	1	1	1	1	1	1	1	1	1	1	1	1	1	1	1	1	1	1	1	1
15	174	222,35	Pyruvate	Carboxylic acids	1	0,6862	0,7088	1	1	1	1	0,6568	1	1	1	1	1	1	1	1	1	1	1	1	1	1	1	1
16	102	227,96	Glycine	Amino acids	4E-06	0,0012	0,0582	1	3E-05	4E-05	0,015	0,0035	1	1	1	1	1	0,0626	0,0063	1	1	1	1	1	1	0,0051	0,0043	1
17	153	228,44	_	Unknown	0,0803	1	1	1	0,1592	0,2427	1	1	1	1	1	1	1	1	1	1	1	1	1	1	1	1	1	1
18	140	233,99	_	Unknown	0,4261	1	1	1	1	0,5441	1	1	1	1	1	1	1	1	1	1	1	1	1	1	1	1	1	1
19	174	234,62	_	Unknown	0,7042	1	1	1	1	0,7435	1	1	1	1	1	1	1	1	1	1	1	1	1	1	1	1	1	1
20	177	245,83	_	Unknown	2E-05	0,0313	1	1	2E-05	0,0049	0,0778	0,2143	1	1	1	1	1	0,0154	0,4983	0,6166	0,7366	1	1	1	1	1	1	1
21	130	248,86	Butyrate, 2-amino-	Amino acids	6E-10	1E-15	2E-06	0,6895	1E-09	8E-07	3E-11	0	0,0015	1	1	0,0039	1	1	2E-11	6E-05	0,0596	1	0,009	9E-08	0,2218	3E-05	0	4E-05
22	89	253,49	_	Unknown	1	0,1868	1	1	1	1	0,5236	0,4764	1	1	1	1	1	1	1	1	1	1	1	1	1	1	1	1
23	184	254,45	_	Unknown	0,3003	1	1	1	1	0,2983	1	1	1	1	1	1	1	1	1	1	1	1	1	1	1	1	1	1
24	116	254,62	_	Unknown	0,0415	1	1	0,7017	0,0541	1	1	1	1	1	1	1	1	1	1	1	1	1	1	1	1	1	1	1
25	104	260,76	_	Unknown	0,2678	1	1	1	1	0,2543	1	1	1	1	1	1	1	1	1	1	1	1	1	1	1	1	1	1
26	147	264,46	Oxalate	Carboxylic acids	5E-07	1	1	1	4E-05	1E-06	1	1	1	1	1	1	0,3344	1	0,2819	1	1	1	1	1	1	1	1	1
27	144	271,67	Valine	Amino acids	5E-05	8E-19	0,1804	0,6031	4E-05	0,0723	0	0	1E-05	1	1	1	1	0,0067	0,0178	0,0011	4E-09	0,1261	1E-05	3E-09	1	4E-09	0	0,3406
28	131	273,85	_	Unknown	4E-06	1E-11	1E-07	0,018	3E-06	0,1461	0,0664	1E-11	3E-07	1	1	0,0068	1	1	4E-10	1	1	1	0,2515	5E-05	1	1	2E-10	2E-09
29	140	275,46	Acetate	Carboxylic acids	0,3546	1	1	1	1	0,4278	1	1	1	1	1	1	1	1	1	1	1	1	1	1	1	1	1	1
30	120	280,02	_	Unknown	1E-07	1	1	0,001	8E-08	0,1093	1	1	1	1	1	0,3068	0,4327	0,0072	0,004	1	1	1	1	1	1	1	1	1
31	152	282,79	Pyridine, 3-hydroxy-	Miscellaneous	2E-10	7E-06	1	0,0066	1E-05	2E-10	0,0473	4E-06	0,2498	1	1	1	1	1	0,0149	1	0,1217	1	1	0,0176	1	1	1	1
32	140	286,66	_	Unknown	2E-06	0,0808	1	0,3043	0,0037	1E-06	1	0,1074	0,6744	1	1	1	1	1	0,2476	1	1	1	1	1	1	1	1	1
33	125	287,52	_	Unknown	0,0002	1	1	0,071	0,0002	1	1	1	1	1	1	1	1	1	0,5541	1	1	1	1	1	1	1	1	1
34	89	288,01	_	Unknown	8E-11	1	0,039	0,3684	2E-10	1E-07	1	1	1	1	1	1	0,0005	3E-07	1	1	1	0,2758	1	1	1	1	1	1
35	103	288,79	_	Unknown	3E-05	0,0441	0,6713	0,1435	0,091	3E-05	1	0,0551	0,469	0,4985	1	1	1	1	1	1	1	1	1	1	1	1	1	1
36	144	289,12	_	Unknown	5E-20	2E-17	7E-16	1	0	0	6E-10	0	4E-08	1	1	1	1	2E-05	0	0,1154	1	1	1	0,3149	1	3E-08	0	0
37	205	291,9	Glycerol	Sugar alcohols	1E-13	1	1	1	0	0	1	1	1	1	1	1	3E-05	1E-06	0,0004	1	1	1	1	1	1	1	1	1
38	241	299,54	_	Unknown	0,0049	3E-11	0,0057	1	0,0052	0,1521	7E-11	6E-08	0,1748	1	1	1	1	0,0094	0,1121	0,0104	0,3691	1	0,4379	1	1	1E-08	3E-06	1
39	158	304,98	Leucine	Amino acids	8E-15	8E-18	1E-08	0,3243	5E-12	1E-11	1E-11	6E-12	8E-05	1	1	0,2823	1	2E-11	2E-11	1	0,0003	1	0,0007	1E-07	0,4231	6E-11	1E-11	0,8396
40	117	305,92	_	Unknown	9E-05	1	1	0,5559	0,1059	6E-05	1	1	1	1	1	1	1	1	1	1	1	1	1	1	1	1	1	1
41	228	306,44	_	Unknown	0,2029	1	1	1	1	0,1794	1	1	1	1	1	1	1	1	1	1	1	1	1	1	1	1	1	1
42	166	308,41	_	Unknown	0,5128	1	0,5408	1	1	0,4812	1	1	1	1	1	1	1	1	1	1	1	1	1	1	1	1	1	1
43	198	309,12	_	Unknown	0,3137	1	0,5401	1	1	0,5397	1	1	1	1	1	0,4087	1	1	1	1	1	1	1	0,8626	1	1	1	1
44	89	309,79	_	Unknown	0,0001	1	0,096	1	0,0002	0,0052	1	1	1	1	1	0,6415	1	0,4538	0,0054	1	1	1	1	1	1	1	1	1
45	103	312,64	Acetone, 1,3-dihydroxy- (Dimer)	Monosaccharides	2E-09	0,1991	0,0193	0,0066	1E-09	0,0002	1	0,1758	1	1	1	0,0047	1	0,0021	1E-06	1	0,0022	1	1	1	1	1	1	1
46	151	313,55	_	Unknown	0,0617	0,0555	1	1	1	0,0678	1	0,0616	0,7351	1	1	1	1	1	1	1	1	1	1	0,5607	1	1	1	1
47	158	318,91	Isoleucine	Amino acids	0,3946	2E-22	0,0046	1	0,3869	1	0	0	4E-08	1	1	1	1	1	0,0008	2E-10	0	1	2E-08	0	0,0041	6E-10	0	4E-06

Mass Spectral Feature			Metabolite Information		2-Way ANOVA (Variance Analysis)			TukeyHSD - Tukey Honest Significant Differences (differences between the means)																				
					p.value (adjusted using BY)			p.value (adjusted using Benjamini, Hochberg, and Yekutieli method (BY))																				
								Genotype (G)			Timepoint (T)			(Mar vs. Mut) × T			(Mar vs. Syn) × T			Mar × T			Mut × T			Syn × T		
#	M/Z	Retention [s]	Metabolite	Class	Genotype (G)	Timepoint / Treatment (T)	G × T	Mut-Mar	Syn-Mar	Syn-Mut	T0-T1	T0-T3	T1-T3	Mar:0-Mut:0	Mar:1-Mut:1	Mar:3-Mut:3	Mar:0-Syn:0	Mar:1-Syn:1	Mar:3-Syn:3	Mar:0-Mar:1	Mar:0-Mar:3	Mar:1-Mar:3	Mut:0-Mut:1	Mut:0-Mut:3	Mut:1-Mut:3	Syn:0-Syn:1	Syn:0-Syn:3	Syn:1-Syn:3
					0,05	0,05	0,05	0,05	0,05	0,05	0,05	0,05	0,05	0,05	0,05	0,05	0,05	0,05	0,05	0,05	0,05	0,05	0,05	0,05	0,05	0,05	0,05	0,05
53	174	325,01	Glycine	Amino acids	4E-06	8E-06	0,0016	1	0,0003	6E-06	0,0085	8E-06	1	1	1	1	1	1	9E-05	0,4793	1	1	1	1	1	0,2827	1E-05	0,4317
54	299	333	Orthophosphate	Miscellaneous	7E-12	0,0375	0,7115	9E-06	0,0004	0	0,0512	0,7764	1	1	0,3798	0,0406	0,0225	0,627	1	1	1	1	1	1	1	1	0,4168	1
55	100	333,52	_	Unknown	3E-11	0,3558	0,0093	1	7E-10	7E-10	0,5274	1	1	1	1	0,1412	0,0225	0,0105	2E-05	1	0,148	1	1	1	0,8123	1	1	1
56	158	336,03	Norleucine	Amino acids	4E-10	0,0088	1	1	8E-09	9E-09	0,0294	0,0298	1	NA	NA	1	NA	2E-06	4E-05	NA	NA	1	NA	NA	NA	0,2772	0,3174	1
57	85	338,44	_	Unknown	4E-06	7E-06	7E-06	1	0,0003	8E-06	1	5E-05	0,0001	1	1	1	1	1	1E-07	1	1	1	1	1	1	1	1E-07	2E-06
58	142	338,55	Proline	Amino acids	1E-10	1E-11	1E-11	1	2E-09	5E-09	1	4E-11	5E-09	1	1	1	1	1	9E-12	1	1	1	1	1	1	1	1E-11	5E-11
59	171	341,14	Urea	Miscellaneous	0,0073	0,764	1	1	0,0093	0,1653	1	1	1	1	1	1	0,4592	1	1	1	1	1	1	1	1	1	1	1
60	103	344,48	Glycerate	Carboxylic acids	2E-09	2E-15	5E-07	0,003	1E-09	0,0002	9E-11	0	0,0007	1	1	6E-05	1	5E-05	7E-11	3E-07	0	0,0002	1E-05	1E-06	1	1	1	1
61	117	344,82	_	Unknown	2E-16	1E-11	2E-06	0,0112	0	0	6E-06	0	0,0021	0,0001	1	1	1	2E-06	2E-11	5E-06	0	0,0086	1	0,0501	1	1	1	1
62	116	345,34	_	Unknown	1E-17	1	1	2E-08	4E-10	0	1	1	1	0,005	0,1425	0,0029	0,015	9E-05	0,0009	1	1	1	1	1	1	1	1	1
63	129	347,51	_	Unknown	5E-10	1	0,3418	1	4E-09	9E-09	1	1	1	1	1	1	1	7E-05	0,0003	1	1	1	1	1	1	1	1	1
64	105	348,23	Benzoate	Miscellaneous	0,0002	1	1	1	0,0003	0,0046	1	1	1	1	1	1	1	0,7926	1	1	1	1	1	1	1	1	1	1
65	240	356,94	_	Unknown	0,0175	0,7613	1	1	0,0147	1	0,9879	1	1	1	1	1	1	1	1	1	1	1	1	1	1	1	1	1
66	204	357,22	Serine	Amino acids	1E-10	1E-16	2E-07	1	2E-08	8E-10	0	0	0,001	1	1	1	1	0,8195	2E-10	0,0007	0,0004	1	0,0025	0,0012	1	2E-07	0	2E-06
67	217	361,29	_	Unknown	1E-20	1	1	1E-09	0	0	1	1	1	0,0005	0,0114	0,0029	3E-06	9E-07	6E-08	1	1	1	1	1	1	1	1	1
68	144	362,2	_	Unknown	1	0,0017	0,145	1	1	1	0,4294	0,0012	1	1	1	0,2947	1	1	1	1	0,0186	0,2915	1	1	1	1	1	1
69	228	363,04	_	Unknown	1	1	0,3714	1	1	1	1	1	1	1	1	1	1	1	1	1	1	1	1	0,4774	1	1	1	1
70	247	365,14	Succinate	Carboxylic acids	4E-06	4E-05	0,0017	1	3E-05	3E-05	0,005	5E-05	1	1	1	1	1	1	9E-05	1	0,0003	0,1975	0,0104	0,5561	1	1	1	1
71	117	367,14	Threonine	Amino acids	5E-16	2E-19	1E-09	1	0	0	0	0	2E-08	1	1	1	1	9E-05	0	0,0004	8E-07	1	0,0075	8E-06	1	6E-10	0	5E-09
72	255	369,12	_	Unknown	0,0121	1	1	0,189	1	0,0221	1	1	1	1	1	1	1	1	1	1	1	1	1	1	1	1	1	1
73	110	370,34	_	Unknown	1	1	1	1	1	1	1	1	1	1	1	1	1	1	1	1	1	1	1	1	1	1	1	1
74	241	370,44	_	Unknown	6E-09	2E-06	1	0,1063	5E-09	6E-05	0,9409	2E-06	0,004	1	1	1	1	0,0014	9E-05	1	1	1	1	0,2405	0,4231	1	0,0017	1
75	245	370,9	Fumarate	Carboxylic acids	0,0004	2E-09	1	0,3043	0,865	0,0003	0,0003	1E-09	0,0071	1	1	0,8384	1	1	1	0,2514	0,047	1	1	8E-05	0,7826	1	0,0013	1
76	156	371,59	_	Unknown	0,0375	0,0389	0,0401	1	0,5409	0,0406	1	0,1001	0,1664	1	1	1	1	1	0,0272	1	0,006	0,151	1	1	1	1	1	1
77	234	372,16	_	Unknown	1E-06	0,0352	0,0105	6E-05	1E-05	1	0,2017	0,0646	1	1	0,0326	0,0027	1	0,0087	0,0006	0,0224	0,0014	1	1	1	1	1	1	1
78	158	372,37	_	Unknown	8E-08	8E-08	7E-07	1	3E-07	4E-06	1	9E-05	3E-07	NA	1	1	1	1	2E-08	1	1	1	NA	NA	1	1	2E-05	3E-08
79	157	373,37	_	Unknown	0,2632	1	1	1	1	0,2321	1	1	1	1	1	1	1	1	1	1	1	1	1	1	1	1	1	1
80	156	374,32	Pipecolate	Amino acids	2E-06	1	1	4E-06	0,0052	0,1543	1	1	1	1	0,0101	0,6415	1	0,1993	1	1	1	1	1	1	1	1	1	1
81	170	374,68	_	Unknown	5E-06	0,0825	1	1	0,0008	8E-06	0,1154	1	1	1	1	1	1	1	0,0757	1	1	1	1	1	1	1	1	1
82	89	375,99	_	Unknown	6E-09	0,0829	0,0125	0,9395	1E-08	7E-06	0,6009	0,1111	1	1	1	1	0,0016	1E-05	1	1	1	1	1	1	1	1	0,0102	1
83	103	383,71	_	Unknown	1E-26	5E-11	0,0001	0,0181	6E-12	5E-12	0,0068	6E-11	4E-06	1	1	1	3E-11	2E-11	1E-11	0,2265	2E-08	0,0013	1	1E-06	0,001	1	1	1
84	136	386,29	Nicotinate	Miscellaneous	1	1	1	1	1	1	1	1	1	1	1	1	1	1	1	1	1	1	1	1	1	1	1	1
85	103	388,94	_	Unknown	6E-09	1E-17	2E-11	1	2E-06	1E-08	1E-06	7E-12	4E-11	1	1	1	1	1	5E-11	0,0008	3E-07	1	1	0,0028	1	0,0318	1E-11	5E-11
86	217	389,43	_	Unknown	2E-17	1	1	4E-09	2E-11	4E-12	1	1	1	0,0015	0,0043	0,0053	5E-05	7E-05	2E-05	1	1	1	1	1	1	1	1	1
87	99	391,87	Uracil	Nucleic acids	0,5037	1	1	1	1	0,4633	1	1	1	1	1	1	1	1	1	1	1	1	1	1	1	1	1	1
88	130	392,29	_	Unknown	0,187	8E-09	0,0727	1	0,1705	1	8E-06	1E-08	1	1	1	1	1	0,0755	1	1	0,2115	1	1	0,0003	1	0,0003	0,013	1
89	117	393,2	_	Unknown	1	1E-05	0,4824	1	1	1	0,1539	8E-06	0,0627	1	1	1	1	1	0,8866	1	1	1	1	0,9538	1	1	0,0027	0,0439
90	100	393,52	_	Unknown	0,2307	0,0427	0,4053	1	1	0,2178	1	0,05	0,5433	1	1	0,2306	1	1	1	1	1	1	1	0,1876	0,8681	1	1	1
91	103	393,67	_	Unknown	4E-25	4E-08	0,0001	0,0143	6E-12	5E-12	0,1105	3E-08	0,0005	1	1	0,0002	3E-11	2E-11	1E-11	1	1	1	0,0213	8E-08	0,0873	1	0,0087	0,2229
92	86	393,95	_	Unknown	0,3747	1	0,716	1	0,3797	1	1	1	1	1	1	1	1	1	1	1	1	1	1	1	1	1	1	1
93	103	397,43	_	Unknown	2E-05	0,1234	0,0246	0,0006	1E-04	1	1	0,1196	1	1	0,7206	0,0041	1	0,1469	0,0007	0,5615	0,0023	1	1	1	1	1	1	1
94	117	397,96	_	Unknown	0,5788	1	1	1	0,9454	1	1	1	1	1	1	1	1	1	1	1	1	1	1	1	1	1	1	1
95	196	401,73	_	Unknown	1E-10	0,2144	1	0,3059	4E-07	2E-10	1	0,2072	1	1	1	1	1	0,0353	0,0035	1	1	1	1	1	1	1	1	1
96	102	403,93	_	Unknown	2E-05	0,0389	0,0508	0,0007	0,0002	1	0,1193	0,13	1	1	0,1608	0,0482	1	0,0178	0,0097	0,0234	0,0198	1	1	1	1	1	1	1
97	218	406,18	_	Unknown	1	3E-06	0,8714	1	1	1	0,1361	2E-06	0,0229	1	1	1	1	1	1	1	0,0004	1	1	1	1	1	0,2749	1
98	269	406,24	_	Unknown	0,7068	0,0135	1	1	1	1	1	0,0131	0,4444	1	1	1	1	1	1	1	1	1	1	1	1	1	1	1
99	97	407,83	_	Unknown	0,0021	1	1	0,0147	1	0,0442	1	1	1	1	1	0,6075	1	1	1	1	1	1	1	1	1	1	1	1

Mass Spectral Feature			Metabolite Information		2-Way ANOVA (Variance Analysis)			TukeyHSD - Tukey Honest Significant Differences (differences between the means)																	
					p.value (adjusted using BY)			p.value (adjusted using Benjamini, Hochberg, and Yekutieli method (BY))																	
								Genotype (G)			Timepoint (T)			(Mar vs. Mut) × T			(Mar vs. Syn) × T			Mar × T			Mut × T			Syn × T		
#	M/Z	Retention [s]	Metabolite	Class	Genotype (G)	Timepoint / Treatment (T)	G × T	Mut-Mar	Syn-Mar	Syn-Mut	T0-T1	T0-T3	T1-T3	Mar:0-Mut:0	Mar:1-Mut:1	Mar:3-Mut:3	Mar:0-Syn:0	Mar:1-Syn:1	Mar:3-Syn:3	Mar:0-Mar:1	Mar:0-Mar:3	Mar:1-Mar:3	Mut:0-Mut:1	Mut:0-Mut:3	Mut:1-Mut:3	Syn:0-Syn:1	Syn:0-Syn:3	Syn:1-Syn:3
					0,05	0,05	0,05	0,05	0,05	0,05	0,05	0,05	0,05	0,05	0,05	0,05	0,05	0,05	0,05	0,05	0,05	0,05	0,05	0,05	0,05	0,05	0,05	0,05
105	85	416,23	_	Unknown	1	1	1	1	1	1	1	1	1	1	1	1	1	1	1	1	1	1	1	1	1	1	1	1
106	143	417,36	_	Unknown	5E-09	1	1	2E-06	1	2E-08	1	1	1	0,0922	1	0,0048	1	1	1	1	1	1	1	1	1	1	1	1
107	117	418,97	_	Unknown	1	0,2266	0,718	1	1	1	1	0,4402	0,8296	1	1	1	1	1	1	1	1	1	1	0,6998	0,8279	1	1	1
108	146	420,9	_	Unknown	2E-08	1	1	7E-07	1	8E-07	1	1	1	0,0492	0,5457	0,0047	1	1	1	1	1	1	1	1	1	1	1	1
109	159	422,33	_	Unknown	1E-18	2E-13	2E-06	0,6263	5E-13	4E-13	2E-10	1E-12	0,3738	1	1	1	0,0004	9E-11	2E-12	4E-07	5E-09	1	6E-07	3E-10	1	1	1	1
110	113	422,79	Thymine	Nucleic acids	0,4513	0,2201	1	1	0,729	1	1	0,9371	0,3979	1	1	1	1	1	1	1	1	1	1	1	1	1	1	1
111	115	425,13	_	Unknown	0,0002	0,0023	0,5971	0,7071	0,0002	0,1177	0,0042	0,116	1	0,3898	1	1	0,014	1	1	1	1	1	0,2033	0,9819	1	1	1	1
112	159	425,37	_	Unknown	5E-07	0,0013	1	1	1E-06	3E-05	1	0,0059	0,0106	1	1	1	0,7954	0,2006	0,0094	1	1	1	1	0,1793	0,3872	1	1	1
113	143	427,91	_	Unknown	3E-05	1	1	1	0,0101	3E-05	1	1	1	1	1	1	1	1	1	1	1	1	1	1	1	1	1	1
114	194	429,02	_	Unknown	5E-13	0,001	0,6198	1	7E-11	4E-12	0,3954	0,0007	1	1	1	1	0,0658	0,0001	1E-06	1	0,0109	1	1	1	1	1	1	1
115	117	430,48	Decanoate	Fatty acids	0,0003	0,0603	1	1	0,0026	0,0009	1	0,0513	1	1	1	1	1	1	1	1	1	1	1	1	1	1	1	1
116	88	433,73	_	Unknown	1E-12	1	1	0,0004	0	3E-07	1	1	1	1	1	0,0623	0,0005	2E-05	4E-07	1	1	1	1	1	1	1	1	1
117	140	433,81	_	Unknown	1	1	1	1	1	1	1	1	1	1	1	1	1	1	1	1	1	1	1	1	1	1	1	1
118	89	433,94	_	Unknown	5E-05	1	1	1	0,0004	6E-05	1	1	1	1	1	1	1	0,5241	0,3835	1	1	1	1	1	1	1	1	1
119	143	434,37	_	Unknown	2E-08	1	1	9E-06	0,8468	8E-08	1	1	1	0,3229	1	0,0044	1	1	1	1	1	1	1	1	1	1	1	1
120	232	435,93	_	Unknown	4E-10	9E-08	2E-06	1	3E-09	2E-08	0,8768	1E-07	0,0002	1	1	1	1	1	6E-10	1	1	1	1	1	1	1	2E-09	4E-06
121	143	436,86	_	Unknown	2E-06	0,9725	1	0,0064	0,2833	1E-06	1	1	1	1	1	0,0792	1	1	1	1	1	1	1	1	1	1	1	1
122	100	437,63	_	Unknown	0,8942	0,0015	0,0938	1	0,8737	1	0,0971	0,0028	1	1	1	1	1	1	NA	1	1	1	1	1	1	0,1719	NA	NA
123	146	440,02	_	Unknown	8E-10	1	1	1E-07	1	5E-09	1	1	1	0,0056	1	0,0106	1	1	1	1	1	1	1	1	1	1	1	1
124	88	440,35	_	Unknown	9E-13	0,1088	1	0,2706	5E-12	9E-11	1	0,0908	1	1	1	1	0,001	7E-07	3E-08	1	1	1	1	1	1	1	1	1
125	133	440,72	Malate	Carboxylic acids	0,0001	1E-05	0,2683	0,075	1	9E-05	0,0536	6E-06	0,3288	1	1	0,0946	1	1	1	1	1	1	1	0,0006	0,3298	1	1	1
126	218	442,18	_	Unknown	0,0004	3E-06	0,0043	1	0,0017	0,0019	0,0043	2E-06	0,469	1	1	1	1	1	4E-05	1	1	1	1	0,2131	1	0,3261	1E-05	0,2301
127	292	442,33	_	Unknown	2E-05	5E-18	0,3399	0,3083	1E-05	0,0413	8E-10	7E-12	1E-10	1	1	0,6426	1	0,0601	5E-05	0,0007	3E-11	8E-06	4E-05	2E-10	0,0025	0,086	1E-08	0,0004
128	85	442,87	_	Unknown	1	1	1	1	1	1	1	1	1	1	1	1	1	1	1	1	1	1	1	1	1	1	1	1
129	146	450,06	_	Unknown	9E-17	0,764	0,1498	0,0005	0	0	1	0,7176	1	1	1	0,0016	0,0003	7E-06	0,0001	1	1	1	1	0,1129	1	1	1	1
130	133	450,2	_	Unknown	0,0009	1	1	0,9395	0,2504	0,0007	1	1	1	1	1	1	1	1	1	1	1	1	1	1	1	1	1	1
131	131	450,31	_	Unknown	5E-12	0,0104	0,665	1	3E-09	1E-11	0,4015	0,0093	1	1	1	1	1	3E-05	0,0008	1	1	1	1	0,6077	1	1	1	1
132	217	451,69	_	Unknown	5E-19	1E-21	3E-18	1	6E-12	5E-12	0,0003	8E-12	3E-11	0,9519	0,7503	0,0029	0,8277	1E-05	1E-11	0,0001	3E-11	6E-11	1E-04	3E-11	4E-11	0,6459	1	1
133	100	452,45	_	Unknown	9E-06	0,0057	0,0284	1	9E-05	7E-05	1	0,0039	1	1	1	1	1	1	0,0001	1	1	1	1	1	1	1	0,0003	0,8755
134	243	453,88	_	Unknown	1	1	1	1	1	1	1	1	1	1	1	1	1	1	1	1	1	1	1	1	1	1	1	1
135	151	454,96	_	Unknown	2E-17	1	1	0,0178	6E-12	5E-12	1	1	1	1	1	1	2E-05	4E-08	2E-07	1	1	1	1	1	1	1	1	1
136	255	455,28	_	Unknown	1	1	1	1	1	1	1	1	1	1	1	1	1	1	1	1	1	1	1	1	1	1	1	1
137	232	457,17	Aspartate	Amino acids	0,0043	1E-12	1	0,1577	0,0066	1	6E-09	0	0,0826	1	1	1	1	1	0,1087	0,213	0,0005	1	0,0075	0,0003	1	0,0002	2E-08	1
138	170	457,41	_	Unknown	0,0035	1E-12	1	0,9911	0,0028	0,8854	3E-08	0	0,051	1	1	1	1	1	0,0796	0,8726	0,0027	1	0,0027	4E-05	1	0,0024	2E-07	1
139	159	458,85	_	Unknown	0,0002	1	1	0,0032	1	0,0015	1	1	1	0,8888	1	1	1	1	1	1	1	1	1	1	1	1	1	1
140	156	464,26	_	Unknown	0,0004	1	1	1	0,1766	0,0006	1	1	1	NA	NA	1	NA	NA	1	NA	NA	NA	1	1	1	1	1	1
141	146	464,33	_	Unknown	2E-17	0,7202	1	2E-08	7E-10	0	1	0,7539	1	0,0133	0,0326	0,0032	0,0172	0,0031	4E-05	1	1	1	1	1	1	1	1	1
142	188	464,6	_	Unknown	0,1129	0,0007	1	1	0,1169	0,8338	1	0,0008	0,0503	1	1	1	1	1	0,2548	1	1	1	1	0,7617	1	1	0,1715	1
143	144	464,87	_	Unknown	2E-05	2E-08	0,0127	1	3E-05	0,0044	0,0053	1E-08	0,0019	1	1	1	1	1	4E-05	1	1	1	1	0,0996	1	0,1272	3E-07	0,0179
144	117	465,49	_	Unknown	0,0022	1	1	1	0,044	0,0033	1	1	1	1	1	1	1	1	1	1	1	1	1	1	1	1	1	1
145	146	467,91	_	Unknown	2E-07	1	1	2E-05	1	2E-06	1	1	1	0,1396	1	0,1551	1	1	1	1	1	1	1	1	1	1	1	1
146	155	468,78	_	Unknown	0,0104	0,0036	1	1	0,0119	0,2238	1	0,0024	0,7891	1	1	1	1	1	0,0728	1	1	1	1	1	1	1	0,0426	1
147	217	469,64	_	Unknown	2E-17	1E-10	2E-05	9E-05	0	0	2E-05	8E-11	0,0002	1	0,3316	1	1	4E-06	9E-12	0,0016	3E-09	0,0004	0,0372	2E-05	0,5139	1	1	1
148	204	470,22	_	Unknown	1E-07	1	1	4E-06	1	2E-06	1	1	1	0,0381	1	0,0634	1	1	1	1	1	1	1	1	1	1	1	1
149	111	470,7	Adipate	Carboxylic acids	1	0,2938	1	1	1	1	0,5023	1	1	1	1	1	1	1	1	1	1	1	1	1	1	1	1	1
150	133	473,17	_	Unknown	6E-14	4E-15	8E-12	1	2E-11	4E-12	2E-08	6E-12	2E-06	0,6158	0,0261	3E-08	1	0,1733	9E-12	0,0075	2E-11	5E-11	0,0004	0,0001	1	0,3416	0,1505	1
151	157	473,37	Malate, 2-isopropyl-	Carboxylic acids	3E-19	1E-23	2E-23	0	0	0,2757	0	0	0	1	1	0	1	0,4848	0	4E-06	0	0	1E-09	1E-09	1	1E-07	3E-07	1

Mass Spectral Feature			Metabolite Information		2-Way ANOVA (Variance Analysis)			TukeyHSD - Tukey Honest Significant Differences (differences between the means)																	
					p.value (adjusted using BY)			p.value (adjusted using Benjamini, Hochberg, and Yekutieli method (BY))																	
								Genotype (G)			Timepoint (T)			(Mar vs. Mut) × T			(Mar vs. Syn) × T			Mar × T			Mut × T			Syn × T		
#	M/Z	Retention [s]	Metabolite	Class	Genotype (G)	Timepoint / Treatment (T)	G × T	Mut-Mar	Syn-Mar	Syn-Mut	T0-T1	T0-T3	T1-T3	Mar:0-Mut:0	Mar:1-Mut:1	Mar:3-Mut:3	Mar:0-Syn:0	Mar:1-Syn:1	Mar:3-Syn:3	Mar:0-Mar:1	Mar:0-Mar:3	Mar:1-Mar:3	Mut:0-Mut:1	Mut:0-Mut:3	Mut:1-Mut:3	Syn:0-Syn:1	Syn:0-Syn:3	Syn:1-Syn:3
					0,05	0,05	0,05	0,05	0,05	0,05	0,05	0,05	0,05	0,05	0,05	0,05	0,05	0,05	0,05	0,05	0,05	0,05	0,05	0,05	0,05	0,05	0,05	0,05
157	217	483,53	_	Unknown	5E-12	1	1	0,0004	5E-06	0	1	1	1	1	1	0,1658	1	0,0436	0,1692	1	1	1	1	1	1	1	1	1
158	118	486,97	_	Unknown	6E-08	1	0,4245	0,0071	4E-08	0,0039	1	1	1	1	0,6156	1	1	0,0327	9E-05	1	1	1	1	1	1	1	1	1
159	142	490,55	Arginine	Amino acids	2E-16	2E-10	1E-09	1	0	0	0,0003	1E-10	0,0007	1	1	1	1	9E-05	0	1	1	1	1	1	1	0,0003	0	9E-07
160	116	490,81	_	Unknown	1E-11	8E-09	5E-06	1	2E-10	4E-10	3E-05	5E-09	0,0478	1	1	1	1	0,0067	6E-10	1	1	1	1	1	1	0,0014	1E-09	0,0003
161	170	491,51	[Homoglutamine]	Amino acids	9E-08	5E-09	0,0004	0,7526	9E-08	8E-05	5E-06	7E-09	1	1	1	0,0135	1	0,0108	2E-07	0,0104	4E-08	0,151	0,0063	0,097	1	1	1	1
162	103	492,76	_	Unknown	1E-15	1	1	3E-07	1E-08	0	1	1	1	0,005	0,0237	0,9927	0,0396	0,0231	0,0003	1	1	1	1	1	1	1	1	1
163	199	493,12	_	Unknown	0,0183	1	1	1	1	0,0145	1	1	1	1	1	1	1	1	1	1	1	1	1	1	1	1	1	1
164	100	494,25	_	Unknown	0,2119	9E-10	0,0582	1	0,3081	1	0,1197	7E-10	2E-05	1	1	0,0946	1	1	0,0228	1	1	1	1	6E-05	0,007	1	1E-05	0,0118
165	195	495,2	_	Unknown	1E-08	1E-09	0,0195	0,0001	0,079	1E-08	0,0026	8E-10	0,0002	1	0,3798	1	1	1	0,0006	1	8E-07	0,0011	1	0,0021	0,5139	1	0,5201	1
166	112	495,6	_	Unknown	2E-05	1E-05	0,0217	1	2E-05	0,0089	0,884	2E-05	0,0065	1	1	0,7709	1	1	1E-05	1	1	1	1	1	1	1	4E-05	0,1374
167	171	496,04	_	Unknown	0,0001	1	1	1	0,0001	0,0335	1	1	1	1	1	1	1	0,0288	0,1833	1	1	1	1	1	1	1	1	1
168	175	497,03	_	Unknown	1	2E-06	1	1	1	1	1	2E-06	0,0022	1	1	1	1	1	1	1	0,0149	0,5253	1	0,0544	1	1	1	1
169	117	498,61	_	Unknown	9E-15	1E-13	4E-12	1	6E-12	5E-12	0,0013	7E-12	3E-09	1	1	1	1	0,0032	1E-11	1	1	1	1	1	1	0,0049	1E-11	5E-11
170	112	498,7	_	Unknown	0,0052	2E-07	0,0544	1	0,0049	0,3164	0,5998	2E-07	0,0003	1	1	0,4275	1	1	0,0016	1	1	1	1	0,0038	0,2525	1	9E-05	0,01
171	177	500,22	_	Unknown	0,6996	0,0024	0,5268	1	1	1	1	0,0038	0,0498	1	1	0,3725	1	1	1	1	1	1	1	0,0262	0,136	1	1	1
172	103	500,64	_	Unknown	1	0,2911	1	1	1	1	1	0,3754	1	1	1	1	1	1	1	1	1	1	1	1	1	1	0,6873	1
173	217	500,79	Ribose (; Ribulose)	Monosaccharides	2E-17	0,0524	1	9E-07	2E-11	4E-12	0,7003	0,0575	1	0,0196	1	0,0391	0,0007	4E-05	2E-05	1	1	1	1	1	1	1	1	1
174	103	502,32	_	Unknown	8E-07	0,0448	0,0017	1	2E-05	5E-06	1	0,0395	1	0,0917	1	0,5091	1	0,0413	0,0041	0,4132	0,0008	1	1	1	1	1	1	1
175	123	505,51	_	Unknown	0,624	0,0108	1	1	1	1	1	0,0454	0,0472	1	1	1	1	1	1	1	1	1	1	0,2436	0,5139	1	1	1
176	156	506,62	Pyroglutamate	Amino acids	4E-05	0,6458	0,0115	1	4E-05	0,0086	1	1	1	1	1	1	0,0003	1	1	1	1	1	1	1	1	0,2127	0,1571	1
177	128	507,76	Glutamate	Amino acids	3E-06	1	0,0032	0,0331	2E-06	0,1416	1	1	1	1	1	1	7E-05	0,0351	1	1	1	1	1	1	1	1	0,0102	1
178	217	510,63	_	Unknown	1E-20	0,5677	0,4867	8E-11	4E-12	4E-12	1	1	0,9951	3E-06	0,0002	0,0049	0,0015	7E-08	3E-10	1	1	1	1	1	1	1	1	1
179	255	510,68	_	Unknown	1	1	1	1	1	1	1	1	1	1	1	1	1	1	1	1	1	1	1	1	1	1	1	1
180	146	510,9	_	Unknown	5E-10	1	1	4E-07	0,6078	1E-09	1	1	1	0,0062	0,1921	0,0423	1	1	1	1	1	1	1	1	1	1	1	1
181	100	512,79	_	Unknown	0,0005	0,003	0,0002	1	0,0008	0,0105	1	0,0022	0,7883	1	1	1	7E-05	1	1	1	1	1	1	1	1	0,0319	4E-06	1
182	179	515,21	Nicotinamide	Miscellaneous	1E-19	1	1	4E-06	4E-12	4E-12	1	1	1	0,0056	0,5759	1	7E-07	6E-07	6E-10	1	1	1	1	1	1	1	1	1
183	129	516,65	_	Unknown	0,1873	0,3164	0,0046	1	0,4958	0,2903	1	0,5292	1	1	1	0,1678	1	1	1	1	0,0093	1	1	1	1	1	1	1
184	174	517,17	Putrescine	Amino acids	0,435	0,016	0,4012	1	1	0,6375	1	0,0148	0,5788	1	1	1	1	1	1	1	0,042	1	1	1	1	1	1	1
185	117	518,8	_	Unknown	5E-14	9E-11	2E-06	4E-11	0	1	0,0971	9E-11	1E-06	1	0,02	4E-10	1	2E-05	8E-12	0,0515	8E-12	2E-06	1	1	1	1	1	1
186	205	518,88	_	Unknown	0,0037	8E-13	0,0032	0,0143	0,0572	1	1	0	2E-09	1	1	0,0462	1	1	9E-05	1	3E-09	7E-07	1	3E-05	0,0039	1	0,5201	1
187	100	519,19	_	Unknown	4E-10	6E-07	5E-06	1	2E-09	3E-08	3E-06	2E-05	1	1	1	1	1E-09	1	0,3496	1	1	1	1	1	1	6E-08	2E-07	1
188	140	520,21	_	Unknown	5E-11	1E-12	4E-12	1	4E-10	4E-09	1	5E-12	1E-09	1	1	1	1	1	0	1	1	1	1	1	1	1	0	0
189	182	520,3	_	Unknown	0,0003	1	0,0029	1	0,0003	0,0173	1	1	1	1	1	0,0091	1	1	0,0023	1	0,0141	1	1	1	1	1	1	1
190	85	520,46	_	Unknown	1	1	1	1	1	1	1	1	1	1	1	1	1	1	1	1	1	1	1	1	1	1	1	1
191	328	521,45	_	Unknown	0,3919	0,2324	1	1	0,5002	1	1	1	0,7141	NA	1	1	1	1	0,8617	1	1	1	NA	NA	1	1	1	1
192	117	521,87	_	Unknown	3E-13	1E-06	0,0044	1	1E-11	1E-11	0,0082	8E-07	0,2	1	1	0,1475	0,0146	3E-05	4E-07	0,213	5E-06	0,3588	1	1	1	1	0,0599	1
193	102	522,75	_	Unknown	4E-21	0,0131	0,7634	1E-09	0	0	1	0,0298	0,0988	0,3566	0,006	8E-06	0	0	0	1	0,0596	0,7253	1	1	1	1	1	1
194	173	523,26	_	Unknown	1E-08	1	1	1	1E-06	6E-08	1	1	1	1	1	1	1	0,023	0,0666	1	1	1	1	1	1	1	1	1
195	200	524,39	_	Unknown	5E-06	0,0282	0,0711	1	0,0002	2E-05	1	0,0234	1	1	1	1	1	1	0,0004	1	1	1	1	1	1	1	0,0044	1
196	100	525,47	_	Unknown	5E-10	3E-07	0,0006	1	2E-09	3E-08	1	8E-07	0,0001	1	1	1	1	1	7E-09	1	1	1	1	0,0487	1	1	8E-06	8E-05
197	133	527,36	Phosphoenolpyruvate	Carboxylic acids	0,9501	0,235	0,0711	1	1	1	1	0,2722	1	1	1	1	1	0,7374	1	1	1	1	1	1	1	1	1	1
198	142	527,62	_	Unknown	1	1	0,1937	1	1	1	1	1	1	1	1	1	1	1	0,3612	1	1	1	1	1	1	1	1	1
199	195	527,67	_	Unknown	0,0003	1	1	1	0,042	0,0003	1	1	1	1	1	1	1	1	0,8572	1	1	1	1	1	1	1	1	1
200	117	527,9	Dodecanoate	Fatty acids	3E-09	0,195	0,2136	1	3E-07	2E-08	0,3072	1	1	1	0,7833	1	0,0057	1	0,0006	0,1588	1	0,404	1	1	1	1	1	1
201	100	528,06	_	Unknown	0,0018	0,0441	1	1	0,0014	0,4105	1	0,0395	1	1	1	1	1	0,0853	1	1	1	1	1	1	1	1	1	1
202	111	528,07	_	Unknown	0,454	1	1	1	1	0,4657	1	1	1	1	1	1	1	1	1	1	1	1	1	1	1	1	1	1
203	288	529,81	_	Unknown	1E-10	1E-05	3E-05	1	1E-09	4E-09	0,0173	8E-06	0,4987	1	1	1	1	0,0033	3E-09	1	1	1	1	1	1	0,005	4E-08	0,0429

Mass Spectral Feature			Metabolite Information		2-Way ANOVA (Variance Analysis)			TukeyHSD - Tukey Honest Significant Differences (differences between the means)																	
					p.value (adjusted using BY)			p.value (adjusted using Benjamini, Hochberg, and Yekutieli method (BY))																	
								Genotype (G)			Timepoint (T)			(Mar vs. Mut) × T			(Mar vs. Syn) × T			Mar × T			Mut × T			Syn × T		
#	M/Z	Retention [s]	Metabolite	Class	Genotype (G)	Timepoint / Treatment (T)	G × T	Mut-Mar	Syn-Mar	Syn-Mut	T0-T1	T0-T3	T1-T3	Mar:0-Mut:0	Mar:1-Mut:1	Mar:3-Mut:3	Mar:0-Syn:0	Mar:1-Syn:1	Mar:3-Syn:3	Mar:0-Mar:1	Mar:0-Mar:3	Mar:1-Mar:3	Mut:0-Mut:1	Mut:0-Mut:3	Mut:1-Mut:3	Syn:0-Syn:1	Syn:0-Syn:3	Syn:1-Syn:3
					0,05	0,05	0,05	0,05	0,05	0,05	0,05	0,05	0,05	0,05	0,05	0,05	0,05	0,05	0,05	0,05	0,05	0,05	0,05	0,05	0,05	0,05	0,05	0,05
209	101	533,06	_	Unknown	2E-08	0,3041	0,6039	1E-07	NA	NA	1	0,9825	0,6247	0,213	0,122	0,0001	NA	NA	NA	1	0,8167	1	1	1	1	NA	NA	NA
210	156	533,75	_	Unknown	1	0,3089	1	1	1	1	1	0,5551	1	1	1	1	1	1	1	1	1	1	1	1	1	1	1	1
211	142	533,85	Proline [+CO2]	Amino acids	5E-05	4E-07	2E-05	1	0,0002	0,0007	1	2E-06	2E-05	1	1	1	1	1	1E-06	1	1	1	1	1	1	1	5E-08	5E-07
212	85	534,93	_	Unknown	0,018	1	1	0,6785	1	0,0171	1	1	1	1	1	0,4797	1	1	1	1	1	1	1	1	1	1	1	1
213	117	536,07	_	Unknown	5E-07	0,1585	1	4E-05	6E-05	0,022	0,9561	1	0,3519	0,9841	1	0,0118	NA	NA	0,0002	1	1	1	1	1	1	NA	NA	NA
214	117	540,01	_	Unknown	8E-11	3E-11	3E-09	1	2E-10	1E-07	0,0093	1E-10	4E-07	NA	1	1	1	0,1055	2E-12	1	1	1	NA	NA	0,4645	0,0452	2E-12	5E-09
215	171	540,51	_	Unknown	4E-05	0,1371	1	1	4E-05	0,0134	1	0,4368	0,37	1	1	1	1	1	0,0026	1	1	1	1	1	1	1	1	1
216	100	540,46	_	Unknown	1	2E-07	0,5847	1	1	1	1	9E-07	3E-05	1	1	1	1	1	1	1	1	1	1	1	1	1	6E-05	0,0434
217	157	541,84	_	Unknown	0,0384	1	1	0,1027	1	0,2655	1	1	1	1	1	1	1	1	1	1	1	1	1	1	1	1	1	1
218	89	542,39	_	Unknown	3E-10	9E-09	0,1008	0,0055	2E-10	1E-05	0,0011	5E-09	0,0063	1	1	1	1	0,0117	2E-07	1	0,1609	1	1	0,1107	1	0,3416	2E-06	0,0335
219	85	543,44	_	Unknown	1	1	1	1	1	1	1	1	1	1	1	1	1	1	1	1	1	1	1	1	1	1	1	1
220	204	548,63	_	Unknown	1	0,0001	1	1	1	1	0,0003	0,0065	1	1	1	1	1	1	1	1	1	1	0,0476	0,1203	1	1	1	1
221	129	549,83	_	Unknown	0,019	1E-09	0,3119	1	0,0428	0,0857	0,0049	8E-10	0,0007	1	1	1	1	0,7201	0,3319	0,2442	4E-05	1	1	3E-05	0,6998	1	1	1
222	116	549,94	Asparagine	Amino acids	0,0006	0,0008	1	1	0,0009	0,0253	0,9146	0,0005	0,4987	1	1	1	1	1	0,3794	1	1	1	1	0,0501	0,8193	1	1	1
223	98	549,97	_	Unknown	4E-13	1	0,0161	1	1E-11	1E-11	1	1	1	1	1	1	7E-07	5E-06	0,2795	1	1	1	1	1	1	1	0,0739	0,115
224	112	550,33	_	Unknown	0,008	1	1	1	0,0167	0,0451	1	1	1	1	1	1	1	1	0,4558	1	1	1	1	1	1	1	1	1
225	243	555,76	Glycerol 2-P	Sugar alcohols	0,9426	0,1611	1	1	1	1	1	1	0,2511	1	1	1	1	1	1	1	1	1	1	1	1	1	1	1
226	101	556,05	_	Unknown	0,0009	0,0276	1	1	0,0299	0,001	1	0,0312	0,4596	1	1	1	1	1	1	1	0,6199	1	1	1	1	1	1	1
227	156	556,19	_	Unknown	8E-10	1	1	1E-07	1	8E-09	1	1	1	0,0133	0,451	0,0124	1	1	1	1	1	1	1	1	1	1	1	1
228	125	556,34	_	Unknown	0,077	0,0096	1	1	0,8269	0,0764	1	0,0084	0,3821	1	1	1	1	1	1	1	1	1	1	0,1199	1	1	1	1
229	204	556,42	_	Unknown	1	0,1809	0,6321	1	1	1	1	0,1865	1	1	1	1	1	1	1	1	1	1	1	1	1	1	1	1
230	99	558,73	_	Unknown	2E-07	0,0425	0,0851	1	7E-07	8E-06	0,2126	0,0865	1	1	1	0,9456	1	0,0344	0,0001	1	0,0137	1	1	1	1	1	1	1
231	217	560,45	Glucosyl	Miscellaneous	1E-05	3E-14	0,0001	0,0502	0,2266	8E-06	1E-07	0	2E-05	1	0,3016	1	1	1	0,0001	0,3904	2E-09	1E-04	1E-04	1E-09	0,3703	1	0,7203	1
232	142	570,43	Ornithine	Amino acids	6E-13	4E-06	1E-05	1	2E-10	0	0,0027	3E-06	1	1	1	1	1	0,0008	5E-10	1	1	1	1	1	1	0,0005	1E-08	0,7716
233	299	573,9	Glycerol 3-P	Sugar alcohols	1	2E-09	0,0037	1	1	1	1	6E-09	6E-07	1	1	1	1	1	1	1	0,0323	0,0042	1	1	1	0,6014	1E-07	0,0026
234	214	575,93	_	Unknown	3E-13	6E-13	6E-13	1	1E-11	2E-11	1	1E-11	1E-10	1	1	1	1	1	1E-11	1	1	1	1	1	1	1	2E-11	5E-11
235	111	576,33	_	Unknown	1	0,0032	0,985	1	1	1	1	0,0085	0,0276	1	1	1	1	1	1	1	1	1	1	0,0701	0,2948	1	1	1
236	142	577,01	_	Unknown	2E-05	0,0015	0,0079	1	0,0001	0,0001	1	0,001	0,3866	1	1	1	1	1	1E-05	1	1	1	1	1	1	1	0,0001	0,0179
237	103	578,95	Fructose	Monosaccharides	6E-05	0,1927	1	1	9E-05	0,0054	0,4403	1	0,9747	1	1	1	1	0,2471	1	1	1	1	1	1	1	1	1	1
238	156	579,99	Glutamate, N-acetyl-	Amino acids	9E-06	1E-06	1	0,0379	0,1705	7E-06	1	3E-06	0,0002	1	1	1	1	1	1	1	0,0462	0,151	1	1	1	1	0,0034	0,6353
239	85	580,6	_	Unknown	2E-11	1	1	1	9E-11	1E-08	1	1	1	1	1	1	0,0004	0,0001	0,0007	1	1	1	1	1	1	1	1	1
240	205	581,54	_	Unknown	0,0024	1	1	0,0156	1	0,0206	1	1	1	1	1	1	1	1	1	1	1	1	1	1	1	1	1	1
241	117	581,88	_	Unknown	0,0603	1	1	0,4228	1	0,1237	1	1	1	1	1	1	1	1	1	1	1	1	1	1	1	1	1	1
242	104	582,11	_	Unknown	0,2238	1	0,9965	1	0,579	0,3746	1	1	1	1	1	1	1	1	1	1	1	1	1	1	1	1	1	1
243	247	583,35	_	Unknown	0,0057	1E-14	0,9654	1	0,0277	0,0157	0	7E-10	0,0013	1	1	1	1	0,1794	1	6E-08	1E-04	1	3E-08	0,0003	1	0,0014	0,1545	1
244	299	586,83	_	Unknown	2E-06	1	1	0,0071	0,3453	2E-06	1	1	1	1	1	1	1	1	1	1	1	1	1	1	1	1	1	1
245	205	587,27	Sorbitol	Sugar alcohols	0,0018	1	1	0,3142	0,0018	1	1	1	1	1	1	0,3162	1	1	0,171	1	1	1	1	1	1	1	1	1
246	128	588,06	_	Unknown	1	3E-11	0,0014	1	1	1	0,0002	1E-11	1E-04	1	1	1	1	1	1	1	3E-05	0,404	0,0223	0,1561	1	1	5E-07	3E-05
247	160	590,08	Glucose	Monosaccharides	0,0048	1	1	0,1024	0,0101	1	1	1	1	1	1	0,1539	1	1	0,1041	1	1	1	1	1	1	1	1	1
248	265	591,55	_	Unknown	2E-10	3E-05	0,0002	0,0082	1E-10	5E-06	1	2E-05	0,0153	1	1	0,0058	1	0,0026	5E-10	0,7326	5E-07	0,0047	1	1	1	1	1	1
249	273	592,46	Citrate	Carboxylic acids	0,0176	5E-10	0,0014	1	0,2769	0,0206	1E-05	3E-10	0,0281	1	1	1	1	1	0,004	1	2E-06	0,0002	1	0,0544	1	0,0003	0,0044	1
250	197	594,67	_	Unknown	0,0112	0,4863	1	1	0,0102	0,437	1	0,4764	1	1	1	1	1	1	1	1	0,8939	1	1	1	1	1	1	1
251	123	595,49	_	Unknown	0,0003	1	1	0,2991	0,5393	0,0002	1	1	1	1	1	1	1	1	1	1	1	1	1	1	1	1	1	1
252	273	597,44	Isocitrate	Carboxylic acids	1E-20	0,004	0,0025	1	0	0	0,0443	1	0,0134	1	1	1	8E-11	0	9E-10	1	1	1	1	1	1	0,0039	1	0,0003
253	156	598,09	Glutamine	Amino acids	3E-09	2E-09	0,0005	0,2575	3E-09	1E-05	2E-05	2E-09	0,2934	1	1	1	1	0,0241	3E-08	1	1	1	1	1	1	0,0009	4E-09	0,1278
254	96	598,75	_	Unknown	3E-07	1E-08	0,0044	1	4E-07	6E-05	0,0095	7E-09	0,0014	1	1	0,3562	1	1	1E-06	1	1	1	1	0,0012	0,7087	0,3573	9E-07	0,015
255	205	598,7	Glucose	Monosaccharides	0,0001	7E-07	0,5489	1	0,0038	0,0002	0,0066	5E-07	0,2959	1	1	1	1	0,2738	0,0804	1	0,9292	1	1	0,9433	1	0,078	0,0001	1

Mass Spectral Feature			Metabolite Information		2-Way ANOVA (Variance Analysis)			TukeyHSD - Tukey Honest Significant Differences (differences between the means)																	
					p.value (adjusted using BY)			p.value (adjusted using Benjamini, Hochberg, and Yekutieli method (BY))																	
								Genotype (G)			Timepoint (T)			(Mar vs. Mut) × T			(Mar vs. Syn) × T			Mar × T			Mut × T			Syn × T		
#	M/Z	Retention [s]	Metabolite	Class	Genotype (G)	Timepoint / Treatment (T)	G × T	Mut-Mar	Syn-Mar	Syn-Mut	T0-T1	T0-T3	T1-T3	Mar:0-Mut:0	Mar:1-Mut:1	Mar:3-Mut:3	Mar:0-Syn:0	Mar:1-Syn:1	Mar:3-Syn:3	Mar:0-Mar:1	Mar:0-Mar:3	Mar:1-Mar:3	Mut:0-Mut:1	Mut:0-Mut:3	Mut:1-Mut:3	Syn:0-Syn:1	Syn:0-Syn:3	Syn:1-Syn:3
					0,05	0,05	0,05	0,05	0,05	0,05	0,05	0,05	0,05	0,05	0,05	0,05	0,05	0,05	0,05	0,05	0,05	0,05	0,05	0,05	0,05	0,05	0,05	0,05
261	95	605,68	_	Unknown	0,1523	1	1	1	0,1434	1	1	1	1	1	1	1	1	1	1	1	1	1	1	1	1	1	1	1
262	157	605,82	Citrulline	Amino acids	2E-13	3E-09	4E-07	1	1E-11	8E-12	0,0003	2E-09	0,0057	1	1	1	1	9E-05	1E-11	1	1	1	1	1	1	0,0002	3E-11	0,0004
263	119	609,44	_	Unknown	0,1326	0,6999	1	1	1	0,1162	1	1	0,9951	1	1	1	1	1	1	1	1	1	1	1	1	1	1	1
264	85	613	_	Unknown	1	1	0,8339	1	1	1	1	1	1	1	1	1	1	1	1	1	1	1	1	1	1	1	1	1
265	217	613,69	_	Unknown	8E-10	0,0276	0,0976	NA	NA	9E-10	NA	NA	0,049	NA	NA	NA	NA	NA	NA	NA	NA	NA	NA	NA	1	NA	NA	0,0837
266	156	615,12	_	Unknown	5E-23	3E-09	7E-16	1	0	0	4E-06	4E-09	0,997	1	1	1	0	2E-11	4E-05	1	1	1	1	0,5262	1	0	0	0,0004
267	205	615,28	_	Unknown	4E-06	1	0,0032	1	1E-05	7E-05	1	1	1	1	1	0,0473	1	1	0,0014	1	0,3757	0,4699	1	0,6638	1	1	1	1
268	117	615,99	Tetradecanoate	Fatty acids	2E-05	0,0091	1	0,0092	1	3E-05	1	0,0078	0,4444	1	0,9459	1	1	1	1	1	1	1	1	1	1	1	1	1
269	197	616,74	_	Unknown	0,0061	1	1	1	0,0071	0,1177	1	1	1	1	1	1	1	1	1	1	1	1	1	1	1	1	1	1
270	217	617,12	_	Unknown	9E-13	2E-24	0,0003	0,0003	8E-07	0	0	0	5E-05	1	0,0228	0,6001	1	1	3E-06	0	0	0,0039	0	0	0,3319	9E-11	0	1
271	95	618,86	_	Unknown	1	1	1	1	1	1	1	1	1	1	1	1	1	1	1	1	1	1	1	1	1	1	1	1
272	197	619,14	_	Unknown	0,002	0,4295	1	1	0,0023	0,0622	1	0,4069	1	1	1	1	0,7266	1	1	1	1	1	1	1	1	1	1	1
273	197	622,93	_	Unknown	0,0063	0,7881	1	1	0,0064	0,1805	1	0,8532	1	1	1	1	1	1	1	1	1	1	1	1	1	1	1	1
274	85	624,45	Nonadecane	Miscellaneous	1E-10	1	1	0,0028	1E-10	3E-05	1	1	1	1	0,3159	1	0,0009	6E-05	0,001	1	1	1	1	1	1	1	1	1
275	294	624,56	_	Unknown	3E-12	0,0773	1	0,0009	5E-07	7E-12	1	0,0625	1	1	0,6156	1	1	0,1853	0,0011	1	1	1	1	1	1	1	1	1
276	204	624,83	_	Unknown	6E-10	5E-05	1	0,0143	4E-05	4E-10	0,2118	3E-05	0,3063	1	1	1	1	0,3446	0,0143	1	0,0639	1	1	0,0499	1	1	1	1
277	103	626,03	_	Unknown	6E-12	5E-12	0,0016	0,0016	1E-06	4E-12	1	2E-11	2E-09	1	1	0,0447	0,4542	1	3E-05	1	0,0001	0,0305	1	1	1	1	3E-08	4E-08
278	100	626,88	[Aspartate, N-carbamyl-]	Amino acids	9E-07	2E-07	0,0014	1	4E-06	3E-05	2E-06	4E-06	1	1	1	1	1	2E-05	0,028	1	1	1	1	1	1	3E-07	6E-05	1
279	95	627,01	_	Unknown	0,8951	1	1	1	0,9938	1	1	1	1	1	1	1	1	1	1	1	1	1	1	1	1	1	1	1
280	197	628,4	_	Unknown	0,0002	1	1	1	0,0007	0,0024	1	1	1	1	1	1	0,4691	1	1	1	1	1	1	1	1	1	1	1
281	143	628,46	_	Unknown	1E-07	1	1	1	8E-05	1E-07	1	1	1	1	1	1	1	0,3586	0,67	1	1	1	1	1	1	1	1	1
282	204	630,93	_	Unknown	0,0466	0,1927	1	0,1099	1	0,4689	1	0,2045	1	1	1	1	1	1	1	1	1	1	1	1	1	1	1	1
283	194	632,11	_	Unknown	0,0014	1	1	1	0,2617	0,001	1	1	1	1	1	1	1	1	1	1	1	1	1	1	1	1	1	1
284	100	632,26	_	Unknown	2E-05	0,0029	1	1	0,0003	5E-05	0,1756	0,0028	1	1	1	1	1	0,1733	0,5929	1	1	1	1	0,0938	1	1	1	1
285	156	632,62	[Glutamate, N-acetyl-]	Amino acids	0,0149	0,8884	1	1	0,6666	0,0123	1	1	1	1	1	1	1	1	1	1	1	1	1	1	1	1	1	1
286	103	632,8	_	Unknown	1	7E-08	0,5622	1	1	1	1E-07	0,0007	0,0927	1	1	1	1	1	1	0,495	1	1	0,8259	1	1	9E-05	0,0276	1
287	117	635,87	_	Unknown	1E-11	1	1	0,0021	0	2E-06	1	1	1	1	1	1	0,0017	6E-05	5E-06	1	1	1	1	1	1	1	1	1
288	174	637,58	_	Unknown	0,0233	1	1	1	0,0333	0,1393	1	1	1	1	1	1	1	1	1	1	1	1	1	1	1	1	1	1
289	102	639,07	_	Unknown	1E-08	7E-09	2E-06	1	2E-08	3E-05	0,3124	6E-08	1E-06	NA	1	1	1	0,4538	3E-08	1	1	1	NA	NA	1	1	1E-08	1E-07
290	133	639,84	_	Unknown	3E-05	1	1	0,189	0,1767	2E-05	1	1	1	1	1	1	1	1	1	1	1	1	1	1	1	1	1	1
291	117	640,11	_	Unknown	6E-05	1	1	0,0332	1	6E-05	1	1	1	1	1	1	1	1	1	1	1	1	1	1	1	1	1	1
292	128	643,12	Methionine sulfoxide	Amino acids	1	3E-12	0,0011	1	1	1	7E-06	0	0,0004	1	1	1	1	1	1	0,2726	7E-06	1	0,0102	0,0978	1	1	3E-08	3E-05
293	117	645,38	_	Unknown	8E-07	1	1	0,0031	0,5814	8E-07	1	1	1	1	1	1	1	1	1	1	1	1	1	1	1	1	1	1
294	299	646,86	Hexadecan-1-ol	Miscellaneous	1E-05	1	1	0,0019	1	2E-05	1	1	1	1	0,1461	1	1	1	1	1	1	1	1	1	1	1	1	1
295	174	647,91	_	Unknown	5E-09	0,0007	0,0092	1	3E-08	4E-07	1	0,0045	0,0071	1	1	1	0,4327	1	5E-07	1	1	1	1	1	1	1	0,0015	0,0004
296	152	651,84	_	Unknown	6E-19	1	1	1E-11	5E-13	2E-10	1	1	1	8E-05	2E-06	2E-05	2E-11	2E-11	4E-11	1	1	1	1	1	1	1	1	1
297	89	652,1	_	Unknown	2E-12	3E-08	0,0147	0,0002	1E-06	6E-12	1	1E-07	8E-06	1	1	0,3725	1	0,0551	1E-05	1	1	1	1	1	1	1	3E-07	0,0005
298	171	652,17	_	Unknown	0,0393	0,0008	0,0019	0,0867	0,6714	1	0,0588	0,0008	1	1	1	0,0006	1	1	1	1	0,0004	1	1	1	1	1	1	1
299	103	653,89	_	Unknown	0,0466	0,9603	0,0278	1	0,072	0,2323	1	1	1	1	1	0,8167	1	1	0,3595	1	1	1	1	1	1	1	1	1
300	156	654,47	_	Unknown	1E-05	8E-05	0,1074	1	9E-05	0,0001	1	0,0001	0,008	1	1	1	1	1	7E-05	1	0,0013	0,0552	1	0,6437	1	1	1	1
301	117	657,26	Pentadecanoate	Fatty acids	0,0019	1	1	0,0813	1	0,0028	1	1	1	1	1	1	1	1	1	1	1	1	1	1	1	1	1	1
302	218	658,17	Tyrosine	Amino acids	1E-14	6E-19	4E-10	0,0001	2E-10	5E-12	3E-11	7E-12	6E-11	1	1	6E-10	1	6E-07	6E-05	2E-06	3E-09	1	1E-06	2E-11	4E-11	1	0,0021	1
303	87	660,53	_	Unknown	1E-05	0,0389	0,0029	0,5559	8E-06	0,0098	0,1217	0,1286	1	1	1	0,004	1	0,0293	0,0012	0,523	0,0021	1	1	1	1	1	1	1
304	128	662,22	_	Unknown	1E-11	5E-11	2E-11	1	2E-10	4E-10	8E-11	8E-05	5E-05	1	1	1	1	2E-11	0,0091	1	1	1	1	1	1	6E-11	0,0006	2E-10
305	103	663,47	_	Unknown	2E-27	6E-07	1	0,7071	0	0	0,0003	8E-07	1	1	1	1	0	0	0	1	0,0507	1	1	0,278	1	0,0739	0,0774	1
306	128	666,82	_	Unknown	1	0,0037	0,4918	1	1	1	0,531	0,0037	1	1	1	1	NA	1	1	1	0,0181	1	1	1	1	NA	NA	1
307	179	669,03	_	Unknown	9E-05	9E-05	0,1714	0,0839	0,7827	8E-05	0,1033	5E-05	0,4461	1	1	0,0487	1	1	1	1	1	1	1	0,0003	0,4734	1	1	1

Mass Spectral Feature			Metabolite Information		2-Way ANOVA (Variance Analysis)			TukeyHSD - Tukey Honest Significant Differences (differences between the means)																	
					p.value (adjusted using BY)			p.value (adjusted using Benjamini, Hochberg, and Yekutieli method (BY))																	
								Genotype (G)			Timepoint (T)			(Mar vs. Mut) × T			(Mar vs. Syn) × T			Mar × T			Mut × T			Syn × T		
#	M/Z	Retention [s]	Metabolite	Class	Genotype (G)	Timepoint / Treatment (T)	G × T	Mut-Mar	Syn-Mar	Syn-Mut	T0-T1	T0-T3	T1-T3	Mar:0-Mut:0	Mar:1-Mut:1	Mar:3-Mut:3	Mar:0-Syn:0	Mar:1-Syn:1	Mar:3-Syn:3	Mar:0-Mar:1	Mar:0-Mar:3	Mar:1-Mar:3	Mut:0-Mut:1	Mut:0-Mut:3	Mut:1-Mut:3	Syn:0-Syn:1	Syn:0-Syn:3	Syn:1-Syn:3
					0,05	0,05	0,05	0,05	0,05	0,05	0,05	0,05	0,05	0,05	0,05	0,05	0,05	0,05	0,05	0,05	0,05	0,05	0,05	0,05	0,05	0,05	0,05	0,05
313	142	680,07	_	Unknown	1E-06	0,0011	0,0618	1	3E-06	6E-05	0,1539	0,005	0,1237	NA	1	1	NA	0,2327	2E-05	NA	NA	1	NA	NA	1	1	0,0102	0,0429
314	117	680,12	_	Unknown	4E-05	1	1	0,0668	0,5409	4E-05	1	1	1	1	1	1	1	1	1	1	1	1	1	1	1	1	1	1
315	97	680,43	_	Unknown	0,0005	1	1	1	0,075	0,0005	1	1	1	1	1	1	1	1	1	1	1	1	1	1	1	1	1	1
316	104	682,33	_	Unknown	3E-08	1	1	0,0005	0,0264	3E-08	1	1	1	1	1	1	1	1	1	1	1	1	1	1	1	1	1	1
317	142	682,58	_	Unknown	2E-11	2E-06	5E-05	1	3E-10	6E-10	0,0733	1E-06	0,0282	1	1	1	1	0,0135	9E-10	1	1	1	1	1	1	0,0712	2E-08	0,0036
318	101	682,72	_	Unknown	0,0008	1	0,1566	1	0,0006	0,1759	1	1	1	1	1	0,2782	1	0,1733	0,8617	1	0,9342	1	1	1	1	1	1	1
319	99	684,89	_	Unknown	1E-05	0,3015	0,049	0,6263	8E-06	0,0131	0,5023	1	1	1	1	0,119	1	0,0096	0,0023	0,7069	0,0669	1	1	1	1	1	1	1
320	156	685,24	_	Unknown	3E-14	1E-18	6E-13	1	3E-12	8E-13	4E-07	5E-13	2E-12	1	1	0,0157	1	8E-06	1E-12	9E-06	2E-12	8E-12	0,2002	3E-12	1E-11	1	1	1
321	128	688,45	_	Unknown	1E-09	7E-13	2E-07	0,2354	1E-09	7E-06	1	8E-12	1E-09	1	1	1	1	0,8327	4E-11	1	3E-10	2E-07	1	2E-08	1E-05	1	1	1
322	115	688,58	_	Unknown	3E-07	0,0007	0,2683	0,3182	0,0003	3E-07	1	0,0012	0,015	1	1	1	1	1	0,003	1	0,0828	1	1	0,1129	0,6681	1	1	1
323	160	689,21	_	Unknown	0,0048	1	0,8835	1	0,0203	0,0155	NA	NA	1	NA	1	1	NA	0,0551	1	NA	NA	1	NA	NA	1	NA	NA	1
324	103	690,4	_	Unknown	0,0005	1	1	0,3083	0,4808	0,0004	1	1	1	1	1	1	1	1	1	1	1	1	1	1	1	1	1	1
325	167	690,71	_	Unknown	0,0003	1	0,0099	0,381	0,3661	0,0002	1	1	1	1	1	0,0087	1	1	1	1	1	1	1	0,4483	0,2324	1	1	1
326	110	692,26	_	Unknown	1E-13	1E-05	3E-07	1	7E-12	2E-11	2E-05	0,3221	0,016	1	1E-05	1	0,4542	4E-11	6E-05	1E-08	1	3E-06	1	1	1	1	1	1
327	149	694,2	_	Unknown	0,0037	1	1	1	0,0372	0,0071	1	1	1	1	1	1	1	1	1	1	1	1	1	1	1	1	1	1
328	174	694,54	Ornithine, N-acetyl-	Amino acids	1E-12	7E-06	2E-06	1	3E-11	9E-12	0,5879	8E-06	0,0137	1	1	1	1	1	1E-10	1	1	1	1	1	1	0,4254	6E-07	9E-06
329	311	695,68	Hexadecenoate, 9Z-	Fatty acids	0,4881	1	1	1	0,4709	1	1	1	1	1	1	1	1	1	1	1	1	1	1	1	1	1	1	1
330	117	696,78	Hexadecanoate	Fatty acids	1	1	1	1	1	1	1	1	1	1	1	1	1	1	1	1	1	1	1	1	1	1	1	1
331	169	698,48	_	Unknown	2E-07	0,1	0,0278	1	0,0001	3E-07	0,3848	0,2164	1	1	1	1	1	0,0004	1	1	1	1	1	1	1	0,0312	1	1
332	94	699,56	_	Unknown	4E-11	1	1	3E-06	7E-11	1E-05	1	1	1	1	0,022	0,1184	0,002	1E-05	4E-05	1	1	1	1	1	1	1	1	1
333	102	700,03	_	Unknown	0,0081	1	1	1	0,1004	0,0109	1	1	1	1	1	1	1	1	1	1	1	1	1	1	1	1	1	1
334	128	701,88	_	Unknown	2E-09	5E-14	2E-11	0,0002	0,003	1E-09	1	6E-12	3E-11	1	1	3E-08	1	1	1E-05	1	7E-06	0,0006	1	2E-11	4E-11	1	1	1
335	138	703,93	_	Unknown	1	0,7202	0,1622	1	1	1	1	1	0,9832	1	1	1	1	1	1	1	0,8124	0,783	1	1	1	1	1	1
336	299	704,5	Ribose 5-P	Monosaccharides	4E-16	0,0002	0,4265	3E-06	1E-10	4E-12	0,0046	0,0007	1	0,0018	0,0352	1	0,0976	0,0004	5E-07	0,8907	0,0026	1	1	1	1	1	1	1
337	174	708,59	_	Unknown	0,0432	2E-12	1	1	0,0833	0,1584	8E-08	0	0,0091	1	1	1	1	0,078	1	0,0009	7E-05	1	0,0084	2E-06	1	1	8E-05	0,3088
338	128	710,1	_	Unknown	2E-07	1E-12	9E-07	1	3E-06	6E-07	0,8024	8E-12	1E-09	1	1	0,1475	1	0,2375	2E-05	1	4E-06	0,0506	1	2E-10	1E-09	1	1	1
339	156	712,18	_	Unknown	1E-20	2E-24	1E-17	0,0005	6E-12	5E-12	2E-08	8E-12	3E-11	1	1	5E-06	1	4E-08	1E-11	3E-07	3E-11	6E-11	0,0006	3E-11	4E-11	1	1	1
340	141	718,8	_	Unknown	0,0001	1	1	0,0005	NA	NA	1	1	1	0,4942	1	1	NA	NA	NA	1	1	1	1	1	1	NA	NA	NA
341	117	718,9	_	Unknown	0,0002	1	1	0,3864	0,2899	0,0001	1	1	1	1	1	1	1	1	1	1	1	1	1	1	1	1	1	1
342	116	723,79	_	Unknown	7E-06	1	0,2441	1	3E-05	9E-05	1	1	1	1	1	1	1	0,0018	1	1	1	1	1	1	1	1	1	1
343	156	724,08	_	Unknown	0,0008	7E-05	0,0011	1	0,0014	0,0138	0,0518	5E-05	1	1	1	1	1	1	1E-05	1	1	1	1	1	1	0,4395	2E-05	0,5174
344	97	724,33	_	Unknown	1E-14	1E-04	1	1	5E-12	4E-12	0,0403	7E-05	1	1	1	1	4E-06	2E-05	1E-05	1	0,3691	1	1	0,1107	1	1	1	1
345	103	726,83	_	Unknown	6E-05	0,1379	0,1862	0,0425	0,7659	6E-05	1	1	0,1864	1	0,2375	1	1	1	1	1	1	1	1	1	0,3298	1	1	1
346	143	733,23	Phytol	Prenol lipids	0,4227	0,0593	1	1	1	0,381	1	0,05	1	1	1	1	1	1	1	1	1	1	1	1	1	1	1	1
347	204	733,39	_	Unknown	2E-14	5E-09	3E-11	1	5E-12	4E-12	1	6E-09	1E-05	1	1	1	1	0,0802	9E-12	1	1	1	1	1	1	0,6792	1E-11	5E-09
348	197	735,84	_	Unknown	1E-19	3E-14	3E-09	1	5E-12	4E-12	1E-11	2E-09	0,0007	0,2798	0,001	1	0,065	2E-11	2E-10	3E-11	6E-07	1E-05	0,0009	0,0008	1	1	1	1
349	156	735,79	_	Unknown	1E-09	4E-08	0,0011	1	6E-08	1E-08	0,0086	2E-08	0,0124	1	1	1	1	0,0034	2E-06	1	1	1	1	1	1	0,0037	2E-08	0,2301
350	103	737,25	_	Unknown	6E-26	5E-06	1E-08	1	6E-12	5E-12	0,0234	3E-06	0,2581	1	0,7028	1	3E-11	2E-11	1E-11	1	1	0,06	1	1	1	1	1E-09	2E-06
351	149	738,57	_	Unknown	4E-09	0,8414	1	0,089	2E-05	5E-09	1	1	1	1	1	1	1	0,0478	0,2563	1	1	1	1	1	1	1	1	1
352	267	739,25	Urocanate	Miscellaneous	0,0005	1	0,0051	1	0,0023	0,0037	1	1	1	1	1	0,1797	1	0,0102	1	1	1	0,4699	1	1	0,8193	1	1	1
353	174	741,43	_	Unknown	8E-11	0,0008	0,0044	1	6E-10	1E-08	0,0084	0,0028	1	1	1	1	1E-07	0,0052	0,5049	1	1	1	1	1	1	0,0029	8E-05	1
354	217	746,87	_	Unknown	9E-17	0,0104	1	1	0	0	0,0169	0,21	1	1	1	1	9E-06	1E-09	4E-07	1	1	1	1	1	1	0,256	1	1
355	183	748,32	_	Unknown	1E-17	0,8028	1	6E-10	4E-08	0	1	0,7539	1	0,0002	0,046	0,0007	0,7954	0,0023	0,0019	1	1	1	1	1	1	1	1	1
356	124	751,17	_	Unknown	4E-09	1	1	0,0545	9E-05	3E-09	1	1	1	1	1	1	1	1	0,3929	1	1	1	1	1	1	1	1	1
357	204	751,57	_	Unknown	7E-08	1	0,0769	0,0787	0,0011	5E-08	1	1	1	1	0,4189	1	1	1	0,0048	1	1	0,3391	1	1	1	1	1	1
358	100	757,33	_	Unknown	8E-06	0,0056	0,082	1	6E-05	8E-05	0,0566	0,0078	1	1	1	1	1	0,0351	0,0031	1	1	1	1	1	1	0,0305	0,0033	1
359	124	760,83	_	Unknown	8E-14	0,1446	1	0,0009	6E-09	0	1	0,1189	1	1	1	0,213	0,0219	0,0004	0,0208	1	1	1	1	1	1	1	1	1

Mass Spectral Feature			Metabolite Information		2-Way ANOVA (Variance Analysis)			TukeyHSD - Tukey Honest Significant Differences (differences between the means)																	
					p.value (adjusted using BY)			p.value (adjusted using Benjamini, Hochberg, and Yekutieli method (BY))																	
								Genotype (G)			Timepoint (T)			(Mar vs. Mut) × T			(Mar vs. Syn) × T			Mar × T			Mut × T			Syn × T		
#	M/Z	Retention [s]	Metabolite	Class	Genotype (G)	Timepoint / Treatment (T)	G × T	Mut-Mar	Syn-Mar	Syn-Mut	T0-T1	T0-T3	T1-T3	Mar:0-Mut:0	Mar:1-Mut:1	Mar:3-Mut:3	Mar:0-Syn:0	Mar:1-Syn:1	Mar:3-Syn:3	Mar:0-Mar:1	Mar:0-Mar:3	Mar:1-Mar:3	Mut:0-Mut:1	Mut:0-Mut:3	Mut:1-Mut:3	Syn:0-Syn:1	Syn:0-Syn:3	Syn:1-Syn:3
					0,05	0,05	0,05	0,05	0,05	0,05	0,05	0,05	0,05	0,05	0,05	0,05	0,05	0,05	0,05	0,05	0,05	0,05	0,05	0,05	0,05	0,05	0,05	0,05
365	117	768	Octadecenoic acid, n-(Z)	Fatty acids	0,056	1	1	1	0,0482	1	1	1	1	1	1	1	1	1	1	1	1	1	1	1	1	1	1	1
366	217	768,41	Fructose 6-P	Monosaccharides	0,0056	2E-19	0,0922	1	0,1823	0,0061	2E-11	1E-10	6E-11	1	1	1	1	1	1	6E-11	0,0005	6E-05	7E-11	0,0002	9E-06	3E-09	0,0013	0,0041
367	204	769,51	_	Unknown	0,0014	0,0208	0,3164	1	0,0412	0,0018	1	0,0296	0,2633	1	1	1	1	1	1	1	1	1	1	0,0521	1	1	1	1
368	91	769,58	[Linolenate, gamma-]	Fatty acids	0,0059	1	0,5779	1	0,0105	0,0582	1	1	1	1	1	1	1	0,4021	1	1	1	1	1	1	1	1	1	1
369	339	770,61	_	Unknown	0,0006	1	1	1	0,0183	0,0008	1	1	1	1	1	1	1	1	1	1	1	1	1	1	1	1	1	1
370	117	770,93	Stearate	Fatty acids	2E-07	0,1092	1	1	3E-05	4E-07	0,5023	0,1976	1	1	1	1	1	0,0108	1	1	1	1	1	1	1	1	1	1
371	95	771,63	[Linolenate, alpha-]	Fatty acids	0,1536	1	1	1	0,2166	0,538	1	1	1	1	1	1	1	1	1	1	1	1	1	1	1	1	1	1
372	322	771,82	_	Unknown	5E-06	1	1	0,0135	8E-06	0,004	1	1	1	1	1	1	NA	0,0084	0,1041	1	1	1	1	1	1	NA	NA	1
373	160	773,09	Glucose 6-P; Galactose 6-P	Monosaccharides	9E-09	2E-19	0,0009	0,568	2E-05	1E-08	0	0	2E-07	1	1	1	1	0,0002	0,1282	0	5E-07	0,0125	0	2E-08	0,0017	9E-06	0,0109	1
374	102	775,03	_	Unknown	1E-09	2E-05	1	0,0066	0,0002	7E-10	0,0002	0,0002	1	1	1	0,68	1	0,0383	1	0,495	1	1	0,0793	0,0674	1	1	1	1
375	156	776,97	[Glutamylleucine, gamma-]	Amino acids	1E-10	1E-15	6E-11	0,3241	3E-07	2E-10	1	0	0	1	1	0,0016	1	1	5E-10	1	2E-09	1E-07	1	0	0	1	1	1
376	299	779,67	Glucose 6-P; Galactose 6-P	Monosaccharides	1E-09	5E-19	0,0001	0,66	2E-06	2E-09	0	0	1E-07	1	1	1	1	5E-06	1	0	1E-05	0,0002	0	9E-09	0,007	0,0003	0,01	1
377	146	785,24	_	Unknown	0,8268	1	1	1	1	0,7831	1	1	1	1	1	1	1	1	1	1	1	1	1	1	1	1	1	1
378	156	785,38	_	Unknown	2E-09	4E-13	5E-07	1	8E-09	2E-07	0,6794	0	1E-09	1	1	1	1	0,1794	1E-09	1	4E-09	6E-05	1	2E-09	5E-08	1	1	1
379	318	789,69	_	Unknown	2E-05	1	1	1	0,0042	2E-05	1	1	1	1	1	1	1	1	1	1	1	1	1	1	1	1	1	1
380	202	790,53	Tryptophan	Amino acids	0,0004	2E-08	0,064	0,3352	0,508	0,0003	0,0384	1E-08	0,001	1	1	0,0258	1	1	1	1	0,3563	1	1	8E-06	0,0014	1	0,2804	1
381	103	790,9	_	Unknown	3E-05	0,0196	0,0011	1	4E-05	0,0087	0,0878	0,0596	1	1	1	0,0042	1	0,0755	0,0013	0,2644	0,0004	1	1	1	1	1	1	1
382	116	790,98	_	Unknown	0,0014	0,0779	1	1	0,0025	0,0127	0,1113	0,8793	1	1	1	1	1	0,3446	1	0,6807	1	1	1	1	1	1	1	1
383	169	794,33	_	Unknown	5E-07	1	1	3E-05	0,2922	2E-05	1	1	1	1	0,1608	0,1658	NA	1	1	1	1	1	1	1	1	NA	NA	1
384	146	795,92	_	Unknown	5E-19	0,3871	0,5703	2E-11	NA	NA	0,8411	0,9258	1	9E-11	4E-11	2E-10	NA	NA	NA	1	1	1	1	1	1	NA	NA	NA
385	299	802,01	_	Unknown	1	7E-09	1	1	1	1	7E-08	3E-07	1	1	1	1	1	1	1	0,0043	0,2579	1	0,3922	0,0012	1	0,0194	0,5499	1
386	146	802,92	_	Unknown	5E-23	1	1	2E-11	3E-12	3E-12	1	1	1	9E-11	4E-11	6E-10	NA	5E-11	1E-11	1	1	1	1	1	1	NA	NA	1
387	146	808,86	_	Unknown	4E-05	0,9433	1	0,0425	0,0294	6E-05	1	1	1	1	1	1	1	1	1	1	1	1	1	1	1	1	1	1
388	174	809,86	_	Unknown	3E-09	3E-05	1E-06	1	4E-09	1E-07	1	0,0008	0,0004	1	1	1	1	1	1E-09	1	1	1	1	1	1	1	3E-07	8E-05
389	156	809,95	_	Unknown	1E-05	7E-06	0,0134	1	0,0005	4E-05	1	1E-05	0,001	1	1	1	1	1	0,0002	1	0,0012	0,5993	1	0,0136	0,0419	1	1	1
390	95	811,66	_	Unknown	2E-06	1	1	0,0005	1	3E-06	1	1	1	1	1	0,036	1	1	1	1	1	1	1	1	1	1	1	1
391	103	813,36	_	Unknown	4E-14	1	0,0013	1	6E-12	0	1	1	1	0,0092	1	1	0,017	5E-06	1E-06	1	1	1	1	0,0086	1	1	1	1
392	146	813,78	_	Unknown	3E-06	1	0,5179	1E-05	NA	NA	1	1	1	0,0021	1	1	NA	NA	NA	1	1	1	1	1	1	NA	NA	NA
393	129	816,44	_	Unknown	3E-05	0,9263	1	0,0914	0,0175	3E-05	1	1	1	1	1	0,3106	1	1	1	1	1	1	1	1	1	1	1	1
394	103	818,63	_	Unknown	0,0031	1	1	0,0103	NA	NA	1	1	1	1	1	1	NA	NA	NA	1	1	1	1	1	1	NA	NA	NA
395	146	819,86	_	Unknown	4E-14	1	1	1E-10	1E-06	2E-12	1	1	1	3E-06	0,0002	0,0009	0,0286	0,0579	0,0826	1	1	1	1	1	1	1	1	1
396	117	822,79	_	Unknown	0,1154	1	0,2014	1	0,1089	1	1	1	1	1	1	1	1	1	0,135	1	0,5025	1	1	1	1	1	1	1
397	85	823,3	_	Unknown	0,0017	1	0,118	0,0612	1	0,0029	1	1	1	0,8977	0,9724	1	1	1	1	1	1	1	1	1	1	1	1	1
398	146	823,71	_	Unknown	1E-07	1	0,0274	7E-07	NA	NA	1	1	1	0,0001	0,046	1	NA	NA	NA	1	1	1	1	0,1203	1	NA	NA	NA
399	204	826,87	_	Unknown	3E-23	1	1	2E-09	5E-12	4E-12	1	1	1	0,0004	0,0085	0,0061	2E-10	1E-10	5E-10	1	1	1	1	1	1	1	1	1
400	146	828,55	_	Unknown	2E-12	1	0,4237	2E-06	7E-08	4E-12	1	1	1	0,0003	0,372	1	0,0714	0,0072	0,002	1	1	1	1	1	1	1	1	1
401	189	831,18	_	Unknown	0,0002	1	0,0078	1	0,0008	0,0018	1	1	1	1	1	0,1185	1	1	0,0015	1	0,1956	0,9417	1	1	1	1	1	1
402	361	840,54	Sucrose	Oligosaccharides	3E-28	4E-22	9E-17	2E-11	5E-12	4E-12	2E-06	6E-12	3E-11	2E-10	5E-11	1E-10	1	4E-05	9E-12	0,0124	2E-11	5E-11	2E-06	2E-11	4E-11	1	1	1
403	387	841,55	_	Unknown	0,0008	6E-20	0,145	1	0,0022	0,0082	0	3E-08	0	1	1	1	1	0,0351	0,6837	2E-10	0,24	5E-06	1E-09	0,4036	8E-05	0	3E-05	1E-07
404	160	843,34	_	Unknown	2E-13	3E-17	4E-12	1	1E-11	1E-11	2E-11	2E-05	3E-11	1	1	1	1	2E-11	0,253	0,1503	1	1	0,002	1	1	6E-11	0,0035	5E-11
405	131	848,49	_	Unknown	0,1069	1	1	1	1	0,0925	1	1	1	1	1	1	1	1	1	1	1	1	1	1	1	1	1	1
406	202	848,65	_	Unknown	3E-10	0,0135	0,0006	1	8E-09	4E-09	0,0365	0,1124	1	1	1	0,0447	1	0,0022	5E-06	0,292	0,0004	1	1	1	0,7234	1	1	1
407	247	849,9	_	Unknown	1E-10	1	1	8E-10	NA	NA	1	1	1	0,0003	0,0006	0,0003	NA	NA	NA	1	1	1	1	1	1	NA	NA	NA
408	132	851,69	_	Unknown	7E-08	0,3551	0,0819	1	9E-08	4E-05	0,5023	1	1	1	1	0,3228	1	0,0011	0,0003	0,7992	0,148	1	1	1	1	1	1	1
409	100	855,21	_	Unknown	0,0095	0,0271	1	0,0839	0,0339	1	1	0,02	1	1	1	1	1	1	1	1	1	1	1	1	1	1	1	1
410	99	855,23	_	Unknown	1E-08	0,0004	0,0008	1	9E-08	3E-07	0,0014	0,0082	1	1	1	0,0652	1	0,0006	0,0002	0,0405	0,0004	1	1	1	0,2447	1	1	1
411	173	857,15	_	Unknown	0,0003	0,0042	0,0045	0,0813	0,0003	1	0,0864	0,0054	1	1	1	0,003	1	0,2088	0,0007	0,2207	0,0001	1	1	1	1	1	1	1

Mass Spectral Feature			Metabolite Information		2-Way ANOVA (Variance Analysis)			TukeyHSD - Tukey Honest Significant Differences (differences between the means)																	
					p.value (adjusted using BY)			p.value (adjusted using Benjamini, Hochberg, and Yekutieli method (BY))																	
								Genotype (G)			Timepoint (T)			(Mar vs. Mut) × T			(Mar vs. Syn) × T			Mar × T			Mut × T			Syn × T		
#	M/Z	Retention [s]	Metabolite	Class	Genotype (G)	Timepoint / Treatment (T)	G × T	Mut-Mar	Syn-Mar	Syn-Mut	T0-T1	T0-T3	T1-T3	Mar:0-Mut:0	Mar:1-Mut:1	Mar:3-Mut:3	Mar:0-Syn:0	Mar:1-Syn:1	Mar:3-Syn:3	Mar:0-Mar:1	Mar:0-Mar:3	Mar:1-Mar:3	Mut:0-Mut:1	Mut:0-Mut:3	Mut:1-Mut:3	Syn:0-Syn:1	Syn:0-Syn:3	Syn:1-Syn:3
					0,05	0,05	0,05	0,05	0,05	0,05	0,05	0,05	0,05	0,05	0,05	0,05	0,05	0,05	0,05	0,05	0,05	0,05	0,05	0,05	0,05	0,05	0,05	0,05
417	129	870,38	_	Unknown	0,6576	0,9412	1	1	1	0,6191	1	1	1	1	1	1	1	1	1	1	1	1	1	1	1	1	1	1
418	99	872,76	_	Unknown	3E-18	1	1	2E-11	4E-12	5E-07	1	1	1	1E-04	4E-07	5E-08	1E-09	6E-09	1E-11	1	1	1	1	1	1	1	1	1
419	115	873,13	_	Unknown	7E-19	0,0281	0,0025	3E-10	0	2E-10	0,0588	0,2234	1	1	0,0013	5E-08	2E-07	0	0	0,0411	0,0016	1	1	1	1	1	1	1
420	202	873,26	_	Unknown	5E-10	0,0104	0,0002	1	5E-09	2E-08	0,0237	0,1196	1	1	1	0,0059	1	0,001	4E-06	0,213	0,0003	1	1	1	0,2562	1	1	1
421	191	875,92	Trehalose, alpha,alpha-	Oligosaccharides	5E-06	0,001	0,0085	7E-05	1	0,0004	1	0,0041	0,0092	1	1	9E-05	1	1	1	1	1	1	1	0,0008	0,0029	1	1	1
422	173	877,28	_	Unknown	0,0002	0,0104	0,0065	0,0103	0,0007	1	0,174	0,0122	1	1	1	0,0019	1	0,132	0,0027	0,2207	0,0003	1	1	1	1	1	1	1
423	129	881	_	Unknown	1	1	1	1	1	1	1	1	1	1	1	1	1	1	1	1	1	1	1	1	1	1	1	1
424	109	887,04	_	Unknown	7E-07	0,0149	0,0005	1	1E-06	0,0002	0,0439	0,0966	1	1	1	0,0029	1	0,0344	7E-05	0,4745	0,0003	1	1	1	0,4734	1	1	1
425	133	887,38	_	Unknown	1E-05	0,0447	0,0305	1	0,0001	7E-05	0,0588	1	1	1	1	0,2947	1	0,9043	0,004	1	0,0587	1	1	1	1	1	1	1
426	239	887,67	_	Unknown	5E-07	0,0108	3E-05	1	6E-07	0,0003	0,0395	0,0616	1	1	1	9E-05	1	0,1071	1E-05	0,8431	4E-05	1	1	1	0,1104	1	1	1
427	99	890,57	_	Unknown	0,0002	0,2464	0,0005	0,881	0,0001	0,0558	0,7829	0,4405	1	1	1	0,001	1	1	0,0003	1	0,0014	1	1	1	0,7247	1	1	1
428	204	906,44	_	Unknown	1	1	1	1	1	1	1	1	1	1	1	1	1	1	1	1	1	1	1	1	1	1	1	1
429	103	915,42	_	Unknown	4E-19	1	1	1E-09	5E-13	4E-13	1	1	1	3E-05	0,0123	0,0023	4E-10	NA	4E-10	1	1	1	1	1	1	NA	1	NA
430	204	921,27	[Melibiose]	Oligosaccharides	6E-29	1	1	1	5E-12	4E-12	1	1	1	1	1	1	3E-11	2E-11	9E-12	1	1	1	1	1	1	1	1	1
431	99	923,86	_	Unknown	1E-12	1	0,8339	6E-11	2E-08	0,002	1	1	1	0,0019	2E-05	1E-06	NA	NA	2E-07	1	1	1	1	1	1	NA	NA	NA
432	171	925,94	_	Unknown	6E-17	1	1	1E-11	2E-09	1	1	1	1	3E-09	9E-10	3E-10	NA	2E-07	NA	1	1	1	1	1	1	NA	NA	NA
433	149	926,68	_	Unknown	0,0718	0,1638	0,0246	1	0,0636	1	0,2975	0,8611	1	1	1	0,1376	1	1	0,3756	1	0,5764	1	1	1	0,4645	1	1	1
434	204	927,27	_	Unknown	1E-21	1	1	1	6E-12	5E-12	1	1	1	1	1	1	6E-11	8E-11	1E-11	1	1	1	1	1	1	1	1	1
435	91	930,08	_	Unknown	0,3182	0,6623	0,3985	1	1	0,4736	1	1	1	1	0,8518	1	1	1	1	1	1	1	0,9867	1	0,8663	1	1	1
436	103	931,46	_	Unknown	0,2588	1	1	1	1	0,2372	1	1	1	1	1	1	1	1	1	1	1	1	1	1	1	1	1	1
437	103	935,28	_	Unknown	5E-06	1	1	1	1E-05	0,0002	1	1	1	1	1	1	0,9597	0,6393	0,1004	1	1	1	1	1	1	1	1	1
438	111	935,55	_	Unknown	2E-18	0,0926	0,4164	1	2E-12	2E-12	1	0,1026	1	1	1	1	7E-10	2E-10	6E-12	1	1	1	1	1	1	1	0,0581	1
439	129	942,09	_	Unknown	0,0003	1	1	1	0,0133	0,0004	1	1	1	1	1	1	1	1	1	1	1	1	1	1	1	1	1	1
440	103	942,07	_	Unknown	2E-11	1	1	0,0104	1E-06	1E-11	1	1	1	1	1	0,1797	1	0,0102	0,0747	1	1	1	1	1	1	1	1	1
441	111	945,63	_	Unknown	1E-06	0,0984	NA	1	3E-05	3E-05	1	0,1539	1	NA	NA	NA	NA	NA	NA	NA	NA	NA	NA	NA	NA	NA	NA	NA
442	101	956,67	_	Unknown	4E-12	1	1	5E-07	4E-08	9E-12	1	1	1	0,0048	0,02	0,1539	NA	0,0041	3E-05	1	1	1	1	1	1	NA	NA	1
443	146	956,78	_	Unknown	1E-11	1	1	1E-10	NA	NA	1	1	1	4E-05	3E-05	0,0002	NA	NA	NA	1	1	1	1	1	1	NA	NA	NA
444	146	964,5	_	Unknown	2E-11	1	1	2E-10	NA	NA	1	1	1	4E-05	4E-05	0,0008	NA	NA	NA	1	1	1	1	1	1	NA	NA	NA
445	103	964,88	_	Unknown	3E-14	1	1	1E-05	1E-07	0	1	1	1	0,0887	0,3564	1	0,319	0,0931	0,0014	1	1	1	1	1	1	1	1	1
446	204	969,81	_	Unknown	4E-26	1	1	1	0	0	1	1	1	1	1	1	0	0	0	1	1	1	1	1	1	1	1	1
447	103	969,82	_	Unknown	2E-13	1	1	1	0	1E-11	1	1	1	1	1	1	1E-05	1E-05	0,0004	1	1	1	1	1	1	1	1	1
448	141	973,16	_	Unknown	8E-06	0,0375	7E-05	1	7E-06	0,0051	0,0664	0,3878	1	1	1	0,0005	1	0,0169	0,0007	0,153	0,0005	1	1	1	0,0873	1	1	1
449	100	975,11	_	Unknown	0,0673	0,0902	0,0829	0,1766	NA	NA	1	0,0738	1	1	1	0,0585	NA	NA	NA	1	0,0342	1	1	1	1	NA	NA	NA
450	91	975,98	_	Unknown	0,3338	0,627	0,4115	1	1	0,5139	1	1	1	1	0,6588	1	1	1	1	1	1	1	1	1	0,8123	1	1	1
451	88	977,6	_	Unknown	2E-05	1	0,2831	9E-05	NA	NA	1	1	1	0,2234	0,0198	1	NA	NA	NA	1	1	1	1	1	1	NA	NA	NA
452	95	979,52	Squalene	Prenol lipids	1E-11	5E-06	0,6039	3E-06	2E-11	0,0011	0,3921	3E-06	0,0137	0,6158	1	0,1658	0,0379	1E-05	1E-07	1	0,0012	1	1	0,097	1	1	1	1
453	204	982,79	_	Unknown	8E-15	1	0,1686	0,0011	6E-10	0	1	1	1	0,295	0,0543	1	0,013	0,086	2E-06	1	1	0,8889	1	1	1	1	1	1
454	89	983,6	_	Unknown	1E-11	1	1	2E-07	0,0522	1E-11	1	1	1	0,9828	0,0292	0,0044	1	1	1	1	1	1	1	1	1	1	1	1
455	146	988,99	_	Unknown	2E-13	1	1	0,0007	1E-08	4E-12	1	1	1	1	0,3316	0,3186	0,0003	0,0288	0,082	1	1	1	1	1	1	1	1	1
456	236	994,66	Adenosine, 5-methylthio-	Nucleic acids	2E-12	4E-17	0,0017	0,002	3E-07	0	0,0003	0	0	1	1	0,1376	1	0,1476	1E-05	1	1E-09	1E-05	0,0441	0	5E-07	1	0,0009	0,0766
457	169	995,73	Uridine-5 P (; UDP; UTP)	Nucleic acids	0,3182	1	1	1	1	0,3703	1	1	1	1	1	1	1	1	1	1	1	1	1	1	1	1	1	1
458	204	998,62	_	Unknown	5E-14	0,7202	1	1	4E-12	0	1	1	1	1	1	1	1E-04	9E-06	2E-07	1	1	1	1	1	1	1	1	1
459	97	998,85	_	Unknown	1E-05	0,0002	0,0032	1	0,0004	7E-05	1	0,0012	0,0134	NA	1	1	NA	1	7E-06	NA	NA	1	1	1	1	1	0,0001	0,0009
460	103	1007,09	_	Unknown	2E-18	0,3871	0,4175	1	0	0	1	0,3567	1	1	1	1	1E-06	8E-09	2E-11	1	1	1	1	1	1	1	0,0723	1
461	204	1007,52	_	Unknown	7E-10	0,6116	1	1	2E-08	1E-08	1	0,5814	1	1	1	1	0,2669	0,0124	4E-05	1	1	1	1	1	1	1	0,7122	1
462	99	1022,66	_	Unknown	6E-09	4E-06	0,003	1	1E-07	7E-08	0,0015	4E-06	0,462	1	1	1	1	0,0003	6E-07	1	1	1	1	1	1	0,0034	8E-07	0,5559
463	156	1049,59	_	Unknown	0,0198	0,0926	1	0,0538	1	0,2976	1	0,6568	0,1654	1	1	1	1	1	1	1	1	1	1	1	1	1	1	1

Mass Spectral Feature			Metabolite Information		2-Way ANOVA (Variance Analysis)			TukeyHSD - Tukey Honest Significant Differences (differences between the means)																			
					p.value (adjusted using BY)			p.value (adjusted using Benjamini, Hochberg, and Yekutieli method (BY))																			
								Genotype (G)			Timepoint (T)			(Mar vs. Mut) × T			(Mar vs. Syn) × T			Mar × T			Mut × T			Syn × T		
#	M/Z	Retention [s]	Metabolite	Class	Genotype (G)	Timepoint / Treatment (T)	G × T	Mut-Mar	Syn-Mar	Syn-Mut	T0-T1	T0-T3	T1-T3	Mar:0-Mut:0	Mar:1-Mut:1	Mar:3-Mut:3	Mar:0-Syn:0	Mar:1-Syn:1	Mar:3-Syn:3	Mar:0-Mar:1	Mar:0-Mar:3	Mar:1-Mar:3	Mut:0-Mut:1	Mut:0-Mut:3	Mut:1-Mut:3	Syn:0-Syn:1	Syn:0-Syn:3	Syn:1-Syn:3
					0,05	0,05	0,05	0,05	0,05	0,05	0,05	0,05	0,05	0,05	0,05	0,05	0,05	0,05	0,05	0,05	0,05	0,05	0,05	0,05	0,05	0,05	0,05	0,05
469	174	1071,85	_	Unknown	NA	NA	NA	NA	NA	NA	NA	NA	NA	NA	NA	NA	NA	NA	NA	NA	NA	NA	NA	NA	NA	NA	NA	NA
470	204	1074,68	_	Unknown	0,0005	0,0389	0,0183	1	0,0215	0,0004	0,4518	0,0448	1	0,5693	1	1	1	1	0,048	1	0,0012	1	1	1	1	1	1	1
471	114	1074,76	_	Unknown	0,0172	0,11	0,0078	0,3043	0,0272	1	0,5849	0,1639	1	1	1	0,0039	1	1	0,0164	1	0,0015	1	1	1	1	1	1	1
472	117	1074,9	_	Unknown	0,6902	1	0,79	1	1	0,9368	1	1	1	1	1	1	1	1	1	1	0,6199	1	1	1	1	1	1	1
473	174	1081,69	_	Unknown	0,0009	1	NA	NA	0,0011	NA	1	1	1	NA	NA	NA	NA	NA	NA	NA	NA	NA	NA	NA	NA	NA	NA	NA	NA
474	204	1083,16	_	Unknown	5E-13	1	0,0767	2E-11	1	3E-09	1	1	1	0,0001	0,0003	2E-08	1	NA	1	1	1	1	1	0,4697	1	NA	1	NA
475	179	1086,71	_	Unknown	8E-06	1	1	0,0254	0,2712	6E-06	1	1	1	1	1	0,267	1	1	1	1	1	1	1	1	1	1	1	1
476	99	1089,53	_	Unknown	3E-12	0,0004	1E-04	2E-10	1	3E-10	0,0009	1	0,0279	0,7255	2E-09	0,1098	1	1	1	1	1	1	7E-06	1	0,0001	1	1	1
477	113	1093,22	_	Unknown	0,2163	1	0,2266	0,9268	0,4423	1	1	1	1	1	1	0,1658	1	1	0,6479	1	0,4049	1	1	1	1	1	1	1
478	113	1098,45	_	Unknown	0,0625	0,2162	0,0025	1	0,0541	1	1	0,1982	1	1	1	0,0045	1	1	0,0337	1	0,0021	0,7178	1	1	1	1	1	1
479	204	1118,68	_	Unknown	4E-05	1	0,5971	1	4E-05	0,0133	1	1	1	1	1	1	1	0,0034	1	1	1	1	1	1	1	1	1	1
480	204	1128,02	Isomaltotriose	Oligosaccharides	2E-08	1	0,0025	0,2513	1E-08	8E-05	1	1	1	1	0,0499	1	0,0016	4E-05	1	1	1	0,0077	1	1	1	1	1	1
481	297	1145,88	Phylloquinone	Prenol lipids	1	1	1	1	1	1	1	1	1	1	1	1	1	1	1	1	1	1	1	1	1	1	1	1
482	596	1150,42	_	Unknown	1	1	1	1	1	1	1	1	1	1	1	1	1	1	1	1	1	1	1	1	1	1	1	1
483	97	1152	_	Unknown	0,1147	1	1	1	1	0,1083	1	1	1	1	1	1	1	1	1	1	1	1	1	1	1	1	1	1
484	204	1163,23	_	Unknown	6E-10	1	0,0088	1	6E-09	2E-08	1	1	1	1	1	0,6075	0,0127	4E-06	1	1	1	0,0711	1	1	1	1	1	1
485	204	1165,79	_	Unknown	3E-09	1	0,0127	1	2E-08	9E-08	1	1	1	1	1	0,4657	0,0051	5E-05	1	1	1	0,1484	1	1	1	1	1	1
486	204	1171,85	_	Unknown	2E-07	1	0,0508	0,6863	2E-07	4E-05	1	1	1	1	1	1	0,0013	0,0011	1	1	1	0,9565	1	1	1	1	1	1
487	93	1173,55	_	Unknown	8E-07	1	0,3418	1	7E-07	0,0007	1	1	1	1	1	1	0,011	0,001	1	1	1	0,5478	1	1	1	1	1	1
488	204	1173,92	_	Unknown	0,0001	1	0,1857	1	0,0009	0,0007	1	1	1	1	1	1	0,8678	0,0213	1	1	1	0,404	1	1	1	1	1	1
489	204	1175,92	_	Unknown	3E-08	1	0,0153	0,9523	4E-08	4E-05	1	1	1	1	1	1	0,0029	6E-05	1	1	1	0,1328	1	1	1	1	1	1
490	91	1201,3	_	Unknown	0,6369	1	1	1	1	1	1	1	1	1	1	1	1	1	1	1	1	1	1	1	1	1	1	1
491	131	1207,92	_	Unknown	1	1	1	1	1	1	1	1	1	1	1	1	1	1	1	1	1	1	1	1	1	1	1	1
492	131	1218,77	_	Unknown	1E-20	1	1	2E-09	0	0	1	1	1	0,0049	0,0134	0,001	0	0	0	1	1	1	1	1	1	1	1	1
493	103	1218,93	_	Unknown	7E-05	1	1	1	0,0195	6E-05	1	1	1	1	1	1	1	1	1	1	1	1	1	1	1	1	1	1
494	95	1234,25	_	Unknown	0,014	0,7297	0,0767	1	0,0119	1	1	1	1	1	1	0,0591	1	1	0,0394	1	0,0588	1	1	1	1	1	1	1
495	129	1237,84	_	Unknown	0,0291	1	1	1	0,2456	0,0386	1	1	1	1	1	1	1	1	1	1	1	1	1	1	1	1	1	1
496	204	1266,5	_	Unknown	1	1	1	1	1	1	1	1	1	1	1	1	1	1	1	1	1	1	1	1	1	1	1	1
497	145	1282,44	_	Unknown	1	8E-06	1	1	1	1	1E-05	1	0,0071	1	1	1	1	1	1	1	1	1	0,1183	1	1	0,3416	1	1
498	129	1283,24	_	Unknown	0,2161	0,0452	1	1	0,4713	0,427	0,0934	1	0,5785	1	1	1	1	1	1	1	1	1	1	1	1	1	1	1
499	204	1283,7	_	Unknown	8E-06	1	0,1432	1	3E-05	0,0002	1	1	1	1	1	1	0,7954	0,0138	1	1	1	1	1	1	1	1	1	1
500	129	1289	_	Unknown	1	1	1	1	1	1	1	1	1	1	1	1	1	1	1	1	1	1	1	1	1	1	1	1
501	87	1308,95	_	Unknown	1	1	1	1	1	1	1	1	1	1	1	1	1	1	1	1	1	1	1	1	1	1	1	1

Materials

Chemicals

Chemical	Provider
Acetic acid	Carl Roth, Karlsruhe, Germany
Acetone	Carl Roth, Karlsruhe, Germany
Acetonitrile	Carl Roth, Karlsruhe, Germany
Ammonium sulphate	Carl Roth, Karlsruhe, Germany
APS	Carl Roth, Karlsruhe, Germany
BICINE	Carl Roth, Karlsruhe, Germany
Boric acid	VEB Laborchemie, Apolda, Germany
BSA	Carl Roth, Karlsruhe, Germany
Calcium chloride dihydrate	Serva, Heidelberg, Germany
Citric acid	Carl Roth, Karlsruhe, Germany
Cobalt(II+) dinitrate hexahydrate	Sigma-Aldrich, Munich, Germany
Copper sulphate pentahydrate	Sigma-Aldrich, Munich, Germany
Dipotassium hydrogen phosphate $\times 3H_2O$	Carl Roth, Karlsruhe, Germany
Disodium carbonate	Carl Roth, Karlsruhe, Germany
Disodium hydrogen phosphate	Carl Roth, Karlsruhe, Germany
DTT	Carl Roth, Karlsruhe, Germany
EDTA	Carl Roth, Karlsruhe, Germany
Ethanol	Carl Roth, Karlsruhe, Germany
Ferric ammonium citrate	Fluka, Buchs, Switzerland
Formaldehyde	Sigma-Aldrich, Munich, Germany
Glycerol	Carl Roth, Karlsruhe, Germany
Glycine	Carl Roth, Karlsruhe, Germany
HEPES	Carl Roth, Karlsruhe, Germany

Hydrogen chloride	Carl Roth, Karlsruhe, Germany
Hydrogen peroxide solution 30 %	Carl Roth, Karlsruhe, Germany
Iodoacetamide	ICN Biomedicals, Aurora, Ohio, USA
Iodoacetic acid	Applichem, Darmstadt, Germany
Isopropanol	Carl Roth, Karlsruhe, Germany
Magnesium Chloride	Carl Roth, Karlsruhe, Germany
Magnesium sulphate heptahydrate	Carl Roth, Karlsruhe, Germany
Manganese chloride tetrahydrate	ICN Biomedicals, Aurora, Ohio, USA
Methanol	Carl Roth, Karlsruhe, Germany
n-Propylgallate	Carl Roth, Karlsruhe, Germany
Phosphoric acid 85 %	Carl Roth, Karlsruhe, Germany
PMSF	Sigma-Aldrich, Munich, Germany
Potassium bicarbonate	Carl Roth, Karlsruhe, Germany
Potassium carbonate	Carl Roth, Karlsruhe, Germany
SDS	Carl Roth, Karlsruhe, Germany
Sodium chloride	Carl Roth, Karlsruhe, Germany
Sodium dihydrogen phosphate,	Carl Roth, Karlsruhe, Germany
Sodium hydroxide	Carl Roth, Karlsruhe, Germany
Sodium molybdate dihydrate	ICN Biomedicals, Aurora, Ohio, USA
Sodium nitrate	Carl Roth, Karlsruhe, Germany
TCA	Carl Roth, Karlsruhe, Germany
TEMED	Carl Roth, Karlsruhe, Germany
TFA	Sigma-Aldrich, Munich, Germany
Tricine	Carl Roth, Karlsruhe, Germany
TRIS	Carl Roth, Karlsruhe, Germany
Triton® X-100	Sigma-Aldrich, Munich, Germany
Tween® 20	Sigma-Aldrich, Munich, Germany
Urea	MP Biochemicals, Illkirch, France
Zinc sulphate heptahydrate	Merck, Darmstadt, Germany

Miscellaneous

Item	Provider
Agarose LE	Biozym Scientific, Oldendorf, Germany
Bacto™ Agar	Becton-Dickson, Sparks, MD, USA
PageRuler™ Prestained Protein Ladder	Fermentas, St. Leon-Rot, Germany
Rotiphorese® Gel 30	Carl Roth, Karlsruhe, Germany
Microcystin LR	Dr. K. Ishida, Jena
Microcystin standards	Enzo Life Sciences, Germany
Nodularin standard	DHI, Denmark
Lysozyme from chicken egg white	Serva, Heidelberg, Germany
Antibodies	
Anti-Microcystin-LR mAB MC10E7	Enzo® Life Sciences, Lörrach, Germany
Anti-RbcL form I, II pAB AS03 037	Agrisera AB, Vannas, Sweden
Sheep Anti-Mouse IgG-Peroxidase	GE Hethcare, Buckinghamshire UK
Goat Anti-Rabbit IgG-Peroxidase	Sigma-Aldrich, St. Louis, MO, USA
FITC-conjugated Goat Anti-Mouse IgG	Jackson-Dianova, Hamburg, Germany
Consumables	
Amicon®Ultra centrifugal filters	Millipore™ Cooperation, Cork, Ireland
Plastibrand® Cuvetts PS, 1.5-3 ml	Carl Roth, Karlsruhe, Germany
Rotiprotect® Nitril gloves	Carl Roth, Karlsruhe, Germany
Glass sample slides 76x26x1 mm	Carl Roth, Karlsruhe, Germany
Cover slides 40x25x0.13-0.16 mm	Carl Roth, Karlsruhe, Germany
Microtiter® Flat bottom 96 well micro plates, sterile	Greiner-bio one, Frickenhausen, Germany
PARAFilm "M" Distensible plastic sealing film	Pechiney Plastic Packaging, Chicago, Il, USA

Pipett tips, TipOne® 0.1-10, 1-200, 101-1250 μl natural tips	Starlab, Ahrensburg, Germany
Safe Lock Tubes Polypropylene reaction tubes, 500 μl	Eppendorf AG, Hamburg, Germany
Serological Pipettes 2 mL, 10 mL, 25 ml, sterile	Carl Roth, Karlsruhe, Germany
Syringe filter 4 mm, Acrodisc®, 0.45 μm nylon membrane	PALL Life Sciences, USA
Syringe filter Whatman®, 0.2 μm sterile	Whatman®, Maidstone, UK
Whatman® 3MM Filter Paper	Whatman® Paper, Maidstone, UK

Technical appliance

Item	**Provider**
PowerPack Basic/ HC	Bio-Rad, Hercules, CA, USA
Mini-PROTEAN® Tetra System	Bio-Rad, Hercules, CA, USA
Haereus Pico 21 Microcentrifuge	Thermo Fisher Scientific Inc. Waltham, MA, USA
Perfect Spin 24R Microcentrifuge	PeqLab Biotechnology GmbH, Germany
200R 21 Microcentrifuge	Hettich, Tuttlingen, Germany
Heraeus Multifuge 1S-R	Thermo Fisher Scientific Inc. Waltham, MA, USA
Sigma 6-16K	Sartorius AG, Göttingen, Germany
Vortex Genie 2™, G560E	Scientific Industries, Bohemia N.Y., USA
Cell mill	Retsch GmbH, Haan, Germany
IKAMAG®RET Magnetic stirrer	IKA GmbH & Co. Kg, Staufen, Germany
Variomag mono	Thermo Fisher Scientific Inc. Waltham, MA, USA
Mini Rotator PTR-25	Grant-bio, Shepreth, England
Stirring bars	Carl Roth, Karlsruhe, Germany
KM-2-SWIP-VARIO Shaker	Edmund Buhler, Germany

DOS-10L Shaker	NeoLab, Migge, Heidelberg, Germany
Sartorius Basic Balance	Sartorius AG, Göttingen, Germany
Kern 572-37 Balance	Kern & Sohn GmbH, Balingen, Germany
Thriller Thermo-shaker block	PeqLab Biotechnology GmbH, Germany
Heat block	PeqLab Biotechnology GmbH, Germany
PCE-PHD multi meter	PCE Deutschland GmbH, Meschede, Germany
FiveEasy™ FE 20 pH Meter	Mettler Toledo AG, Schwerzenbach, Switzerland
LE 409 pH Sond	Mettler Toledo AG, Schwerzenbach, Switzerland
Sonorex TK 52	Bandelin Electronic, Berlin, Germany
Sonopuls UW 3100	Bandelin Electronic, Berlin, Germany
Sonotrode MS 72	Bandelin Electronic, Berlin, Germany
UV-1800 Spectrophotometer	Shimadzu, Japan
Varioskan™ Flash Plate Reader	Thermo Fisher Scientific Inc. Waltham, MA, USA
Li-250 Spherical photometer	Li-COR, inc., Lincoln, NE, USA
ChemiDoc™ XRS+ Imager	BioRad, USA
Milli-Q Reference A^+	Merck Millipore, Darmstadt, Germany
SpeedVac Vacuum concentrator	Eppendorf, Hamburg, Germany
MZ 2C Vacuum Pump	Vacuubrand, Wertheim, Germany
PC 2004 Vario Vacuum Pump	Vacuubrand, Wertheim, Germany
ÄKTAprime plus™ FPLC	GE Healthcare, USA

HPLC

DGU-20 A5 Degasser	Shimadzu, Japan
CBM-20 A System controler	Shimadzu, Japan
LC-20 AD Liquid chromatograph	Shimadzu, Japan
SPD-M20A Diode array detector	Shimadzu, Japan
SIL-20 AD Auto injector	Shimadzu, Japan
Column oven CTO-10 ASVP	Shimadzu, Japan
Fraction Collector FRC-10 A	Shimadzu, Japan

SymmetryShield™RP18 end-capped 3.5 μm, 4.6×100 mm C18 colum	Waters, Milford, MA, USA
Agilent 2900 series HPLC	Agilent, Waldbronn, Germany
Purospher STAR RP-18 end-capped 3 μm, 30×4 mm	Merck, Darmstadt, Germany
API 5500 QTrap MS	AB Sciex, USA
Microscopy	
AMG EVOS fl	Peqlab, Erlangen, Germany
Canon PowerShot A520	Canon, Tokyo, Japan
CM100 TEM	Philips, Eindhoven, The Netherlands
Wilozyt H500	Hund, Wetzler, Germany
Software	
ExPASy proteomics server	Swiss Institute of Bioinformatics
Image Lab™	BioRad, USA
ImageBrowser EX for Windows	Canon, Tokyo, Japan
ImageJ analysis software	Rasband WS. ImageJ, U.S. National Institutes of Health, Bethesda, Maryland, USA
Kyoto Encyclopedia of Genes and Genomes (KEGG)	Kyoto, Japan
LaTeX	www.latex-project.org
LCsolution HPLC software	Shimadzu, Japan
Microsoft Office 2010	Microsoft®, Redmond, WA, USA
NCBI	National Center for Biotechnology Information, USA
Prime View FPLC software	GE Healthcare, USA
R 3.0.2	R Development Core Team, 2013
UV Probe spectroscopy software	Shimadzu, Japan
Windows 7 Professional OS	Microsoft®, Redmond, WA, USA

Publications

Zilliges, Y., Kehr, J.-C., **Meissner, S.**, Ishida, K., Mikkat, S., Hagemann, M., Kaplan, A., Börner, T., and Dittmann, E. (2011)

The cyanobacterial hepatotoxin microcystin binds to proteins and increases the fitness of *Microcystis* under oxidative stress conditions

PLoS ONE, 6: e17615

Meissner, S., Fastner, J., and Dittmann, E. (2013)

Microcystin production revisited: conjugate formation makes a major contribution

Environmental Microbiology, 15(6):1810–1820

Meissner, S., Steinhauser, D., and Dittmann, E. (2014)

Metabolomic analysis indicates a pivotal role of the hepatotoxin microcystin in high light adaptation of *Microcystis*

Environmental Microbiology, pages n/a–n/a

Deutsche Zusammenfassung

Effekte der Produktion von Microcystin in *Microcystis aeruginosa* PCC 7806

Cyanobakterien produzieren etwa 40 Prozent der primären Biomasse auf der Welt, aber auch giftige Peptide wie das leberschädigende Microcystin . Massenvorkommen, so genannte Blaualgenblüten, gefährden vielerorts regelmäßig die Trinkwasserversorgung. Diese Arbeit hatte zum Ziel, den Einfluss der Microcystinproduktion auf physiologische Abläufe in dem weit verbreiteten blütenbildenden Cyanobakterium *Microcystis aeruginosa* zu charakterisieren.

Zum einen, wurde hierfür der Einfluss der Beleuchtungsintensität auf die Produktion von Microcystin und dessen Bindung an zelluläre Proteine ermittelt. Hierzu wurden etablierte Quantifizierungstechniken mit biochemischen Methoden kombiniert. RubisCO, das Schlüsselenzym zur primären Kohlenstofffixierung, war ein Hauptinteraktionspartner von Microcystin. Hohe Beleuchtungsintensität erhöhte die Menge von an Proteine gebundenem Microcystin. Bis zu 60 Prozent des gesamten zellulären Microcystins lag an Proteine gebunden vor, d.h. es wurde durch Standardquantifizierungsmethoden nicht erfasst. Die Notwendigkeit, zur Quantifizierung des gesamten Microcystins die Proteinfraktion mit einzubeziehen, wurde auch in Freilandproben demonstriert. Die Entwicklung einer immunofluoreszenzbasierten Methode erlaubte die Unterscheidung von

toxischen und nichttoxischen *Microcystis* Kolonien in Freilandproben.
Die starklichtinduzierte Interaktion von Microcystin mit Proteinen deutete auf einen möglichen Einfluss des Sekundärmetabolits auf den Primärstoffwechsel von Microcystis hin. Um dieser Frage nachzugehen, wurde ein umfassender GC/MS-basierter Versuch durchgeführt, um die Akkumulation von Metaboliten im Microcystin produzierenden Stamm *Microcystis aeruginosa* PCC 7806 und dessen microcystinfreier *mcyB*-mutierten Variante vergleichen zu können. Es zeigte sich, dass Microcystin einen Einfluss auf die Akkumulation von 85 (17 Prozent) aller 501 detektierten Metabolite unter erhöhter Beleuchtungsstärke hatte. Besonders die vermehrte Synthese osmotisch aktiver Substanzen in der *mcyB* Mutante, verstanden als generelle Reaktion auf allgemeinen Stress, deutet auf eine Beteiligung von Microcystin in der metabolischen Justierung von *Microcystis* hin.
Die Parallelanalyse des Modellstamms *Synechocystis* PCC 6803 offenbarte grundsätzliche metabolische Unterschiede zwischen verschiedenen Cyanobakterienspezies. Demnach produzierte *Microcystis* vor allem Kohlehydrate und *Synechocystis* eher Aminosäuren. Die GC/MS-basierten Ergebnisse wurden durch elektronmikroskopische Aufnahmen und die Quantifizierung von Speichermetaboliten gestützt. Innerhalb drei Stunden bewirkte Starklicht die Akkumulation von Glykogen in *Microcystis* auf ca. 8.5 prozent des Frischgewichts, wohingegen *Synechocystis* mehr Cyanophycin produzierte. Die Ergebnisse zeigten, dass im Hinblick auf die biotechnologische Nutzung von Cyanobakterien, die Charakterisierung speziesspezifischer metabolischer Eigenschaften mehr Beachtung finden sollte.